

ADSORPTION OF PURE AND MULTICOMPONENT
GASES ON WET COAL

By

XUDONG LIANG

Bachelor of Science

East China University of Science and Technology

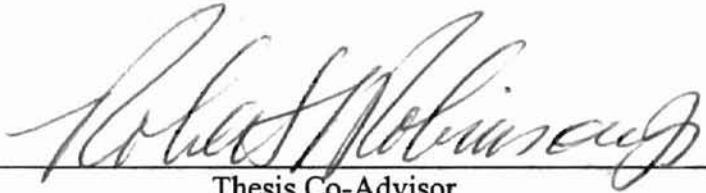
Shanghai, China

1991

Submit to the Faculty of the
Graduate College of the
Oklahoma State University
in partial fulfillment of
the requirements for
the Degree of
MASTER OF SCIENCE
DECEMBER 1999

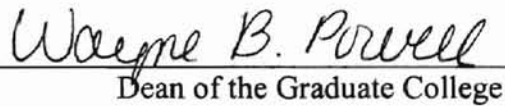
ADSORPTION OF PURE AND MULTICOMPONENT
GASES ON WET COAL

Thesis Approved :


Thesis Co-Advisor


Thesis Co-Advisor




Dean of the Graduate College

mathematical models to correlate the experimental data precisely. Results show that the models correlate the pure gas experimental data less than 3%.

PREFACE

The purpose of this research was to investigate the competitive adsorption behavior of methane, carbon dioxide and nitrogen on the surface of coal. Measurements were focused on the adsorption of the pure gases methane, nitrogen, carbon dioxide and their mixtures. Experiments were conducted on wet Fruitland and Illinois-6 coals at $115^{\circ}F$.

Mathematical models have been applied to describe the observed behavior. Five models: Langmuir, Loading-Ratio-Correlation (LRC), Zhou-Gasem-Robinson (ZGR) equation of state, Park-Gasem-Robinson (PGR) equation of state and Simplified-Local-Density (SLD) approach were used to correlate the experimental data of pure methane, carbon dioxide and nitrogen adsorption on wet Fruitland and Illinois-6 coals at $115^{\circ}F$. The LRC model and the ZGR equation of state were used to correlate the adsorption measurements of binary mixtures involving methane, carbon dioxide and nitrogen on wet Fruitland coal at $115^{\circ}F$.

Precise pure gas adsorption on wet Fruitland and Illinois-6 coals and binary mixture adsorption data on wet Fruitland coal have been obtained. The uncertainty for pure gas adsorption is less than 5% for pressures from 100 to 1800 psia, and the uncertainty for the total adsorption in binary gas mixtures is within 7%.

The mathematical models can correlate the experimental data precisely. Results show that all five models can represent the pure gas experimental data less than 3% average absolute error.

ACKNOWLEDGMENT

I express my appreciation to my thesis advisors for giving me their

I would like to thank Dr. Robert L. Johnson

office to make sure that I am

and of the present

and for giving me the

to the

ACKNOWLEDGEMENT

I wish to express my sincere appreciation to my thesis advisers for giving me their guidance and intelligence on this project. I would like to thank Dr. Robert L. Robinson, Jr., Amoco Chair, for giving me the chance to work on this project. His guidance and assistance was critical to the success of the project. I would like to thank Dr. Khaled A. M. Gasem, R.N. Maddox Professor, for giving me many encouragement, assistance and supervision through my research. Also, I like to thank Dr. Arland. H. Johannes for his time and advice to my thesis.

I also acknowledge the financial support of the U.S Depart of Energy.

I would like to thank all the people who have offered me support and assistance through my research work. Especially, my wife, Jun, and my parents for their patience, understanding, and support during my program.

Chapter	Page
V. EXPERIMENTAL RESULTS AND DISCUSSION	10
Wet Coal Substrate	32
TABLE OF CONTENTS	34
RESULTS	35
DISCUSSION	55

Chapter	Page
I. INTRODUCTION.....	1
II. THEORY	5
Adsorption Thermodynamics	5
Langmuir Model	7
ZGR Equation of State	8
PGR Equation of State	10
Simplified-Local-Density Model	11
III. EXPERIMENTAL APPARATUS.....	14
Experimental Techniques	14
Experimental Apparatus.....	15
Positive Displacement Injection Pump	17
Equilibrium Cell	17
Pressure Measurements.....	17
Temperature Measurements.....	18
Cell Section.....	18
Air/Water Bath Temperature Controllers.....	19
Gas Mixture Sampling and Analysis.....	19
IV. EXPERIMENTAL PROCEDURE.....	21
Governing Equation.....	21
Pressure Calibration	23
Temperature Calibration.....	24
Wet Coal Substrate.....	25
Equilibrium Cell Void Volume	25
Pure Component Adsorption.....	26
Binary Mixture Adsorption.....	28
Gas Chromatograph Calibration.....	28
Gibbs/Absolute Adsorption Relation.....	29

Chapter	Page
V. EXPERIMENTAL RESULTS AND DISCUSSION. BASIS.....	132
APPENDIX A - PURE COMPONENT ADSORPTION ON WET FRUITLAND COAL.....	132
Pure Component Adsorption on Wet Fruitland Coal.....	34
Binary Mixture Adsorption Data.....	39
Previous Data.....	55
VI. ANALYSIS OF EXPERIMENTAL ERRORS.....	73
Experimental Uncertainties in Pure Gas Adsorption.....	73
Experimental Uncertainties in Binary Gas Adsorption.....	75
Experimental Uncertainty.....	77
Discussion of Error Analysis.....	78
VII. DATA CORRELATION.....	81
Single Langmuir Model for Pure Components.....	81
LRC Model.....	81
ZGR Equation of State.....	86
PGR Equation of State.....	88
SLD Model.....	94
Discussion.....	96
LRC Model for Binary Mixture.....	98
ZGR Equation of State for Binary Mixture.....	105
VIII. CONCLUSIONS AND RECOMMENDATIONS.....	115
Conclusions.....	115
Recommendations.....	116
BIBLIOGRAPHY.....	117
APPENDICES.....	120
APPENDIX A - GAS COMPRESSIBILITY FACTORS.....	121
APPENDIX B - DERIVATION OF FUGACITY FOR ZHOU-GASEM-ROBINSON EQUATION OF STATE.....	135
APPENDIX C - DERIVATION OF FUGACITY FOR PARK-GASEM-ROBINSON EQUATION OF STATE.....	138

Chapter	Page
APPENDIX D - ADSORPTION ON ORGANIC COAL BASIS.	142
APPENDIX E - EXPERIMENTAL ADSORPTION DATA.	145

OF TABLES

Table	Page
1. Porosity of the parent and oxidized lignites in water	22
2. Adsorption of CO_2 on parent and oxidized lignites	29
3. Adsorption of CO_2 on parent and oxidized lignites	31
4. Adsorption of CO_2 on parent and oxidized lignites	31
5. Adsorption of CO_2 on parent and oxidized lignites	31
6. Adsorption of CO_2 on parent and oxidized lignites	31
7. Adsorption of CO_2 on parent and oxidized lignites	31
8. Adsorption of CO_2 on parent and oxidized lignites	31
9. Adsorption of CO_2 on parent and oxidized lignites	31
10. Adsorption of CO_2 on parent and oxidized lignites	31
11. Adsorption of CO_2 on parent and oxidized lignites	31
12. Adsorption of CO_2 on parent and oxidized lignites	31
13. Adsorption of CO_2 on parent and oxidized lignites	31
14. Adsorption of CO_2 on parent and oxidized lignites	31
15. Adsorption of CO_2 on parent and oxidized lignites	31
16. Adsorption of CO_2 on parent and oxidized lignites	31
17. Adsorption of CO_2 on parent and oxidized lignites	31
18. Adsorption of CO_2 on parent and oxidized lignites	31
19. Adsorption of CO_2 on parent and oxidized lignites	31
20. Adsorption of CO_2 on parent and oxidized lignites	31
21. Adsorption of CO_2 on parent and oxidized lignites	31
22. Adsorption of CO_2 on parent and oxidized lignites	31
23. Adsorption of CO_2 on parent and oxidized lignites	31
24. Adsorption of CO_2 on parent and oxidized lignites	31
25. Adsorption of CO_2 on parent and oxidized lignites	31
26. Adsorption of CO_2 on parent and oxidized lignites	31
27. Adsorption of CO_2 on parent and oxidized lignites	31
28. Adsorption of CO_2 on parent and oxidized lignites	31
29. Adsorption of CO_2 on parent and oxidized lignites	31
30. Adsorption of CO_2 on parent and oxidized lignites	31
31. Adsorption of CO_2 on parent and oxidized lignites	31
32. Adsorption of CO_2 on parent and oxidized lignites	31
33. Adsorption of CO_2 on parent and oxidized lignites	31
34. Adsorption of CO_2 on parent and oxidized lignites	31
35. Adsorption of CO_2 on parent and oxidized lignites	31
36. Adsorption of CO_2 on parent and oxidized lignites	31
37. Adsorption of CO_2 on parent and oxidized lignites	31
38. Adsorption of CO_2 on parent and oxidized lignites	31
39. Adsorption of CO_2 on parent and oxidized lignites	31
40. Adsorption of CO_2 on parent and oxidized lignites	31
41. Adsorption of CO_2 on parent and oxidized lignites	31
42. Adsorption of CO_2 on parent and oxidized lignites	31
43. Adsorption of CO_2 on parent and oxidized lignites	31
44. Adsorption of CO_2 on parent and oxidized lignites	31
45. Adsorption of CO_2 on parent and oxidized lignites	31
46. Adsorption of CO_2 on parent and oxidized lignites	31
47. Adsorption of CO_2 on parent and oxidized lignites	31
48. Adsorption of CO_2 on parent and oxidized lignites	31
49. Adsorption of CO_2 on parent and oxidized lignites	31
50. Adsorption of CO_2 on parent and oxidized lignites	31

Table	Page
1. Parameters in Equation for Gas Solubilities in Water	22
2. Gas Chromatograph Response Factor and Retention Time	29
3. Pure Methane Adsorption on Wet Fruitland Coal at 115 °F	33
4. Pure Nitrogen Adsorption on Wet Fruitland Coal at 115 °F	33
5. Pure Carbon Dioxide Adsorption on Wet Fruitland at 115 °F	34
6. Pure Methane Adsorption on Wet Illinois-6 Coal at 115 °F	38
7. Pure Nitrogen Adsorption on Wet Illinois-6 Coal at 115 °F	38
8. Methane/Carbon Dioxide Adsorption on Wet Fruitland Coal at 115 °F	50
9. Methane/Nitrogen Adsorption on Wet Fruitland Coal at 115 °F	52
10. Nitrogen/Carbon Dioxide Adsorption on Wet Fruitland Coal at 115 °F	54
11. Experimental Uncertainty Analysis	77
12. Simple Langmuir Model Representation of Adsorption on Fruitland Coal	86
13. Simple Langmuir Model Representation of Adsorption on Illinois-6 Coal	87
14. LRC Model Representation of Adsorption on Fruitland Coal ($\eta = 0.87$)	87

LIST OF TABLES

Table	Page
1. Parameters in Equation for Gas Solubilities in Water	22
2. Gas Chromatograph Response Factor and Retention Time	29
3. Pure Methane Adsorption on Wet Fruitland Coal at 115 °F	33
4. Pure Nitrogen Adsorption on Wet Fruitland Coal at 115 °F	33
5. Pure Carbon Dioxide Adsorption on Wet Fruitland at 115 °F	34
6. Pure Methane Adsorption on Wet Illinois-6 Coal at 115 °F	38
7. Pure Nitrogen Adsorption on Wet Illinois-6 Coal at 115 °F	38
8. Methane/Carbon Dioxide Adsorption on Wet Fruitland Coal at 115 °F	50
9. Methane/Nitrogen Adsorption on Wet Fruitland Coal at 115 °F	52
10. Nitrogen/Carbon Dioxide Adsorption on Wet Fruitland Coal at 115 °F	54
11. Experimental Uncertainty Analysis	77
12. Simple Langmuir Model Representation of Adsorption on Fruitland Coal	86
13. Simple Langmuir Model Representation of Adsorption on Illinois-6 Coal	87
14. LRC Model Representation of Adsorption on Fruitland Coal ($\eta = 0.87$)	87

Table	Page
15. LRC Model Representation of Adsorption on Illinois-6 Coal ($\eta = 0.87$)	88
16. ZGR Equation of State Representation of Adsorption on Fruitland Coal.	92
17. ZGR Equation of State Representation of Adsorption on Illinois-6 Coal.	92
18. Pure Fluid Parameters for PGR Equation of State	92
19. Universal Constants for PGR Equation of State	93
20. PGR Equation of State Representation of Adsorption on Fruitland Coal.	93
21. SLD Model Representation of Adsorption on Fruitland Coal.	94
22. SLD Model Representation of Adsorption on Fruitland Coal.	96
23. Regression Results for Adsorption of Methane, Nitrogen and Carbon Dioxide on Wet Fruitland Coal at 115 °F	97
24. Summary of Model Results for Gas Adsorption on Wet Fruitland Coal at 115 °F	98
25. LRC Model Representation of Adsorption for Binary Mixtures.	112
26. ZGR Equation of State Representation of Adsorption for Binary Mixtures	113
27. Comparison of LRC Model and ZGR Equation of State Prediction of Binary Mixtures Adsorption	114
28. Regressed R-K EOS Constants for Different Gases	128
29. Regressed Binary Mixture Interaction Parameters.	129
30. Accuracy of Pure Binary Mixture Compressibility Factor Simulation Model	130
31. Organic Coal Content of Coal Sample	143
32. Pure Methane Adsorption Data on Wet Fruitland Coal (Run2)	146

Table	Page
33. Pure Methane Adsorption Data on Wet Fruitland Coal (Run2)	147
34. Pure Methane Adsorption Data on Wet Fruitland Coal (Run3)	148
35. Pure Carbon Dioxide Adsorption Data on Wet Fruitland Coal (Run1)	149
36. Pure Carbon Dioxide Adsorption Data on Wet Fruitland Coal (Run2)	150
37. Pure Carbon Dioxide Adsorption Data on Wet Fruitland Coal (Run3)	151
38. Pure Nitrogen Adsorption Data on Wet Fruitland Coal (Run1)	152
39. Pure Nitrogen Adsorption Data on Wet Fruitland Coal (Run2).	153
40. Pure Nitrogen Adsorption Data on Wet Fruitland Coal (Run3).	154
41. Pure Methane Adsorption Data on Wet Illinois-6 Coal (Run1)	155
42. Pure Methane Adsorption Data on Wet Illinois-6 Coal (Run2)	156
43. Pure Nitrogen Adsorption Data on Wet Illinois-6 Coal (Run1)	157
44. Pure Nitrogen Adsorption Data on Wet Illinois-6 Coal (Run2)	158
45. Methane/Carbon Dioxide (80%/20%) Adsorption Data on Wet Fruitland Coal	159
46. Methane/Carbon Dioxide (60%/40%) Adsorption Data on Wet Fruitland Coal.	160
47. Methane/Carbon Dioxide (40%/60%) Adsorption Data on Wet Fruitland Coal.	161
48. Methane/Carbon Dioxide (20%/80%) Adsorption Data on Wet Fruitland Coal	162
49. Methane/Nitrogen (80%/20%) Adsorption Data on Wet Fruitland Coal	163
50. Methane/Nitrogen (60%/40%) Adsorption Data on Wet Fruitland Coal	164
51. Methane/Nitrogen (40%/60%) Adsorption Data on Wet Fruitland Coal	165

Table	Page
52. Methane/Nitrogen (20%/80%) Adsorption Data on Wet Fruitland Coal	166
53. Nitrogen/Carbon Dioxide (80%/20%) Adsorption Data on Wet Fruitland Coal	167
54. Nitrogen/Carbon Dioxide (60%/40%) Adsorption Data on Wet Fruitland Coal	168
55. Nitrogen/Carbon Dioxide (40%/60%) Adsorption Data on Wet Fruitland Coal	169
56. Nitrogen/Carbon Dioxide (20%/80%) Adsorption Data on Wet Fruitland Coal	170

Figure	Page
14. Methane/Nitrogen Binary Mixture Adsorption on Wet Fruitland Coal at 115°F	49
15. Nitrogen/Carbon Dioxide Binary Mixture Adsorption on Wet Fruitland Coal at 115°F	57

LIST OF FIGURES

Figure	Page
1. Schematic Diagram of Adsorption Apparatus	16
2. Response Factor of Gas Chromatograph.	31
3. Gas Adsorption on Wet Fruitland Coal	35
4. Pure Carbon Dioxide Adsorption on Wet Fruitland Coal at 115°F	36
5. Gas Adsorption on Wet Illinois-6 Coal at 115°F	37
6. Methane/Carbon Dioxide Binary Mixture Adsorption on Wet Fruitland Coal at 115°F : Methane.	40
7. Methane/Carbon Dioxide Binary Mixture Adsorption on Wet Fruitland Coal at 115°F : Carbon Dioxide.	41
8. Methane/Carbon Dioxide Binary Mixture Adsorption on Wet Fruitland Coal at 115°F : Total	42
9. Methane/Nitrogen Binary Mixture Adsorption on Wet Fruitland Coal at 115°F : Methane.	44
10. Methane/Nitrogen Binary Mixture Adsorption on Wet Fruitland Coal at 115°F : Nitrogen.	45
11. Methane/Nitrogen Binary Mixture Adsorption on Wet Fruitland Coal at 115°F : Total	46
12. Nitrogen/Carbon Dioxide Binary Mixture Adsorption on Wet Fruitland Coal at 115°F : Nitrogen	47
13. Nitrogen/Carbon Dioxide Binary Mixture Adsorption on Wet Fruitland Coal at 115°F : Carbon Dioxide	48

Figure	Page
14. Nitrogen/Carbon Dioxide Binary Mixture Adsorption on Wet Fruitland Coal at 115 °F : Total	49
15. Data Comparison for Pure Nitrogen Adsorption on Wet Fruitland Coal at 115 °F	57
16. Data Comparison for Pure Methane Adsorption on Wet Fruitland Coal at 115 °F	58
17. Data Comparison for Pure Carbon Dioxide Adsorption on Wet Fruitland Coal at 115 °F	59
18. Reevaluation of Hall's Carbon Dioxide Adsorption Data on Wet Fruitland Coal at 115 °F	60
19. Data Comparison for Methane/Carbon Dioxide Binary Mixture Adsorption on Wet Fruitland Coal at 115 °F : Methane	61
20. Data Comparison for Methane/Carbon Dioxide Binary Mixture Adsorption on Wet Fruitland Coal at 115 °F : Carbon Dioxide	62
21. Data Comparison for Methane/Carbon Dioxide Binary Mixture Adsorption on Wet Fruitland Coal at 115 °F : Total	63
22. Data Comparison for Methane/Carbon Dioxide Binary Mixture Adsorption on Wet Fruitland Coal at 115 °F : Methane/Amoco	64
23. Data Comparison for Methane/Carbon Dioxide Binary Mixture Adsorption on Wet Fruitland Coal at 115 °F : Carbon Dioxide/Amoco	65
24. Data Comparison for Methane/Carbon Dioxide Binary Mixture Adsorption on Wet Fruitland Coal at 115 °F : Total/Amoco	66
25. Data Comparison for Methane/Nitrogen Binary Mixture Adsorption on Wet Fruitland Coal at 115 °F : Methane	67
26. Data Comparison for Methane/Nitrogen Binary Mixture Adsorption on Wet Fruitland Coal at 115 °F : Nitrogen	68
27. Data Comparison for Methane/Nitrogen Binary Mixture Adsorption on Wet Fruitland Coal at 115 °F : Total	69

Figure	Page
28. Data Comparison for Nitrogen/Carbon Dioxide Binary Mixture Adsorption on Wet Fruitland Coal at 115°F : Nitrogen	170
29. Data Comparison for Nitrogen/Carbon Dioxide Binary Mixture Adsorption on Wet Fruitland Coal at 115°F : Carbon Dioxide	171
30. Data Comparison for Nitrogen/Carbon Dioxide Binary Mixture Adsorption on Wet Fruitland Coal at 115°F : Total	172
31. Uncertainty Associated with Pure Gas Adsorption on Wet Fruitland Coal at 115°F	179
32. Uncertainty Associated with Pure Gas Adsorption on Wet Illinois-6 Coal at 115°F	80
33. Simple Langmuir Representation of Pure Gas Adsorption on Wet Fruitland Coal at 115°F	82
34. Simple Langmuir Representation of Pure Gas Adsorption on Wet Illinois-6 Coal at 115°F	83
35. LRC Representation of Pure Gas Adsorption on Wet Fruitland Coal at 115°F	84
36. LRC Representation of Pure Gas Adsorption on Wet Illinois-6 Coal at 115°F	85
37. ZGR Representation of Pure Gas Adsorption on Wet Fruitland Coal at 115°F	89
38. ZGR Representation of Pure Gas Adsorption on Wet Illinois-6 Coal at 115°F	90
39. PGR Representation of Pure Gas Adsorption on Wet Fruitland Coal at 115°F	91
40. SLD Representation of Pure Nitrogen Adsorption on Wet Fruitland Coal at 115°F	95
41. LRC Representation of Methane/Nitrogen Binary Mixture Adsorption on Wet Fruitland Coal at 115°F : Methane	99

Figure	Page
42. LRC Representation of Methane/Nitrogen Binary Mixture Adsorption on Wet Fruitland Coal at 115 °F : Nitrogen	100
43. LRC Representation of Methane/Carbon Dioxide Binary Mixture Adsorption on Wet Fruitland Coal at 115 °F : Methane	101
44. LRC Representation of Methane/Carbon Dioxide Binary Mixture Adsorption on Wet Fruitland Coal at 115 °F : Carbon Dioxide.	102
45. LRC Representation of Nitrogen/Carbon Dioxide Binary Mixture Adsorption on Wet Fruitland Coal at 115 °F : Nitrogen	103
46. LRC Representation of Nitrogen/Carbon Dioxide Binary Mixture Adsorption on Wet Fruitland Coal at 115 °F : Carbon Dioxide.	104
47. ZGR Representation of Methane/Nitrogen Binary Mixture Adsorption on Wet Fruitland Coal at 115 °F : Methane	106
48. ZGR Representation of Methane/Nitrogen Binary Mixture Adsorption on Wet Fruitland Coal at 115 °F : Nitrogen	107
49. ZGR Representation of Methane/Carbon Dioxide Binary Mixture Adsorption on Wet Fruitland Coal at 115 °F : Methane	108
50. ZGR Representation of Methane/Carbon Dioxide Binary Mixture Adsorption on Wet Fruitland Coal at 115 °F : Carbon Dioxide.	109
51. ZGR Representation of Nitrogen/Carbon Dioxide Binary Mixture Adsorption on Wet Fruitland Coal at 115 °F : Nitrogen	110
52. ZGR Representation of Nitrogen/Carbon Dioxide Binary Mixture Adsorption on Wet Fruitland Coal at 115 °F : Carbon Dioxide.	111
53. Deviation Between Calculated and Tabulated Compressibility Factors for Helium.	123
54. Deviation Between Calculated and Tabulated Compressibility Factors for Methane.	125
55. Deviation Between Calculated and Tabulated Compressibility Factors for Nitrogen.	126

Figure	Page
56. Deviation Between Calculated and Tabulated Compressibility Factors for Carbon Dioxide	127
57. Methane/Nitrogen Binary Mixture Compressibility Factor Calibration	131
58. Methane/Carbon Dioxide Binary Mixture Compressibility Factors Calibration: Reamer	132
59. Methane/Carbon Dioxide Binary Mixture Compressibility Factors Calibration: Holste-Hall	133
60. Nitrogen/Carbon Dioxide Binary Mixture Compressibility Factor Calibration	134
61. Data Comparison of Pure Gas Adsorption from OSU and Amoco (Organic Coal Basis)	144

NOMENCLATURE

a	specific molar area; 3-D EOS model constant
a_2	2-D analog of 3-D EOS model constant a
A	ash content; molar Helmholtz energy; surface area per mass of absorbent
AAPD	average absolute percentage deviation
b	3-D EOS model constant
b_2	2-D analog of 3-D EOS model constant b
B	Langmuir model constant
$B(T)$	second virial coefficient
c	critical state
CH_4	methane
CO_2	carbon dioxide
C_{ij}	EOS binary interaction parameter, dimensionless
D_{ij}	EOS binary interaction parameter, dimensionless
EOS	equation of state
F	fugacity
G	molar Gibbs free energy
G_i	molar Gibbs free energy of component i
k_i	2D-EOS model constant of component i
L	Langmuir model constant

M	general property
m	2-D ZGR EOS model constant
M_S	mass of absorbent
n	number of moles
n_i	number of moles of component i
N_A	Avogadro's number
N₂	nitrogen
P	pressure
PB	Peng-Robinson equation of state
PGR	Park-Gasem-Robinson equation of state
R	universal gas constant
R_f	relative response factor
RK	Redlich-Kwong equation of state
RMSE	root mean square error
S	sulfur content; objective function; entropy
T	temperature
T*	characteristic temperature parameter in PGR EOS
\tilde{T}	reduced temperature (T/T^*)
U	ZGR/PGR EOS model parameter, molar internal energy
v	molar volume
v*	characteristic volume
V	volume
W	ZGR/PGR EOS model parameter

x_i	mole fraction of component i in absorbed phase
y_i	mole fraction of component i in gas phase
Y	temperature-dependent function in the PGR EOS at low density limit
z	compressibility factor
z_k	pump section feed gas mixture composition for component k
Z_a	compressibility factor for absorbed phase
Z_M	PGR equation of state constant
ZGR	Zhou-Gasem-Robinson equation of state

Greek Letters

α	2-D EOS model constant
β	2-D EOS model constant
ϕ_i	fugacity coefficient of i as a pure component
γ_i	activity coefficient of component i in a mixture
μ_i	chemical potential of component i
π	2-dimensional pressure
ε_{fs}/k	fluid-solid contribution
θ	fraction of monolayer coverage
ρ	density
η	loading ratio correlation constant
σ	uncertainty of experimental data; surface density
τ	geometrical constant in PGR equation of state

Γ^{ex} excess adsorption
 ω total amount adsorbed per mass adsorbent

ω_i amount adsorbed of component i per mass adsorbent

ψ fugacity coefficient

Ω R-K EOS constant

Superscripts

g gas phase

o standard state

Subscripts

Abs absolute adsorption

Ads adsorbed phase

Ash ash content in coal

c cell section

f final reading

i initial reading

i, j components i, j

sulfur sulfur content in coal

inj injected gas

pump pump section

sol amount of gas dissolved in the water

unads amount of unadsorbed gas in the cell section

Large quantities of natural gas (methane) are stored in coal deposits. The amount of gas currently in coalbeds in the U.S. is estimated to be 400 trillion cubic feet (Tcf) of which about 95 Tcf is recoverable under current technology [1]. Coalbed methane production grew to 2.9 Bcf/d of gas supply during 1997, accounting for about 6% of total U.S. natural gas production [28]. Thus, coalbed methane can represent a valuable addition to the national energy reserve. However, the current state of scientific and engineering knowledge on coalbed methane is inadequate to develop optimum strategies for its recovery.

In addition, large quantities of carbon dioxide are generated by industry. The amount of carbon dioxide released to the environment increases every year. Carbon dioxide can increase the greenhouse effect, which leads to warmer weather worldwide. This is a serious environmental problem. Researchers have proposed carbon dioxide sequestration in oceans, oil fields and coalbeds. Sequestering carbon dioxide in coalbeds has the added benefit of enhancing coalbed methane production, which is an attractive way to reduce carbon dioxide.

Coalbed methane is stored primarily in the form of an adsorbed layer on the coal surface, where it exhibits liquid-like density [24]. So, a significant amount of methane can be stored on a given volume of coal. Knowledge of this adsorption behavior is critical for accurate description of production processes to recover the adsorbed gas. Typical coalbed gas is 95% methane, with the remaining gases including ethane, carbon

dioxide, nitrogen, helium and hydrogen. In addition to the gases formed, large quantities of water are released during the maturation process for coal. Methane is retained in coals in one of three states: as adsorbed molecules on the organic surfaces, as free gas within the pores or fractures, and dissolved in aqueous solution within coalbed. The primary mechanism of methane retention in coalbed is adsorption on the coal surface within the matrix pore structure. In coalbed methane production, due to the presence of a gas phase, methane gas recovery can be enhanced either by reducing the partial pressure of methane through the introduction of a lower-adsorbing gas such as nitrogen or displacement by the introduction of a high-adsorbing gas such as carbon dioxide. A two-step injection process involving a strongly adsorbable fluid followed by a weakly adsorbable gas can be used to simulate the release of residual methane from the coalbed. The strong adsorber, carbon dioxide, displaces and desorbs the methane while the inert gas nitrogen forces the excess carbon dioxide to move through the coalbed. As the fluid moves through the coalbed, it desorbs more methane from the coal matrix [24].

The flue gas generated from power plants and refineries contains about 85 percent carbon dioxide and 15 percent nitrogen, which can be used to generate coalbed methane by enhanced gas recovery [7].

The gas sorbed on coal is not always pure methane. Coal can also contain appreciable amounts of carbon dioxide, nitrogen, and heavier hydrocarbons. The injected flue gas is not pure gas, it contains carbon dioxide, nitrogen and other residual gases. In these cases, a description of multi-component gas adsorption is needed in order to predict methane gas-in-place, rates and reserves. Thus, a spectrum of compositions will develop

through time and position in the bed during primary or enhanced gas production. An injected gas can be nitrogen and/or carbon dioxide. The complete adsorption data on the pure methane, nitrogen and carbon dioxide and their binary mixtures is necessary before we can comprehensively understand the adsorption and desorption behavior in such systems.

Previous studies have been conducted on the adsorption of mixed gases on coals. Measurements have been reviewed by DeGance [3] for the adsorption of various gases on carbon substrates. Data bibliographies have been provided by Yang [32], Valenzuel and Myers [29]. Greaves [6] investigated the adsorption of methane + carbon dioxide mixtures on dry Sewickley coal at $73^{\circ}F$ at pressures to 1,000 psia. Pure carbon dioxide and methane, along with mixtures containing 90% and 75% methane, were studied. A much more comprehensive study was done by Stevenson, who measured the adsorption of methane, nitrogen, and carbon dioxide, and of their binary and ternary mixtures, on dry coal from the Westcliff Bulli seam in New South Wales at $86^{\circ}F$ and pressures to 750 psia.

Some studies on wet coal have been performed. Harpalani [10] studied the adsorption of pure carbon dioxide, methane and one mixture (93% methane, 5% carbon dioxide, 2% nitrogen) on wet Fruitland coal at $112^{\circ}F$ and pressure to 1,400 psia. Also, Arri [1] measured the adsorption at $115^{\circ}F$ on wet Fruitland coal of pure methane, carbon dioxide, nitrogen and several mixtures at pressure to 1,500 psia.

Several models are used to correlate experimental adsorption data. Among them, the Langmuir model and loading-ratio-correlation (LRC) model are simple and widely used to correlate pure and binary experimental data. Equations of state are applied to the

pure and binary gas adsorption results [34]. Lira and coworkers have successfully applied the simplified-local-density model to pure gas adsorption on carbon adsorbent [21]. Oklahoma State University started research of gas adsorption on wet Fruitland coal at $115^{\circ}F$ in 1991 by Robinson, Gasem and Hall [8]. Hall collected data of pure and binary gas for nitrogen, methane and carbon dioxide adsorption on coal at the pressures from 100 psia to 1800 psia, and he correlated the experimental data by Langmuir and LRC models. Zhou developed a new general cubic type equation of state model to correlate the adsorption experimental data [33].

Objectives of the present work are to:

- Measure the adsorption of pure methane, nitrogen and carbon dioxide and their binary mixtures on wet Fruitland and Illinois-6 coals at $115^{\circ}F$ at pressures from 100 to 1800 psia,
- Test the Langmuir, the LRC, the Zhou-Gasem-Robinson (ZGR) equation of state and simplified-local-density (SLD) models to correlate the pure gases and their binary mixture adsorption data; develop the Park-Gasem-Robinson (PGR) equation of state to correlate the pure gas adsorption data, and
- Provide engineering data to facilitate the evaluations of techniques for carbon dioxide (flue gas) injection into coalbeds to simultaneously reduce carbon dioxide and increase the supply of natural gas.

CHAPTER II

THEORY

The surface of a solid represents a discontinuity of its structure. Research shows that the forces acting at the surface are unsaturated [32]. Hence, when the solid is exposed to a gas, the gas molecules will interact with it and become attached. This phenomena is termed adsorption.

Numerous theories and models have been developed to correlate pure and mixture gas adsorption [32]. Among them are the Langmuir model, statistical model, potential model, vacancy solution model, ideal adsorbed solution theory, heterogeneous Langmuir model, heterogeneous ideal adsorbed solution theory, and two-dimensional equations of state. Each of these models has its strengths and limitations.

Adsorption Thermodynamics

For a homogeneous three-dimensional fluid phase treated as an open system, the fundamental thermodynamic property relation is [30]:

$$d(nU) = Td(nS) - Pd(nV) + \sum(\mu_i dn_i) \quad 2-1$$

For a two-dimensional phase, the fundamental property relation is:

$$d(nU) = Td(nS) - \pi d(nA) + \sum(\mu_i dn_i) \quad 2-2$$

$$d(nU) = Td(nS) - \pi d(nA) + \sum(\mu_i dn_i) \quad 2-3$$

The difference between the three-dimensional and two-dimensional expression is that the pressure is replaced by the spreading pressure and the molar volume by the molar area. The two-dimensional equation can be expanded to a new equation:

$$dU = TdS - \pi dA + \sum(\mu_i dx_i) \quad 2-4$$

$$U = TS - \pi dA + \sum (\mu_i x_i) \quad \text{Langmuir Model} \quad 2-5$$

The two equations can be derived because both n and dn are independent and arbitrary.

Similar equations can be derived for Gibbs free energy:

$$d(nG) = -(nS)dT + (nA)d\pi + \sum (\mu_i dx_i) \quad 2-6$$

$$dG = -SdT + Ad\pi + \sum (\mu_i dx_i) \quad 2-7$$

The chemical potential can be defined as

$$\bar{G}_i = \left(\frac{\partial(nG)}{\partial n_i} \right) = \mu_i \quad 2-8$$

From fundamental thermodynamics equation, we can have

$$d(nG) = \sum (\mu_i dn_i) + \sum (n_i d\mu_i) \quad 2-9$$

Then, the Gibbs-Duhem equation for the two-dimensional phase is

$$SdT - Ad\pi + \sum (x_i d\mu_i) = 0 \quad 2-10$$

At the constant temperature, the equation becomes

$$- Ad\pi + \sum (x_i d\mu_i) = 0 \quad 2-11$$

For the two-dimensional phase, the adsorbate is always in equilibrium with a gas phase. The equilibrium condition means the chemical potential of each specie is the same in the equilibrium phases. That is

$$\begin{aligned} \mu_i &= \mu_i^g \\ d\mu_i &= d\mu_i^g \end{aligned} \quad 2-12$$

The Gibbs adsorption isotherm becomes,

$$Ad\pi - \sum (x_i d\mu_i^g) = 0 \quad 2-13$$

The simplest and still most useful isotherm, for both physical and chemical adsorption, is the Langmuir isotherm [33]. Its form is based on the following assumptions:

- a. The adsorbed molecules or atoms are held at definite, localized sites.
- b. Each site can accommodate one and only one molecule or atom, which is monolayer.
- c. The energy of adsorption is a constant over all sites and there is no interaction between neighboring adsorbates.

At equilibrium, all sites have already been occupied and are no longer available for adsorption, the dynamic equilibrium is between the rates of condensation (adsorption) and evaporation (desorption). These assumption leads to the following equation [32]:

$$\theta = \frac{\omega}{L} = \frac{BP}{1 + BP} \quad 2-14$$

This is the Langmuir isotherm. L is the maximum amount of gas that can be adsorbed on the solid surface, ω is the amount adsorbed on the solid surface at the specified pressure, B is the Langmuir adsorption constant and θ is the fraction of monolayer coverage. B is dependent on the temperature, and its value typically decreases with increase in temperature.

Langmuir [32] also considered the dissociative adsorption for the case of each molecule occupying two sites. Then two sites are needed for both adsorption and desorption. When the adsorbate occupies n sites, the equation becomes the following:

$$\theta = \frac{\omega}{L} = \frac{BP^{1/n}}{1 + BP^{1/n}} \quad 2-15$$

This equation is also recognized as the LRC model.

Langmuir simple model and revised model can be easily extended to multicomponent gas adsorption. The simple Langmuir model can be extended to:

$$\theta_i = \frac{\omega_i}{L_i} = \frac{B_i P y_i}{1 + \sum_j B_j P y_j} \quad 2-16$$

The LRC model becomes,

$$\theta_i = \frac{\omega_i}{L_i} = \frac{B_i (P y_i)^{1/n}}{1 + \sum_j B_j (P y_j)^{1/n}} \quad 2-17$$

ZGR Equation of State

The 2-dimensional Van der Waals (2-D VDW) equation of state (EOS) has been applied to pure gas adsorption by various researchers, including Hill, de Boer and Ross and Olivier. Hoory and Prausnitz extended the 2-D VDW EOS to binary mixtures by using mixing rules [26]. Recently, DeGance [3] used the 2-D virial and Eyring EOS to correlate pure adsorption isotherms for several adsorption systems. Zhou developed a generalized cubic EOS to correlate the data for adsorption on coal [34].

The adsorbate on the solid surface is treated like a liquid phase, so the adsorption can be treated as a gas-liquid equilibrium. The equilibrium can be described by the following equation from van Ness [30]:

$$Z_a \phi_i \omega_i = k_i f_i^g \quad 2-18$$

where, Z_a is the adsorbed gas compressibility factor in liquid phase, ϕ_i is the adsorbed gas fugacity coefficient in liquid phase, ω_i is the adsorbed amount, f_i^g is the unadsorbed gas fugacity, k_i is a constant.

The adsorbed phase fugacity coefficient can be expressed by the following equation:

$$\ln \phi_i = \int_0^{\omega} \left\{ \frac{1}{RT\omega} \left[\frac{\partial(A\pi)}{\partial \omega_i} \right]_{T,ms,n_i} - \frac{1}{\omega} \right\} d\omega - \ln Z_a \quad 2-19$$

where A is the surface area per unit mass of solid, π is the 2-D spreading pressure, ms is the mass of adsorbent. The gas-phase fugacity f_i^g can be calculated by 3-dimensional (3-D) equation of state. The generalized 3-D cubic EOS can be expressed as

$$\left[P + \frac{a}{v^2 + Ubv + Wb^2} \right] [v - b] = RT \quad 2-20$$

This equation can be reduced to two-dimensional equation of state by analogy

$$\left[\pi + \frac{a_2 \sigma^2}{1 + Ub_2 \sigma + W(b_2 \sigma)^2} \right] [1 - b_2 \sigma] = \sigma RT \quad 2-21$$

After rearrangement, the pressure can be related to the adsorption amount.

$$\left[A\pi + \frac{\alpha \omega^2}{1 + U\beta \omega + W(\beta \omega)^2} \right] [1 - \beta \omega] = \omega RT \quad 2-22$$

where, α and β are model constants. The above 2-D EOS can be developed to a new form, as assumed by Zhou [34]:

$$\left[A\pi + \frac{\alpha \omega^2}{1 + U\beta \omega + W(\beta \omega)^2} \right] [1 - (\beta \omega)^m] = \omega RT \quad 2-23$$

The m is the added constant. The number m is very important to the calculation of the EOS. In the current model, m set to 1/3, U=0 and W=0 as suggested by Zhou [34].

This revised EOS can be extended to correlate binary gas adsorption. For the binary gas, the constants can be calculated by following mixing rules by Zhou [34]:

$$\alpha = \sum_i \sum_j x_i x_j \alpha_{ij}$$

$$\beta = \sum_i \sum_j x_i x_j \beta_{ij} \quad 2-24$$

where,

$$\alpha_{ij} = (1 - C_{ij})(\alpha_i + \alpha_j)/2$$

$$\beta_{ij} = (1 + D_{ij})\sqrt{\beta_i \beta_j}$$

PGR Equation of State

A perturbed-hard-chain theory equation of state has been introduced by Park and coworkers in 1994 [26] and is named the Park-Gasem-Robinson (PGR) equation of state [19]. The strength of this equation is that it has a more accurate repulsive term, which is required for precise representation of adsorption behavior. This equation is expressed as:

$$\frac{Pv}{RT} = 1 + c \left(\frac{\beta_1 \tau}{v_r - \beta_2 \tau} - \frac{Z_M Y v_r}{v_r^2 + U v_r + W} - \frac{Q_1 Z_M Y}{v_r + Q_2} \right) \quad 2-25$$

where,

$$v_r = \frac{v}{v^*}$$

$$Y = \exp(F_r) - 1$$

$$F_r = \omega_1 \left(\frac{1}{2\tilde{T}} \right)^{1/2} + \omega_2 \left(\frac{1}{2\tilde{T}} \right) + \omega_3 \left(\frac{1}{2\tilde{T}} \right)^{3/2} + \omega_4 \left(\frac{1}{2\tilde{T}} \right)^2$$

$$\tilde{T} = \frac{T}{T^*}$$

The first term inside the parenthesis is the repulsive term, the second and third terms are attractive terms.

As with the ZGR equation of state, the PGR equation of state can be reduced to 2-D equation of state and can be applied to gas adsorption. The reduced 2-D equation of state is:

$$A\pi = \omega RT + cRT\omega \left(\frac{\beta_1 \tau v l \omega}{1 - \beta_2 \tau l \omega} - \frac{Z_M Y l \omega}{1 + U l \omega + W(l\omega)^2} - \frac{Q_1 Z_M Y l \omega}{1 + Q_2 l \omega} \right) \quad 2-26$$

where ω is the adsorption amount and $l = V^* / A$.

Simplified-Local-Density Model

The simplified-local-density (SLD) model is developed from statistical mechanical theory [19]. It assumes the adsorbent provides a molecularly smooth, nonporous, energetically homogeneous surface. The adsorption is expressed by the surface excess adsorption (Γ^{ex}), the excess number of moles per unit area of adsorbent or

$$\Gamma^{ex} = \int_{z_0}^{\infty} (\rho(z) - \rho_{bulk}) dz \quad 2-27$$

Where ρ is the local density, z is the distance between gas molecule and solid atom.

The lower limit of integration is the surface of the solid, and is taken as the plane at

$$z_0 = \sigma_{ff} / 2 \quad 2-28$$

σ_{ff} is the molecular distance between two molecules of adsorbate.

In adsorption, the attractive potential between the fluid and solid, at any point z , is assumed to be independent of z . At equilibrium, the chemical potential is calculated by contributions from fluid-fluid and fluid-solid interaction.

$$\mu = \mu_{bulk} = \mu_{ff}(z) + \mu_{fs}(z) \quad 2-29$$

where the subscript bulk refers to the bulk fluid, ff refers to fluid-fluid interactions, fs refers to the fluid-solid interactions.

The fluid-solid potential can be expressed by Avogadro Number N_A and molecular potential $\Psi(z)$.

$$\mu_{fs} = N_A \Psi(z) \quad 2-30$$

The fluid-fluid potential can be expressed as:

$$\mu_{ff} = \mu_{bulk} - N_A \Psi(z) \quad 2-31$$

$$\Psi(z) = 4\pi\rho_{atom} \epsilon_{fs} \sigma_{fs}^6 \left(\frac{\sigma_{fs}^6}{5x_1^{10}} - \frac{1}{2} \sum_{i=1}^4 \frac{1}{x_i^4} \right)$$

where $\Psi(z)$ is the potential model.

For non-ideal fluid,

$$\begin{aligned} \mu_{bulk} &= \mu_o + RT \ln(f_{bulk} / f_o) \\ \mu_{ff} &= \mu_o + RT \ln(f_{ff}(z) / f_o) \end{aligned} \quad 2-32$$

after rearrangement,

$$f_{ff}(z) = f_{bulk} \exp[-\Psi(z)/(kT)] \quad 2-33$$

The fugacity can be calculated by equation of state. The Peng-Robinson (PR) EOS was used to calculate the fugacity in the present work.

$$\begin{aligned} f_{bulk} &= RT / (v - b) \exp[b / (v - b) - 2a_{bulk} / (vRT)] \\ f_{ff} &= RT / [v(z) - b] \exp\{b / [v(z) - b] - 2a(z) / [v(z)RT]\} \end{aligned} \quad 2-34$$

where a_{bulk} is P-R EOS constant, $a(z)$ is evaluated from the following equation suggested by Lira [21]:

$$a(z) = a_{bulk} \left(\frac{5}{16} + \frac{6}{16} \frac{z}{\sigma_{ff}} \right) \quad \text{for} \quad 0.5 \leq \frac{z}{\sigma_{ff}} \leq 1.5$$

$$a(z) = a_{bulk} \left[1 - \frac{1}{8 \left(\frac{z}{\sigma_{ff}} - \frac{1}{2} \right)^3} \right] \text{ for } 1.5 \leq \frac{z}{\sigma_{ff}} < \infty$$

Experimental Techniques

The procedure of calculating the surface excess is to calculate the fugacity, f_{bulk} , from the equation of state of pure gas-solid isothermal adsorption is relatively straightforward. The adsorbed equilibrium is commonly determined by one of two methods. $\rho(z)$ and ρ_{bulk} can be calculated from $f_{ff}(z)$ and f_{bulk} by the PR EOS. Then the Γ^{ex} can be calculated from Equation 2-27.

determined by the weight gain on the solid. This is done

by measuring the fixed gas retention volume, V_{ret} , at various pressures.

There are two methods that can be used:

1. Constant volume method

2. Constant pressure method

For the constant volume method, the amount of adsorbate, n_{ads} , can be calculated

from the initial gas pressure, P_0 , and the final gas pressure, P_f , and the initial

and final volumes, V_0 and V_f , respectively, by using the ideal gas equation:

$n_{ads} = \frac{P_0 V_0 - P_f V_f}{RT}$

For the constant pressure method, the amount of adsorbate, n_{ads} , can be calculated

from the initial and final pressures, P_0 and P_f , and the initial and final

retention volumes, $V_{ret,0}$ and $V_{ret,f}$, respectively, by using the ideal gas equation:

$n_{ads} = \frac{P(V_{ret,f} - V_{ret,0})}{RT}$

where n_{ads}

is the amount of

adsorbate per unit

isotherm). The **EXPERIMENTAL TECHNIQUES AND APPARATUS** ental equipment and used. The amount of **Experimental Techniques** by a simple flow apparatus.

3. **By** The measurement of pure gas-solid isothermal adsorption is relatively straightforward. The adsorbed equilibrium is commonly determined by one of two are and methods: (1) the volumetric method where the pressure before and after adsorption in a closed system is measured; (2) the gravimetric method, where the amount adsorbed is determined by the weight gain on the solid in a flow system.

Measurements of mixed-gas isothermal adsorption are somewhat complicated.

There are four methods that can be used.

1. Constant-Volume Method

The pressure and composition of the gas mixture are measured before and after adsorption takes place. The amount and composition of adsorbed phase can be calculated from these data, since the total amount of gas mixture can be determined from pressure and volume, using an EOS. The experimental apparatus contains two compartments: the injection pump section and the equilibrium cell. A mixed gas of known-composition is injected from the pump to the equilibrium cell. In this method, a circulation pump is used to circulate the gas in the equilibrium cell to increase the rate of adsorption. It takes several hours to obtain the equilibrium pressure and composition. The gas composition is determined by a gas chromatograph.

2. Gravimetric Method

In the gravimetric technique, only the measurement of the total amount of adsorbate is required. The adsorbate composition can be calculated by a rigorous

thermodynamic technique suggested by van Ness [30], using the Gibbs adsorption isotherm. The van Ness method can yield tremendous savings in experimental equipment and time. The total amount of adsorbate can be measured by a simple flow apparatus.

3. Dynamic Method

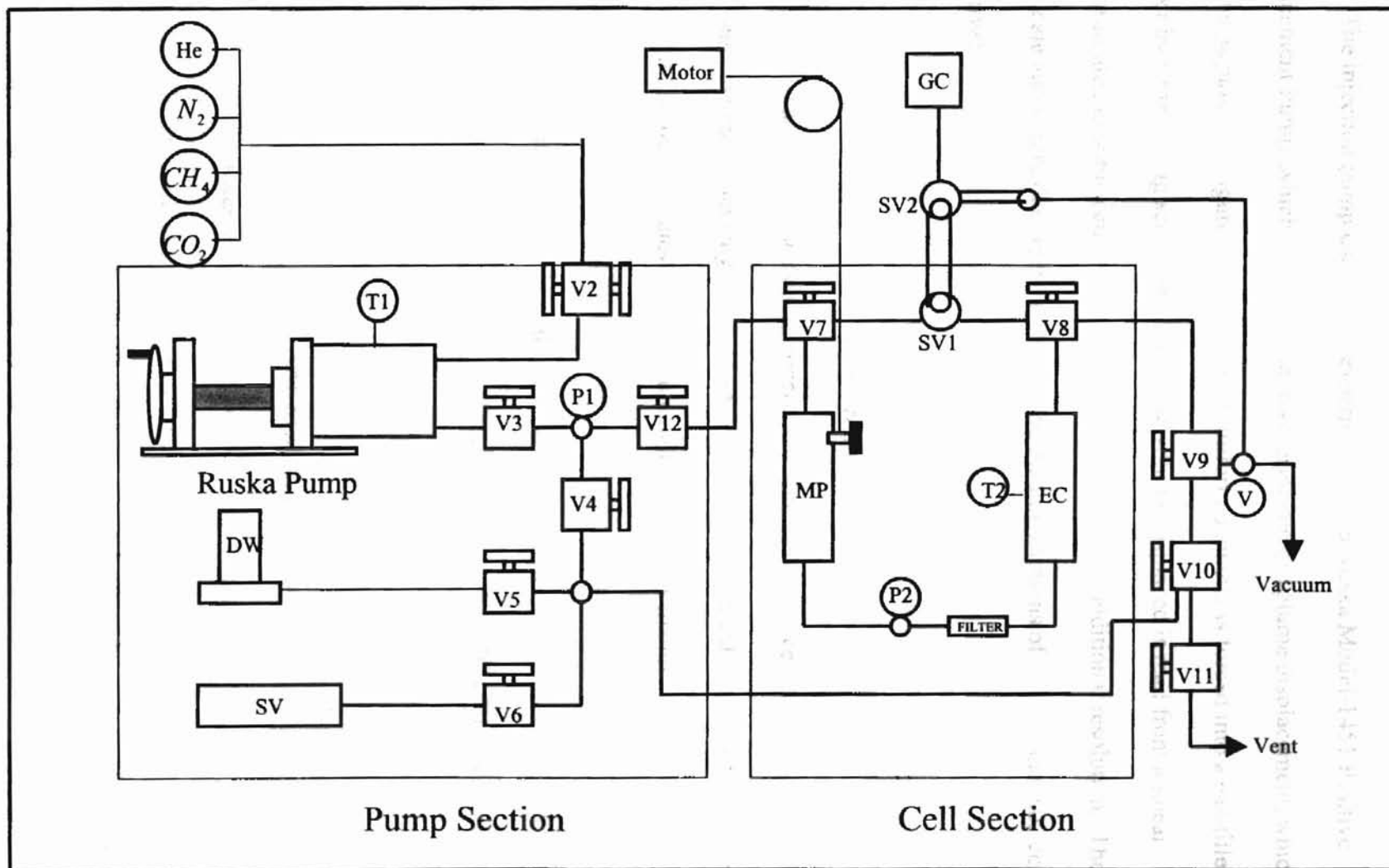
This is a flow method in which the equilibrium is attained at constant pressure and gas phase composition. Then the sample compartment is isolated and the adsorbate mixture is desorbed by evacuation or heating. The desorbed mixture is warmed to ambient temperature, and the composition is measured directly by gas chromatograph.

Experimental Apparatus

In the present work, the volumetric method is used to conduct the pure and mixture gas adsorption on the wet coal surface. The experimental apparatus, which was constructed by Hall, is composed of two compartments: pump section and cell section. The schematic diagram of the experimental apparatus is shown in the Figure 1. The pure or mixed gases to be injected are stored in the pump section, and the adsorption on the coal occurs in the cell section. The pump section consists of a positive displacement injection pump, and the cell section consists of a high-pressure vessel containing the adsorbent.

A known amount of pure or mixed gas is injected by the pump into the cell section for adsorption; the amount of remaining gas in the cell after adsorption completed is known from the P-V-T relationship. The difference of injected gas and unadsorbed gas is the amount adsorbed on the coal surface. The detailed procedure, including the governing equations, is presented in Chapter IV.

Figure 1. Schematic Graph for Experimental Apparatus



resolution of 0.1 psi on the **Positive Displacement Injection Pump** pressure measurement is estimated. The injection pump used in the experiment was a Ruska Model-1451 Positive Displacement Pump, which works on the basic principle of volume displacement, which is shown as *pump* on Figure 1. A plunger of uniform diameter is forced into a gas-filled cylinder by a measuring screw (spindle). The volume displaced is read from a linear scale calibrated in cubic centimeters. A vernier dial provides additional resolution. The linear scale and vernier dial on the pump can be read in divisions of 2.00 cc and 0.02 cc, respectively.

Equilibrium Cell

The cell section of the system consists of a high-pressure vessel capable of holding approximately seventy grams of adsorbent. The cell is a thick-walled container, two inches in diameter by eleven inches in length. The cell is manufactured by High Pressure Equipment (Model 2779) and is shown as *EC* on Figure 1.

The coal sample was held in the cell between two porous disks. These disks allow the gas to pass but contain the coal. The end space in the cell is filled with glass wool.

Pressure Measurements

Pressures are measured in combination with two digital pressure readouts and two pressure transducers calibrated to read absolute pressures from zero to 2000 psia. The pressure gage is Sensotec 450D, and the pressure transducers are Super TJE, which are shown as P1 and P2 on Figure 1. The digital pressure readings are displayed with

resolution of 0.1 psi on the readouts. The uncertainty of the pressure measurements is estimated to be 0.2 psi. The pressure transducers and digital readouts are mounted in temperature-controlled air baths to reduce the effect of variations in ambient temperature on their readings.

Temperature Measurements

The pump section and cell sections are in separate air baths. The temperatures are controlled by OMEGA CN9000A Series Miniature Autotune Microprocessor Controllers, which are shown as T1 and T2 on Figure 1. The temperature controllers maintain pump and cell temperatures within $0.1^{\circ}F$ of their set points.

Azonix Model A1011 Precision RTD Thermometer and probes are used to measure the temperatures in the pump and cell sections. The thermometer built-in microprocessor can be programmed to accept Callendar-van Dusen, IPTS-68, or ITS-90 coefficients for each of up to four probes. Two probes are used, one is on the wall of the Ruska pump plunger to measure the pump temperature, the other is on the wall of the cell to measure the cell temperature. The resolution of both temperatures is $0.002^{\circ}F$.

Cell Section

The cell is mounted inside a Despatch LFD oven, Series 1-42, with a Class-A explosion-relief rating, which is shown as *Cell Section* on the Figure 1. The adsorbing gas within the equilibrium cell is circulated by a magnetic circulation pump (Precision manufacturing, *MP*), but the pump is easy to be jammed, because the coal can come into the pump. The jam can be judged by the cell pressure reading: if the pressure readings is

up and down 0.5 psia when the pump is turned on, the pump is in good shape; if the pressure readings does not show this variation, the pump is jammed. The circulation pump can increase the rate of adsorption and mix the gas in the cell. A high-pressure filter is used to prevent coal particles from flowing out of the cell. Two valves (V7, V8) are used to isolate the cell section circulation from the pump section.

Air/Water Bath Temperature Controllers

Both air and water baths are used to maintain the temperatures of the pump and cell sections. A water bath is used to heat the Ruska pump jacket. The water is stored, heated and circulated by a HAAKE-B water bath circulator. The temperature can be controlled within 0.1°C . Air baths are used to heat the Ruska pump and the cell oven. The Ruska pump is isolated from the surroundings by a plastic cover. The air inside the cover is heated by the wire from a hair dryer and circulated by a fan. The oven is heated by a 300-watt light bulb and the air is circulated by a fan. In both air baths, OMEGA CN9000 controllers are used to maintain the temperatures at 96.6°F and 115°F , respectively. The pump temperature is controlled above the critical temperature of carbon dioxide to make sure all the fluids are in the gas phase.

Gas Mixture Sampling and Analysis

For analysis of gas mixture adsorption, the composition of the unadsorbed gas must be measured at equilibrium. Gas chromatography is used to determine the gas composition, and the gas sample is sent to the chromatograph from the equilibrium cell directly. Two valves are used to send a gas sample from the cell to the gas

chromatograph. One is the sampling valve, the other is a switching valve. Both valves are UW model Valco six-port valves, which are shown as SV1 and SV2 on Figure 1. By operating the sampling and switching valves in the correct sequence (see Hall for details [9]), the gas sample is removed from the cell to the gas chromatograph directly for analysis. The gas chromatograph is a combination of analyzer, console and interface. The analyzer is Perkin-Elmer Sigma 2 GC, which has three detector systems. Some gas parts, such as the oven temperature controller and the carrier gas flow rate controller do not work very well. In this experiment, a thermal conductivity detector was used to measure the composition of the gas mixture. The console is Perkin-Elmer Sigma 1B Console, which is shown as GC on Figure 1. This is a laboratory data system whereby keyboard directives and conversations can be used to establish the analyzer chromatographic conditions, collect and reduce data and print analysis reports. An interface is used to link the chromatograph and the console.

In the chromatograph, an Alltech Permanent Gases packed column is used. The column was filled with 20 feet of HayeSepD 100/120. It can separate light hydrocarbons, nitrogen, carbon dioxide and carbon monoxide mixtures. According to manufacturer recommendations, the column temperature was set at 60 °C, the detector temperatures for detector zone 1 and zone 2 were 140 °C. The flow rate of carrier gas was 30 cc/minute. The area sensitivity and baseline sensitivity are set at 140°C and 10°C. Prior to adsorption measurements, a series of known composition mixtures were used to calibrate the GC. For each composition, a response factor was found, and a linear relation was developed to correlate the response factor to mixture composition. (Details appear in Chapter IV).

CHAPTER IV

EXPERIMENTAL PROCEDURE

Governing Equations

The amount of pure gas adsorption on the coal surface is determined by the difference between the amount of gas injected from the positive displacement pump and the amount of unadsorbed gas remaining inside the equilibrium cell. The amount of gas remaining unadsorbed inside the cell at equilibrium is the sum of the unadsorbed gas and the gas dissolved in the water.

$$n_{ads} = n_{inj} - n_{unads} - n_{sol} \quad 4-1$$

where, n_{ads} is the number of moles gas adsorbed, n_{inj} is the number of moles gas injected from the pump, n_{unads} is the number of moles gas unadsorbed in the cell, n_{sol} is the number of moles gas dissolved in the water.

The amount of gas injected into the cell is evaluated as the product of density and volume injected. The gas density can be found from experimental data at known pressure and temperature. The volume injected is known from readings on the injection pump. The amount of unadsorbed gas is decided by the product of density and void volume in the equilibrium cell. (Density is calculated by a suitable equation of state).

$$n_{inj} = \left(\frac{P \Delta V}{zRT} \right)_{pump} \quad 4-2$$

The void volume is determined by helium injections before the experiment. (Details appear later in this chapter).

$$n_{unads} = \left(\frac{P_f V_{void}}{z_f RT} - \frac{P_i V_{void}}{z_i RT} \right)_{cell} \quad 4-3$$

P_i is the initial pressure of the cell section when the experiment starts, z_i is the compressibility factor at this pressure. The initial pressure is set at 3 psia to prevent water from evaporation. P_f is the final pressure of the cell section when the experiment ends, z_f is the compressibility factor at this pressure. Normally this pressure is set at 3.0 psia in order to avoid the water vaporization from the wet coal sample. Some of the gas will dissolve in the water. For nitrogen and methane, the amount of gas dissolved in the water is minimal. For the carbon dioxide, about 8% of the gas will be dissolved in the water. An equation is used to estimate the gas solubility in the water [9].

$$x = P / (a + bP + cP^2) \quad 4-4$$

$$n_{sol} = n_{water} x / (1 - x) \quad 4-5$$

where x is the mole fraction of gas dissolved in the water, n_{water} is the moles of water, a, b, c are the coefficients to calculate x . For different gas, they are listed in the Table 1.

TABLE 1. Parameters in Equation for Gas Solubilities in Water

	a (psia)	b	c (psia ⁻¹)
Nitrogen	1480000	127.3	0.000635
Methane	769000	150.4	0.005369
Carbon Dioxide	39840	9.452	0.00833

For mixture adsorption, the adsorption of each component should be calculated in a similar way to the pure gas adsorption. The mixture compressibility factor instead of pure component compressibility factor is used in the calculation. The injected gas is calculated by,

$$n_{inj} = z_i P \Delta V / (z_{mix} RT)_{pump} \quad 4-6$$

The unadsorbed gas is calculated by the following equation:

$$n_{unads} = y_i [(P_i V_{void})_{cell} / (z_{mixf} RT)_{cell} - (P_f V_{void})_{cell} / (z_{mixi} RT)_{cell}] \quad 4-10 \quad 4-7$$

z_{mixi} and z_{mixf} are the initial and final pressure in the cell and are calculated by the Redlich-Kwong equation of state. (Details appear in Appendix A). z_i is the gas mole composition in injected, y_i is the gas composition unadsorbed in the cell. The amount of each gas dissolved in the water can be decided by the solubility equation, but the pressure should be replaced by partial pressure $P_i = y_i P$.

$$x_i = P y_i / (a + b P y_i + c (P y_i)^2) \quad 4-8$$

$$n_{sol} = n_{total} x_i / (1 - x_i) \quad 4-9$$

The composition of unadsorbed gas is measured by gas chromatograph. Each sample (about 20 microliter) is sent to the GC for analysis.

Pressure Calibration

The pump and cell pressures are measured by Sensotec Super TJE pressure transducers. The pressure transducers are calibrated using a Ruska Dead Weight Gage Model 2470-710-00. The principle of the pressure calibration is to compare the pressure gage reading pressure with the Dead Weight Tester pressure. The Dead Weight Tester pressure is recognized as the standard pressure, which is calculated from the weights on the tester and the area of the tester piston. A series of weights can be added on the tester, different weights generating different pressures. The equation used to calculate the Dead Weight Tester pressure is listed below.

$P_{DWT} = F / A$

$$F = M_{std} \left(\frac{g_l}{g_s} \right) \left[1 - \left(\frac{\rho_{air}}{\rho_{std}} \right) \right] \quad 4-10$$

$$A = A_{ref} (1 + k\Delta t)$$

Where g_l is the local gravity, g_s is the gravity. The force is calibrated by the local gravity, and the air buoyancy is considered in this case. The area A is calibrated by the operation temperature; A_{ref} is the reference area at 23 °C. M_{std} is the mass of dead weight, k is the temperature coefficient, Δt is the difference between operation temperature and 23 °C. The gage pressure is calculated from the above equation, and atmosphere pressure P_{atm} should be added to get the absolute pressure.

$$P_{DWT} = \left[\frac{M_{std}}{A_{ref} (1 + k\Delta t)} \right] \left[\frac{g_l}{g_s} \right] \left[1 - \left(\frac{\rho_{air}}{\rho_{std}} \right) \right] + P_{atm} \quad 4-11$$

The constants are reported by Hall [9]:

$$g_l = 9.7977 m / sec^2$$

$$g_s = 9.80665 m / sec^2$$

$$\rho_{air} = 0.0012 g / cc$$

$$\rho_{std} = 9.80665 g / cc$$

$$A_{ref} = 8.40024 E - 6 m^2$$

$$k = 9.1 E - 6 / ^\circ C$$

Units of M is kg, and P is kg / m^2 .

Temperature Calibration

The temperature is controlled by the Omega Temperature Controller and is measured by Azonix Model 1011 RTD Thermometer and platinum probes. The probes

are mounted directly on the surface of the equilibrium cell and the pressure transducer to monitor the cell section temperature. The pump section temperature is measured by a thermocouple mounted to the inside of Ruska injection pump jacket surrounding the pump injection cylinder. The Azonix thermometer can calibrate the temperature by knowing parameters of the thermocouple, all the parameters of the thermocouple are reported by Hall in his thesis supplementary material [9]. Another Azonix platinum probe is mounted on the surface of the pump plunger. These two temperatures are controlled to within $0.1^{\circ}F$, which can reduce the temperature profile in the pump section.

Wet Coal Substrate

The equilibrium cell is filled with moistened, finely ground coal substrate. The coal sample is ground to $200\ \mu m$ size of particles. The coal is moistened with water content from 4 to 14 percent, which is above the equilibrium coal moisture content. The wet coal has lower adsorption capacity than the dry coal because water occupies some of the sites available for gas adsorption.

The water content in the coal sample has an impact on the character of the gas adsorption. Dry coal has higher adsorption capacity than wet coal, because the water molecules occupy some of the adsorption sites [1]. However, if the water content is greater than the equilibrium water content in the coal, it has little influence on the adsorption capacity. The equilibrium water content of the Fruitland coal is about 2.4%, as tested in the lab.

The amount of unadsorbed gas remaining in the equilibrium cell is decided by the product of density and void volume. The void volume is measured using helium before running an experiment as follows:

Pure helium is treated as being unadsorbed on the coal surface. Thus, the amount of helium injected into the cell will wholly occupy the void volume in the cell section.

$$n_{inj} = \left(\frac{P\Delta V}{zRT} \right)_{pump} \quad 4-12$$

The known amount of helium is injected into the cell section can be calculated from the pressure and temperature by the following formula:

$$n_{cell} = \left(\frac{P_f V_{void}}{z_f RT} - \frac{P_i V_{void}}{z_i RT} \right)_{cell} \quad 4-13$$

The injected helium is equal to the amount of helium in the cell section, the amount is calculated as,

$$n_{inj} = n_{cell} \quad 4-14$$

$$V_{void} = \frac{\left(\frac{P\Delta V}{zRT} \right)_{pump}}{\left(\frac{P_f}{z_f RT} - \frac{P_i}{z_i RT} \right)} \quad 4-15$$

The initial pressure is set at 3 psia to prevent water from evaporation. The Equations 4-12 and 4-13 should be equal to each other. In the void volume test, the pump pressure was maintained at 1000.5 psia. The temperatures of pump section and cell section were maintained at 96.6 °F and 115 °F , respectively.

The equilibrium cell void volume was measured at six pressure points, from 100~1000 psia. The average absolute deviation was typically 0.01-0.10 cc.

Pure Component Adsorption

After the temperature and pressure instruments are calibrated, the adsorption measurements can be started. The positive displacement pump is filled with pure gas. It takes about two hours for the gas to reach stable pressure and temperature. The pressure is maintained at 1000.5 psia, where the compressibility is relatively insensitive to changes in pressure.

The cell section is evacuated before the experiment starts. The cell section should be flushed by the test fluid to remove any impure gas, such as air. At the start of the experiment, the cell section should be evacuated above 3.0 psia to prevent water evaporation from the wet coal sample (the water-saturated vapor pressure is 3.0 psia at 115 °F). Pure gas adsorption data were measured from 100 psia to 1800 psia at 115 °F, which is the Fruitland coalbed temperature. The circulation pump was used after the gas was pumped to the cell section to accelerate the rate of adsorption on the coal surface. It takes from six to eight hours to reach the equilibrium in the cell. The equilibrium is identified when the temperature and pressure are stable for at least one hour.

The amount of gas injected to the cell section is calculated by the pump section temperature, pressure, compressibility factor and volume change. The amount of unadsorbed gas is calculated by the cell section equilibrium temperature, pressure, void volume and corresponding compressibility factor. A certain amount of pure gas is

dissolved in the water; it is deducted from the amount of gas injected into the cell section. The amount of gas dissolved in the water can be calculated by Equation 4-4.

Binary Mixture Adsorption

The measurement of mixed gas adsorption on the coal is more complicated than for pure gases, because it involves preparing known-composition mixed gases and measuring the composition of unadsorbed gas in the cell section.

Binary gases of known composition were prepared by as follows. Known volumes of two pure gases were pumped to a sample cylinder from the pump at a certain pressure, for example 1500 psia, then the sample cylinder was rotated for about eight hours for mixing. The composition can be calculated by the pump injection pressure of 1500 psia, volume and corresponding compressibility factor at 1500 psia, using an equation of state. The uncertainty of the composition is estimated to be 0.002 mole fraction. The mixture is injected into the cell section. The cell is evacuated to 3.0 psia before the experiment. It takes six to eight hours for the gas mixture to reach equilibrium on the coal surface. After equilibrium is reached, the composition of the unadsorbed remaining gas in the cell section is determined by gas chromatography.

The injected gas volume is calculated from the mixture compressibility factor and gas composition by Equation 4-6. The unadsorbed gas in the cell section is calculated from equivalent information by Equation 4-7.

Gas Chromatograph Calibration

A Perkin-Elmer Sigma 2B gas chromatograph is used to determine the binary mixture composition. The GC was calibrated to find the response factor for each mixture. For different mixtures, the GC has different retention times and response factors. The response factor is defined by the following equation.

$$R_f = (A_1 / A_2) / (y_1 / y_2) \quad 4-16$$

where A_1 / A_2 is the chromatograph area ratio, y_1 / y_2 is the known mixture composition ratio, as described above. In the test, the composition ratio is determined by response factor times the area ratio. Binary mixture samples of known composition are analyzed by the GC to find the response factor. Usually, the response factor changes slightly with composition, so a series of known-composition mixtures were used for calibration, and the relationship between composition and response factor was established in terms of composition.

In this GC calibration, 20/80, 40/60, 60/40 and 80/20 molar composition of binary mixtures were prepared. The retention times and response factors for different binary mixtures are listed in the Table 2 and Figure 2.

Gibbs/Absolute Adsorption Relation

The Gibbs adsorption is the measured adsorption divided by the dry coal mass, but it does not account for the fact that the adsorbed material has occupied part of what was the original void volume in the equilibrium. A correction is required, based on the density of the adsorbed phase. The Gibbs adsorption is related to the true absolute adsorption by the following expression [8]:

$$n_{ads}^{Gibbs} = n_{ads}^{Abs} \left[1 - \left(\frac{\rho_{gas}}{\rho_{ads}} \right) \right]$$

4-17

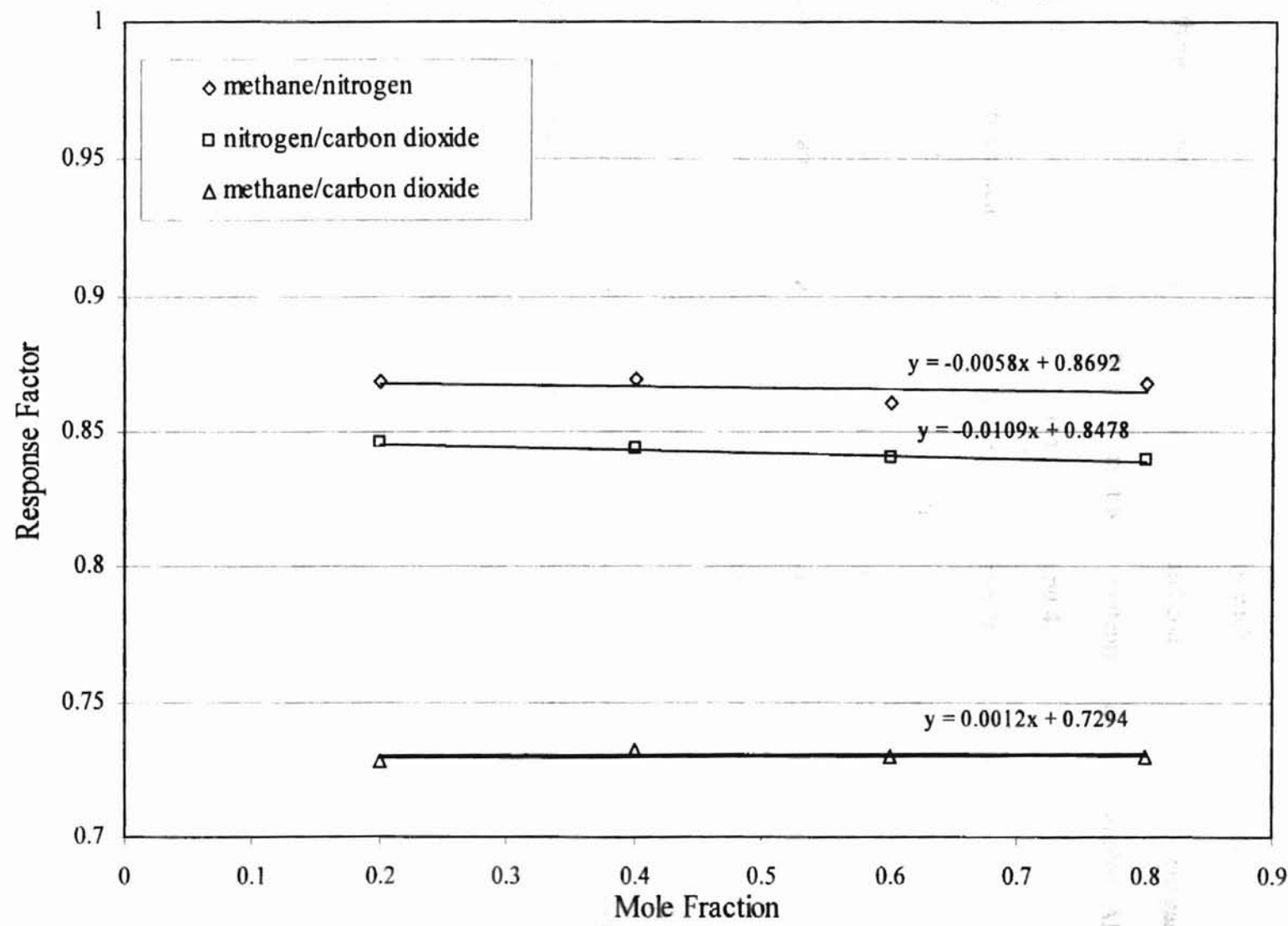
In this case, the adsorbed phase density is treated as saturated liquid. The density of adsorbed nitrogen and methane at boiling point under 1 atmosphere should be known.

The liquid densities of nitrogen, methane and at atmospheric pressure are 0.808 and 0.421, respectively. Carbon dioxide density does not have normal boiling point, its triple point density 1.18 gram/cc is used [25].

TABLE 2. Gas Chromatograph Response Factor and Retention Time (Minute)

Composition	CH_4 / CO_2			N_2 / CH_4			N_2 / CO_2		
	Retention time			Retention time			Retention time		
	CH_4	CO_2	R_f	N_2	CH_4	R_f	N_2	CO_2	R_f
19.5/79.5	4.60	9.10	0.728	2.65	4.55	0.868	2.70	9.20	0.845
40.2/59.8	4.60	9.10	0.732	2.65	4.55	0.869	2.70	9.20	0.843
59.2/40.8	4.60	9.10	0.730	2.65	4.55	0.861	2.70	9.20	0.840
80.4/19.6	4.60	9.10	0.729	2.65	4.55	0.867	2.70	9.20	0.839

Figure 2. Response Factor of Gas Chromatograph



CHAPTER V

DATA PRESENTATION AND DISCUSSION

Pure Component Adsorption on Fruitland Coal

Three replicate experiments were conducted for each of the pure gas nitrogen, methane and carbon dioxide adsorption on wet Fruitland coal at $115^{\circ}F$. Each pure gas adsorption data was measured at three different water contents on the coal samples. All the data are shown in the Tables 3 to 5 and Figures 3 and 4.

The pure methane adsorption amount ranges from 0.20 to 0.86 mmole/g coal at pressures from 100 psia to 1800 psia, where 1 mmole/g coal is equal to 759.4 SCF/ton coal. Figure 3 shows that the methane adsorption on the coal exhibits type-I adsorption based on the Langmuir model. Water content in the coal sample does not have strong impact on the amount of adsorption if it is over moisture equilibrium, which is about 2.4%, as measured in the lab. The amount of methane dissolved in the water is trivial.

The pure replicated nitrogen adsorption amount ranges from 0.05 to 0.40 mmole/g coal at pressures from 100 psia to 1800 psia. The result shows that the nitrogen adsorption on the coal exhibits type-I adsorption. The amount of nitrogen gas dissolved in the water in the coal sample is trivial.

The pure carbon dioxide adsorption amount ranges from 0.5 to 2.1 mmole/g coal at pressures from 100 psia to 1800 psia. The carbon dioxide adsorption on the coal can be explained as type-I adsorption from 100 psia to 1200 psia, but at higher pressures, the adsorption amount increases very fast, which looks like type IV adsorption character. The adsorption result is shown in Figure 4. Water content in the coal sample is more important in the carbon dioxide adsorption. About 8% carbon dioxide dissolves in the

water. For the adsorption amount, carbon dioxide has the highest adsorption on the coal, nitrogen is the lowest.

TABLE 3. Pure Methane Adsorption on Wet Fruitland Coal at 115 °F

Run 1 (9.7% Moisture)		Run 2 (8.3% Moisture)		Run 3 (7.6% Moisture)	
Pressure (psia)	Adsorption (mmole/g coal)	Pressure (psia)	Adsorption (mmole/g coal)	Pressure (psia)	Adsorption (mmole/g coal)
112.1	0.2377	102.6	0.1942	106.9	0.2018
208.1	0.3427	208.1	0.3169	209.1	0.3213
395.1	0.4780	398.9	0.4650	403.7	0.4645
607.2	0.5855	608.0	0.5771	602.0	0.5674
805.0	0.6590	808.0	0.6547	804.1	0.6462
1008.2	0.7188	1004.8	0.7160	1006.4	0.7085
1214.8	0.7431	1207.0	0.7538	1207.9	0.7504
1404.9	0.7859	1407.3	0.7931	1405.9	0.7971
1602.8	0.8274	1605.7	0.8325	1601.8	0.8317
1801.8	0.8703	1802.3	0.8676	1800.4	0.8710

* 1 mmole/g coal=759.4 SCF/ton.

TABLE 4. Pure Nitrogen Adsorption on Wet Fruitland Coal at 115 °F

Run 1 (10.2% Moisture)		Run 2 (9.9% Moisture)		Run 3 (6.2% Moisture)	
Pressure (psia)	Adsorption (mmole/g coal)	Pressure (psia)	Adsorption (mmole/g coal)	Pressure (psia)	Adsorption (mmole/g coal)
107.8	0.0489	105.6	0.0522	102.6	0.0470
210.6	0.0939	206.7	0.0902	201.9	0.0850
403.7	0.1487	402.5	0.1511	399.5	0.1495
602.5	0.2000	616.5	0.2050	603.3	0.2043
805.9	0.2498	804.9	0.2447	802.8	0.2511
1007.9	0.2812	1008.5	0.2848	1002.4	0.2912
1207.9	0.3155	1204.4	0.3167	1203.0	0.3215
1405.9	0.3419	1406.7	0.3527	1402.5	0.3516
1607.6	0.3640	1607.8	0.3817	1601.1	0.3800
1805.0	0.3934	1801.8	0.4041	1799.9	0.4002

TABLE 5. Pure Carbon Dioxide Adsorption on Wet Fruitland Coal at 115 °F

Run 1 (9.0% Moisture)		Run 2 (6.3 % Moisture)		Run 3 (5.1% Moisture)	
Pressure (psia)	Adsorption (mmole/g coal)	Pressure (psia)	Adsorption (mmole/g coal)	Pressure (psia)	Adsorption (mmole/g coal)
104.7	0.5162	105.2	0.5105	102.1	0.4702
209.4	0.7096	200.5	0.6810	210.7	0.7065
401.2	0.9430	399.2	0.9318	407.5	0.9452
611.3	1.0723	602.9	1.0739	601.2	1.0617
796.6	1.1583	803.5	1.1773	802.3	1.1819
1005.1	1.2163	1007.0	1.2539	1000.0	1.2669
1203.6	1.2373	1201.6	1.3524	1203.1	1.3059
1385.2	1.3177	1383.5	1.5372	1396.3	1.5809
1487.8	1.5744	1547.8	1.7943	1559.6	1.8792
1789.0	1.6498	1772.3	1.8952	1781.8	1.9014

Pure Component Adsorption on Illinois-6 Coal

Pure nitrogen and methane adsorption on wet Illinois-6 coal was also measured.

Two replicated experimental runs were made for each gas. The results are shown in Tables 6 and 7 and Figure 5.

The pure methane adsorption ranges from 0.08 to 0.46 mmole/g coal at pressures from 100 psia to 1800 psia. The methane adsorption on the coal can be explained as type-I adsorption from 100 psia to 1800 psia. The pure nitrogen adsorption ranges from 0.02 to 0.20 mmole/g coal at pressures from 100 psia to 1800 psia. The result shows that the nitrogen adsorption on the coal is type-I adsorption.

Both methane and nitrogen adsorption on wet Illinois-6 are about half of that adsorbed on wet Fruitland coal at the same conditions.

Figure 3. Gas Adsorption on Wet Fruitland Coal at 115 °F

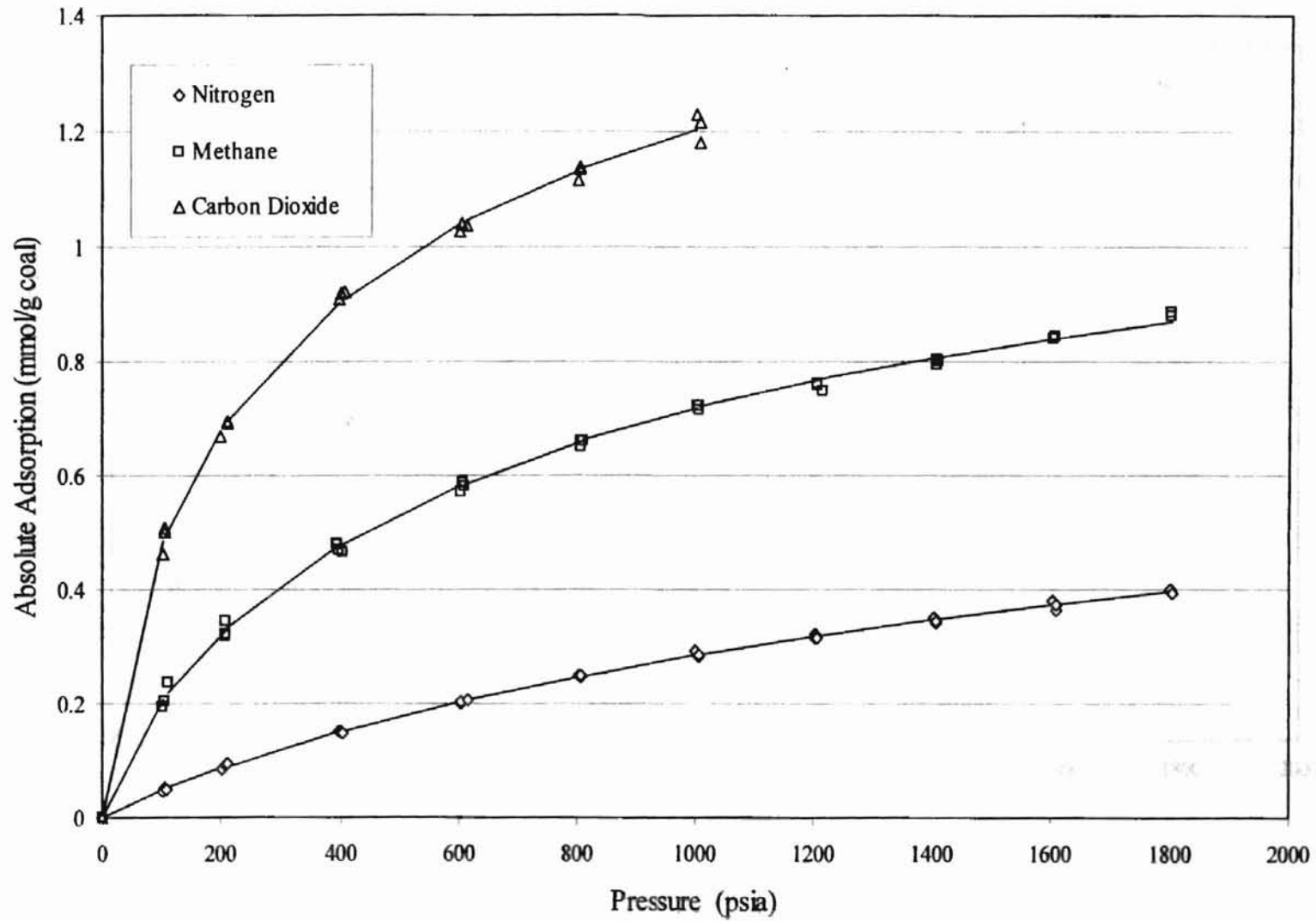


Figure 4. Pure Carbon Dioxide Adsorption on Wet Fruitland Coal at 115 °F

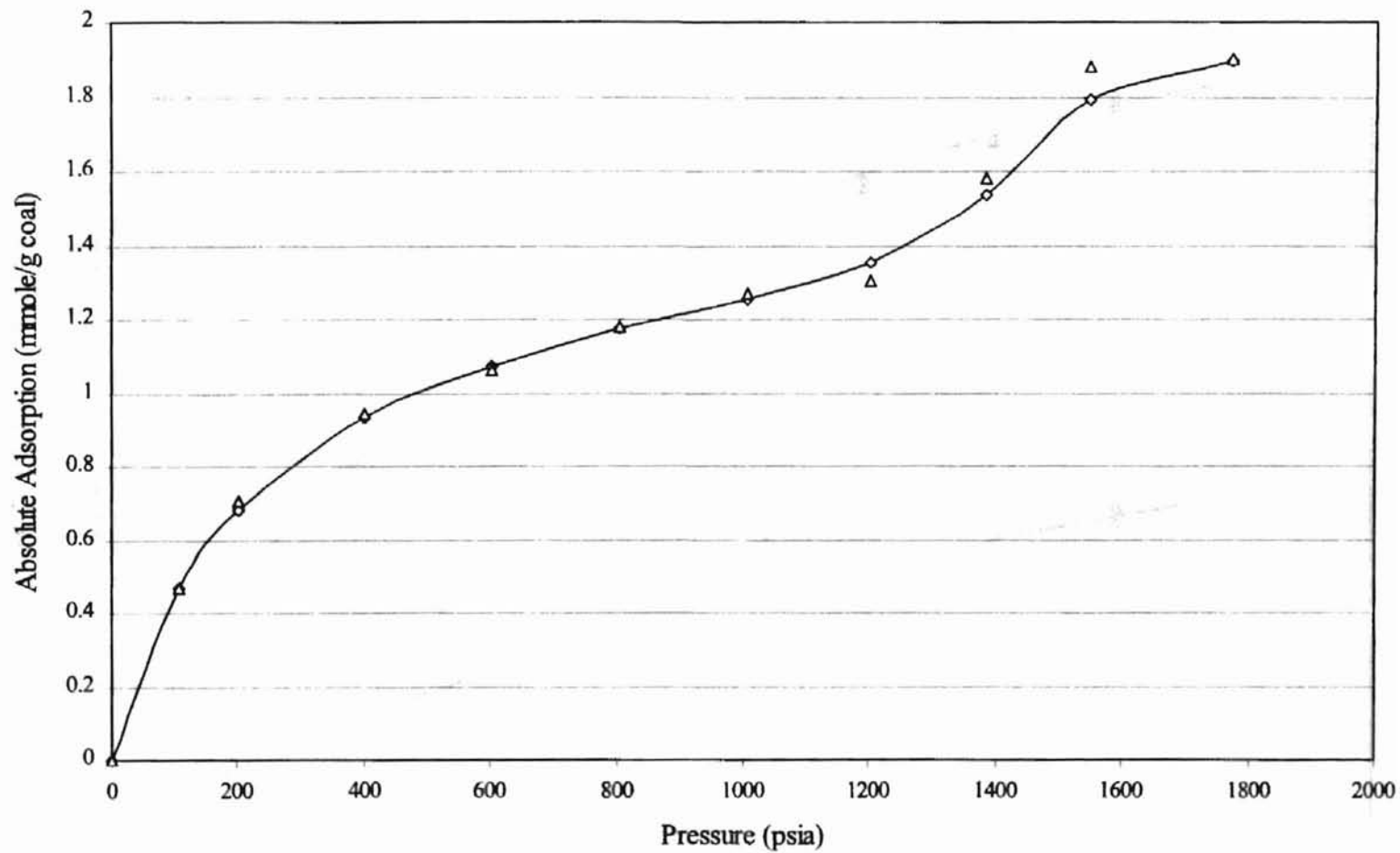


Figure 5. Gas Adsorption on Wet Illinois-6 Coal at 115 °F

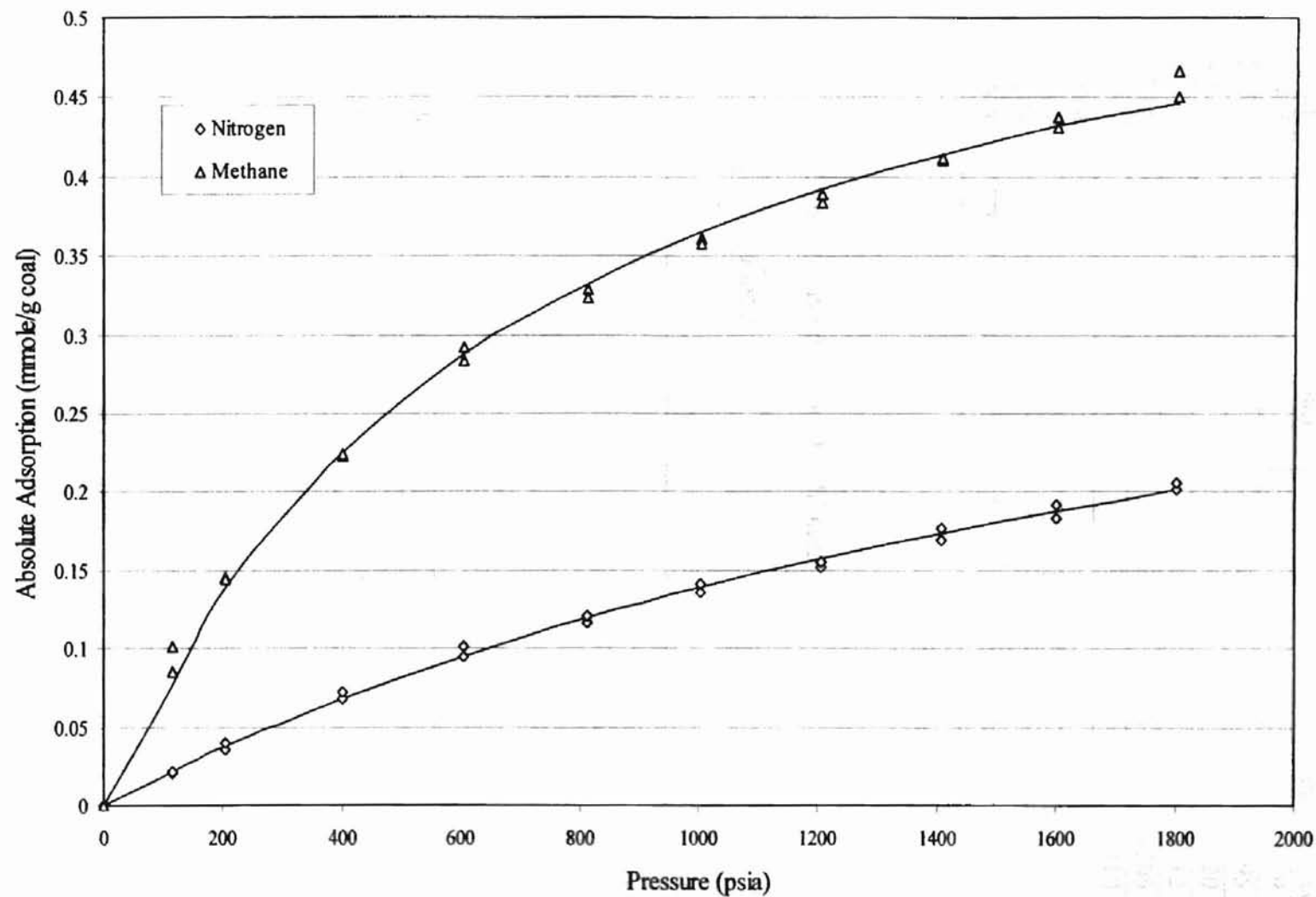


TABLE 6. Pure Nitrogen Adsorption on Wet Illinois-6 Coal at 115 °F

Run 1 (15.6% Moisture)		Run 2 (14.6% Moisture)	
Pressure (psia)	Adsorption (mmole/g coal)	Pressure (psia)	Adsorption (mmole/g coal)
114.5	0.0209	99.9	0.0219
203.8	0.0351	202.9	0.0395
401.5	0.0681	403.6	0.0720
603.9	0.0943	625.5	0.1012
810.8	0.1168	803.6	0.1206
1003.7	0.1362	996.3	0.1410
1204.4	0.1518	1199.7	0.1552
1405.5	0.1687	1405.7	0.1769
1600.5	0.1837	1600.1	0.1918
1801.1	0.2010	1799.0	0.2062

TABLE 7. Pure Methane Adsorption on Wet Illinois-6 Coal at 115 °F

Run 1 (13.6% Moisture)		Run 2 (12.6% Moisture)	
Pressure (psia)	Adsorption (mmole/g coal)	Pressure (psia)	Adsorption (mmole/g coal)
99.8	0.0852	98.3	0.1010
204.4	0.1455	202.6	0.1445
395.8	0.2226	398.8	0.2237
604.5	0.2836	604.2	0.2923
801.8	0.3287	806.5	0.3237
1001.8	0.3611	1004.0	0.3574
1206.0	0.3836	1207.2	0.3893
1371.5	0.4104	1401.9	0.4114
1600.9	0.4378	1601.7	0.4314
1807.9	0.4662	1798.7	0.4508

Binary Mixture Adsorption Data

Binary adsorption of methane, nitrogen and carbon dioxide at a series of compositions has been measured on the wet Fruitland coal at $115^{\circ}F$. For each mixture, the nominal compositions were 20%/80%, 40%/60%, 60%/40%, 80%/20%. The actual gas compositions are shown in Appendix E. The experiments were conducted at pressures from 100 psia to 1800 psia. The experimental data are listed in the Tables 8 to 10 and Figures 6 to 14.

Methane and carbon dioxide binary mixture adsorption results are shown on Figures 6 to 8. For the pure gas adsorption, carbon dioxide has higher adsorption than methane. In the binary mixture, carbon dioxide is more strongly adsorbed than methane. At the composition of methane/carbon dioxide of 80%/20%, methane has more absolute adsorption than carbon dioxide. At the compositions of methane/carbon dioxide of 60%/40%, 40%/60%, 20%/80%, the absolute carbon dioxide adsorption is higher than methane adsorption. As the composition of carbon dioxide goes up, the absolute carbon dioxide adsorption increases, the absolute methane adsorption decreases. The total absolute adsorption increases when more carbon dioxide is in the mixtures. The total adsorption is above the absolute adsorption amount of pure methane, but less than the absolute adsorption of pure carbon dioxide.

Similar to the pure methane adsorption, the absolute adsorption amount of methane in the methane/carbon dioxide binary mixture can be described by the Langmuir model. Unlike pure carbon dioxide adsorption, which has a sharp rise above 1200 psia, the carbon dioxide adsorption in the binary mixture does not show such behavior, actually, it can be fit by Langmuir model.

Figure 6. Methane/Carbon Dioxide Binary Mixture Adsorption on Wet Fruitland Coal at 115 °F: Methane

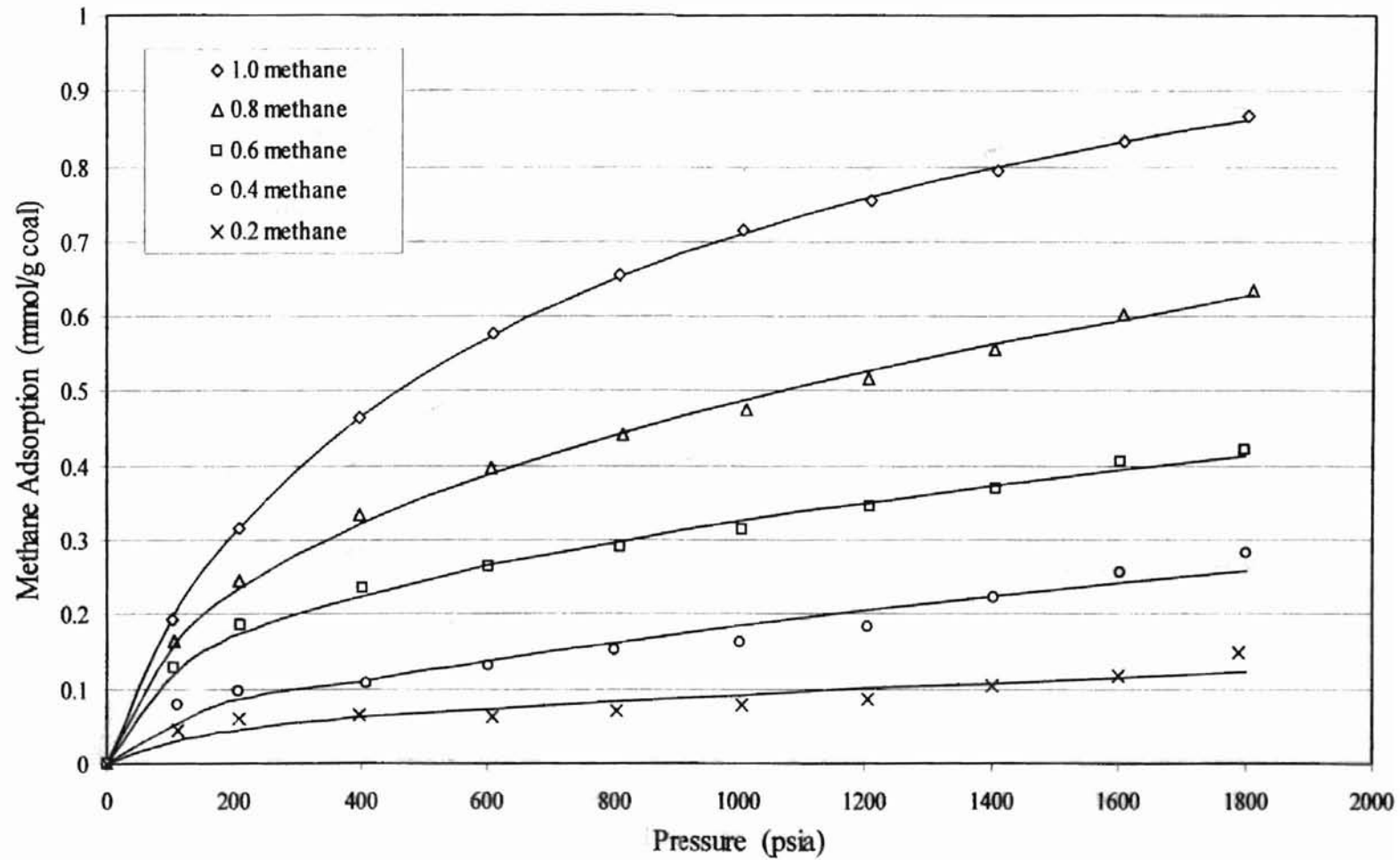


Figure 7. Methane/Carbon Dioxide Binary Mixture Adsorption on Wet Fruitland Coal at 115 °F: Carbon Dioxide

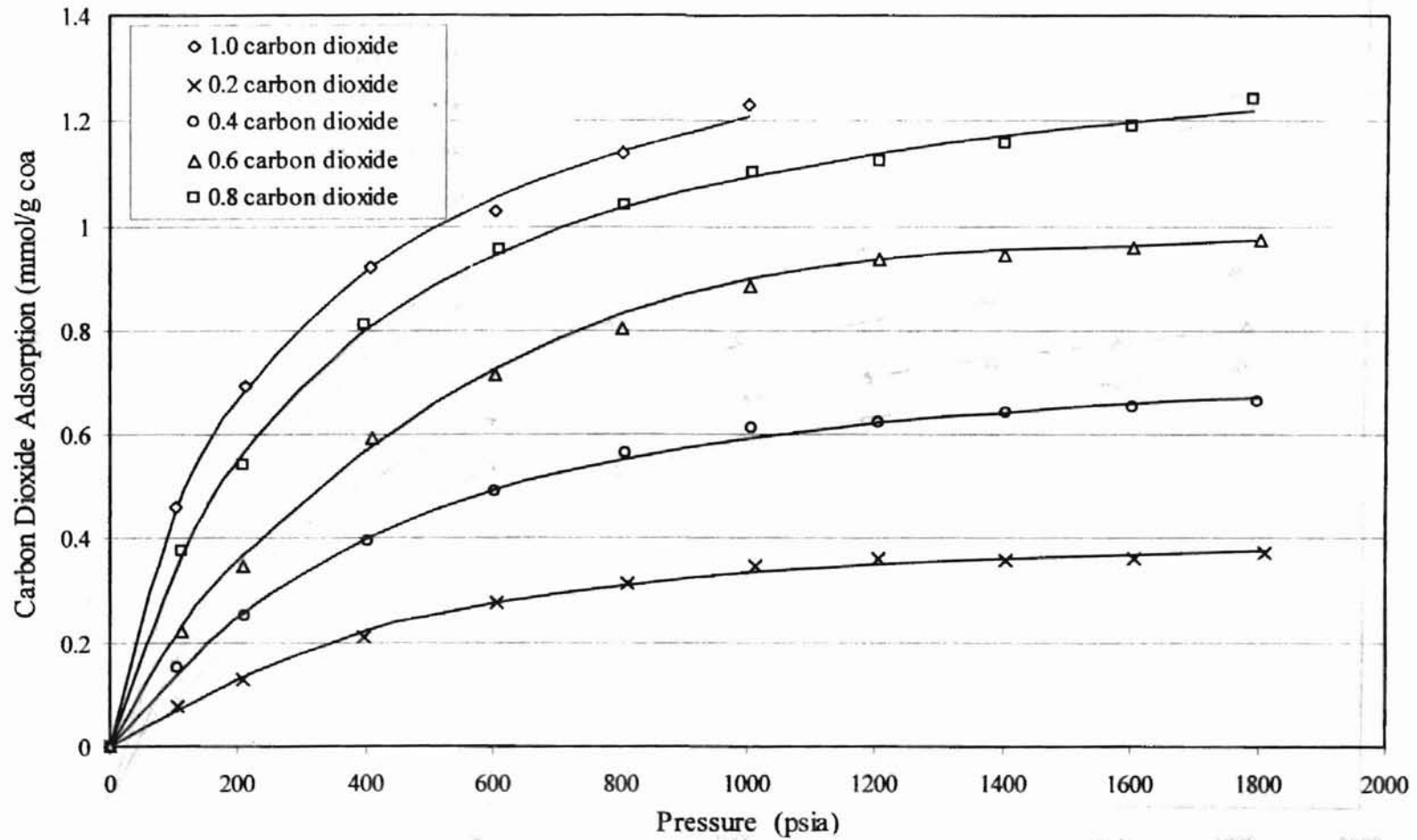
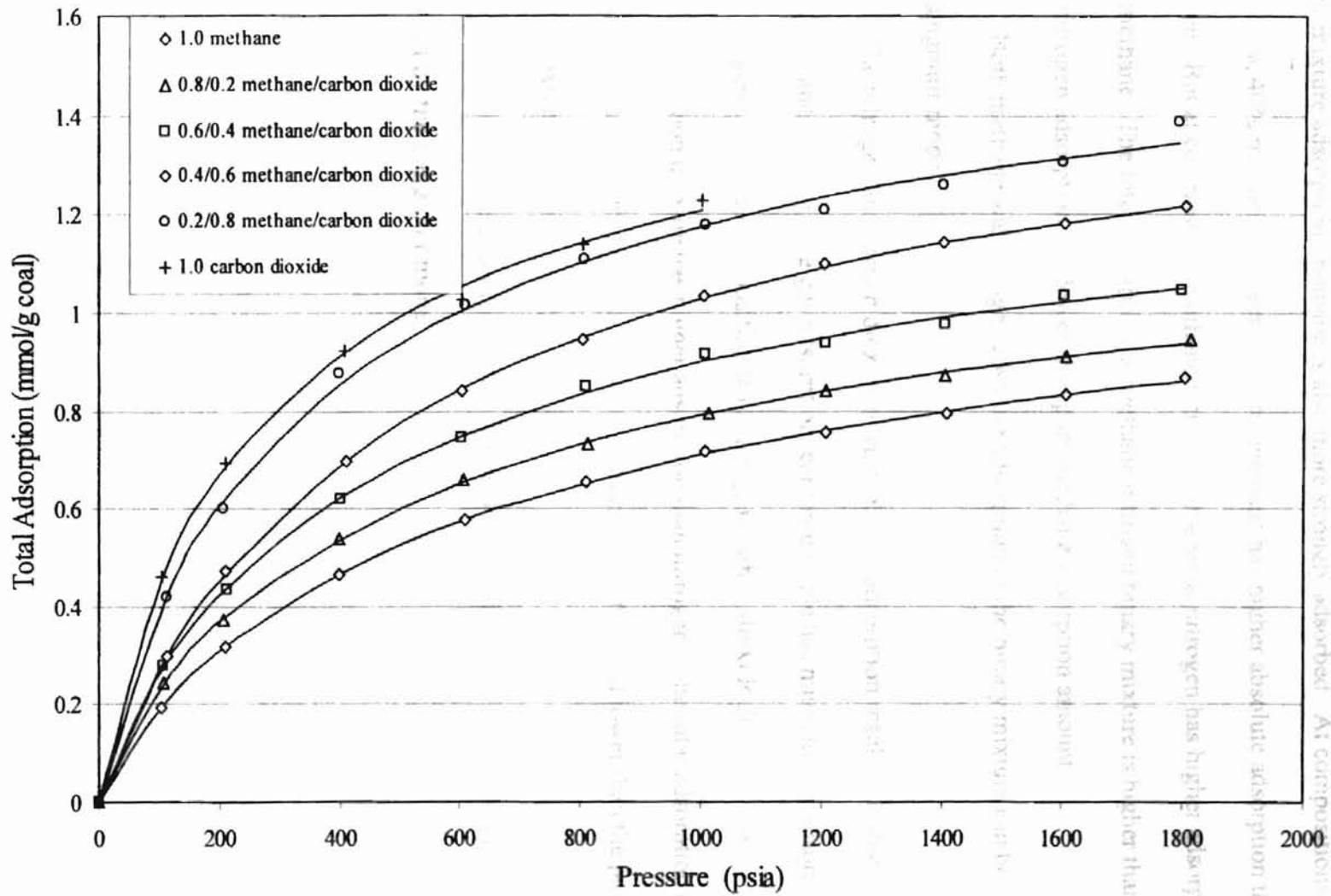


Figure 8. Methane/Carbon Dioxide Binary Mixture Adsorption on Wet Fruitland Coal at 115 °F: Total



The methane and nitrogen binary mixture adsorption results are shown on Figures 9 to 11. Pure methane has higher adsorption than pure nitrogen. In the methane/nitrogen binary mixture adsorption, methane is also more strongly adsorbed. At compositions of 80%, 60%, 40% methane/nitrogen mixture, methane has higher absolute adsorption than nitrogen. But at composition methane/nitrogen 20%/80%, nitrogen has higher adsorption than methane. The total adsorption of methane/nitrogen binary mixture is higher than the pure nitrogen adsorption and lower than pure methane adsorption amount.

Both methane and nitrogen absolute adsorption in the binary mixture can be fit by the Langmuir model.

The nitrogen and carbon dioxide binary mixture adsorption results are shown on Figures 12 and 13. For pure gas adsorption, carbon dioxide has much higher adsorption than nitrogen. With the composition from nitrogen/carbon dioxide 20%/80% to 80%/20%, carbon dioxide has higher adsorption than nitrogen. The total adsorption of this binary mixture is higher than the pure nitrogen adsorption and lower than the pure carbon dioxide adsorption.

Both the nitrogen adsorption and carbon dioxide adsorption in the binary mixture can be fit by the Langmuir model.

Figure 9. Methane/Nitrogen Binary Mixture Adsorption on Wet Fruitland Coal at 115 °F: Methane

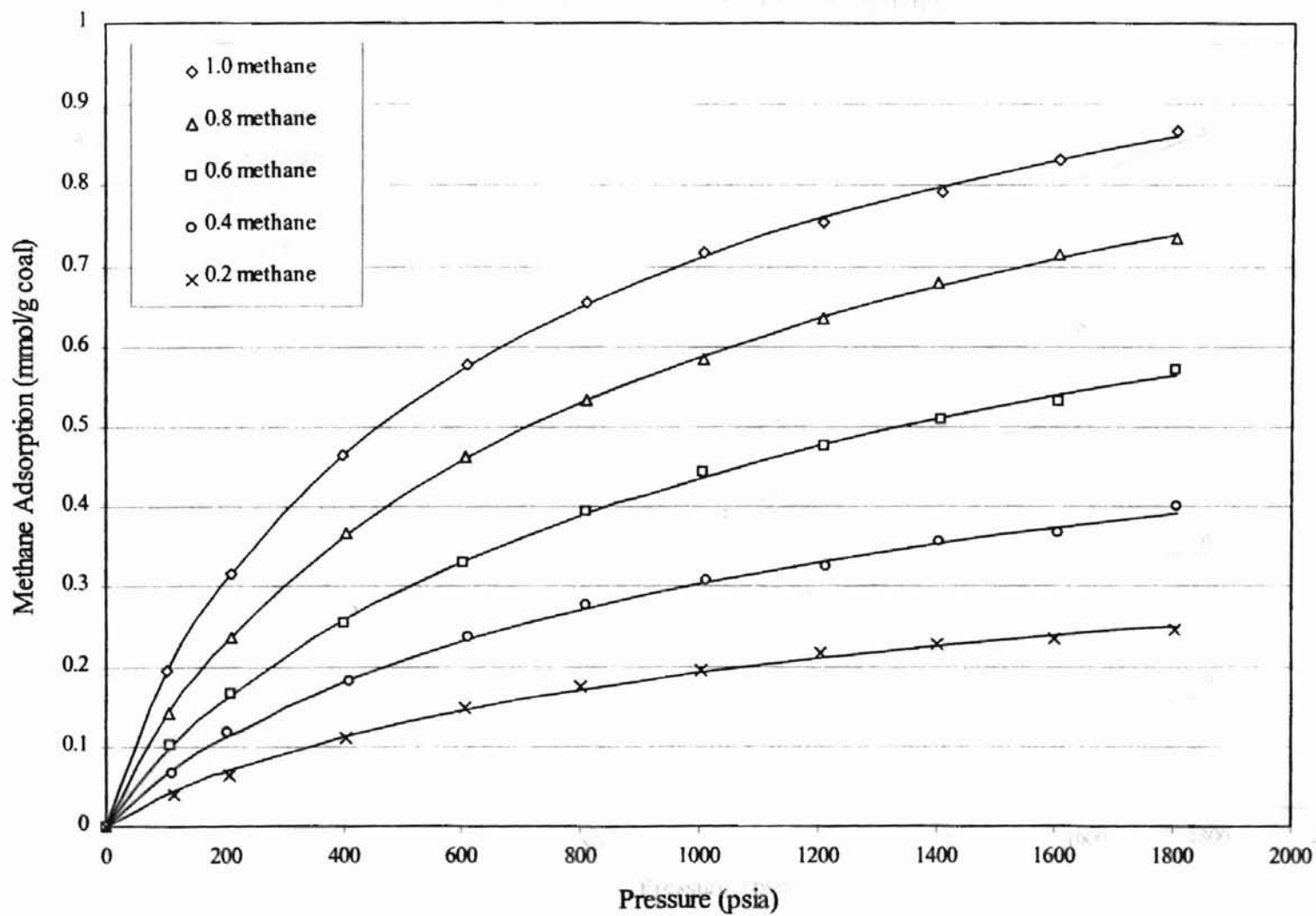


Figure 10. Methane/Nitrogen Binary Mixture Adsorption on Wet Fruitland Coal at 115 °F: Nitrogen

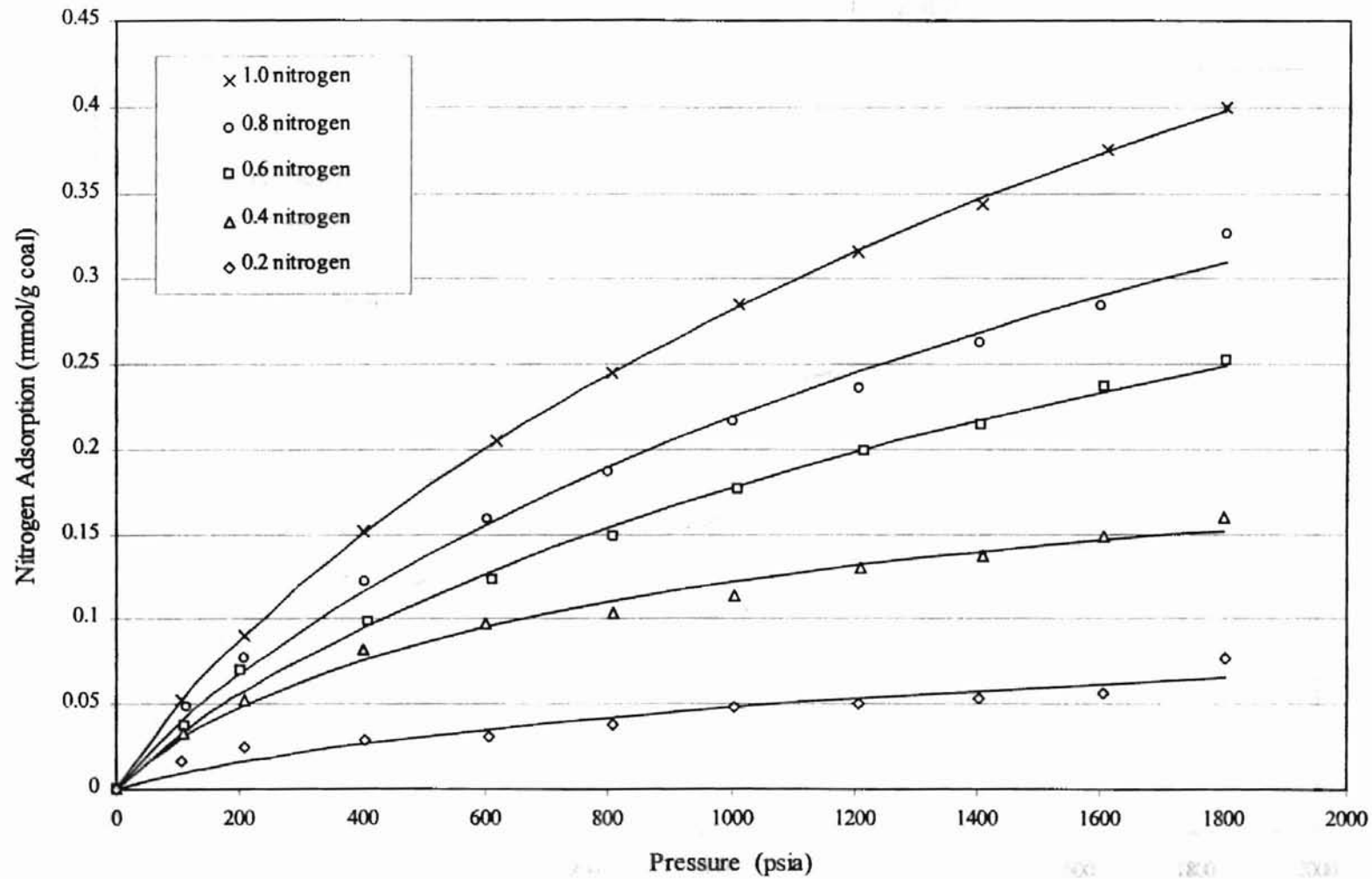


Figure 11. Methane/Nitrogen Binary Mixture Adsorption on Wet Fruitland Coal at 115 °F: Total

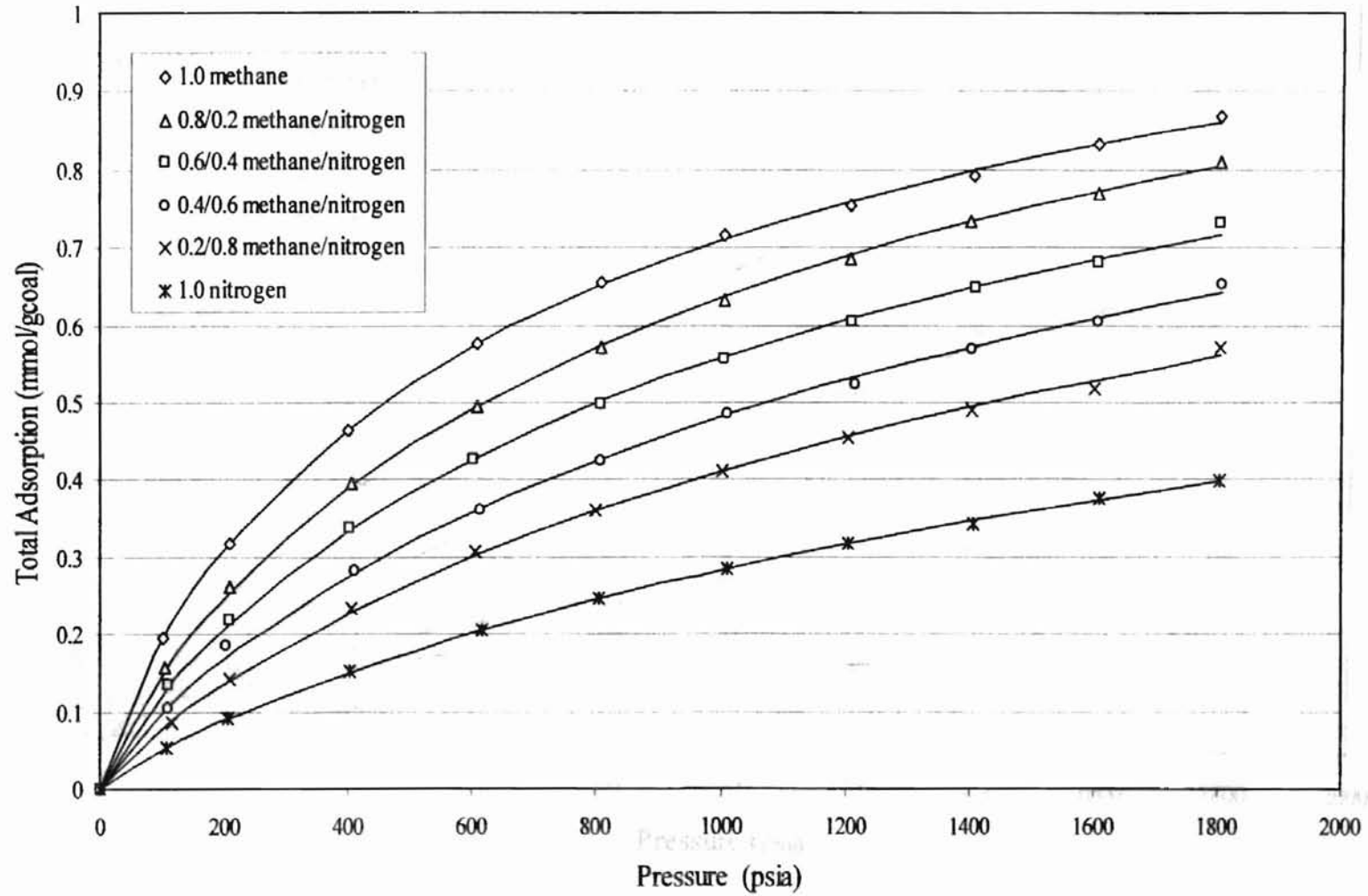


Figure 12. Nitrogen/Carbon Dioxide Binary Mixture Adsorption on Wet Fruitland Coal at 115 °F: Nitrogen

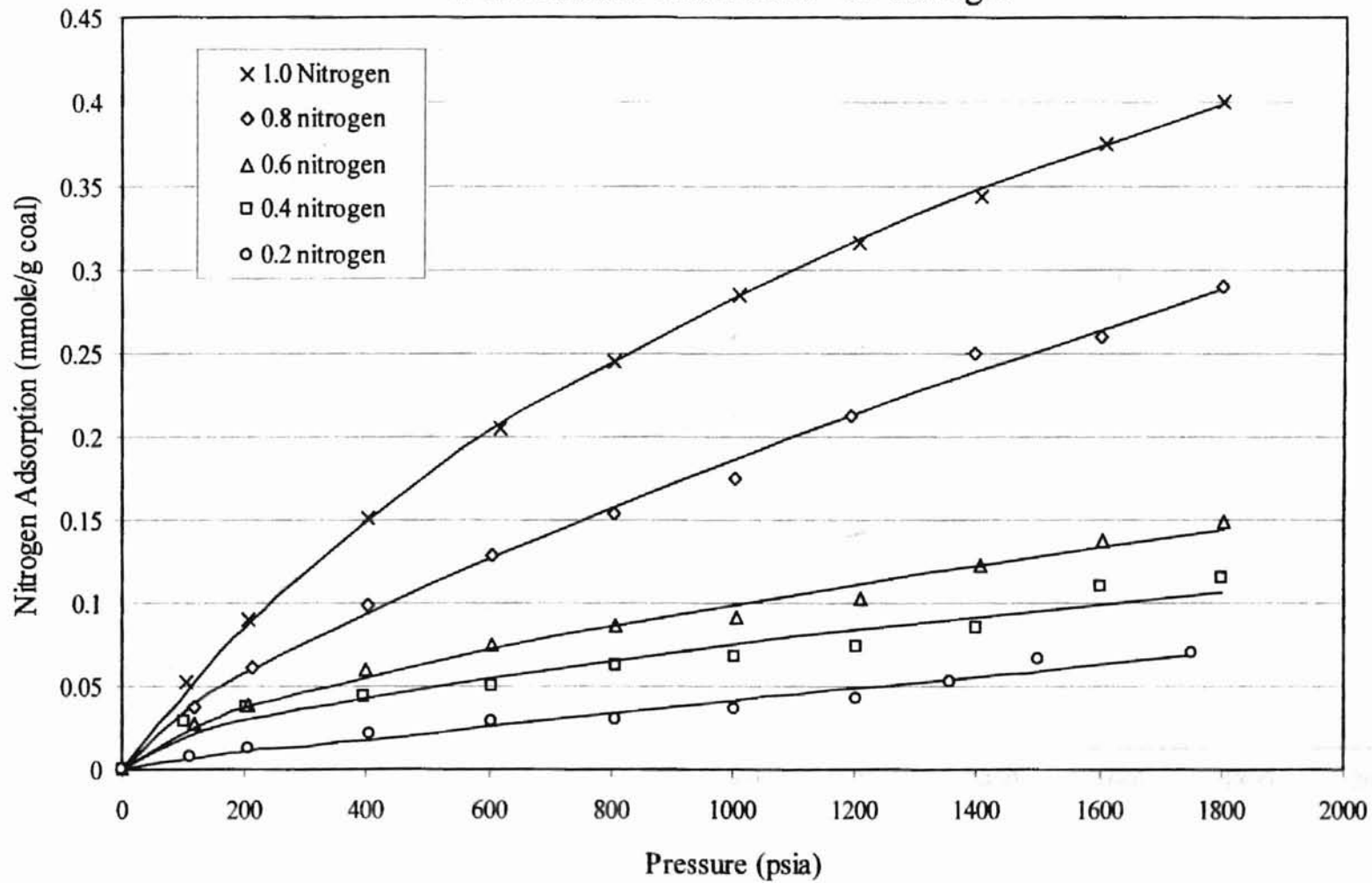


Figure 13. Nitrogen/Carbon Dioxide Binary Mixture Adsorption on Wet Fruitland Coal at 115 °F: Carbon Dioxide

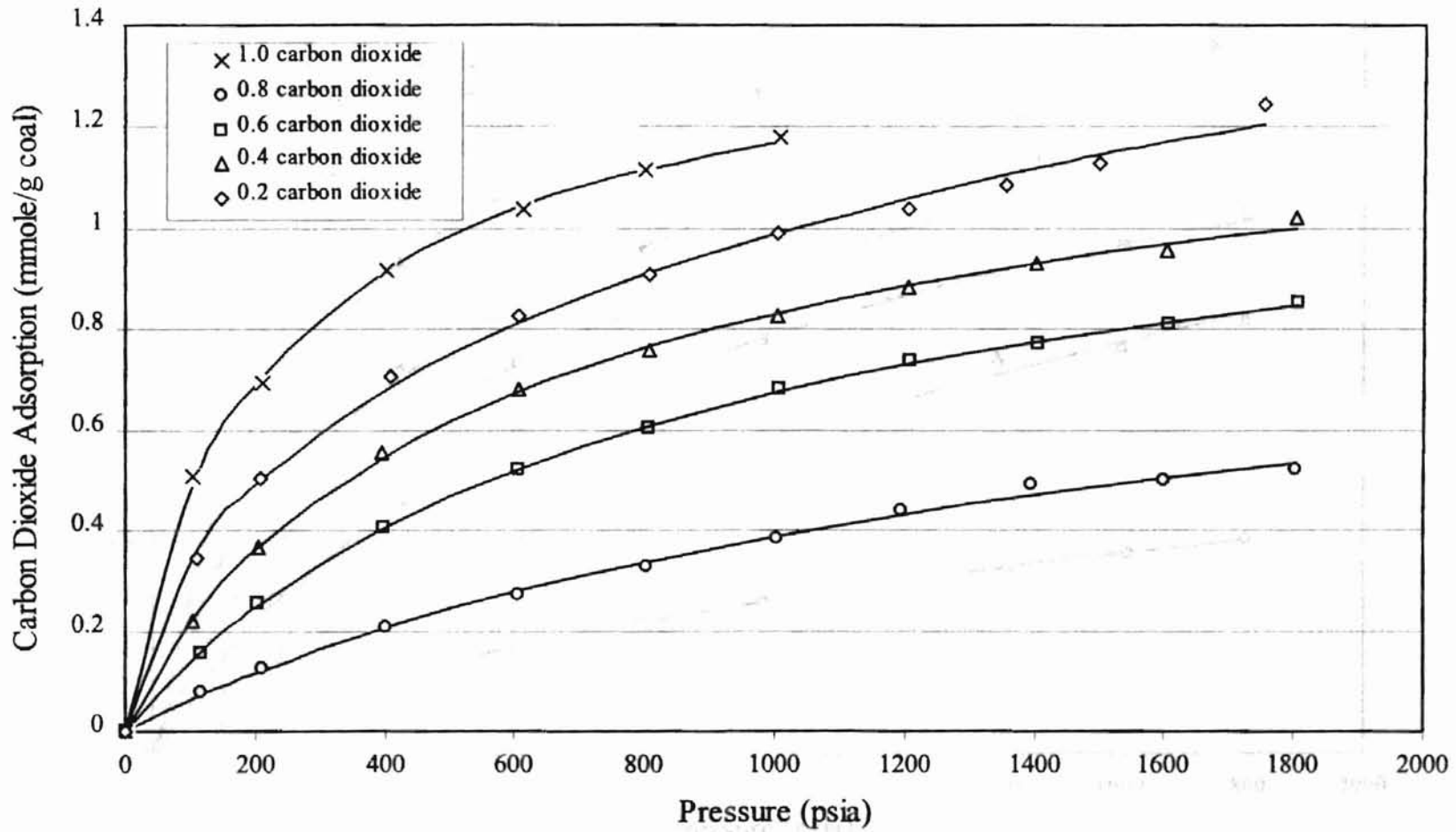


Figure 14. Nitrogen/Carbon Dioxide Binary Mixture Adsorption on Wet Fruitland Coal at 115 °F: Total

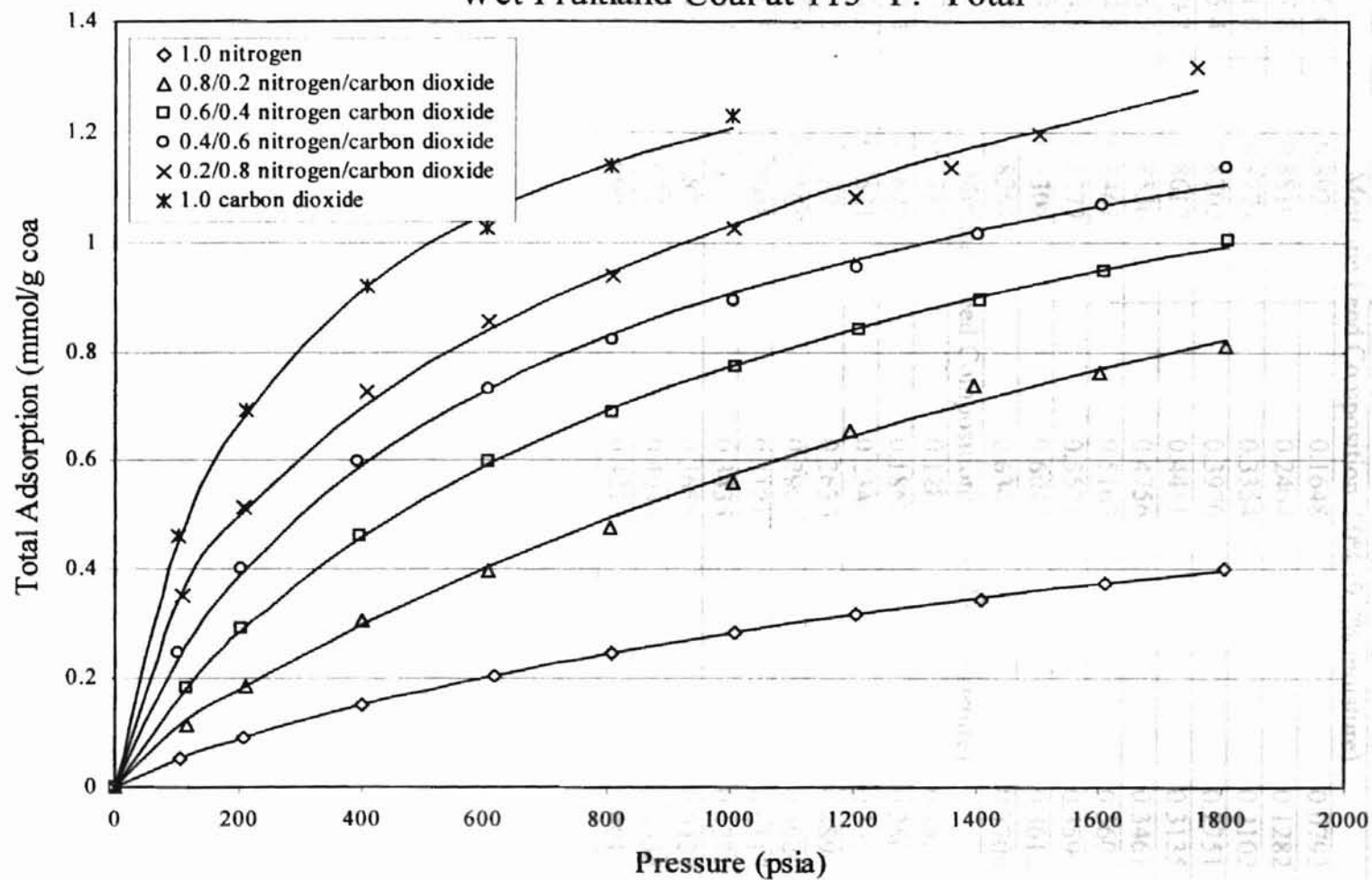


TABLE 5. Nitrogen/Carbon Dioxide Mixture Adsorption on Wet Fruitland Coal at 115 °F

TABLE 8. Methane/Carbon Dioxide Mixture Adsorption on Wet Fruitland
Coal at 115°F (continued)

Pressure (psia)	Methane Gas Mole Fraction	Absolute Methane Adsorption (mmole/g coal)	Absolute Carbon Dioxide Adsorption (mmole/g coal)
Methane Feed Composition: 80% (9.7% moisture)			
105.0	0.8921	0.1648	0.0792
207.8	0.8810	0.2464	0.1282
401.0	0.8774	0.3354	0.2102
605.4	0.8702	0.3970	0.2751
810.2	0.8612	0.4411	0.3135
1008.5	0.8536	0.4756	0.3461
1204.8	0.8461	0.5163	0.3601
1404.3	0.8377	0.5571	0.3590
1603.2	0.8302	0.6042	0.3612
1805.8	0.8261	0.6347	0.3709
Methane Feed Composition: 60% (9.6% moisture)			
107.6	0.7787	0.1283	0.1526
209.4	0.7625	0.1860	0.2502
403.5	0.7521	0.2340	0.3927
602.2	0.7323	0.2636	0.4896
807.9	0.7165	0.2901	0.5620
1005.5	0.7048	0.3121	0.6117
1206.8	0.6921	0.3435	0.6231
1404.9	0.6831	0.3685	0.6427
1605.3	0.6731	0.4040	0.6535
1801.0	0.6662	0.4210	0.6617

TABLE 8. Methane/Carbon Dioxide Mixture Adsorption on Wet Fruitland Coal at 115 °F (Continued)

Pressure (psia)	Methane Gas Mole Fraction	Absolute Methane Adsorption (mmole/g coal)	Absolute Carbon Dioxide Adsorption (mmole/g coal)
Methane Feed Composition: 40% (9.2% moisture)			
111.4	0.5916	0.0774	0.2204
208.2	0.5850	0.0957	0.3466
410.2	0.5826	0.1065	0.5935
602.7	0.5512	0.1313	0.7152
802.1	0.5288	0.1508	0.8039
1002.8	0.5148	0.1623	0.8851
1203.8	0.5009	0.1833	0.9351
1402.2	0.4865	0.2224	0.9439
1601.5	0.4768	0.2555	0.9572
1801.6	0.4700	0.2822	0.9721
Methane Feed Composition: 20% (7.6 % moisture)			
112.0	0.3318	0.0445	0.3744
207.7	0.3089	0.0586	0.5422
398.2	0.2950	0.0651	0.8094
608.6	0.2764	0.0619	0.9535
804.8	0.2607	0.0688	1.0383
1006.1	0.2486	0.0764	1.1001
1203.8	0.2386	0.0854	1.1250
1400.0	0.2308	0.1020	1.1566
1600.3	0.2253	0.1143	1.1911
1790.0	0.2202	0.1477	1.2403

TABLE 9. Methane/Nitrogen Mixture Adsorption on Wet Fruitland Coal at 115 °F

Pressure (psia)	Methane Gas Mole Fraction	Absolute Methane Adsorption (mmole/g coal)	Absolute Nitrogen Adsorption (mmole/g coal)
Methane Feed Composition: 80% (8.5% moisture)			
105.1	0.7424	0.1411	0.0164
208.8	0.7483	0.2363	0.0249
405.3	0.7525	0.3664	0.0287
606.2	0.7577	0.4633	0.0311
808.2	0.7640	0.5331	0.0379
1005.2	0.7697	0.5836	0.0480
1205.8	0.7720	0.6358	0.0499
1402.0	0.7742	0.6792	0.0534
1605.2	0.7762	0.7135	0.0564
1803.2	0.7802	0.7336	0.0768
Methane Feed Composition: 60% (8.7% moisture)			
108.8	0.5442	0.1010	0.0333
208.1	0.5535	0.1654	0.0525
402.2	0.5639	0.2547	0.0820
601.5	0.5678	0.3298	0.0973
808.1	0.5699	0.3943	0.1036
1004.5	0.5728	0.4423	0.1136
1209.3	0.5780	0.4752	0.1299
1408.0	0.5810	0.5092	0.1377
1605.1	0.5835	0.5311	0.1487
1801.8	0.5848	0.5705	0.1594

Oklahoma State University Library

TABLE 9. Methane/Nitrogen Mixture Adsorption on Wet Fruitland Coal at 115 °F₃₁
(Continued)

Pressure (psia)	Methane Gas Mole Fraction	Absolute Methane Adsorption (mmole/g coal)	Absolute Nitrogen Adsorption (mmole/g coal)
Methane Feed Composition: 40% (9.4% moisture)			
109.7	0.3326	0.0672	0.0368
202.6	0.3435	0.1166	0.0697
409.4	0.3539	0.1820	0.0987
612.2	0.3606	0.2366	0.1227
808.7	0.3662	0.2757	0.1487
1011.1	0.3719	0.3082	0.1764
1213.9	0.3769	0.3254	0.1984
1404.6	0.3792	0.3551	0.2141
1605.7	0.3825	0.3670	0.2373
1805.0	0.3841	0.4000	0.2526
Methane Feed Composition: 20% (8.1% moisture)			
115.2	0.1481	0.0388	0.0478
207.8	0.1526	0.0645	0.0769
404.1	0.1581	0.1106	0.1223
603.7	0.1634	0.1473	0.1592
800.2	0.1683	0.1741	0.1870
1002.4	0.1731	0.1948	0.2160
1205.0	0.1753	0.2177	0.2354
1402.4	0.1792	0.2289	0.2621
1600.2	0.1828	0.2345	0.2839
1803.5	0.1854	0.2448	0.3264

TABLE 10. Nitrogen/Carbon Dioxide Mixture Adsorption on Wet Fruitland Coal at 115°F

Pressure (psia)	Nitrogen Gas Mole Fraction	Absolute Nitrogen Adsorption (mmole/g coal)	Absolute Carbon Dioxide Adsorption (mmole/g coal)
Nitrogen Feed Composition: 80% (10.5% moisture)			
117.4	0.9605	0.0380	0.0754
211.2	0.9491	0.0602	0.1252
402.8	0.9328	0.0989	0.2080
605.9	0.9176	0.1286	0.2695
802.5	0.9094	0.1531	0.3255
1004.2	0.9050	0.1745	0.3847
1193.3	0.9014	0.2129	0.4402
1395.0	0.8972	0.2495	0.4900
1602.0	0.8912	0.2620	0.5144
1803.0	0.8662	0.2770	0.5544
Nitrogen Feed Composition: 60% (10.0% moisture)			
116.2	0.8193	0.0271	0.1537
205.0	0.8128	0.0380	0.2542
398.7	0.8011	0.0581	0.4034
604.9	0.7753	0.0725	0.5222
806.0	0.7549	0.0837	0.6024
1006.1	0.7427	0.0882	0.6803
1208.0	0.7304	0.0990	0.7359
1405.8	0.7190	0.1176	0.7725
1606.3	0.7106	0.1322	0.8098
1805.3	0.7046	0.1433	0.8519

TABLE 10. Nitrogen/Carbon Dioxide Mixture Adsorption on Wet Fruitland Coal at 115 °F (Continued)

Pressure (psia)	Nitrogen Gas Mole Fraction	Absolute Nitrogen Adsorption (mmole/g coal)	Absolute Carbon Dioxide Adsorption (mmole/g coal)
Nitrogen Feed Composition: 40% (7.7% moisture)			
102.5	0.6664	0.0287	0.2186
202.9	0.6343	0.0375	0.3666
394.8	0.5904	0.0429	0.5582
604.5	0.5553	0.0487	0.6891
805.8	0.5293	0.0606	0.7697
1002.0	0.5132	0.0657	0.8383
1202.6	0.5004	0.0713	0.8956
1400.0	0.4898	0.0833	0.9456
1602.0	0.4791	0.1069	0.9756
1802.0	0.4744	0.1122	1.0397
Nitrogen Feed Composition: 20% (10.5% moisture)			
110.6	0.3983	0.0170	0.3363
206.5	0.3703	0.0152	0.5021
406.7	0.3240	0.0190	0.7111
605.7	0.2967	0.0249	0.8369
807.5	0.2795	0.0257	0.9222
1003.7	0.2682	0.0300	1.0065
1202.5	0.2566	0.0449	1.0596
1354.7	0.2505	0.0541	1.1069
1500.1	0.2454	0.0664	1.157
1752.0	0.2392	0.0750	1.208

Previous Data

Amoco has collected data for pure nitrogen, methane and carbon dioxide adsorption on wet Fruitland coal at 115 °F at pressures from 100 psia to 1400 psia. Hall at Oklahoma State University has also performed similar experiments extending to 1800 psia. His data are shown with Amoco's and the present data on the Figures 15 to 17. For carbon dioxide, the current data are significantly different from Hall's data, as shown in Figure 17. The reason is that Hall used a less accurate equation of state to calculate the carbon dioxide compressibility factor. Hall's carbon dioxide data have been reevaluated and compared with current data; results are shown in Figure 18.

Comparison of these data indicates that the current data for methane and carbon dioxide pure gases are about 3% lower than Amoco's data and nitrogen is about 10% lower. The reason is that coal samples were from the different wells, and have different ash content. A data comparison based on organic content is given in Appendix D, which shows the current data to be 5% higher than Amoco's data.

For the binary mixture adsorption, the current experimental data have been compared with the data collected by Hall and Amoco. The results are shown in Figures 18 to 30. The current data are very similar to those of Hall. For methane and carbon dioxide mixture adsorption, the overall methane adsorption amount is 8% lower than Hall, the overall carbon dioxide adsorption is very close at low pressure and is 8% lower at the high pressure.

For methane and nitrogen adsorption, the current data are 10% overall lower than the data collected by Hall at compositions of methane/nitrogen of 60%/40% and 40%/60%.

For nitrogen and carbon dioxide adsorption, the current data are very similar to the data from Hall. Current data are about 5% overall lower than Hall's data. There is a 10% lower for the nitrogen adsorption at the composition of nitrogen/carbon dioxide of 20%/80%, the others compositions are about 2 to 3% lower than Hall's data.

The data collected by Amoco are limited to 550, 1050 and 1560 psia for methane/carbon dioxide and methane/nitrogen. The current data agree with the Amoco data in a qualitative sense, but there are substantial differences for the methane/nitrogen adsorption with composition of 0.925/0.075.

The error analysis of the experimental data is shown in Chapter VI.

Figure 15. Data Comparison for Pure Nitrogen Adsorption on
Wet Fruitland Coal at 115 °F

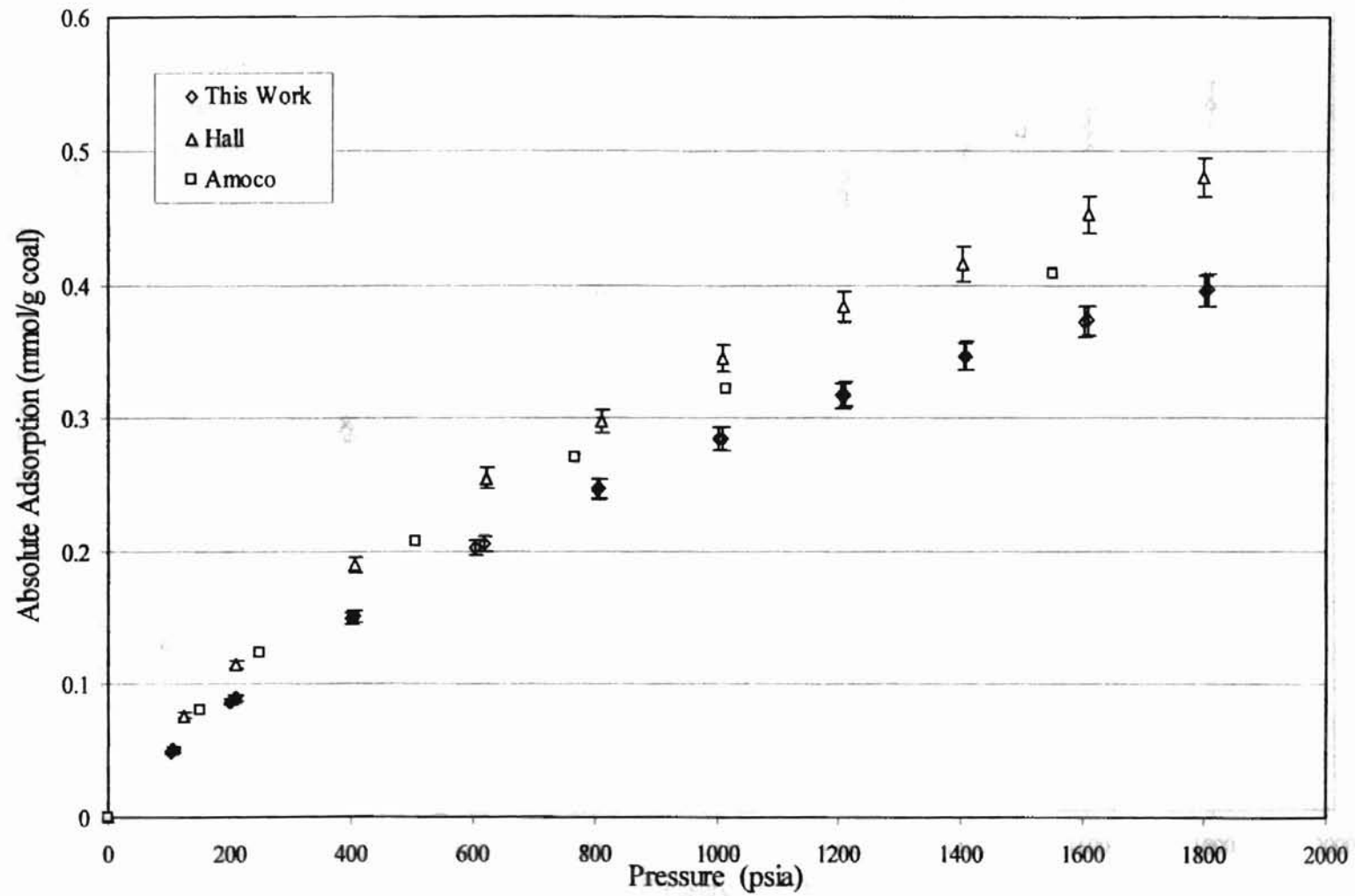


Figure 16. Data Comparison for Pure Methane Adsorption on
Wet Fruitland Coal at 115 °F

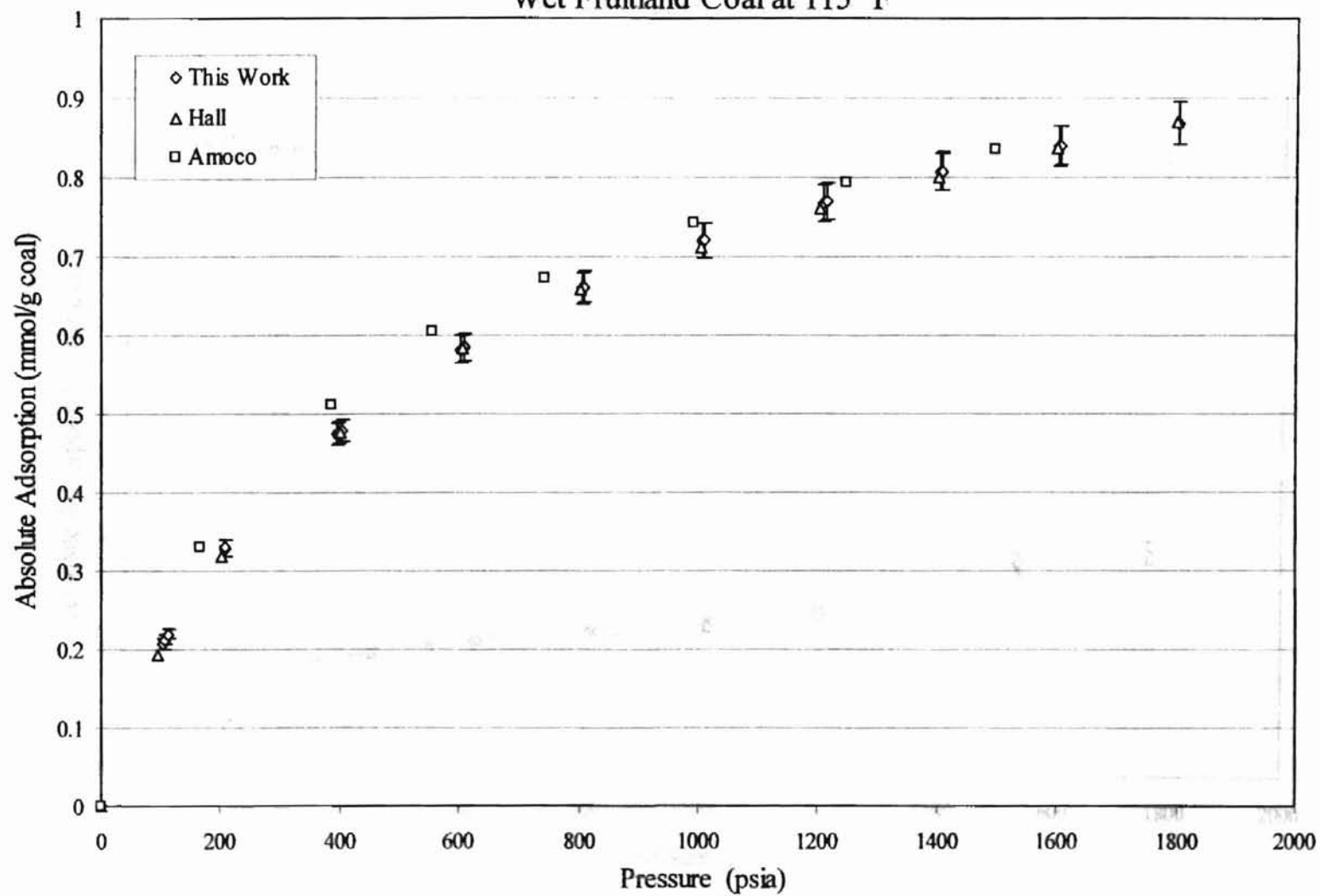


Figure 17. Data Comparison for Pure Carbon Dioxide Adsorption on Wet Fruitland Coal at 115 °F

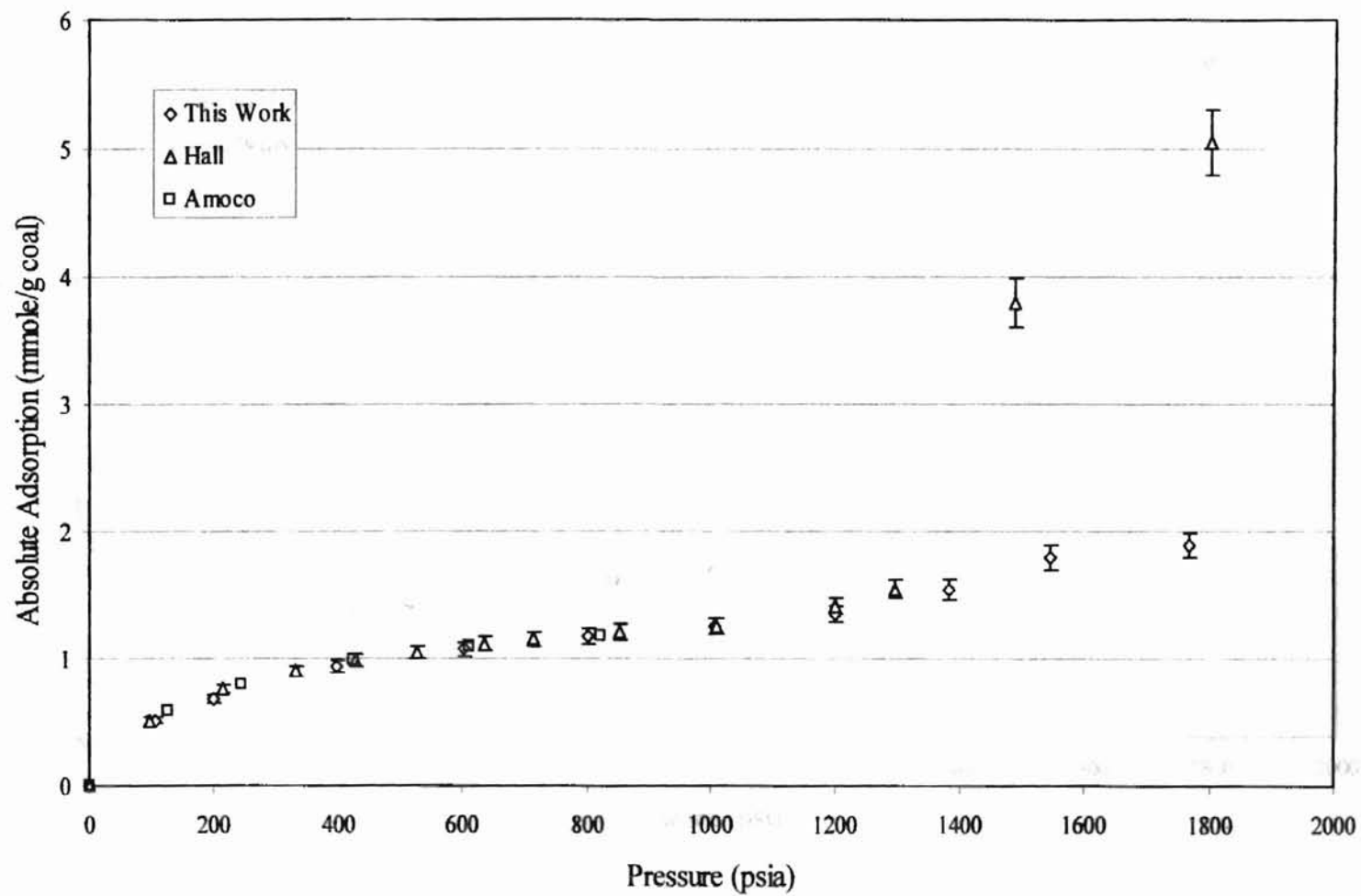


Figure 18. Revaluation of Hall's Carbon Dioxide Adsorption Data on Wet Fruitland Coal at 115 °F

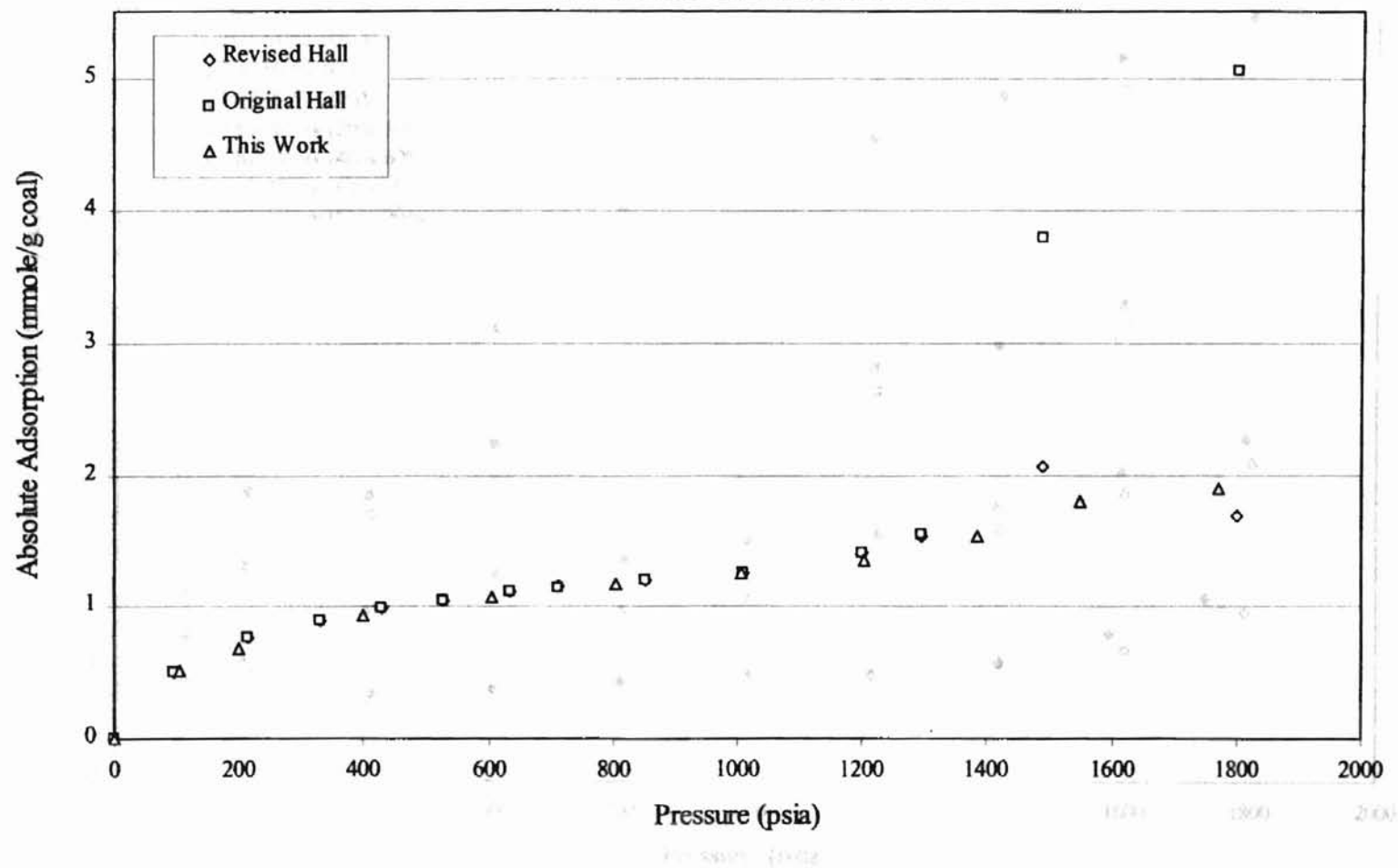


Figure 19. Data Comparison for Methane/Carbon Dioxide Binary Mixture
Adsorption on Wet Fruitland Coal at 115 °F: Methane

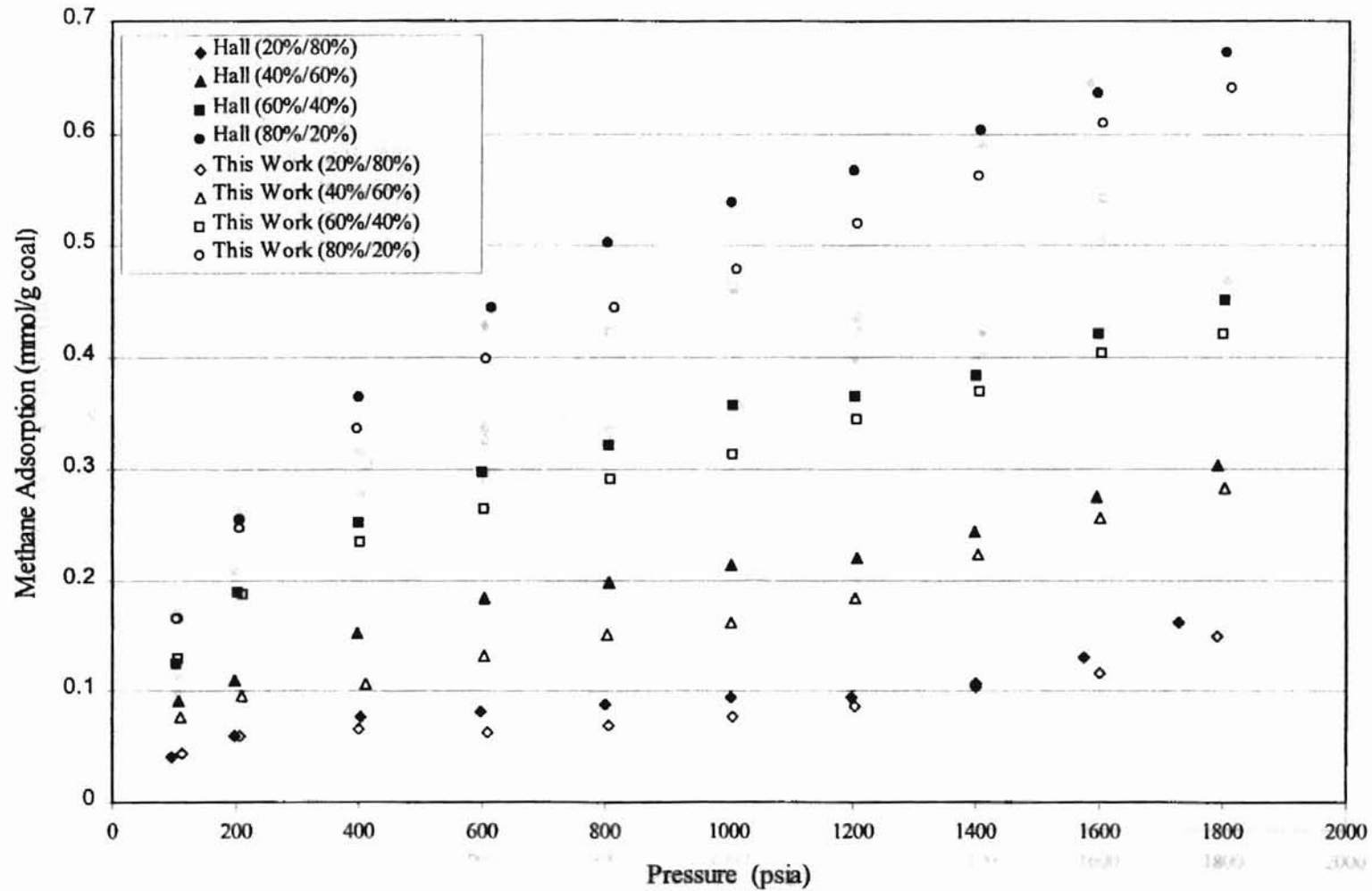


Figure 20. Data Comparison for Methane/Carbon Dioxide Binary Mixture Adsorption on Wet Fruitland Coal at 115 °F: Carbon Dioxide

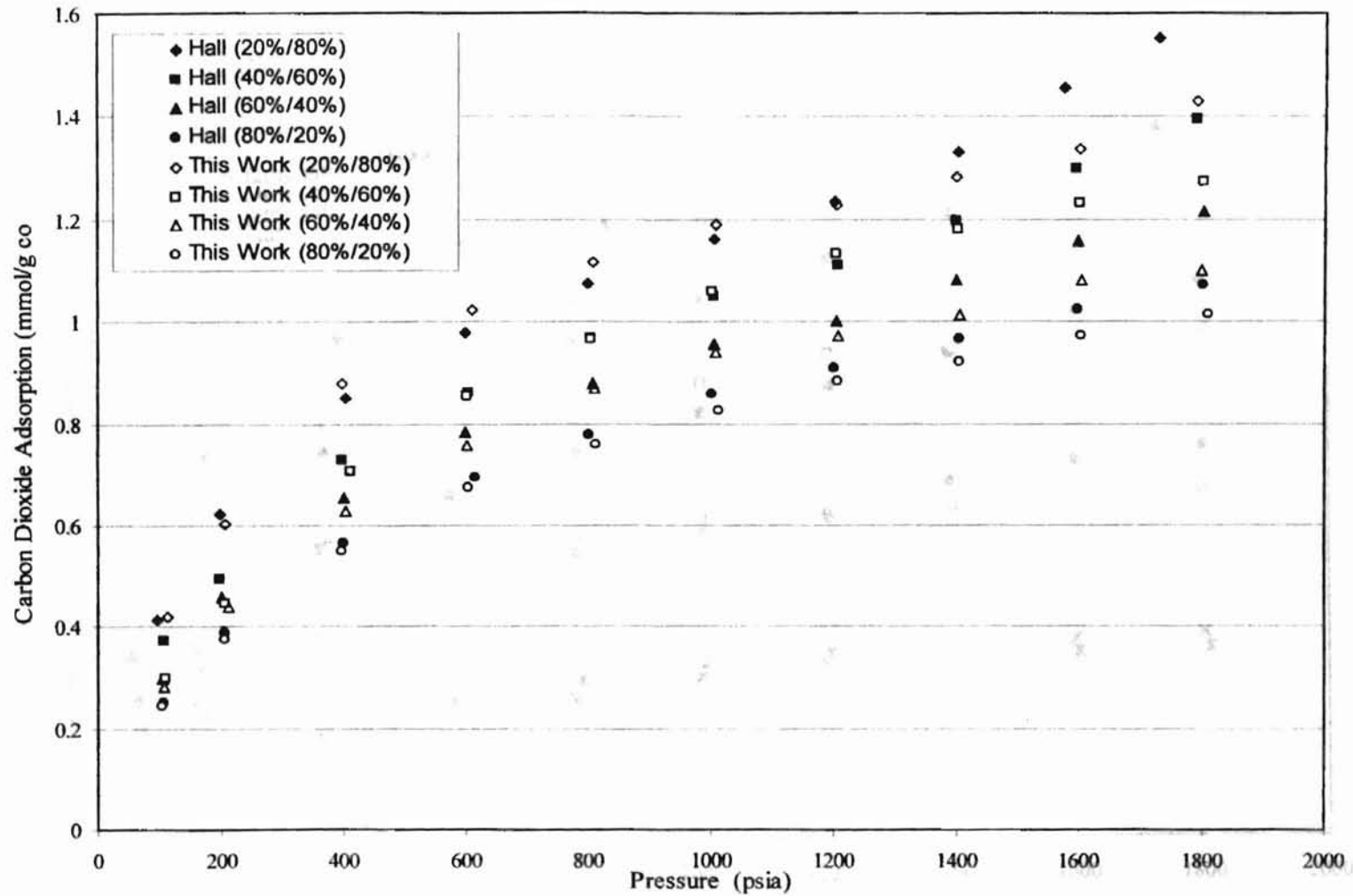


Figure 21. Data Comparison for Methane/Carbon Dioxide Binary Mixture Adsorption on Wet Fruitland Coal at 115 °F: Total

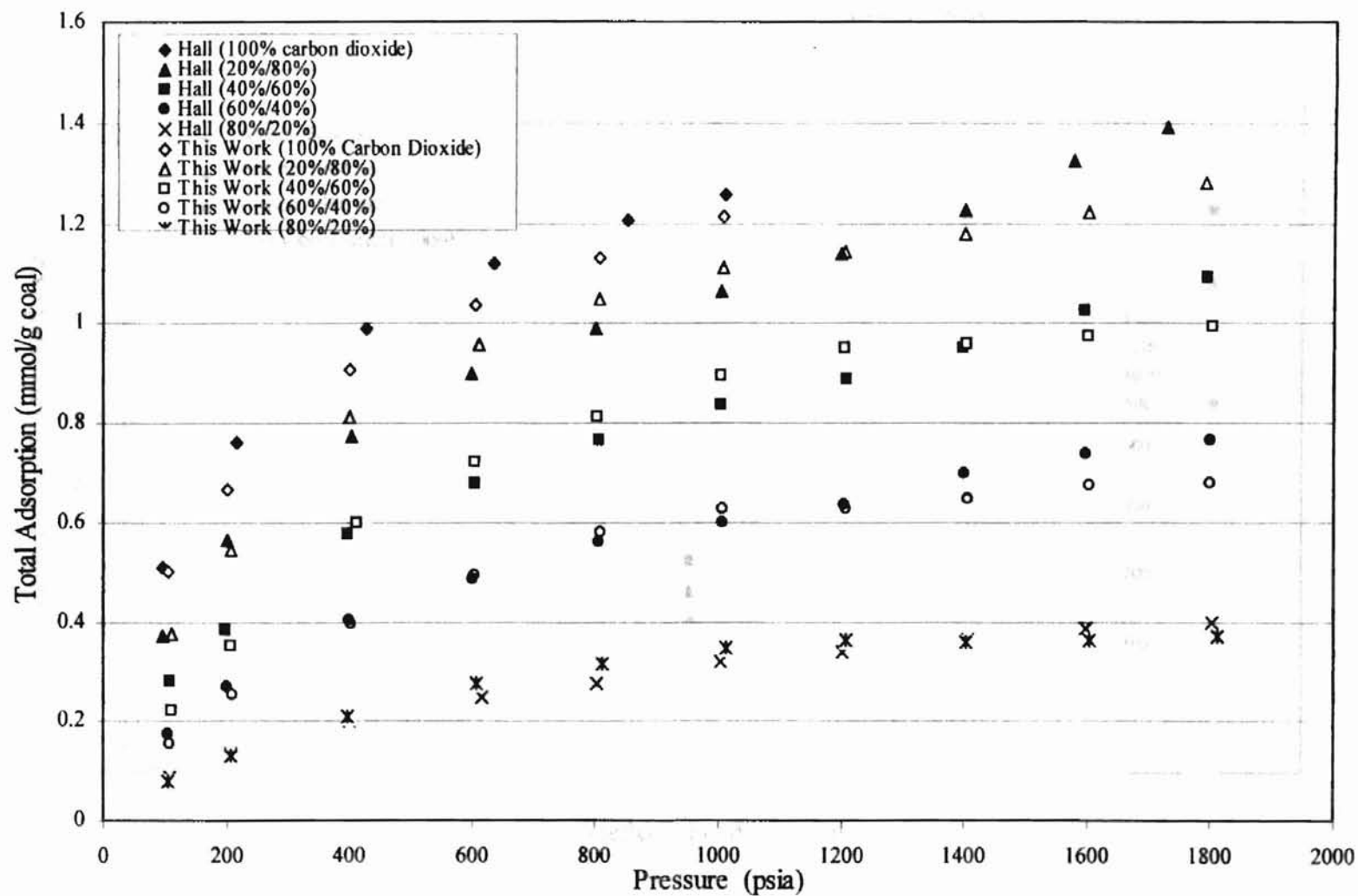


Figure 22. Data Comparison for Methane/Carbon Dioxide Binary Mixture Adsorption on Wet Fruitland Coal at 115 °F: Methane/Amoco

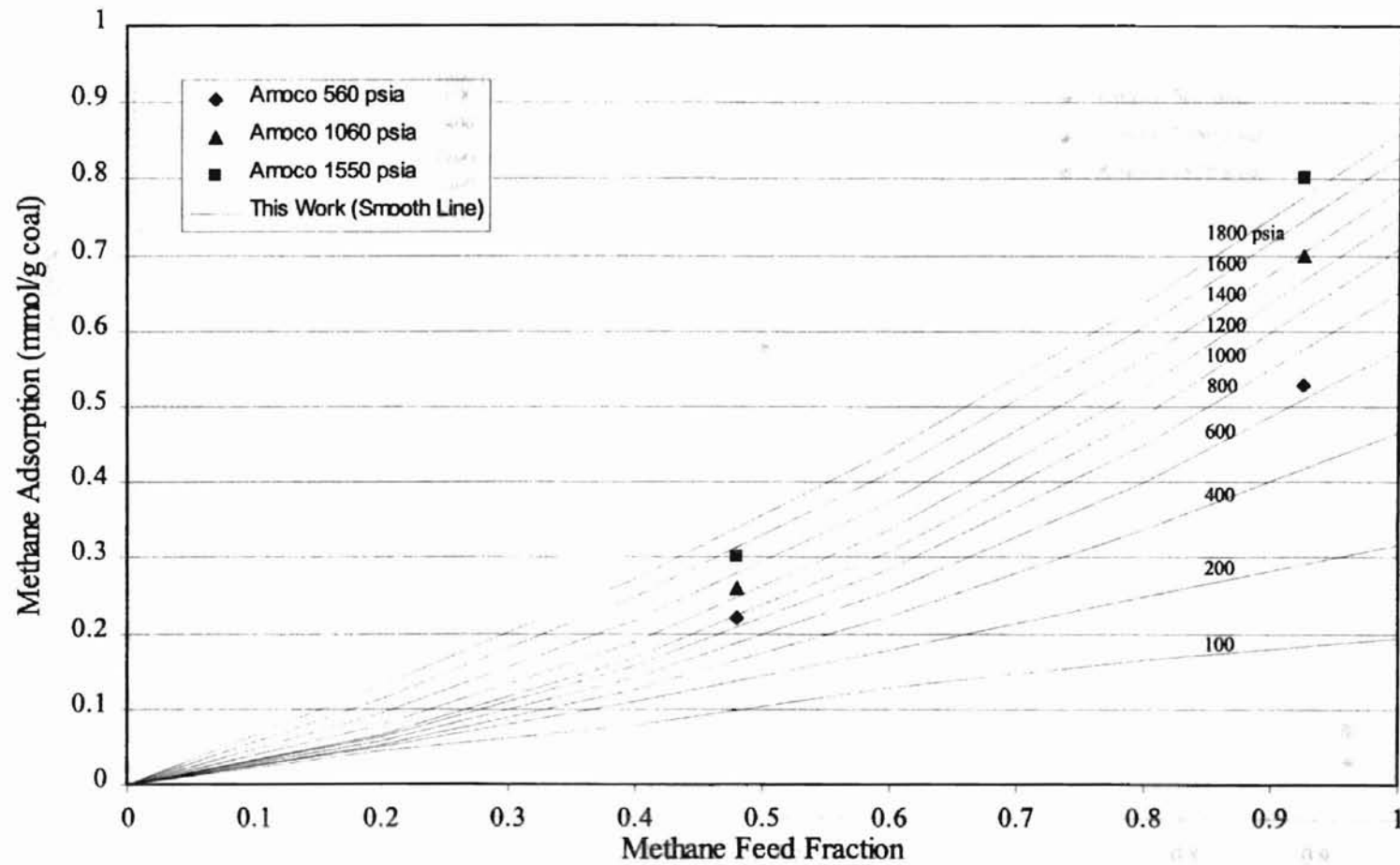


Figure 23. Data Comparison for Methane/Carbon Dioxide Binary Mixture Adsorption on Wet Fruitland Coal at 115 °F: Carbon Dioxide/Amoco

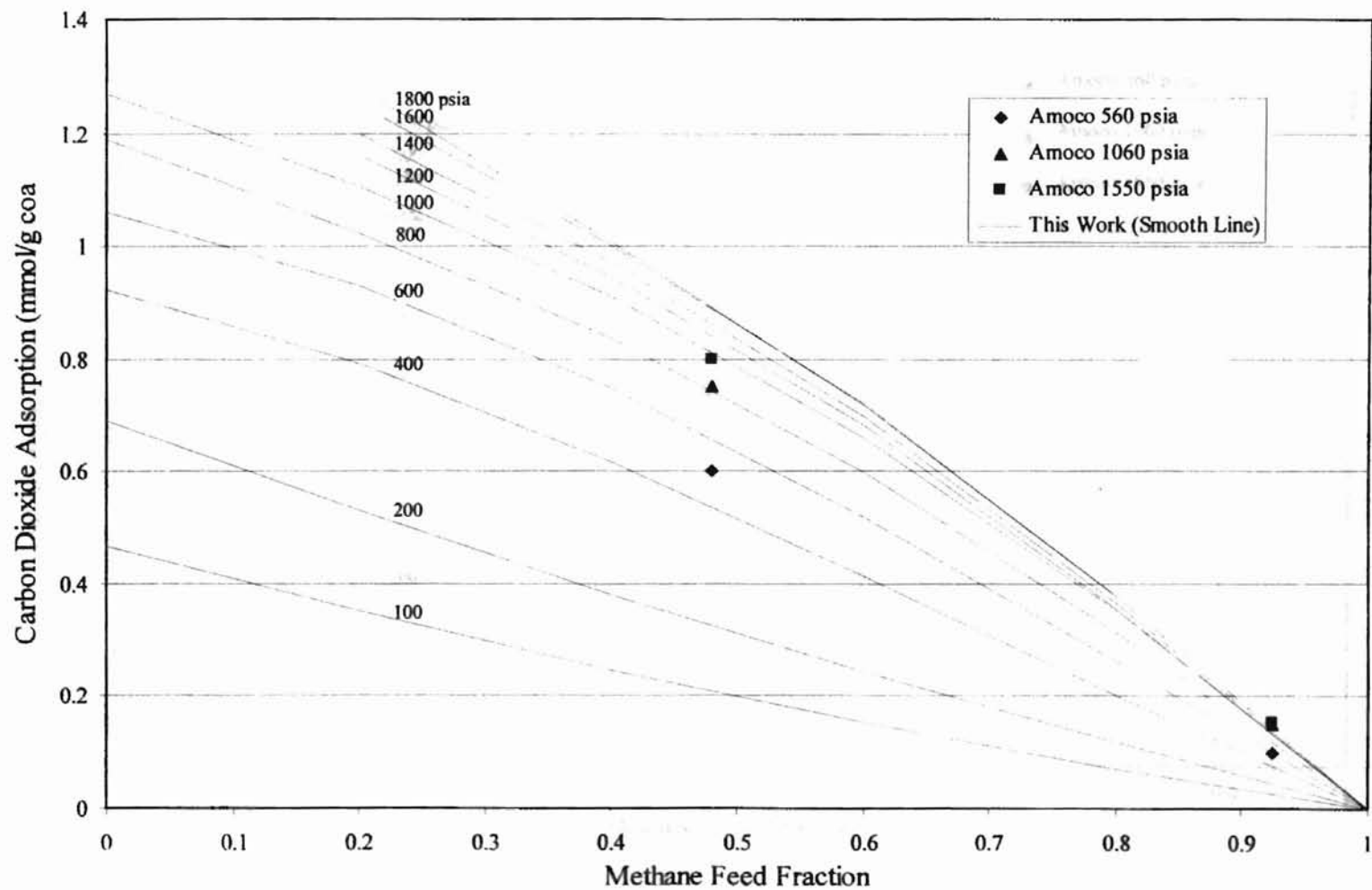


Figure 24. Data Comparison for Methane/Carbon Dioxide Binary Mixture Adsorption on Wet Fruitland Coal at 115 °F: Total/Amoco

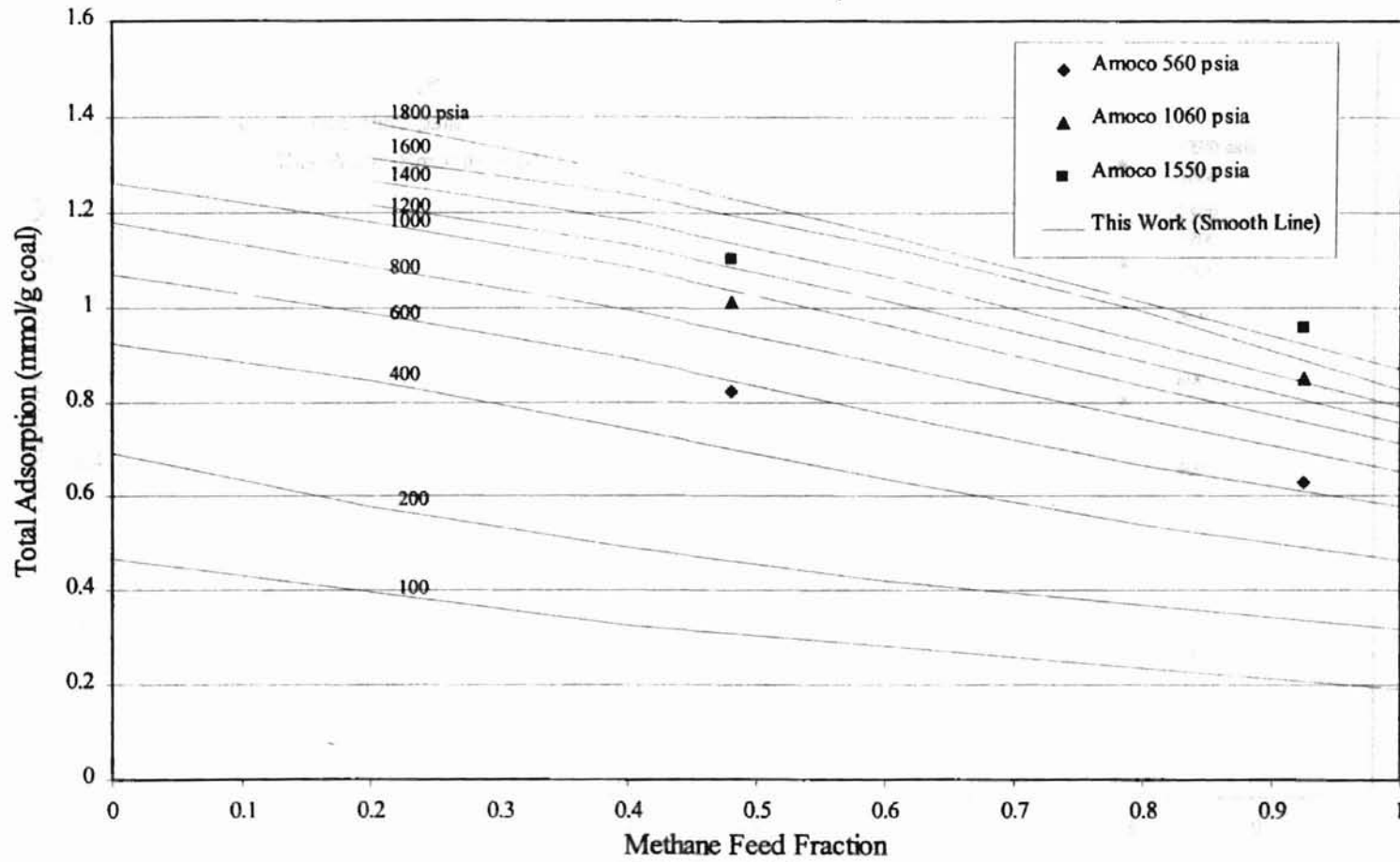


Figure 25. Data Comparison for Methane/Nitrogen Binary Mixture Adsorption on Wet Fruitland Coal at 115 °F: Methane

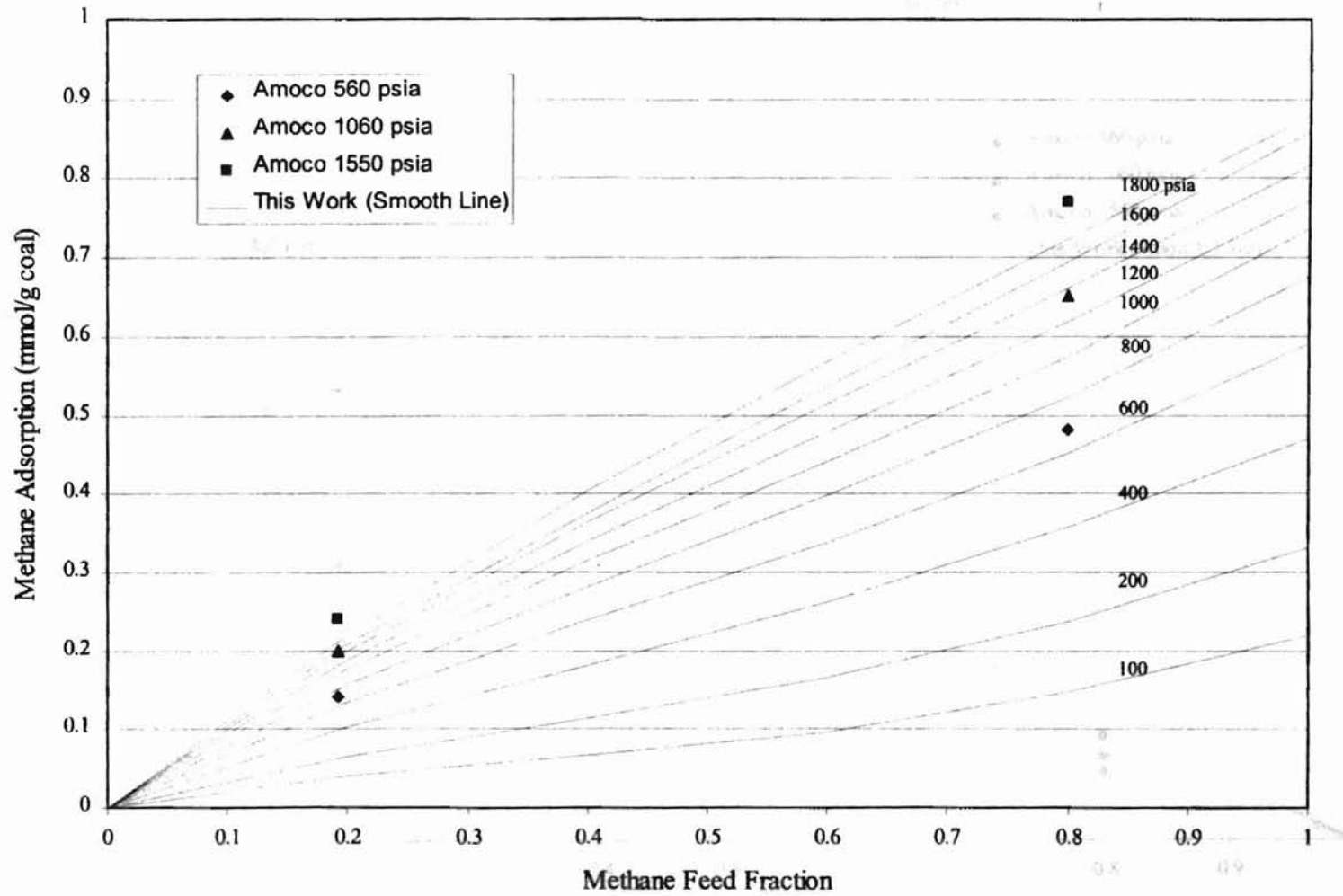


Figure 26. Data Comparison for Methane/Nitrogen Binary Mixture Adsorption on Wet Fruitland Coal at 115 °F: Nitrogen

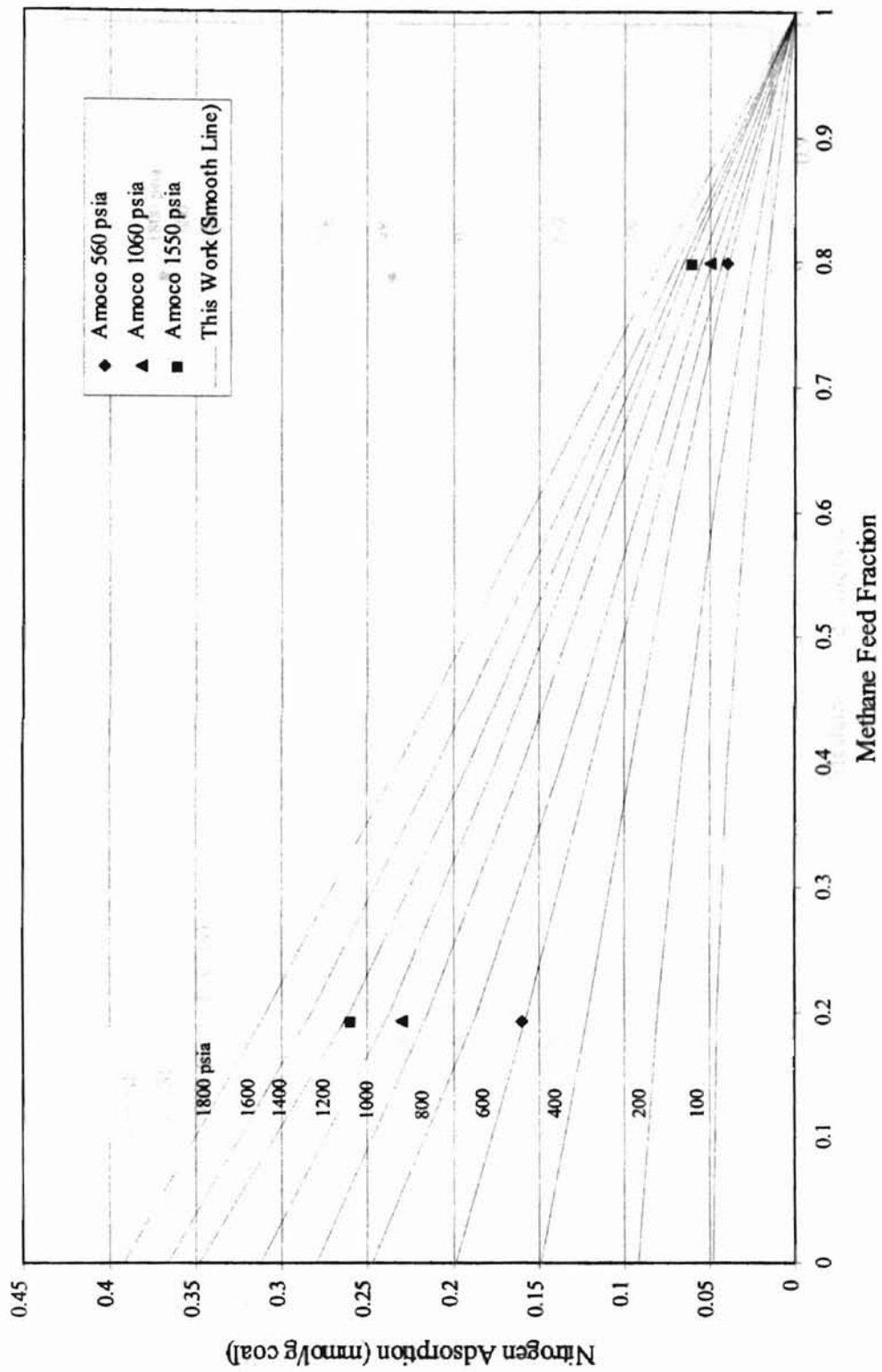


Figure 27. Data Comparison for Methane/Nitrogen Binary Mixture Adsorption on Wet Fruitland Coal at 115 °F: Total

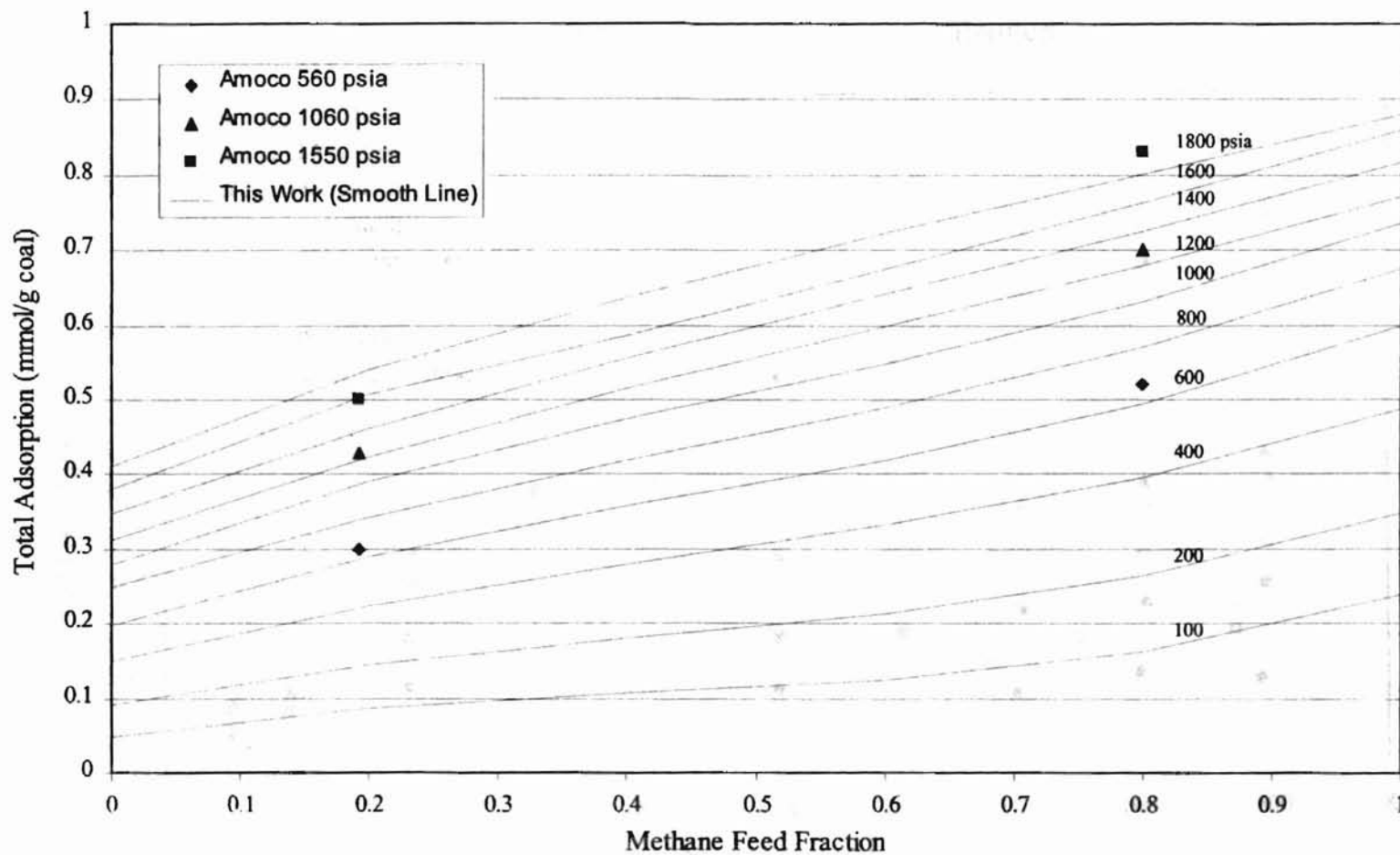


Figure 28. Data Comparison for Nitrogen/Carbon Dioxide Binary Mixture Adsorption on Wet Fruitland Coal at 115 °F: Nitrogen

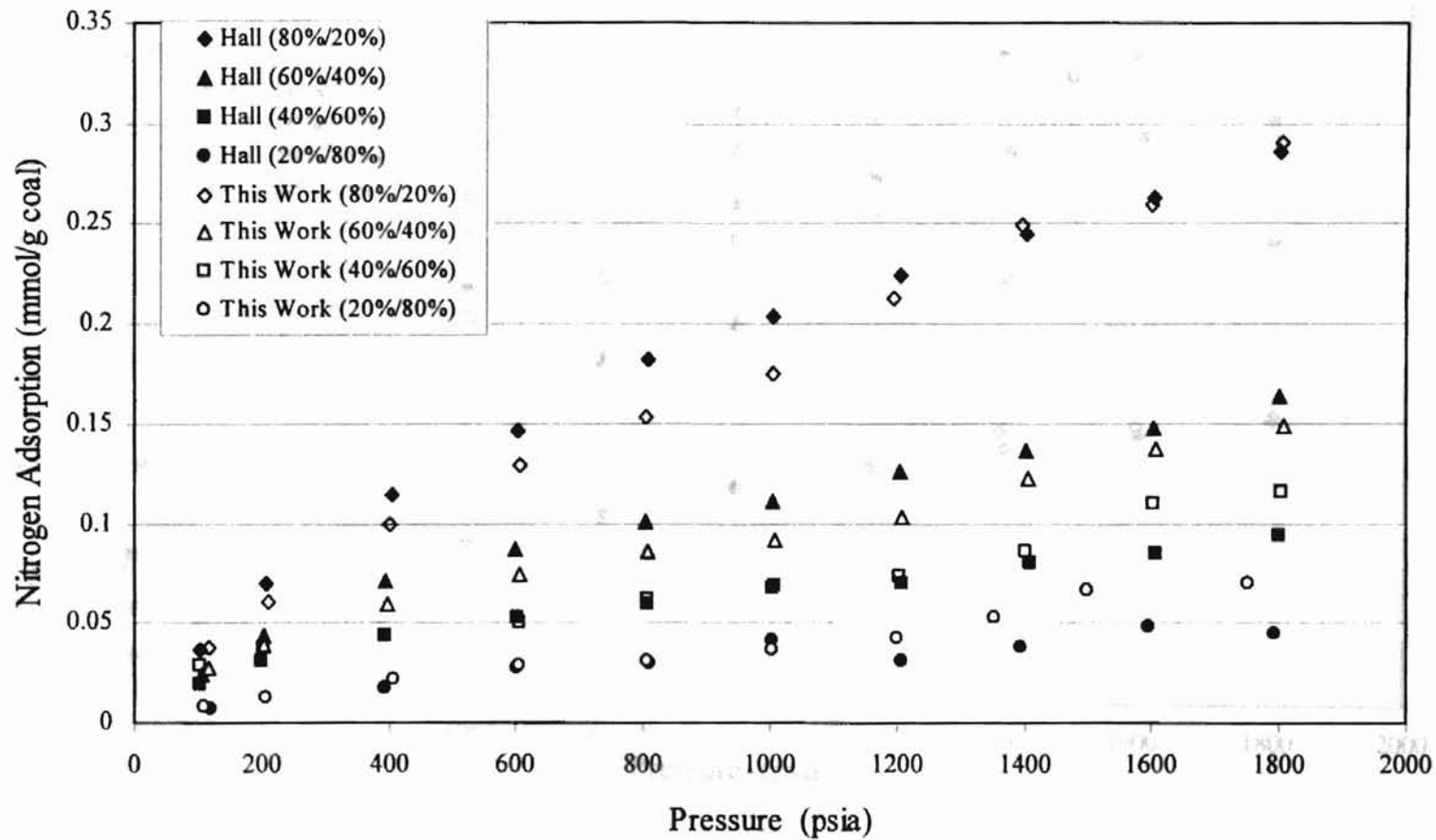


Figure 29. Data Comparison for Nitrogen/Carbon Dioxide Binary Mixture
 Adsorption on Wet Fruitland Coal at 115 °F: Carbon Dioxide

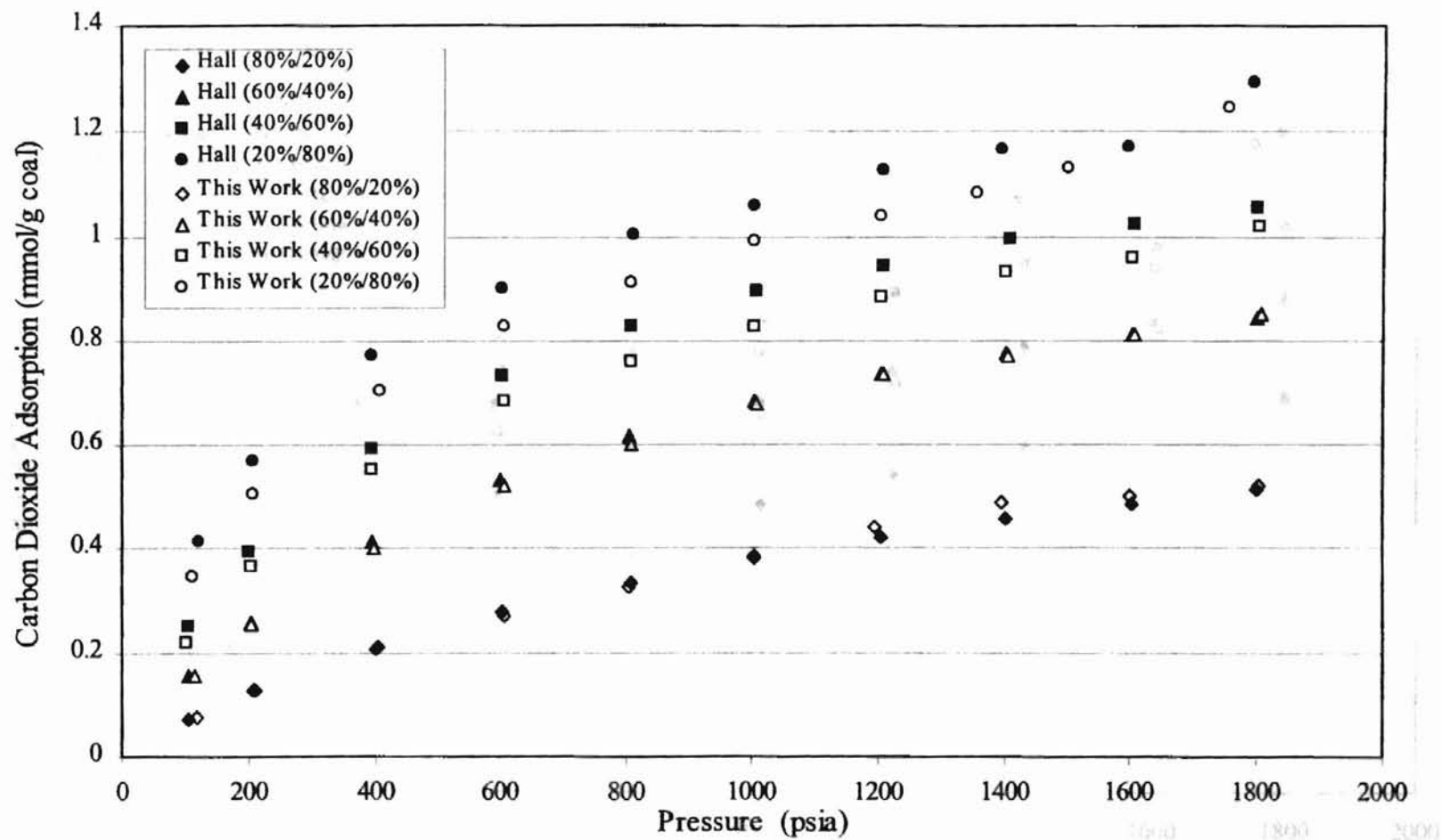
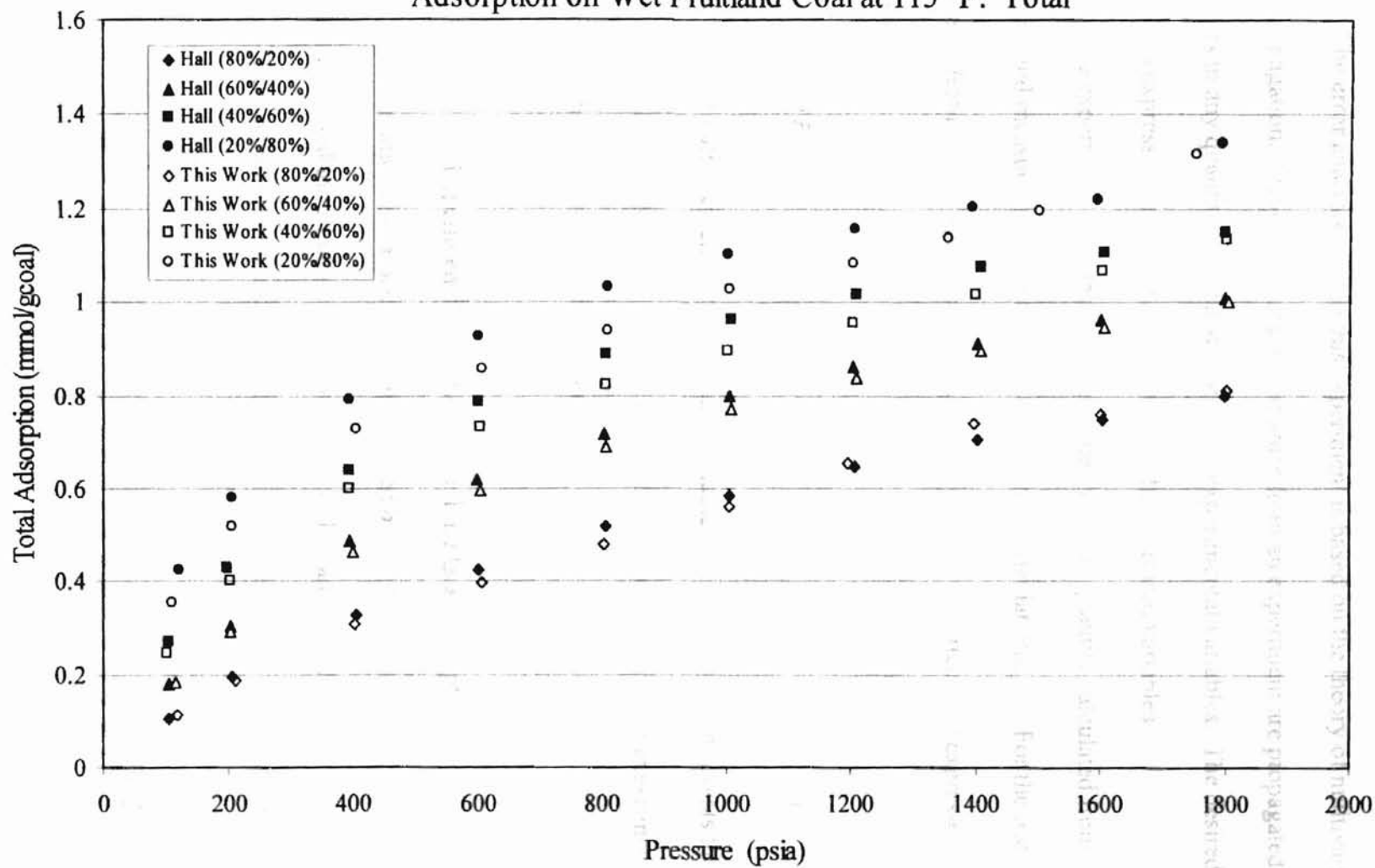


Figure 30. Data Comparison for Nitrogen/Carbon Dioxide Binary Mixture

Adsorption on Wet Fruitland Coal at 115 °F: Total



CHAPTER VI

ANALYSIS OF EXPERIMENTAL ERRORS

The error analysis used in this experiment is based on the theory of multivariate error propagation. Errors in measured variables from an experiment are propagated into the errors in any quantity calculated from these experimental variables. The desired error quantity is expressed as an analytic function of the measured variables.

The experiment uncertainty is associated with the quantity calculated from experimental measurements, in terms of their standard deviations, σ . For the result, R , calculated from a set of variables $(X_1, X_2, X_3, \dots, X_n)$ the uncertainty is expressed as follows:

$$\sigma_R^2 = \sum_{i=1}^N [(\partial R / \partial X_i)^2 \sigma_{x_i}^2] \quad 6-1$$

where the summation extends over all input variables X_i . This equation reveals the uncertainty in R depends on the rate of change of R with respect to each experimental variable and the uncertainty in that experimental variable.

Experimental Uncertainties in Pure Gas Adsorption

The amount of adsorbed gas is determined by the difference between the amount of injected gas and the amount of unadsorbed gas. The amount of injected gas from the positive displacement pump and the amount of unadsorbed gas in the cell section contribute uncertainties.

$$n_a = n_i - n_{unads} \quad 6-2$$

The overall uncertainty is the sum of these two terms:

$$\sigma_{n_g}^2 = \sigma_{n_i}^2 + \sigma_{n_{unads}}^2 \quad 6-3$$

the uncertainty in the amount injected and the uncertainty in the amount of unadsorbed gas in the cell section.

The amount of injected gas is determined by the density and the injected volume and can be expressed as the following formula:

$$n_i = \sum_j (\rho_1 V_{p1} - \rho_2 V_{p2})_j \quad 6-4$$

thus the uncertainty is:

$$\sigma_{n_i}^2 = \sum_j [(\rho_1)^2 \sigma_{V_{p1}}^2 + (\rho_2)^2 \sigma_{V_{p2}}^2 + (V_{p1})^2 \sigma_{\rho_1}^2 + (V_{p2})^2 \sigma_{\rho_2}^2]_j \quad 6-5$$

where j denotes the injection number from pump to cell. In this operation, the initial and final pressures are kept equal, so,

$$\begin{aligned} \rho_2 &= \rho_1 \\ \sigma_{\rho_2} &= \sigma_{\rho_1} \\ \sigma_{V_{p2}} &= \sigma_{V_{p1}} \\ \Delta V_p &= V_{p2} - V_{p1} \end{aligned}$$

the uncertainty becomes,

$$\sigma_{n_i}^2 = \sum_j [(\Delta V_p)^2 \sigma_{\rho}^2 + 2(\rho)^2 \sigma_{V_p}^2]_j \quad 6-6$$

The amount of unadsorbed gas is determined by the density and the void volume, it can be expressed as the following formula:

$$n_{unads} = \rho_g V_{void} \quad 6-7$$

thus the uncertainty is [8]:

$$\sigma_{n_{unads}}^2 = (\rho_g)^2 \sigma_{V_{void}}^2 + (V_{void})^2 \sigma_{\rho_g}^2 \quad 6-8$$

The void volume is the difference between the helium calibrated volume and the volume occupied by the adsorbed phase. Thus the uncertainty is the sum of uncertainties by V_{He} and V_{ads} .

The uncertainty in the helium calibration includes the amount of helium injected and the helium gas density at the cell condition. The uncertainty of V_{void} is expressed as:

$$\sigma_{V_{void}}^2 = \sigma_{V_{He}}^2 + \sigma_{V_{ads}}^2 \quad 6-9$$

the molar volume of the adsorbed phase V_{ads} and V_{He} can be expressed as

$$V_{ads} = n_{ads} v_{ads}$$

$$V_{He} = n_{He} / \rho_{He}$$

Thus,

$$\sigma_{V_{ads}}^2 = (n_{ads})^2 \sigma_{v_{ads}}^2 + (v_{ads})^2 \sigma_{n_{ads}}^2 \quad 6-10$$

and

$$\sigma_{V_{He}}^2 = (1 / \rho_{He})^2 \sigma_{n_{He}}^2 + (n_{He} / \rho_{He}^2)^2 \sigma_{\rho_{He}}^2 \quad 6-11$$

so,

$$\sigma_{V_{void}}^2 = \sigma_{V_{He}}^2 + (n_{ads})^2 \sigma_{v_{ads}}^2 + (v_{ads})^2 \sigma_{n_{ads}}^2 \quad 6-12$$

By combining all these equations, the uncertainty of the pure gas adsorption can be expressed by the following [3]:

$$\sigma_{n_a}^2 = \sum_j [(\Delta V)^2 \sigma_{\rho}^2 + 2\rho^2 \sigma_{v_p}^2] + (\rho_g)^2 \sigma_{V_{He}}^2 + (\rho_g)^2 (n_{ads})^2 \sigma_{v_{ads}}^2 + (V_{void})^2 \sigma_{\rho_g}^2$$

6-13

Experimental Uncertainties in Binary Gas Adsorption

In the adsorption of mixture, for each component, the calculation is the same as pure component adsorption except a z_k , the mole fraction is introduced to account for variation in composition. In a mixture, the amount of specific component k adsorbed, n_{a_k} is given by a relation comparable to Equation 6-2.

$$n_{a_k} = n_{i_k} - n_{c_k} \quad k = 1, 2, \dots, N \quad 6-14$$

therefore,

$$\sigma_{n_{a_k}}^2 = \sigma_{n_{i_k}}^2 + \sigma_{n_{c_k}}^2 \quad 6-15$$

In the pump side, the composition of mixture z_k is introduced to this equation, then

$$n_{i_k} = z_k \sum_j (\rho_1 V_{p1} - \rho_2 V_{p2})_j \quad 6-16$$

similar to equation 6-5

$$\sigma_{n_{i_k}}^2 = (z_k)^2 \sum_j [(\Delta V_p)^2 \sigma_\rho^2 + 2(\rho)^2 \sigma_{V_p}^2]_j + (\sum_j \rho \Delta V_p)_j^2 \sigma_{z_k}^2 \quad 6-17$$

In the cell section, the amount of unadsorbed component k in the equilibrium cell is expressed by

$$n_{c_k} = y_k \rho_c V_c \quad k = 1, 2, \dots, N \quad 6-18$$

where y_k is the mole fraction of component of k in the equilibrium gas mixture in the cell. The n_{c_k} becomes the following:

$$\sigma_{n_{c_k}}^2 = (y_k \rho_c)^2 \sigma_{V_c}^2 + (y_k V_c)^2 \sigma_{\rho_c}^2 + (\rho_c V_c)^2 \sigma_{y_k}^2 \quad 6-19$$

By combining $\sigma_{n_{i_k}}^2$ and $\sigma_{n_{c_k}}^2$ terms, the uncertainty is expressed as:

$$\sigma_{n_{ak}}^2 = (z_k)^2 \left\{ \sum_j [2(\rho_p)^2 \sigma_{V_p}^2 + \Delta V_p^2 \sigma_{\rho_p}^2] \right\} + \left(\sum_j [\rho_p \Delta V_p] \right) \sigma_{z_k}^2 + (y_k \rho_c)^2 [\sigma_{V_{He}}^2 + n_a^2 \sigma_{v_a}^2 + v_a^2 \sigma_{n_a}^2] + (y_k V_C)^2 \sigma_{\rho_c}^2 + (\rho_c V_C)^2 \sigma_{y_k}^2 \quad 6-20$$

Experimental Uncertainty

The above equation requires the specification of several variables. The estimates are listed below:

1. Molar density of the adsorbed phase has been estimated as in Chapter IV. They can be converted to molar volume as 38.0, 34.6 and 37.2 cc/g mole for methane, nitrogen and carbon dioxide respectively.
2. The individual measured variables are assigned as follows in Table 11:

TABLE 11. Experimental Uncertainty

Measured Variables	Uncertainty	
	Symbol	Value
Temperature	σ_T	0.1K
Pressure	σ_P	0.2 psi
Displacement Pump Volume	σ_{V_p}	0.02 cc
Adsorbed Phase Molar Volume	$\sigma_{v_{ads}}$	0.15 v_{ads}
Pure Component Density	$\sigma_{\rho_{pure}}$	0.001 ρ
Mixture Density	$\sigma_{\rho_{mix}}$	0.002 ρ
Helium Injection	$\sigma_{V_{He}}$	0.003 V_{void}
Pump Gas Composition*	σ_{z_k}	0.002
Cell Gas Composition*	σ_{y_k}	0.002

* Estimated from gas chromatographic analysis

Discussion of the Error Analysis

The uncertainties for pure component of nitrogen, methane and carbon dioxide on wet Fruitland coal were calculated by Equation 6-13 and results are shown in Figure 31. Uncertainty of nitrogen is 0.5 ~5%, for methane is 0.5~3% and for pure carbon dioxide is 0.5~2.5% over the pressure ranges from 100 to 1800 psia.

The uncertainties for pure component nitrogen and methane on wet Illinois-6 coal were calculated by Equation 6-13 and results are shown in the Figure 32. Uncertainty of nitrogen is 0.5 ~5%, for pure methane is 0.5~3% with the pressure from 100 to 1800 psia, which are similar to uncertainties on Fruitland coal.

The uncertainties for binary mixtures vary at different compositions and with different mixtures; they were calculated by Equation 6-20. In general, the overall methane/carbon dioxide mixture has 2~7% uncertainty from 100 to 1800 psia, the overall methane/nitrogen mixture has 2~9% uncertainty from 100 to 1800 psia, the overall nitrogen/carbon dioxide mixture has 2~7% uncertainty from 100 to 1800 psia.

In the error analysis, the void volume and the amount of coal loaded in the equilibrium cell have important effects on the overall uncertainty. The other factors, such as temperature, pressure, pump volume readings, gas density and gas compositions do not have a large influence. In order to reduce the uncertainty, the more coal should be loaded and the void volume should be reduced in the cell section. Void volume can be reduced by reducing the tubing and loading more coal sample in the cell.

Figure 31. Uncertainty Associated with Pure Gas Adsorption on Wet Fruitland Coal at 115 °F

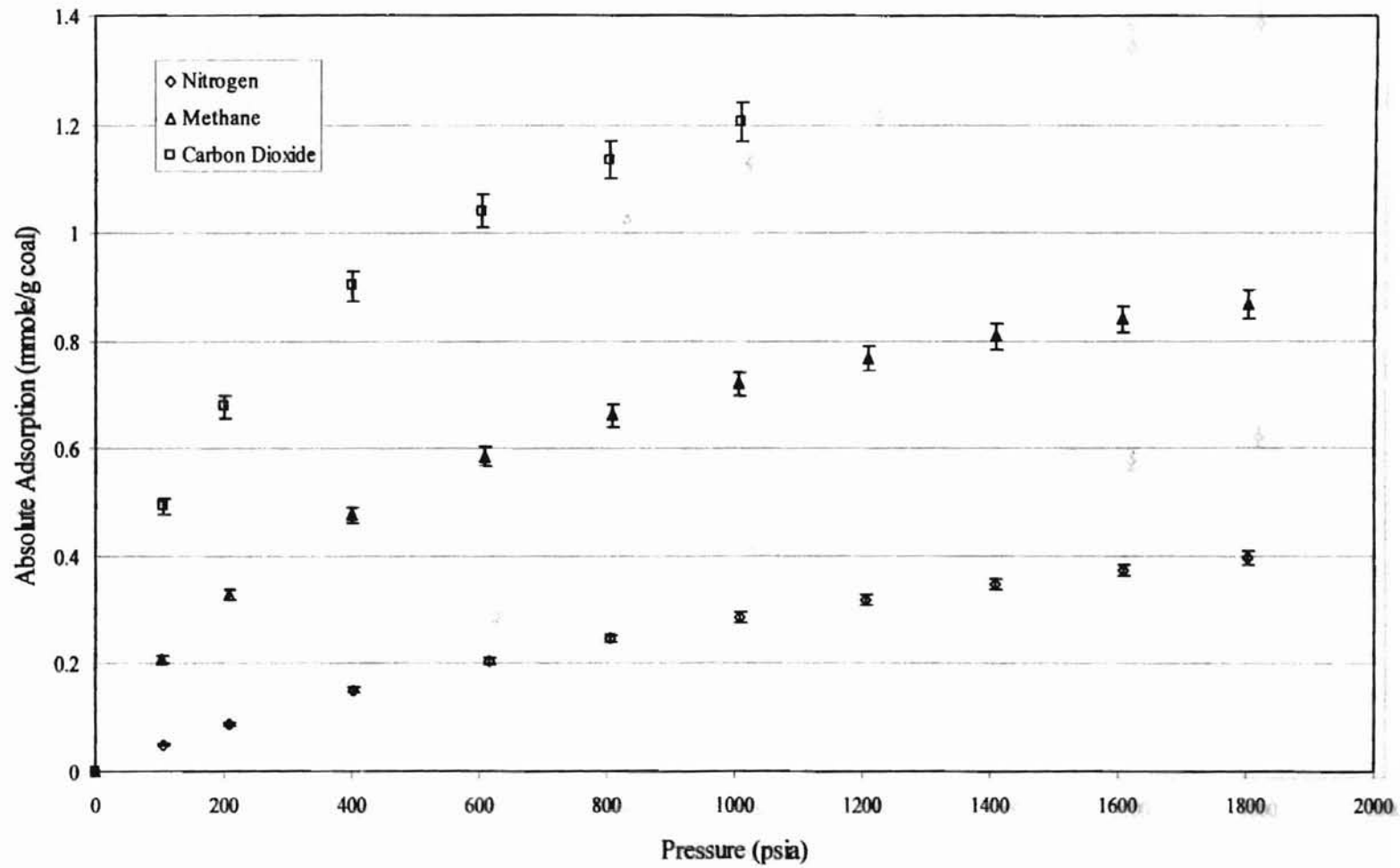
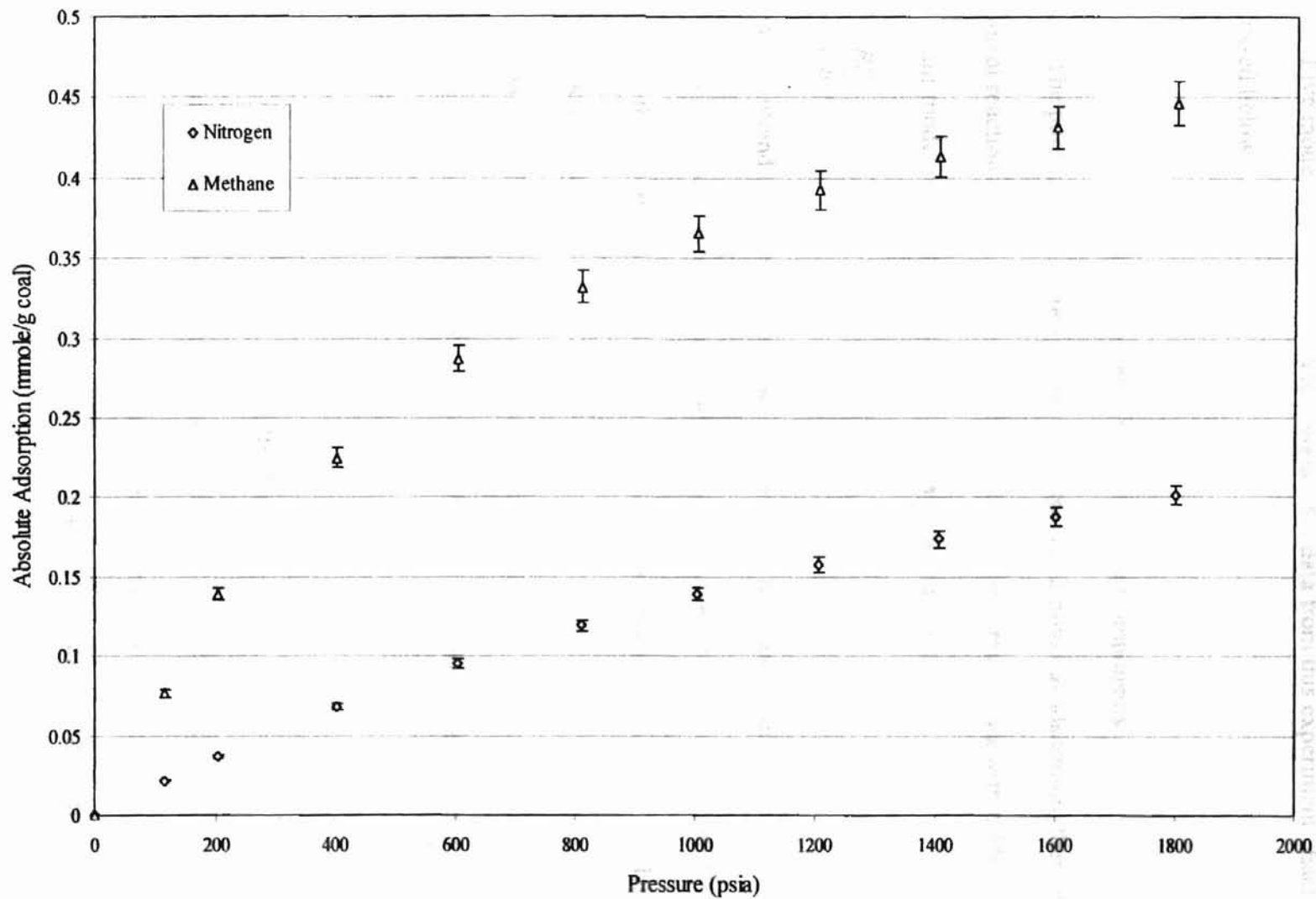


Figure 32. Uncertainty Associated with Gas Adsorption on Wet Illinois-6 Coal at 115 °F



CHAPTER VII

DATA CORRELATION

Five models have been used to correlate the data from this experiment. Each is discussed below.

Simple Langmuir Model for Pure Components

The pure gas adsorption on coal is recognized as physical adsorption; there is no chemical reaction. The Langmuir model can describe the present data within 3%. The Langmuir model relates the adsorption to pressure as Equation 2-14:

$$\theta = \frac{BP}{1 + BP} \quad 7-1$$

On wet Fruitland coal, for pure nitrogen and methane, this model can describe the adsorption volume to pressure from 100 to 1800 psia. For carbon dioxide, from 100 to 1000 psia, the adsorption can be described by Langmuir model. The results are shown in Table 12 and Figure 33.

On wet Illinois-6 coal, for pure nitrogen and methane, this model can relate the adsorption volume to pressure from 100 to 1800 psia. The results are shown in Table 13 and Figure 34.

LRC Model

Langmuir model assumes one gas molecule occupies one site on the solid surface. It is not true for every physical adsorption. Researchers have assumed one gas molecule can be adsorbed on more than one site on the solid surface, and they have modified the Langmuir model as follow [32]:

Figure 33. Simple Langmuir Representation of Gas Adsorption on Wet Fruitland Coal at 115 °F

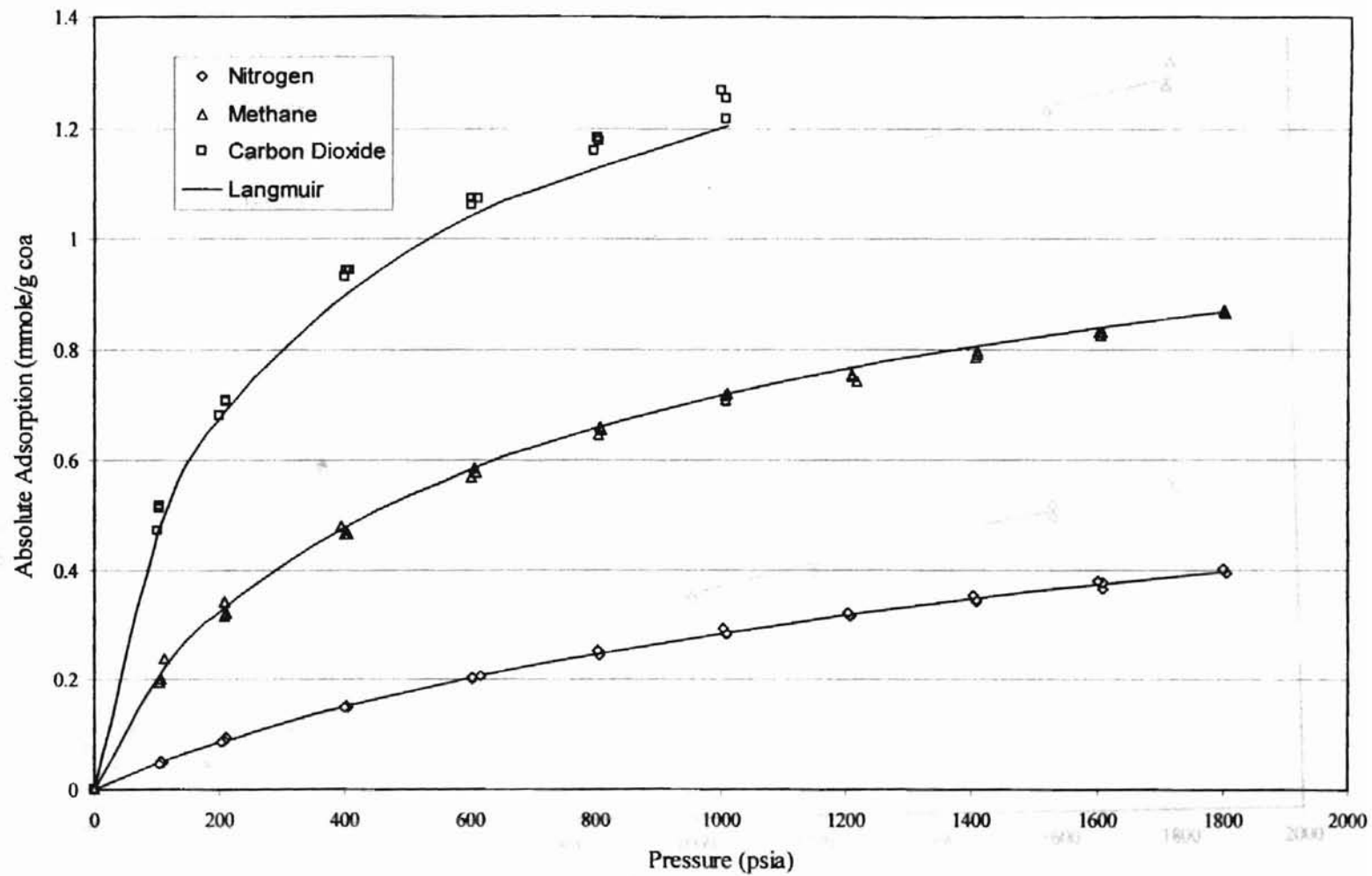


Figure 34. Simple Langmuir Representation of Gas Adsorption on Wet Illinois-6 Coal at 115 °F

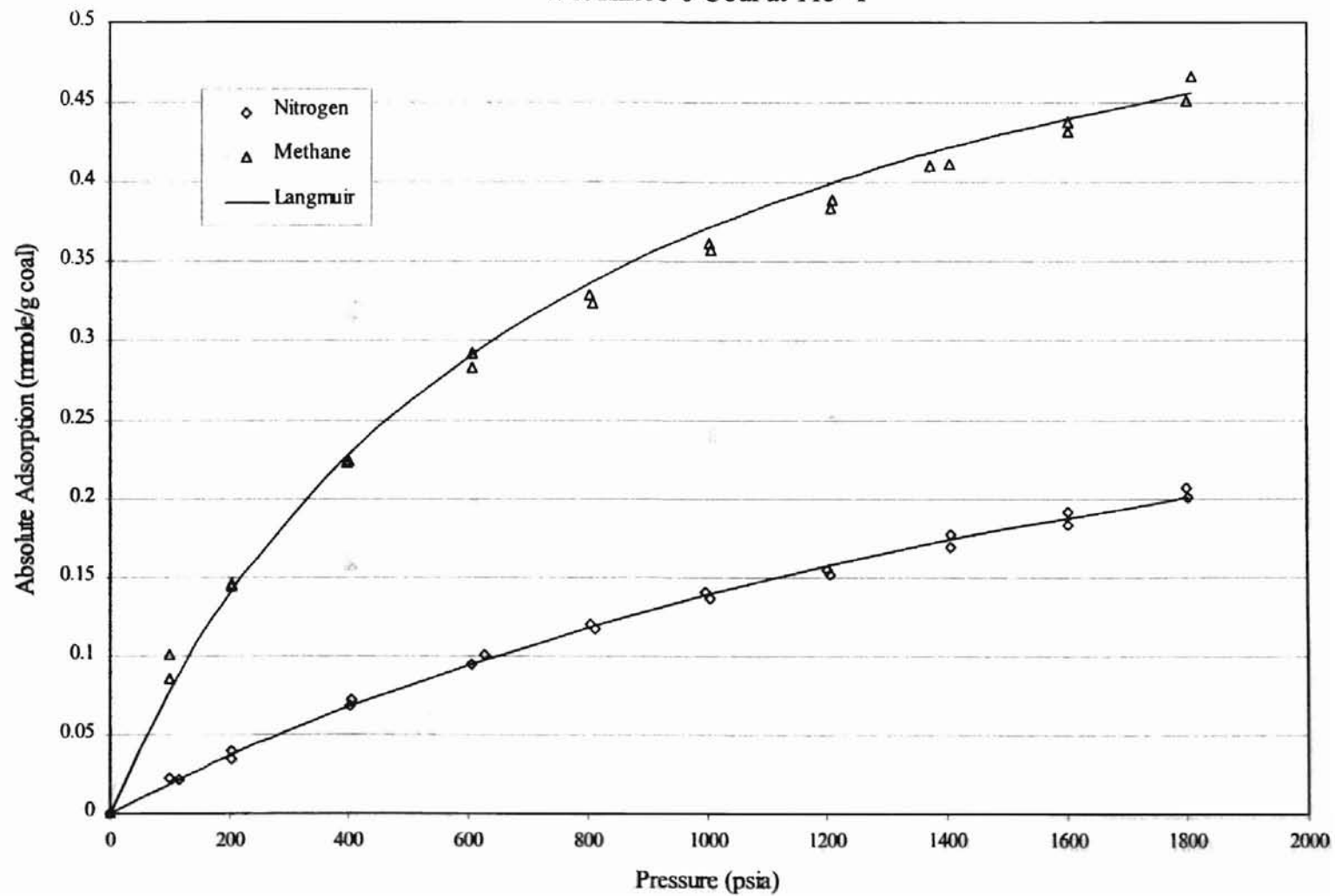


Figure 35. LRC Representation of Gas Adsorption on Wet Fruitland Coal at 115 °F

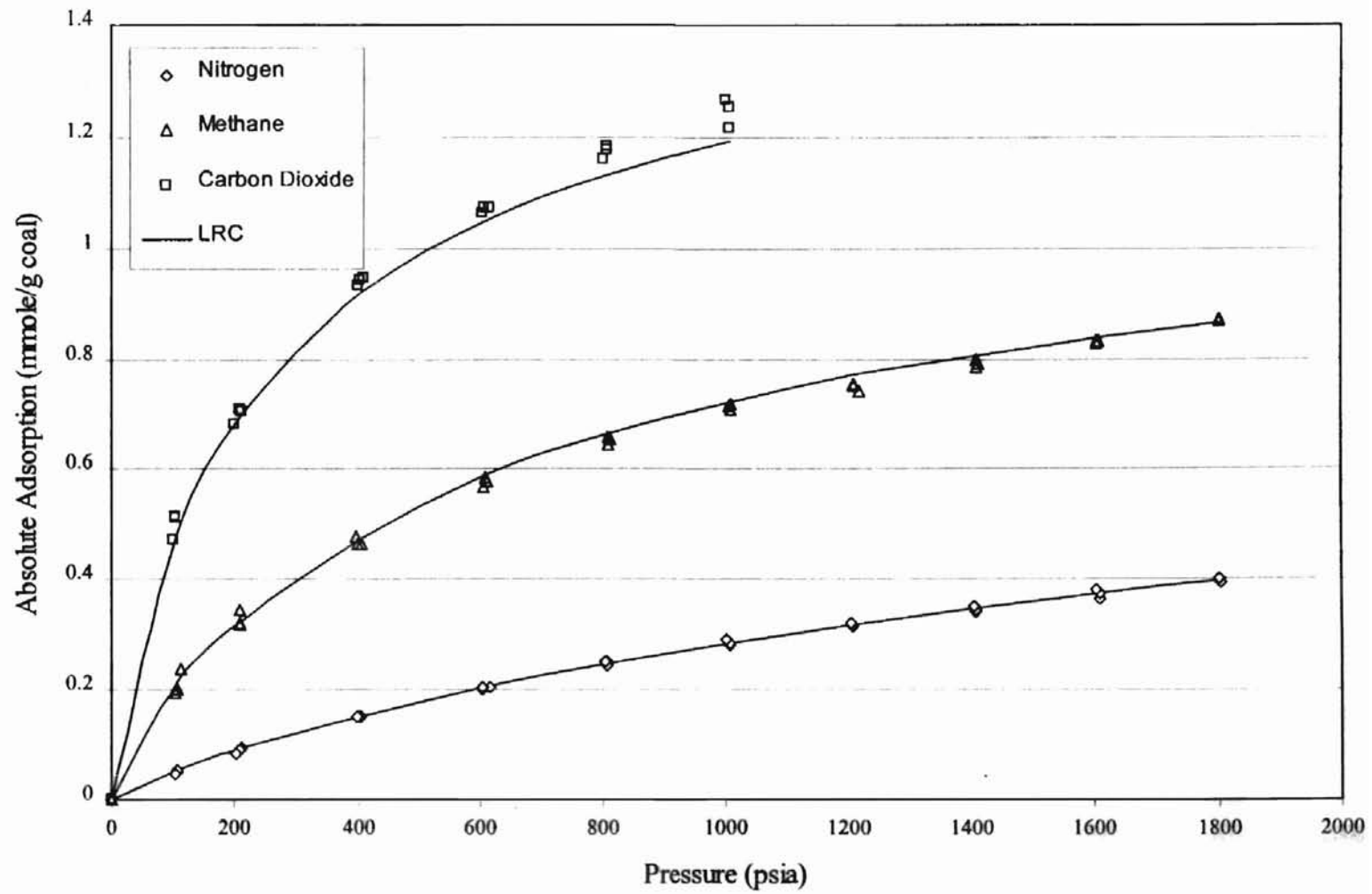
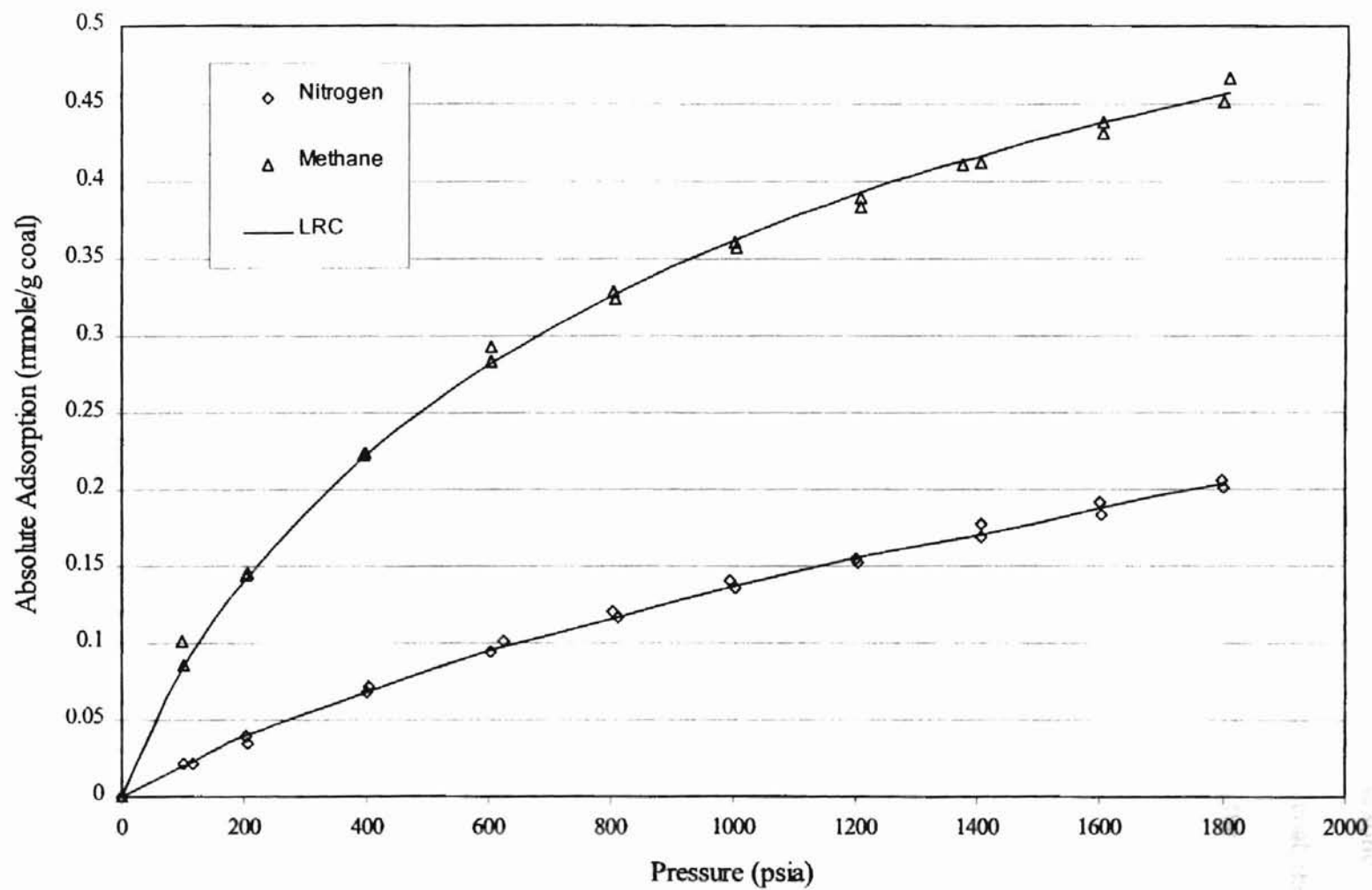


Figure 36. LRC Representation of Gas Adsorption on Wet Illinois-6 Coal at 115 °F



$$\theta = \frac{BP^{1/n}}{1 + BP^{1/n}}$$

7-2

In this model, n equals the number of sites one gas molecule occupies on the solid surface, and $\eta = 1/n$. In this work, we set the $\eta = 0.87$ [32]. For Fruitland coal, the correlation results are shown in Table 14 and Figure 35. For Illinois-6 coal, the correlation results are shown in Table 15 and Figure 36.

TABLE 12. Simple Langmuir Model Representation of Adsorption on Fruitland Coal

Component	L (mmole/g coal)	B (psia ⁻¹)	RMSE	AAPD
CH ₄ (Run1)	1.077	0.00208	0.0188	3.26
CH ₄ (Run2)	1.107	0.00184	0.0096	1.89
CH ₄ (Run3)	1.112	0.00180	0.0126	2.43
CH ₄ (Overall)	1.099	0.00195	0.0196	2.93
N ₂ (Run1)	0.715	0.000656	0.0033	1.63
N ₂ (Run2)	0.751	0.000613	0.0038	2.49
N ₂ (Run3)	0.766	0.000606	0.0013	0.78
N ₂ (Overall)	0.742	0.000626	0.0042	2.05
CO ₂ (Run1)	1.395	0.00497	0.0158	1.75
CO ₂ (Run2)	1.456	0.00441	0.0226	2.46
CO ₂ (Run3)	1.488	0.00411	0.0199	1.77
CO ₂ (Overall)	1.445	0.00448	0.0229	2.28

ZGR Equation of State

A 2-D equation of state developed from generalized cubic equation of state by Zhou is used to correlate the experiment data [33]. The equation is expressed as follow:

$$\left[A\pi + \frac{\alpha\omega^2}{1 + U\beta\omega + W(\beta\omega)^2} \right] [1 - (\beta\omega)^m] = \omega RT \quad 7-4$$

TABLE 13. Simple Langmuir Model Representation of Adsorption on Illinois-6 Coal

Component	L (mmole/g coal)	B (psia ⁻¹)	RMSE	AAPD
CH ₄ (Run1)	0.638	0.00134	0.0070	2.51
CH ₄ (Run2)	0.602	0.00153	0.0083	3.13
CH ₄ (Overall)	0.620	0.00143	0.0083	2.97
N ₂ (Run1)	0.461	0.000416	0.0016	1.18
N ₂ (Run2)	0.455	0.000452	0.0019	2.00
N ₂ (Overall)	0.457	0.000435	0.0031	2.99

TABLE 14. LRC Model Representation of Adsorption on Fruitland Coal ($\eta=0.87$)

Component	L (mmole/g coal)	B (psia ⁻¹)	RMSE	AAPD
CH ₄ (Run1)	1.203	0.00367	0.0124	1.9
CH ₄ (Run2)	1.249	0.00324	0.004	0.43
CH ₄ (Run3)	1.258	0.00317	0.0057	0.9
CH ₄ (Overall)	1.234	0.00344	0.0166	2.01
N ₂ (Run1)	0.959	0.00101	0.0029	1.72
N ₂ (Run2)	1.028	0.000930	0.0012	0.31
N ₂ (Run3)	1.053	0.000916	0.0029	1.86
N ₂ (Overall)	1.011	0.000953	0.0037	1.68
CO ₂ (Run1)	1.513	0.00839	0.0088	0.92
CO ₂ (Run2)	1.595	0.00738	0.0148	1.64
CO ₂ (Run3)	1.640	0.00684	0.0136	1.05
CO ₂ (Overall)	1.580	0.00751	0.0166	1.55

where ω is the absolute adsorption volume, $m=1/3$, $U=0$, $W=0$, which are optimized by Zhou [32]. This model can predict the adsorption on wet Fruitland coal within 2.0 AAPD. The results are listed in the Table 16 and Figure 37. For Illinois-6 coal, the AAPD is within 3.0. Results are shown in Table 17 and Figure 38.

TABLE 15. LRC Model Representation of Adsorption on Illinois Coal ($\eta=0.87$)

Component	L (mmole/g coal)	B ($psia^{-1}$)	RMSE	AAPD
CH ₄ (Run1)	0.747	0.00231	0.0042	0.93
CH ₄ (Run2)	0.693	0.00267	0.0053	2.15
CH ₄ (Overall)	0.719	0.00248	0.0056	1.58
N ₂ (Run1)	0.744	0.000539	0.0019	3.12
N ₂ (Run2)	0.698	0.000616	0.0014	1.36
N ₂ (Overall)	0.719	0.000578	0.0031	3.20

PGR Equation of State

A new 2-D equation of state developed from the PGR equation of state was also used to correlate the experiment data. The equation is expressed as follow (details appear in Appendix D)

$$A\pi = \omega RT + cRT\omega \left(\frac{\beta_1 \tau l \omega}{1 - \beta_2 \tau l \omega} - \frac{Z_M Y l \omega}{1 + U l \omega + W (l \omega)^2} - \frac{Q_1 Z_M Y l \omega}{1 + Q_2 l \omega} \right) \quad 7-3$$

where

$$Y = \exp(F_i) - 1$$

$$F_i = \omega_1 \left(\frac{1}{2\tilde{T}} \right)^{1/2} + \omega_2 \left(\frac{1}{2\tilde{T}} \right) + \omega_3 \left(\frac{1}{2\tilde{T}} \right)^{3/2} + \omega_4 \left(\frac{1}{2\tilde{T}} \right)^2$$

$$\tilde{T} = \frac{T}{T^*}$$

where ω is the absolute adsorption. The other universal constants and gas parameters are listed in Tables 18 and 19, as regressed by Park [27].

This model can predict the adsorption on wet Fruitland coal within 2.0 AAPD. The result is listed in the below Table 20 and Figure 39.

Figure 37. ZGR Representation of Gas Adsorption on Wet Fruitland Coal at 115 °F

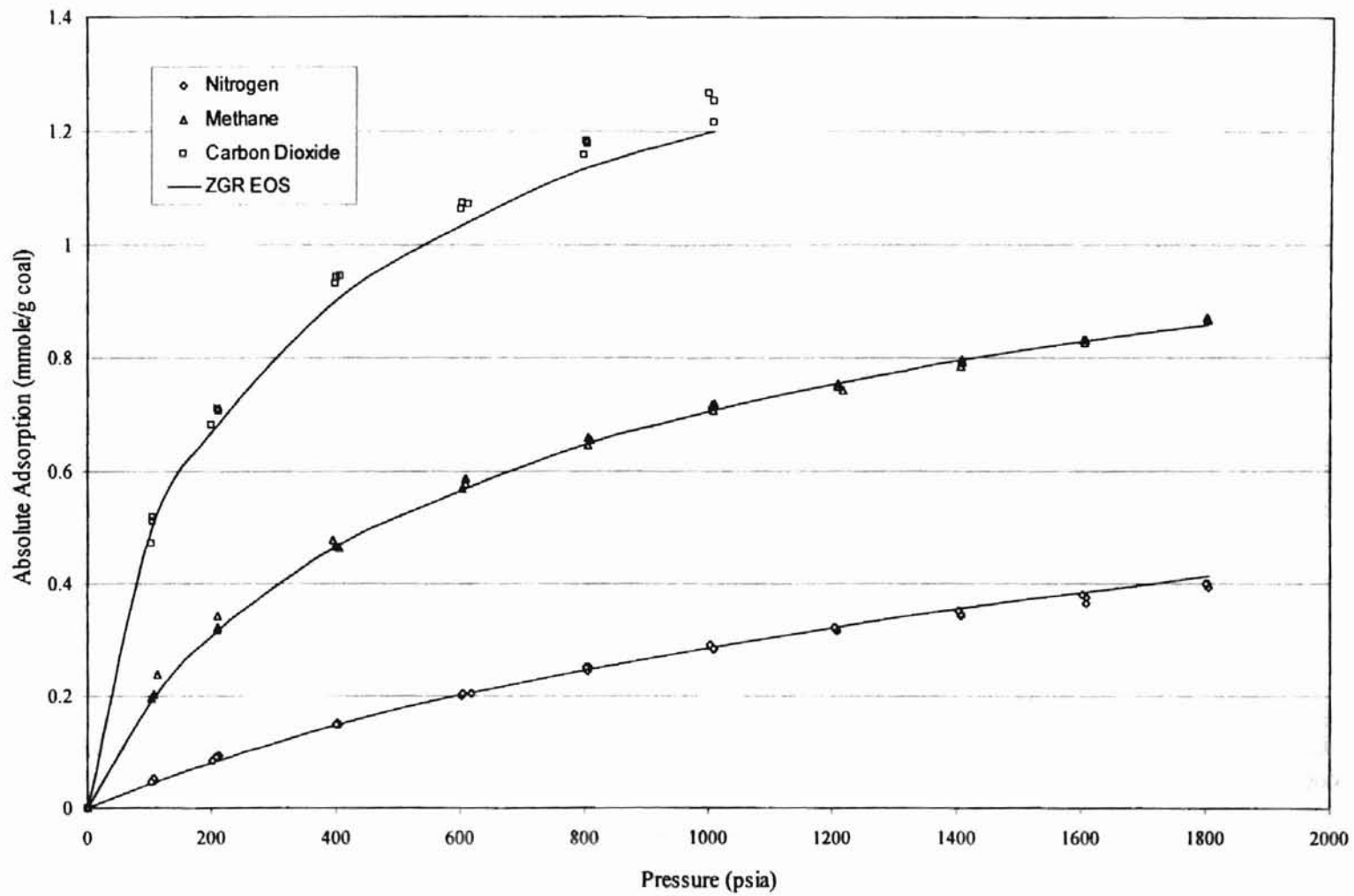
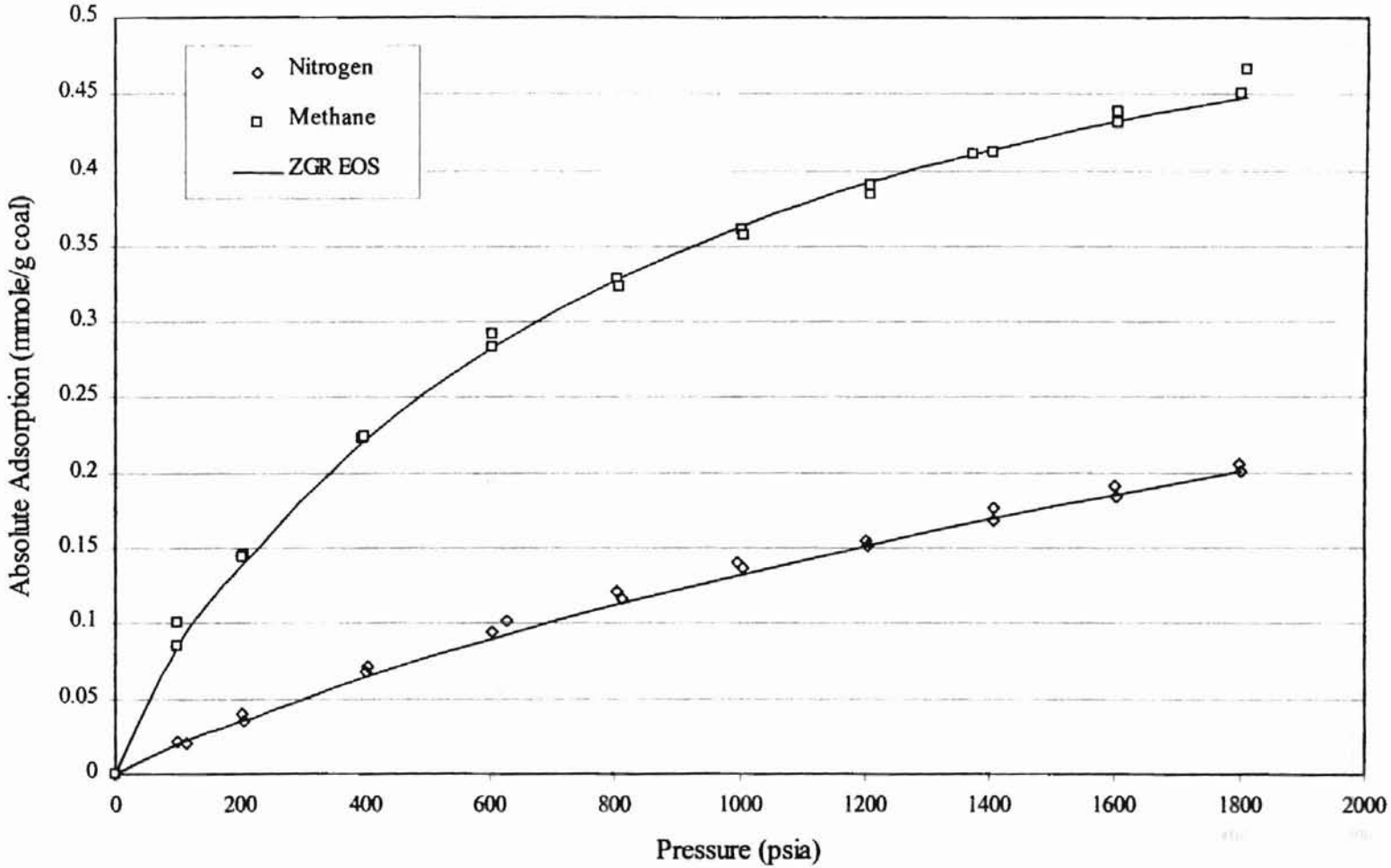


Figure 38. ZGR Representation of Gas Adsorption on Wet Illinois-6 Coal at 115 °F



06

Figure 39. PGR Representation of Gas Adsorption on Wet Fruitland Coal at 115 °F

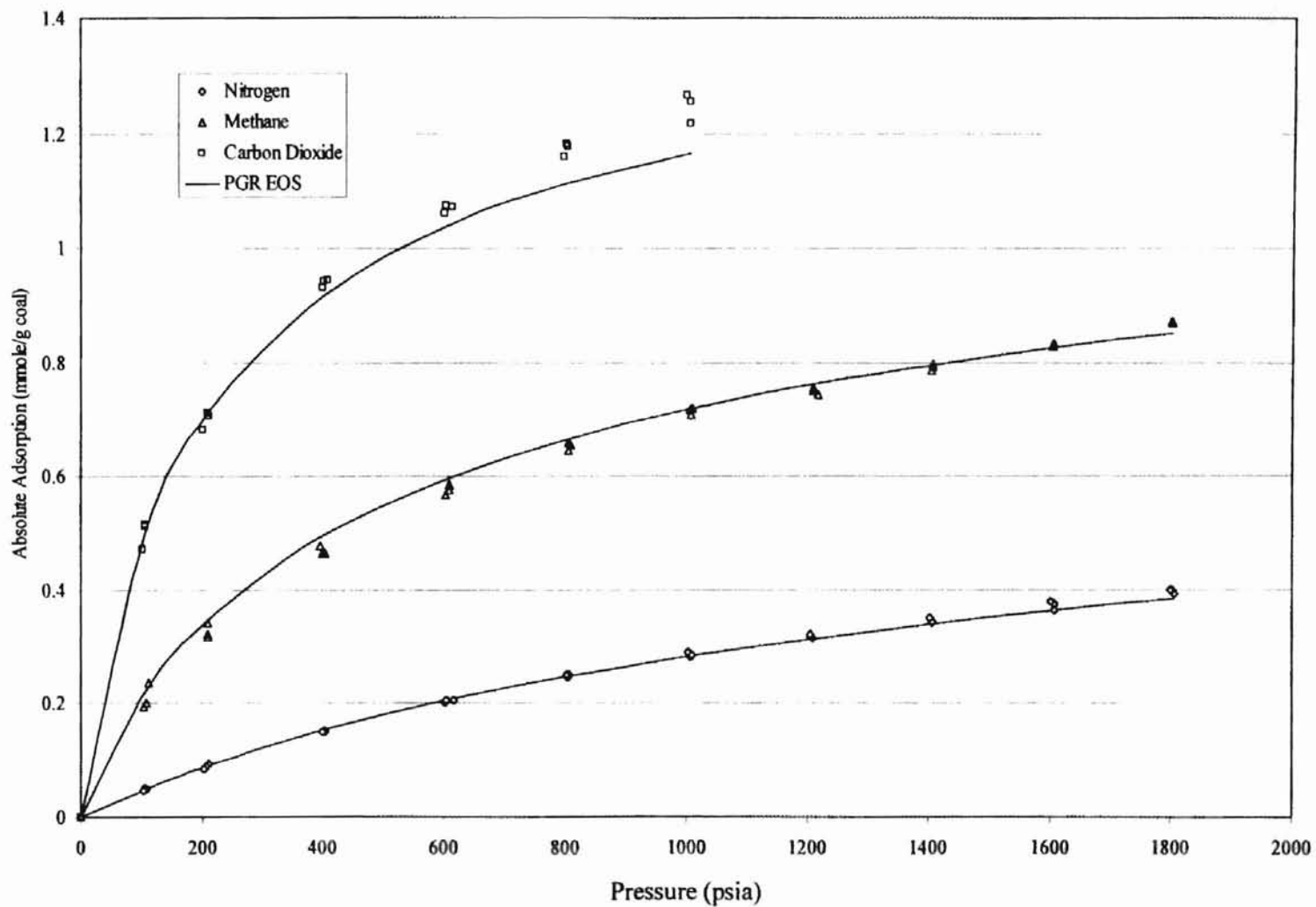


TABLE 16. ZGR Equation of State Representation of Adsorption on Fruitland Coal

Component	α	β	$-\ln k$	RMSE	AAPD
CH_4 (Run1)	34992	0.3612	1.56	0.0087	0.69
CH_4 (Run2)	55500	0.4479	1.84	0.0052	0.61
CH_4 (Run3)	47546	0.4122	1.79	0.0051	0.69
CH_4 (Overall)	50800	0.4298	1.77	0.0105	1.61
N_2 (Run1)	-24030	0.0010	4.72	0.0032	1.55
N_2 (Run2)	-17878	0.0069	4.56	0.0013	0.27
N_2 (Run3)	-19101	0.0010	4.79	0.0048	1.18
N_2 (Overall)	-22611	0.0010	4.73	0.0041	1.55
CO_2 (Run1)	7333	0.1692	0.37	0.0079	0.43
CO_2 (Run2)	6208	0.1509	0.48	0.0092	0.70
CO_2 (Run3)	33100	0.2973	0.60	0.0172	0.97
CO_2 (Overall)	8265	0.1661	0.45	0.0145	1.33

TABLE 17. ZGR Equation of State Representation of Adsorption on Illinois-6 Coal

Component	α	β	$-\ln k$	RMSE	AAPD
CH_4 (Run1)	113270	0.853	2.77	0.0069	1.25
CH_4 (Run2)	40935	0.486	2.56	0.0053	1.53
CH_4 (Overall)	100760	0.802	2.69	0.0060	1.65
N_2 (Run1)	-25915	0.001	5.78	0.0028	2.02
N_2 (Run2)	-31879	0.003	5.53	0.0013	0.74
N_2 (Overall)	-19545	0.014	5.46	0.0031	3.09

TABLE 18. Pure Fluid Parameters for PGR Equation of State [6]

Component	T^* (K)	C
Methane	81.287	1.0
Nitrogen	95.0	1.0
Carbon Dioxide	111.31	1.6565

TABLE 19. Universal Constants of PGR Equation of State

Constants	Value
τ	0.74048
U	-2.8969
W	2.6944
Q_1	10.5121
Q_2	1.0226
Z_M	0.4
ω_1	0.076354
ω_2	2.0124
ω_3	-0.22322
ω_4	-0.70301

TABLE 20. PGR Equation of State Representation of Adsorption on Wet Fruitland Coal

Component	l	$-\ln k$	RMSE	AAPD
CH_4 (Run1)	0.284	3.16	0.0141	1.84
CH_4 (Run2)	0.259	3.34	0.0046	0.72
CH_4 (Run3)	0.262	3.33	0.0074	0.96
CH_4 (Overall)	0.267	3.28	0.0111	1.78
N_2 (Run1)	0.441	4.91	0.0045	1.61
N_2 (Run2)	0.440	4.88	0.0055	1.89
N_2 (Run3)	0.391	4.95	0.0015	0.64
N_2 (Overall)	0.420	4.92	0.0046	1.77
CO_2 (Run1)	0.174	2.08	0.0102	1.04
CO_2 (Run2)	0.165	2.15	0.0189	1.98
CO_2 (Run3)	0.155	2.25	0.0166	1.05
CO_2 (Overall)	0.164	2.17	0.0184	1.78

SLD Model

The SLD model was used to correlate the experimental data. The constants, such as fluid-fluid distance, fluid-solid distance, layer of solid and molecule density, are listed below [21].

$$\sigma_{ff} = 3.82nm$$

$$\sigma_{fs} = 5.2nm$$

$$\alpha = 3.35nm$$

$$\rho_{atom} = 0.382atom / \text{\AA}^2$$

The regression results are shown in Table 21 and Figure 40 for Fruitland coal adsorption, in Table 22 for Illinois-6 coal.

TABLE 21. SLD Model Representation of Adsorption on Fruitland Coal

Component	$\varepsilon_{ff} / k(K)$	SA(m^2)	RMSE	AAPD
CH ₄ (Run1)	47.46	119.9	0.0134	1.21
CH ₄ (Run2)	43.58	129.5	0.0076	0.86
CH ₄ (Run3)	43.54	129.3	0.0084	0.83
CH ₄ (Overall)	44.9	125.9	0.0122	1.94
N ₂ (Run1)	24.67	122.6	0.0047	2.45
N ₂ (Run2)	23.61	131.3	0.0057	3.74
N ₂ (Run3)	23.2	136.4	0.0028	1.95
N ₂ (Overall)	24.04	128.4	0.0055	2.86
CO ₂ (Run1)	45.12	105.7	0.0479	4.99
CO ₂ (Run2)	51.90	84.36	0.0422	4.27
CO ₂ (Run3)	53.47	80.79	0.0490	5.75
CO ₂ (Overall)	49.16	92.01	0.0474	5.13

Figure 40. SLD Representation of Gas Adsorption on Wet Fruitland Coal at 115 °F

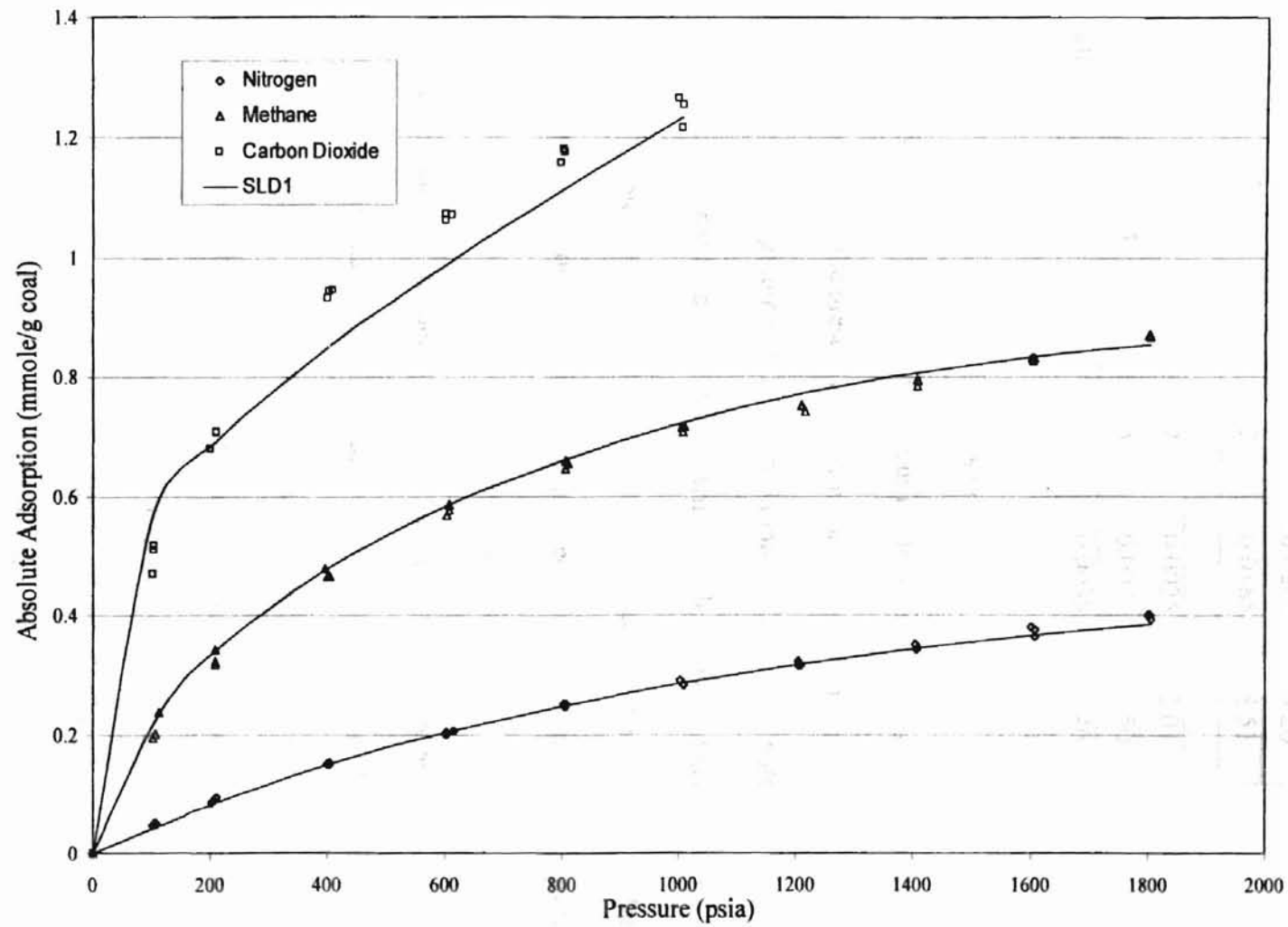


Fig. 40. SLD1 Representation of Gas Adsorption on Wet Fruitland Coal

R² = 0.999
 RMSE = 0.010
 CAPD = 0.20
 0.51

TABLE 22. SLD Model Representation of Adsorption on Illinois-6 Coal

Component	$\varepsilon_f / k(K)$	SA(m^2)	RMSE	AAPD
CH ₄ (Run1)	29.51	102.6	0.0163	7.73
CH ₄ (Run2)	28.61	101.8	0.0204	9.20
CH ₄ (Overall)	29.05	102.2	0.0185	8.51
N ₂ (Run1)	16.91	99.14	0.0025	2.01
N ₂ (Run2)	18.64	90.45	0.0030	3.50
N ₂ (Overall)	18.18	91.79	0.0038	3.46

Discussion

Tables 23 to 25 present a summary of our model evaluation results for the five models we used to correlate the present adsorption data for methane, nitrogen, and CO₂. The models include the Langmuir and LCR correlation, the ZGR and PGR 2-D EOS, and the PR-SLD model. The model parameters, shown in Table 23, were determined by minimizing the sum of squares of percentage errors in the calculated adsorption, ω , for the pure gas of interest. The quality of the fit, expressed in terms of the average absolute percentage deviation (AAPD), is given in Table 24. Figures illustrate the abilities of the LRC, the ZGR EOS, and SLD model to describe the present pure-fluid adsorption data.

Our results indicate that the LRC produces better quality fit than the Langmuir correlation for the three gases studied (within 2 AAPD), reflecting in part the use of one additional parameter ($\eta=0.87$) in the model. The results also reveal the ability of the ZGR EOS to represent the present systems well within their expected experimental uncertainty (within 2 AAPD). By comparison, the PR-SLD model exhibits good representation for methane adsorption comparable to the LRC, but it exhibits larger deviations for the nitrogen and CO₂ (2.9% and 5.9%, respectively). The PR-SLD model

results are not surprising in light of the assumptions made regarding the structure of the coal surface and the accuracy of the density predictions from of the PR EOS.

In these regressions, the data for CO₂ were restricted to pressures below 1000 psia, and the regression result is not good. The results indicate that the SLD model may be a suitable choice for modeling the coalbed gas adsorption. However, model improvements are required to (a) account for coal heterogeneity and structure complexity, and (b) provide for more accurate equations of state, which are capable of modeling coalbed gas environments.

TABLE 23. Regression Results for Adsorption of Methane, Nitrogen, and Carbon Dioxide on Wet Fruitland Coal at 115 °F

Models	Model Parameters	Pure Gas Adsorbed		
		Methane (0-1800 psia)	Nitrogen (0-1800 psia)	Carbon Dioxide (0-1000 psia)
Langmuir	$B_i(1/\text{psia})$	0.001953	0.000626	0.004487
	$L_i(\text{mmole/g coal})$	1.099	0.7428	1.445
LCR	η_i	0.87	0.87	0.87
	$B_i(1/\text{psia})$	0.003448	0.000954	0.007518
	$L_i(\text{mmole/g coal})$	1.234	1.011	1.580
ZGR EOS	$\alpha_i \times 10^{-4}$	5.080	-2.261	0.8265
	$\beta I(\text{g coal/mmole})$	0.4298	0.001	0.1661
	$-\ln k_i$	1.779	4.736	0.4587
PGR EOS	Z_M	0.40	0.40	0.40
	$V^* / A (\text{m})$	0.2675	0.4205	0.1649
	$-\ln k_i$	3.289	4.922	2.171
PR-SLD	$\epsilon_{fs} / k (\text{K})$	44.9	24.04	49.16
	$SA (\text{m}^2)$	125.90	128.40	92.01

TABLE 24. Summary of the Model Results for Gas Adsorption on Wet Fruitland Coal at 115 °F

Model	No. of Regressed Parameters	AAPD		
		Methane (30)*	Nitrogen (30)	Carbon Dioxide (18)
Langmuir	2	2.9	2.1	2.3
LRC	2	2.0	1.7	1.6
ZGR EOS	3	1.6	1.6	1.3
PGR EOS	3	1.8	1.8	1.8
PR-SLD	2	1.9	2.9	5.1

* Number of data points

LRC Model for Binary Mixture

LRC model can be extended to correlate the binary mixture adsorption. The equation can be expressed as:

$$\theta = \frac{\omega}{L} = \frac{B_i(Py_i)^\eta}{1 + \sum B_j(Py_j)^\eta} \quad 7-5$$

where $\eta = 0.87$, and y_i is the equilibrium gas mole fraction, which is obtained from the GC analysis.

The results are shown in Table 25 and Figures 41 to 46. The regression results for different binary mixture adsorption show that the LRC model can regress the experimental data within 5% at some compositions, but not all. The AAPD values of the correlation are shown in the Table 25. The total adsorption can be correlated within 5%, but for the individual gas, the regression results are not very good, some of them yield up to 30.0 AAPD.

Figure 41. LRC Representation of Methane/Nitrogen Binary Mixture Adsorption on Wet Fruitland Coal at 115 °F: Methane

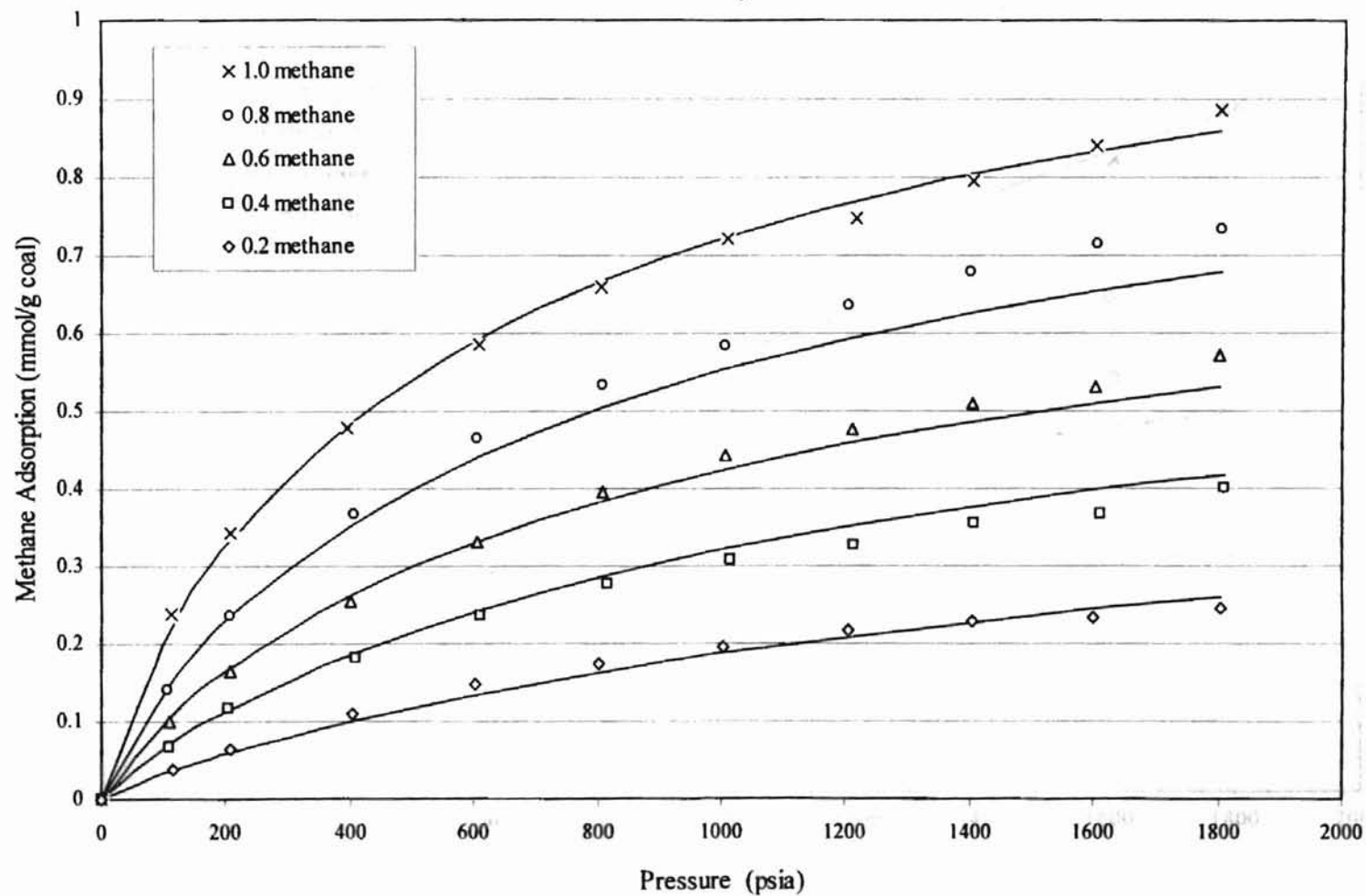


Figure 42. LRC Representation of Methane/Nitrogen Binary Mixture Adsorption on Wet Fruitland Coal at 115 °F: Nitrogen

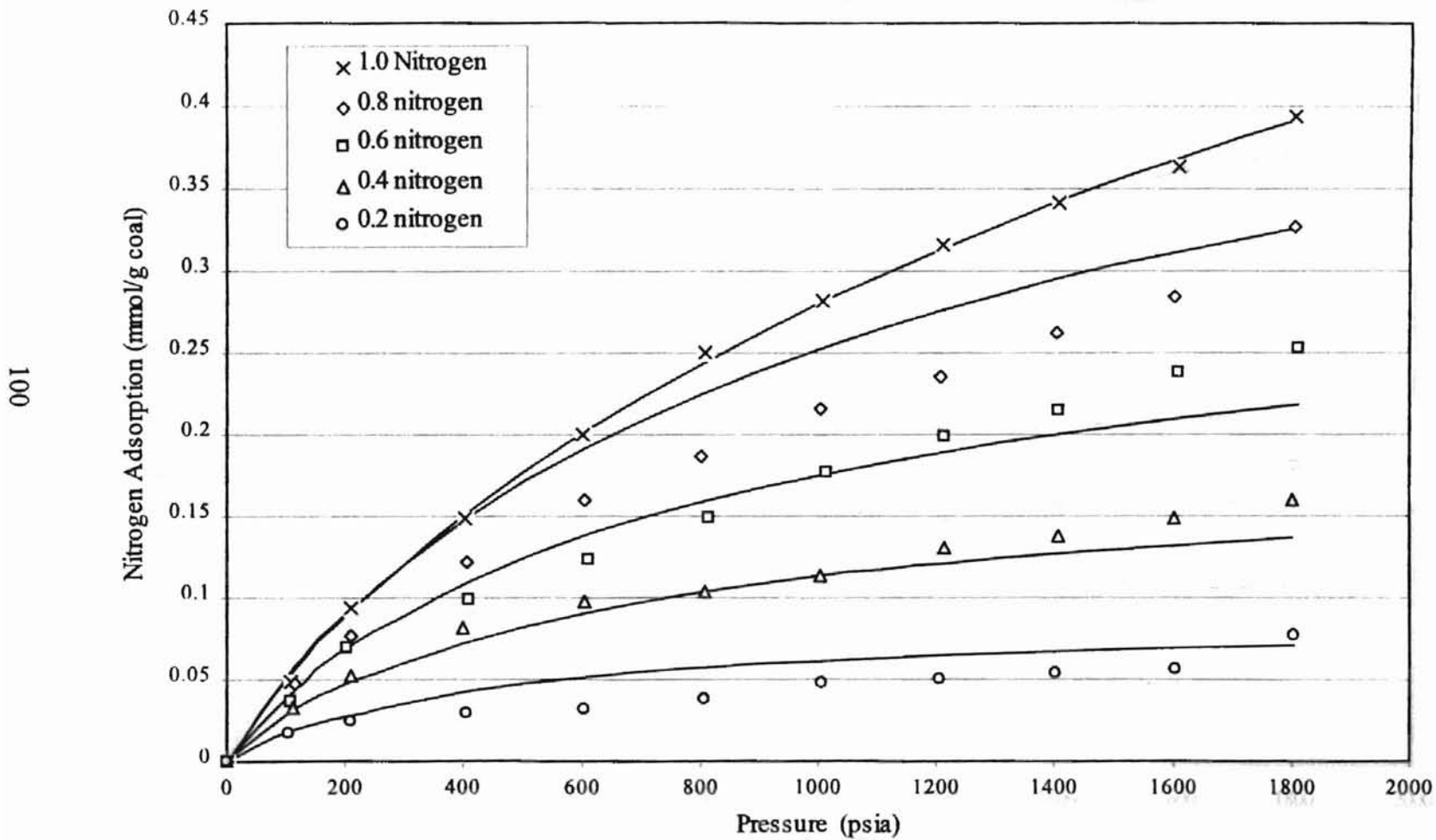


Figure 43. LRC Representation of Methane/Carbon Dioxide Binary Mixture Adsorption on Wet Fruitland Coal at 115 °F: Methane

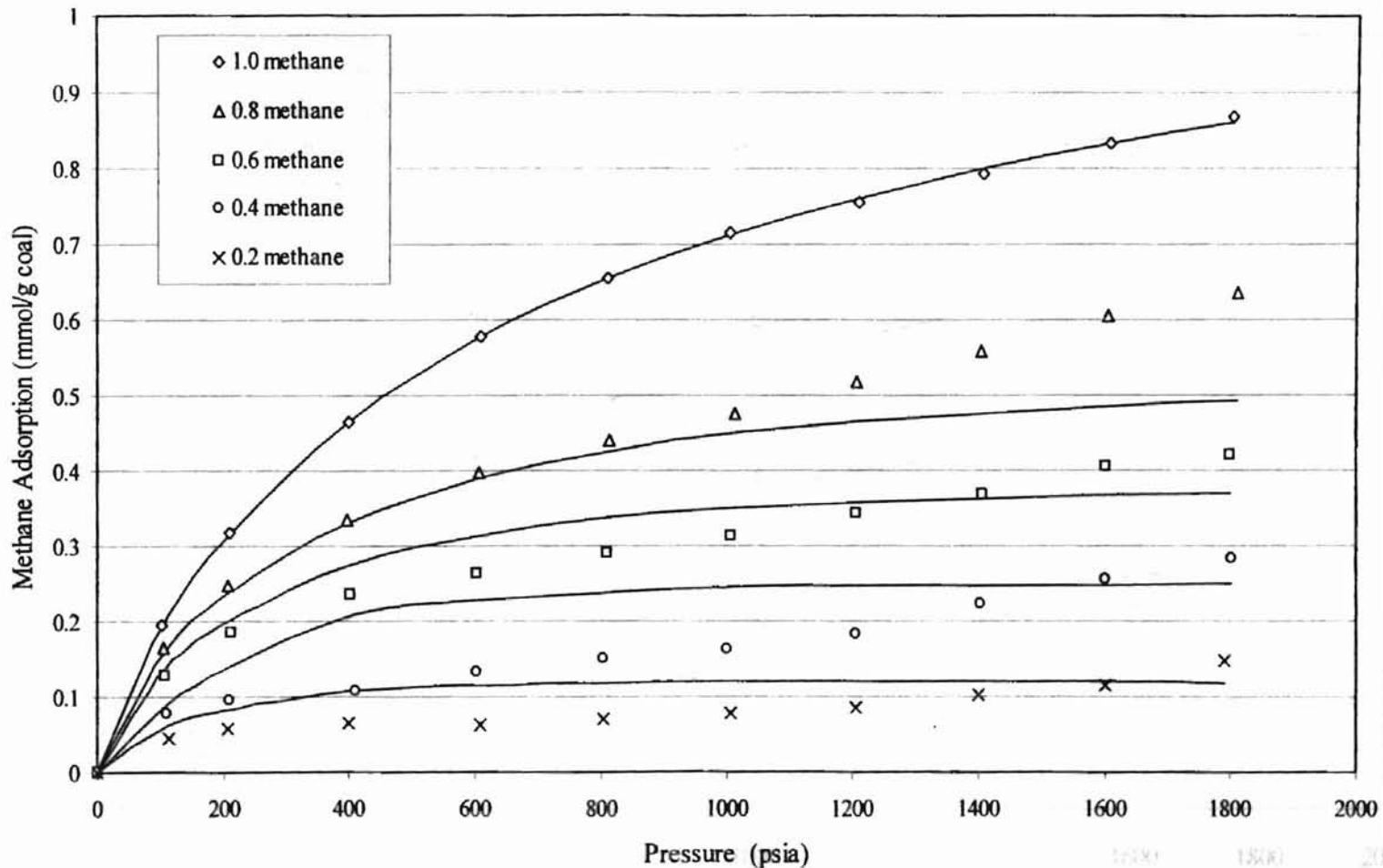


Figure 44. LRC Representation of Methane/Carbon Dioxide Binary Mixture
Adsorption on Wet Fruitland Coal at 115 °F: Carbon Dioxide

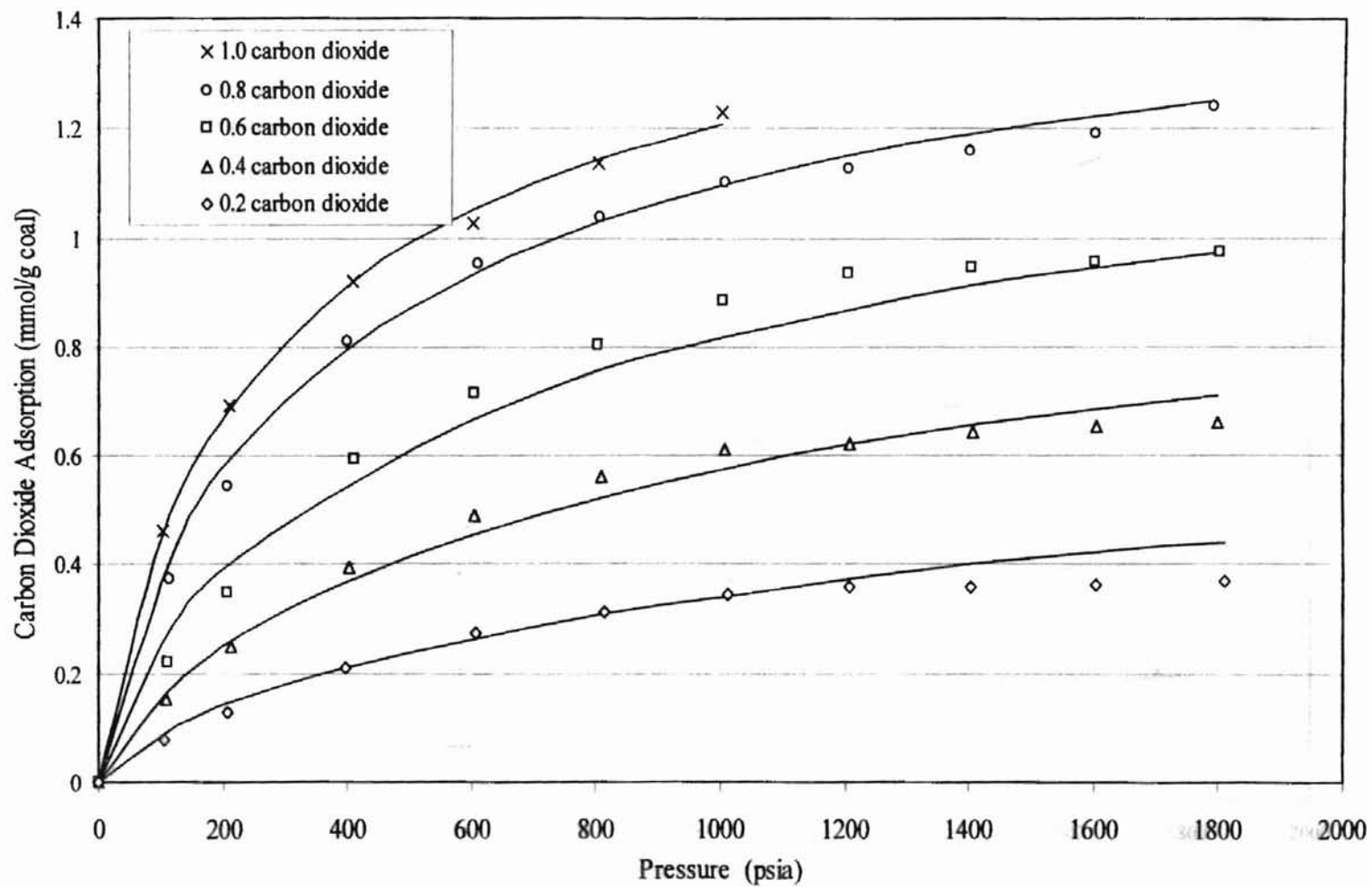


Figure 45. LRC Representation of Nitrogen/Carbon Dioxide Binary Mixture Adsorption on Wet Fruitland Coal at 115 °F: Nitrogen

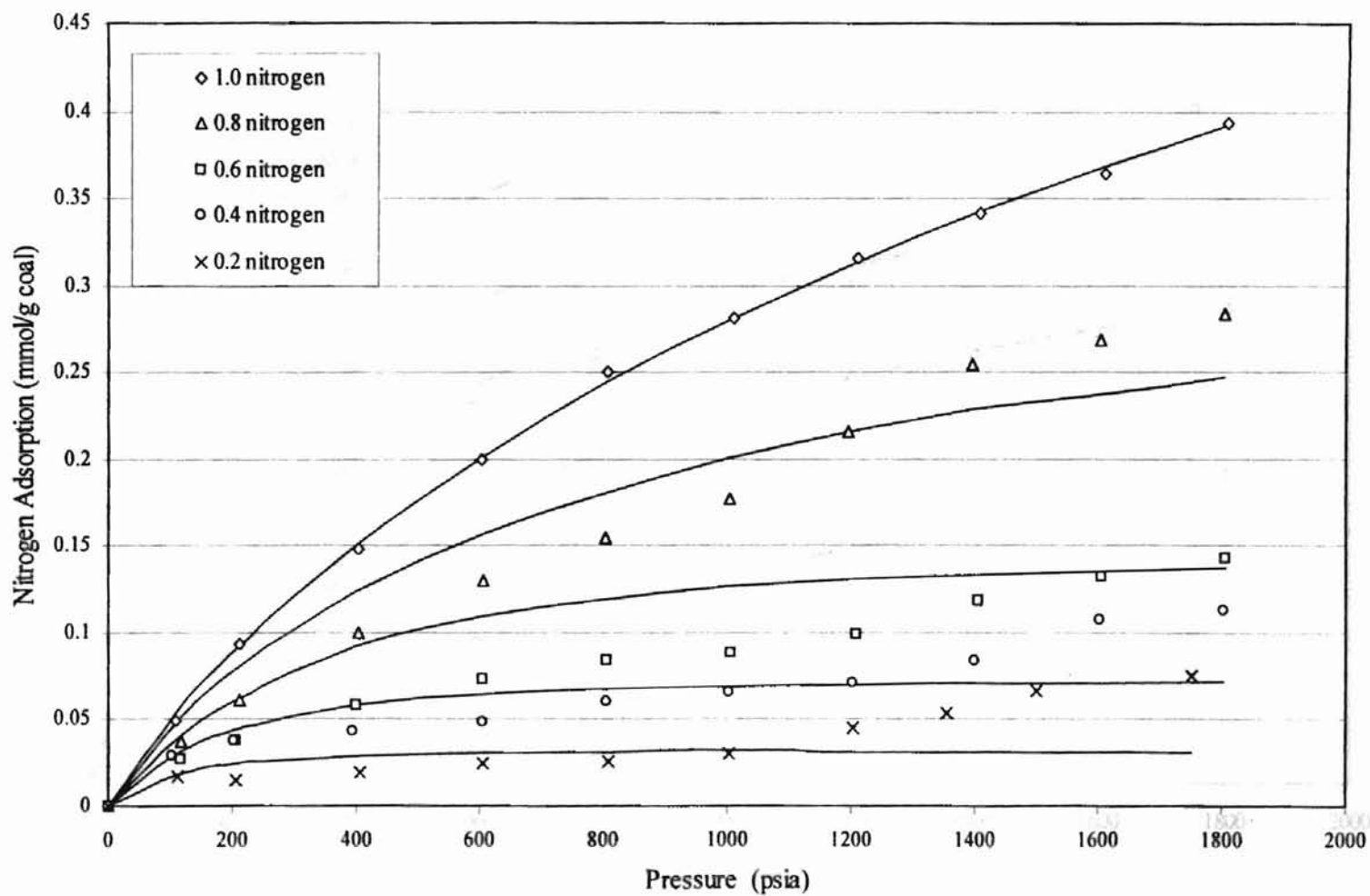
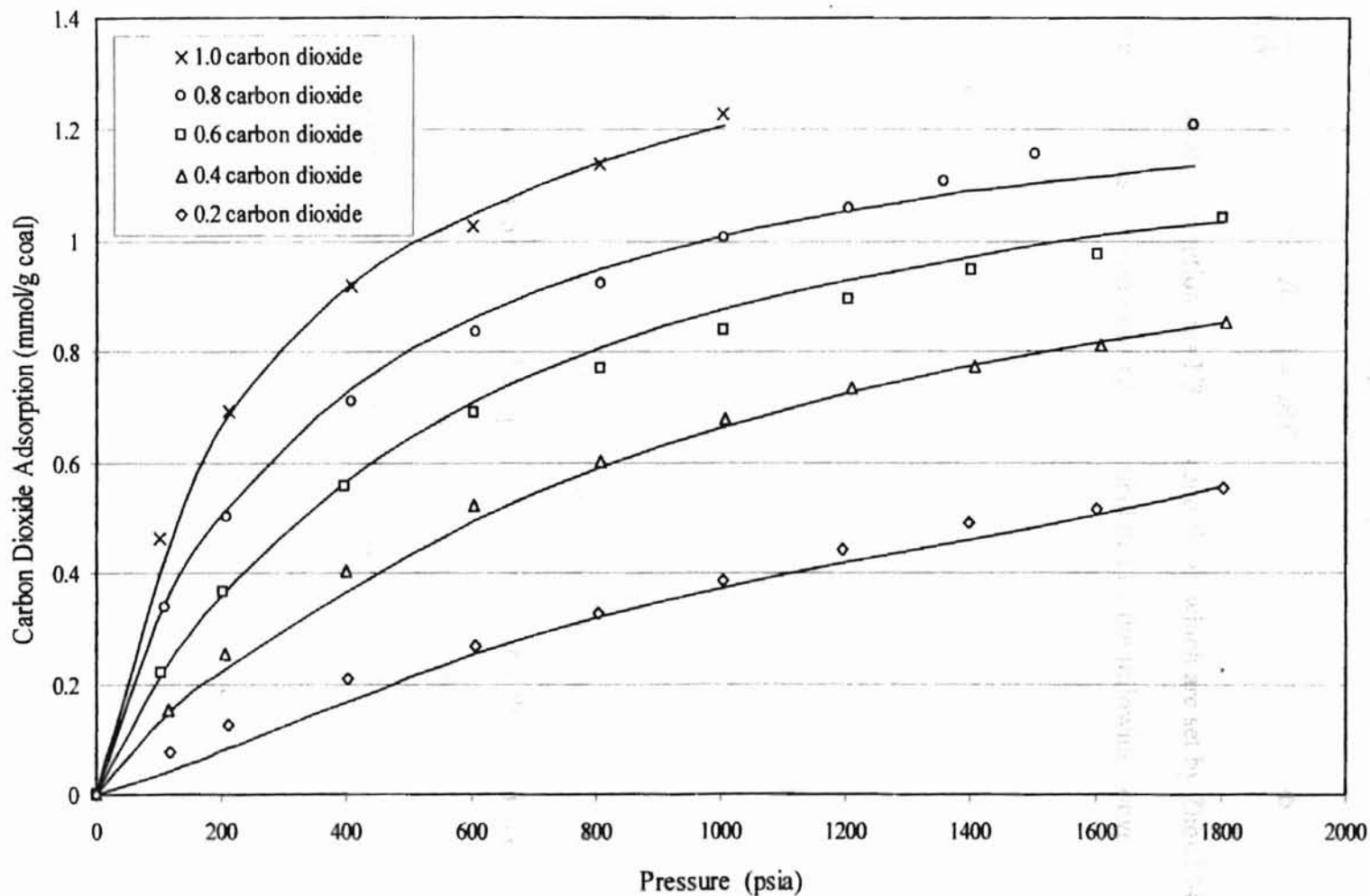


Figure 46. LRC Representation of Nitrogen/Carbon Dioxide Binary Mixture Adsorption on Wet Fruitland Coal at 115 °F: Carbon Dioxide



ZGR Equation of State for Binary Mixture

A 2-D equation of state developed from general cubic EOS by Zhou is used to correlate the experiment data [34]. The equation is expressed as follow:

$$\left[A\pi + \frac{\alpha\omega^2}{1 + U\beta\omega + W(\beta\omega)^2} \right] [1 - (\beta\omega)^m] = \omega RT \quad 7-6$$

where ω is the absolute adsorption, $m=1/3$, $U=0$ and $W=0$, which are set by Zhou [34].

For the binary gas, the constants can be calculated by the following conventional mixing rules [32].

$$\alpha = \sum_i \sum_j x_i x_j \alpha_{ij}$$
$$\beta = \sum_i \sum_j x_i x_j \beta_{ij}$$

where,

$$\alpha_{ij} = (1 - C_{ij})(\alpha_i + \alpha_j)/2$$

$$\beta_{ij} = (1 + D_{ij})\sqrt{\beta_i\beta_j}$$

The regression results are showed in the Table 26 and Figures 47 to 52. Similar to LRC model, the total adsorption can be regressed within 5%, but the individual gas can produce deviations up to 30% deviation. The AAPD and RMSE are shown in Table 26.

The comparison of both models is shown in Table 27. ZGR has better correlation results than LRC model.

Figure 47. ZGR Representation of Methane/Nitrogen Binary Mixture
Adsorption on Wet Fruitland Coal at 115 °F: Methane

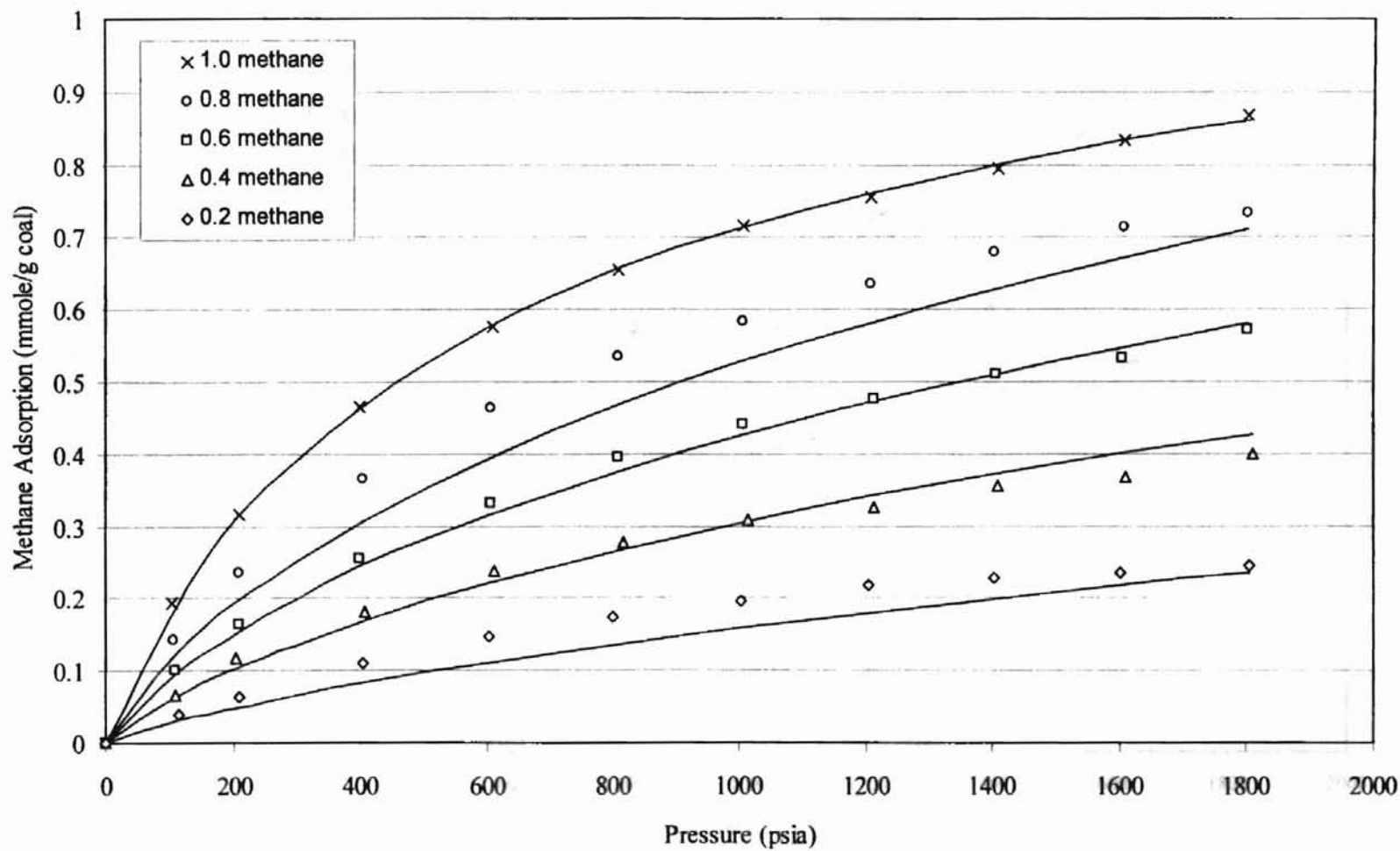


Figure 48. ZGR Representation of Methane/Nitrogen Binary Mixture
Adsorption on Wet Fruitland Coal at 115 °F: Nitrogen

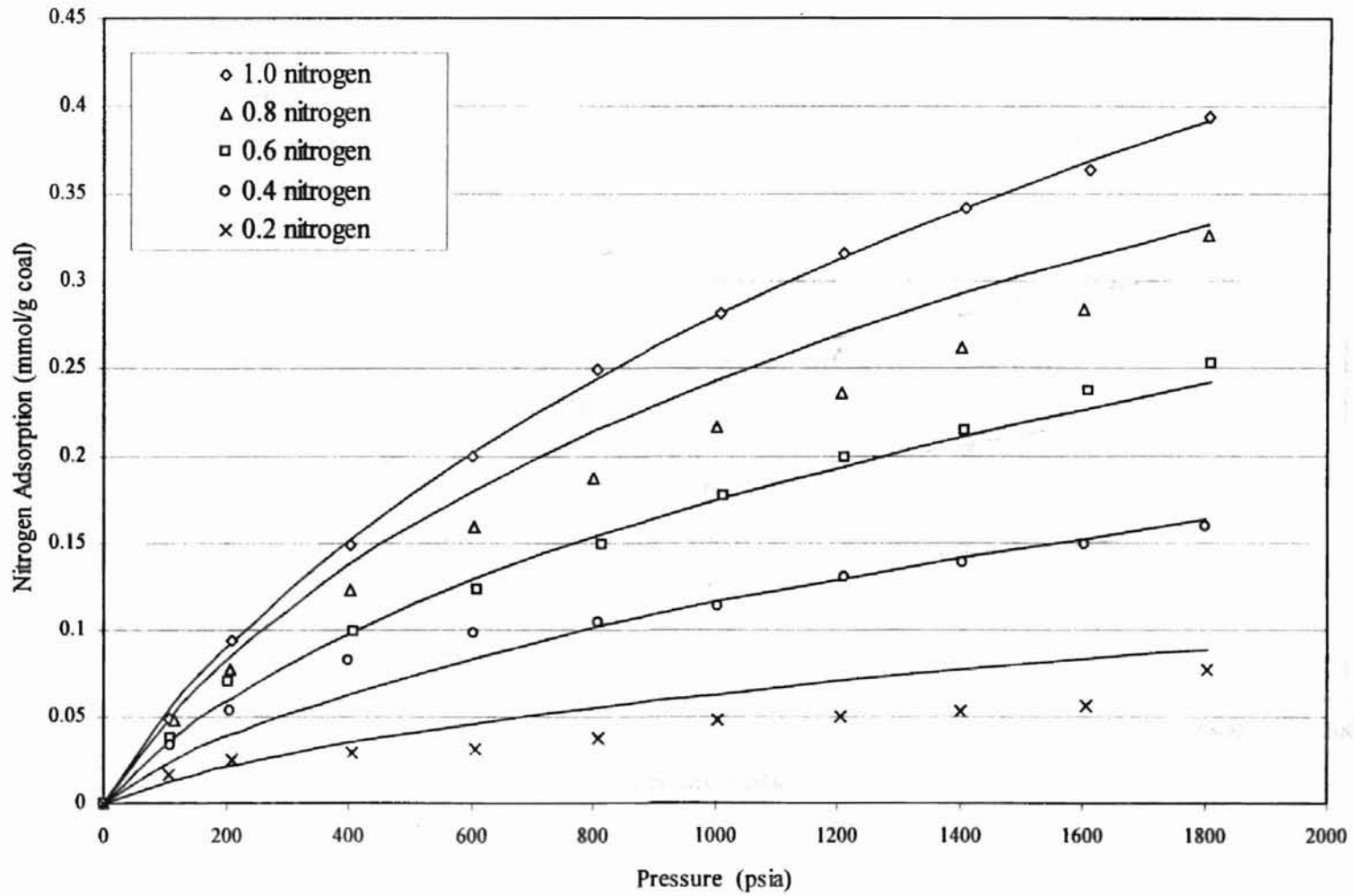


Figure 49. ZGR Representation of Methane/Carbon Dioxide Binary Mixture Adsorption on Wet Fruitland Coal at 115 °F: Methane

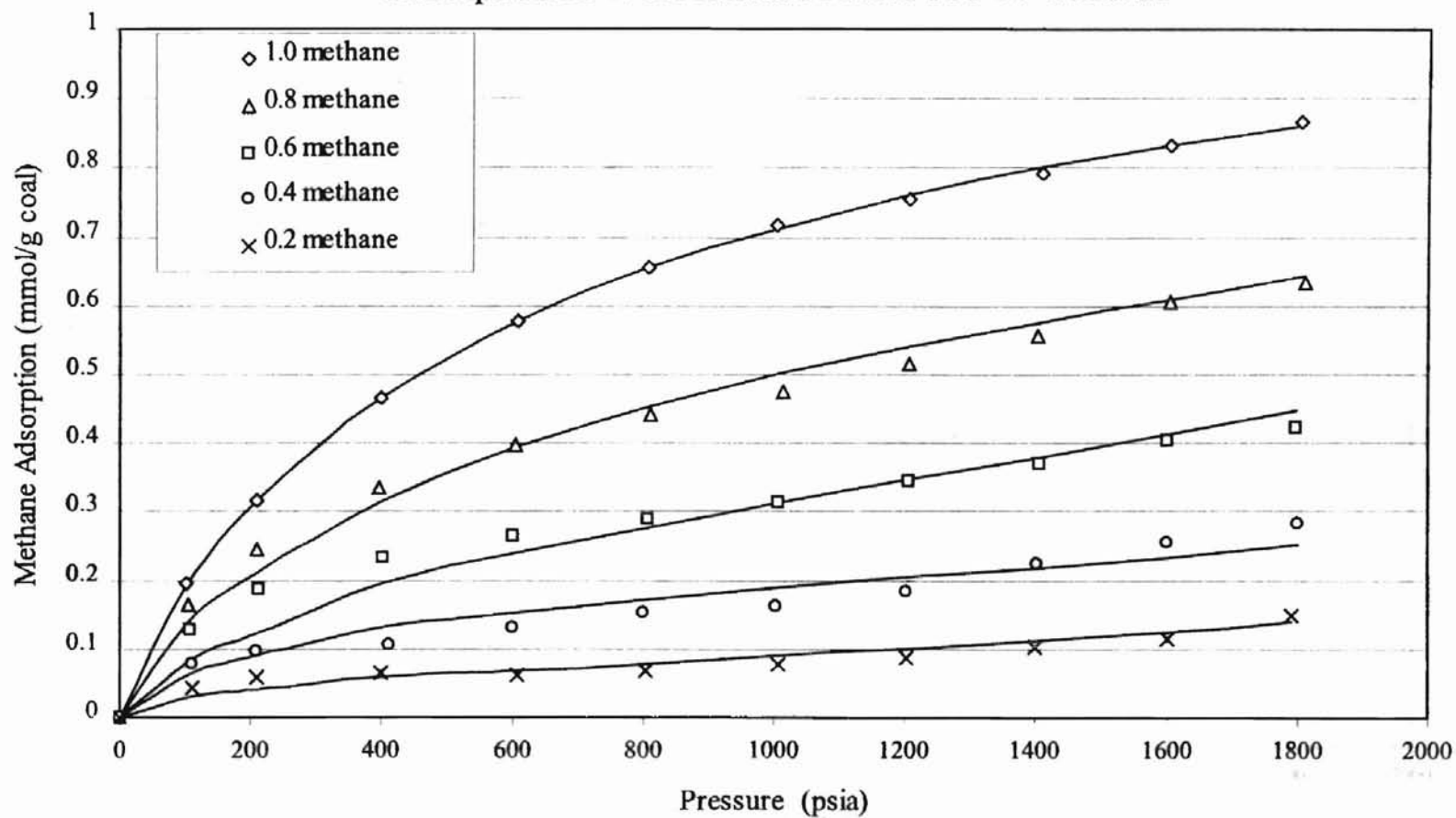


Figure 50. ZGR Representation of Methane/Carbon Dioxide Binary Mixture
 Adsorption on Wet Fruitland Coal at 115 °F: Carbon Dioxide

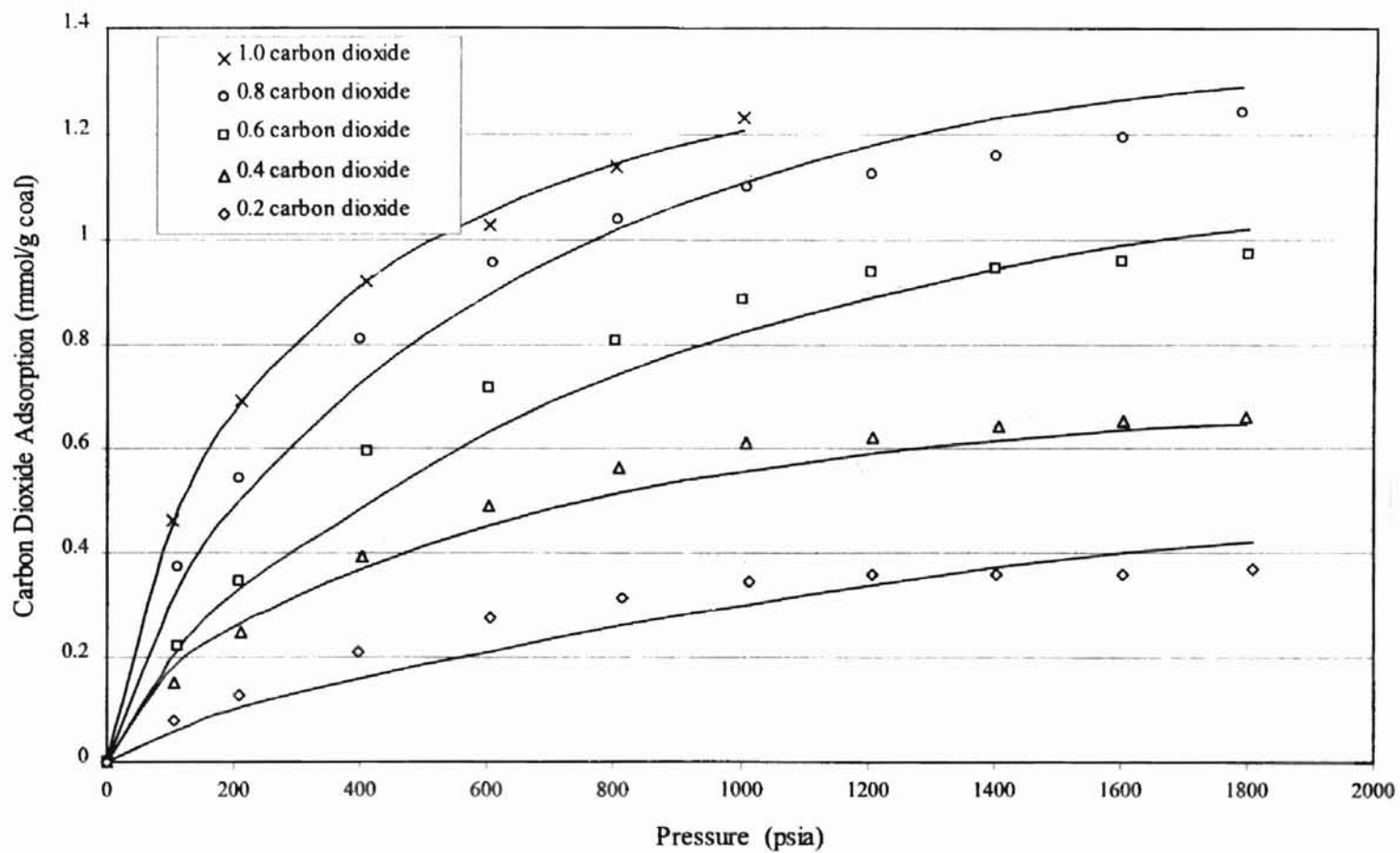


Figure 51. ZGR Representation of Nitrogen/Carbon Dioxide Binary Mixture Adsorption on Wet Fruitland Coal at 115 °F: Nitrogen

110

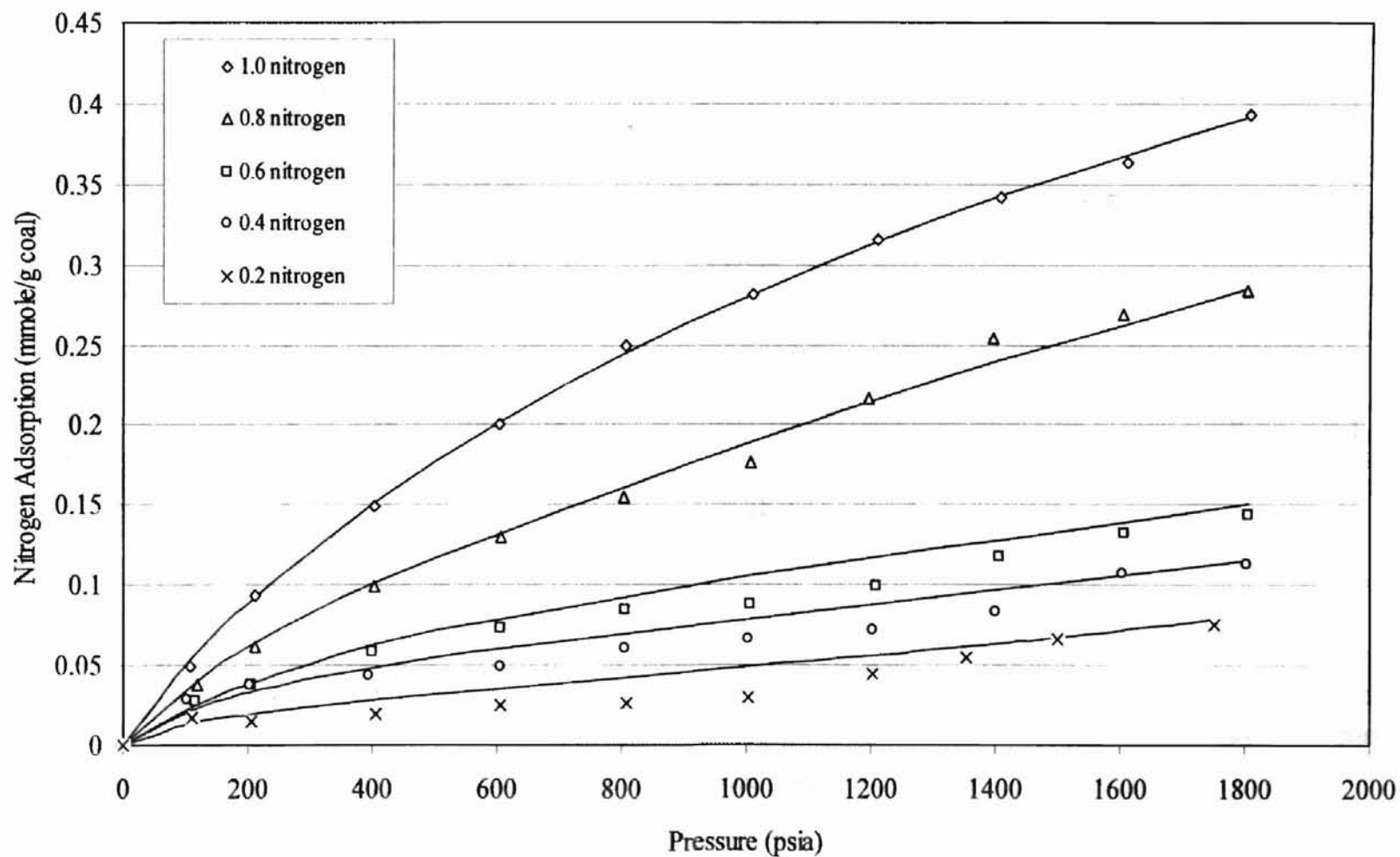


Figure 52. ZGR Representation of Nitrogen/Carbon Dioxide Binary Mixture
Adsorption on Wet Fruitland Coal at 115 °F: Carbon Dioxide

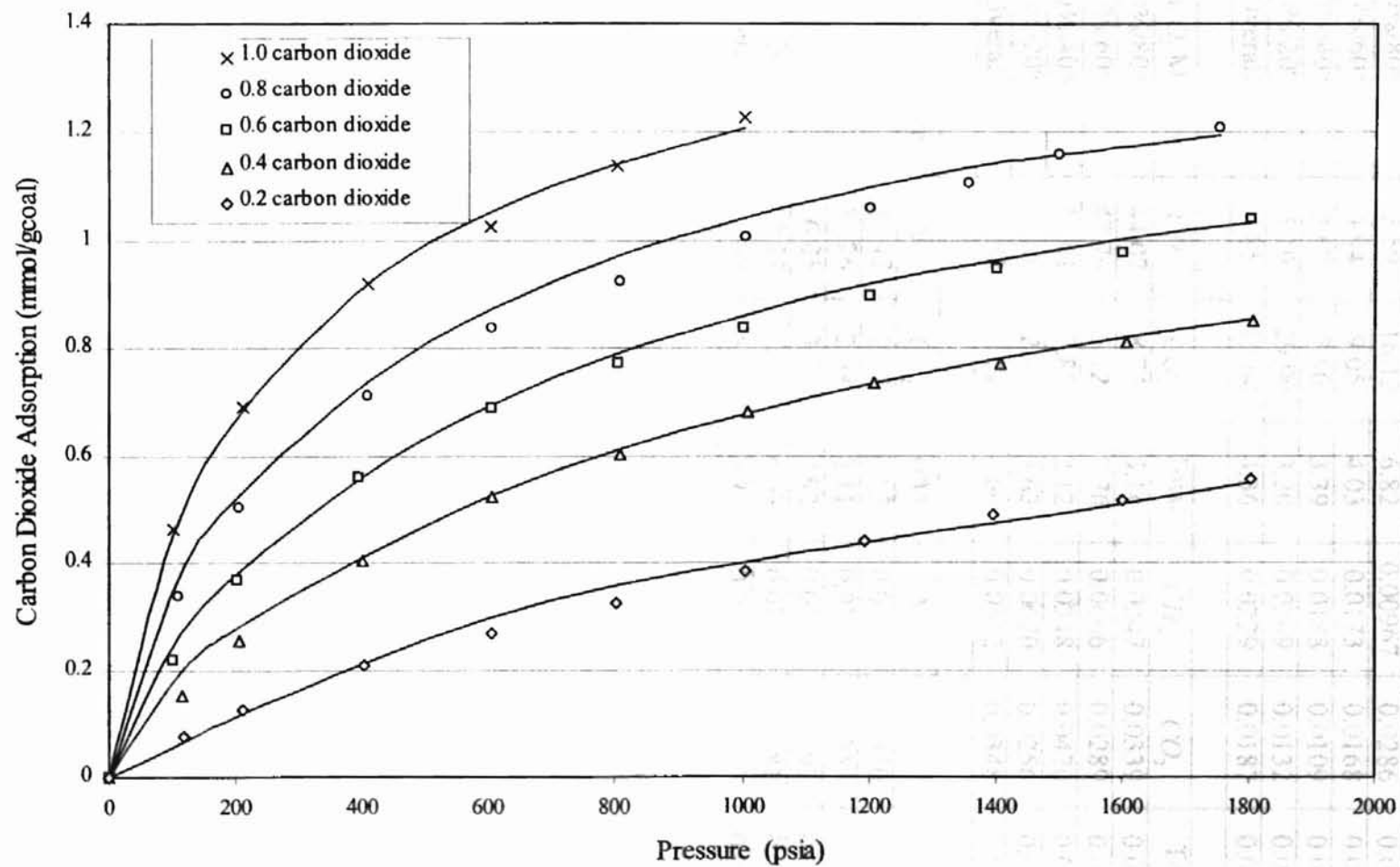


TABLE 25. LRC Model Representation of Adsorption of Binary Mixtures

Mixture Molar Ratio	AAPD			RSME		
	CH_4	N_2	Total	CH_4	N_2	Total
CH_4 / N_2 Mixture						
20%/80%	5.59	16.12	6.82	0.00967	0.0286	0.0237
40%/60%	4.94	9.05	4.03	0.0173	0.0168	0.0152
60%/40%	3.67	7.50	3.39	0.0188	0.0109	0.0282
80%/20%	5.19	29.90	3.20	0.0369	0.0132	0.0294
Overall	4.85	15.64	4.36	0.0229	0.0187	0.0248
CH_4 / CO_2 Mixture						
20%/80%	44.07	8.74	5.14	0.0347	0.0339	0.0459
40%/60%	43.79	5.12	7.76	0.0666	0.0289	0.0532
60%/40%	10.61	7.85	2.12	0.0348	0.0470	0.0138
80%/20%	8.80	2.99	3.62	0.0670	0.0256	0.0367
Overall	26.82	6.17	4.66	0.0532	0.0348	0.0403
N_2 / CO_2 Mixture						
20%/80%	35.47	2.77	6.05	0.0202	0.0330	0.0525
40%/60%	19.26	2.68	2.11	0.0193	0.0252	0.0296
60%/40%	36.05	3.77	2.92	0.0269	0.0192	0.0157
80%/20%	17.57	12.67	4.09	0.0245	0.0281	0.0269
Overall	27.09	5.47	3.79	0.0227	0.0263	0.0312

TABLE 26. ZGR Equation of State Representation of Adsorption of Binary Mixture

Mixture Molar Ratio	AAPD			RMSE		
	CH_4	N_2	Total	CH_4	N_2	Total
CH_4 / N_2 Mixture						
20%/80%	17.58	11.05	2.89	0.0281	0.0229	0.0092
40%/60%	6.07	3.77	3.61	0.0174	0.0066	0.0140
60%/40%	3.37	10.34	4.98	0.0119	0.0093	0.0190
80%/20%	10.94	33.33	8.34	0.0505	0.0163	0.0380
Overall	9.48	14.63	4.95	0.0270	0.0138	0.0200
CH_4 / CO_2 Mixture						
20%/80%	15.28	15.91	8.04	0.0112	0.0542	0.0607
40%/60%	12.64	7.26	5.24	0.0210	0.0549	0.0371
60%/40%	11.03	6.33	4.07	0.0297	0.0328	0.0421
80%/20%	5.46	5.83	6.17	0.0202	0.0419	0.0491
Overall	11.10	8.84	5.88	0.0206	0.0459	0.0472
N_2 / CO_2 Mixture						
20%/80%	31.80	3.94	4.54	0.0100	0.0320	0.0411
40%/60%	15.24	2.96	2.97	0.0097	0.0188	0.0249
60%/40%	9.15	4.70	4.91	0.0098	0.0177	0.0213
80%/20%	3.46	4.75	3.65	0.0070	0.0157	0.0211
Overall	14.92	4.09	4.02	0.0092	0.0211	0.0271

TABLE 27. Comparison of LRC Model and ZGR Equation of State Representation of Binary Mixture Adsorption on Wet Fruitland Coal at 115 °F

	AAPD		RSME	
	LRC	ZGR	LRC	ZGR
<i>CH₄</i> / <i>N₂</i> Mixture				
<i>CH₄</i>	4.85	9.48	0.0229	0.0270
<i>N₂</i>	15.64	14.63	0.0187	0.0138
Total	4.36	4.95	0.0248	0.0200
<i>CH₄</i> / <i>CO₂</i> Mixture				
<i>CH₄</i>	26.82	11.10	0.0532	0.0206
<i>CO₂</i>	6.17	8.84	0.0348	0.0459
Total	4.66	5.88	0.0403	0.0472
<i>N₂</i> / <i>CO₂</i> Mixture				
<i>N₂</i>	27.09	14.92	0.0227	0.0092
<i>CO₂</i>	5.47	4.09	0.0263	0.0211
Total	3.79	4.02	0.0312	0.0271

CONCLUSIONS AND RECOMMENDATIONS

Conclusions

1. For pure gas adsorption, carbon dioxide has the highest adsorption capacity, methane is intermediate, and nitrogen is the lowest. Carbon dioxide has about twice the adsorption of methane and four times that of nitrogen adsorbed on the wet Fruitland coal.
2. Nitrogen and methane display type-I adsorption character at pressures from 100 psia to 1800 psia on wet Fruitland and Illinois-6 coals. Carbon dioxide displays type-I adsorption from 100 to 1000 psia; it has a jump at 1200 psia, which is characteristic of type-IV adsorption.
3. The water content of the coal sample does not influence the adsorption character at levels between 4~14%.
4. The uncertainty for the pure gas adsorption propagated from the measured variables is from 1% to 5%; for binary mixtures, the overall uncertainty for each component is 2% to 7%.
5. The simple Langmuir model and the LRC model can correlate the pure methane and nitrogen adsorption data from 100 to 1800 psia, and carbon dioxide from 100 to 1000 psia. The LRC has 2% accuracy and simple Langmuir model has 3% accuracy in correlating the adsorption data.
6. The PGR and ZGR equation of state can be reduced to 2-D EOS and applied to correlate the pure gas adsorption on wet Fruitland coal. PGR has 2% accuracy in correlating the data. The ZGR has 1.5% accuracy in correlating the data.

7. The SLD model can correlate the pure methane and nitrogen adsorption on the coal. It has 2% accuracy in correlating methane and nitrogen adsorption data, 5% accuracy in correlating carbon dioxide.
8. The carbon dioxide has highest adsorption amount on the coal surface; it replaces the methane and nitrogen adsorption sites in binary mixture adsorption.
9. Both LRC and ZGR equation of state can be used to correlate the binary mixture adsorption data; the ZGR has better correlation results.

Recommendations

1. The magnetic pump used in the cell section jams easily. A high capacity circulation pump is suggested to increase the rate of adsorption.
2. The gas chromatograph is obsolete, some parts, such as oven temperature controller and carrier gas flow rate controller do not work very well; a new GC is suggested to increase the accuracy of the gas component analysis.
3. All parameters in SLD model should be investigated to increase the accuracy of correlate the carbon dioxide adsorption data.
4. All parameters in PGR 2-D equation of state should be investigated to give better results in correlating adsorption data.

BIBLIOGRAPHY

1. Arri, L.E., D. Yee, W.D. Morgan, and M.W. Jeasome, "Modeling Coalbed Methane Production with Binary Gas Adsorption", SPE Report 24363 (1992).
2. DeGance, A.E., "Multicomponent High Pressure Adsorption Equilibria on Carbon Substrates", Amoco Production Company, Report 90319ART0008, Tulsa, Oklahoma (1990).
3. Darwish, N.A., Hall, F.E., Gasem, K.A.M., Robinson, R.L., Jr., "Analysis of Error in Adsorption Measurements Using a Volumetric Technique", Oklahoma State University, March (1992).
4. Gasem, K. A. M., Personal Communication, Oklahoma State University (1999).
5. Gasem, K. A. M., Robinson, R. L. Jr., Liang, X. D., Fitzgerald, J. E., "Sequestration CO_2 in Coalbeds", Oklahoma State University (1999).
6. Greaves, K. H., and Owen, L. B., "Multi-component Gas Adsorption-Desorption Behavior of Coal", Paper 9353, presented at the Coalbed Methane Symposium, The University of Alabama, Tuscaloosa, May 17-21 (1993).
7. Gunter, W.D., Gentzis, T., Rottenfusser, B.A., and Richardson, R. J. H., "Deep Colbed Methane in Alberta, Canada: a Fuel Resource with the Potential of Zero Greenhouse Gas Emissions", Energy Conversion Management., Vol. 38., Suppl., pp. S217-222 (1997).
8. Hall, F.E., Jr., "Adsorption of Pure and Multi-component Gases on Wet Fruitland Coal", M.S. Thesis, Oklahoma State University, Stillwater, Oklahoma (1993).
9. Hall, F.E., "Adsorption Experiment Supplementary Material", Oklahoma State University, Stillwater, Oklahoma (1993).
10. Harpalani, S., and Pariti, U. M., "Study of Coal Sorption Isotherms Using a Multicomponent Gas Mixture", Paper 9353, presented at the Coalbed Methane Symposium, The University of Alabama, Tuscaloosa, May 17-21 (1993).
11. Haney, R.D., and H. Bliss, "Compressibilities of Nitrogen-Carbon Dioxide Mixtures" Journal of Engineering. Chemistry., Vol. 36, No. 11, pp. 989-993, November (1944).

12. Holste, J.C., et. al., "Properties of CO_2 Mixtures with N_2 and with CH_4 ", Gas Processors Association and Gas Research Institute, Research Report RR-122, Tulsa, Oklahoma (1989).
13. "International Thermodynamic Tables of the Fluid State: Carbon Dioxide", International Union of Pure and Applied Chemistry (1976).
14. "International Thermodynamic Tables of the Fluid State: Helium", International Union of Pure and Applied Chemistry (1976).
15. "International Thermodynamic Tables of the Fluid State: Nitrogen", International Union of Pure and Applied Chemistry (1979).
16. "International Thermodynamic Tables of the Fluid State: Methane", International Union of Pure and Applied Chemistry (1978).
17. Keyes, F. G., and H. G. Burks, "The Equation of State for Binary Mixtures of Methane and Nitrogen", Journal of American Chemical Society, Vol. 50, pp. 1100-1106, Apr. (1928).
18. Lamberson, M. N., Bustin, R. M., "Coalbed Methane Characteristics of Gates Formation Coals, Northeastern British Columbia: Effect of Maceral Composition", The American Association of Petroleum Geologists, Vol. 77, No. 12, pp. 2062-2076 (1993).
19. McQuarrie, D.A., "Statistical Mechanics of Non-Ideal Fluids", Butterworths, Stoneham, Massachusetts (1988).
20. Parson, E. A., Keith, D. W., "Fossil Fuel without CO_2 Emission", Science, Vol. 282, pp. 1053-1054 November (1998).
21. Rangarajan, B., Lira, C. T., "Simplified Local Density Model for Adsorption over Large Pressure Ranges", AIChE, Vol. 41, pp. 460-465 (1995).
22. Reid, R. C., Prausnitz, J. M., and Poling, B.E., "The Properties of Gases and Liquids", 4th Edition, McGraw-Hill Book Co., New York (1987).
23. Reamer, H. H., R. H. Olds, B. H. Sage, and W. N. Lacey, "Phase Equilibria in Hydrocarbon Systems", Industrial & Engineering Chemistry, Vol. 36, No2, pp. 88-92 January (1944).
24. Rightmire, C.T., Eddy, Greg. E., Kirr, J. N., "Coalbed Methane Resources of the United States", The American Association of Petroleum Geologists, Tulsa, Oklahoma (1984).
25. Robinson, R. L. Personal Communication, Oklahoma State University (1999).

26. Ross, S. and Olivier, J. P., "On Physical Adsorption", Interscience Publishers, New York (1964).
27. Row, K. H., "Evaluation of the Modeling Park-Gasem-Robinson Equation of State and Calculation of Calorimetric Properties Using Equation of State", Ph. D. Dissertation, Oklahoma State University, Stillwater, Oklahoma (1998).
28. Stevens, S. H., Spector, D., Riemer, P., "Enhanced Coalbed Methane Recovery Using CO_2 Injection: Worldwide Resource and CO_2 Sequestration Potential", 1998 SPE International Conference and Exhibition in China, Beijing, China, November (1998).
29. Valenzuela, D. P., and Myers, A. L., "Adsorption Equilibria Data Handbook", Prentice Hall, Englewood Cliffs, New Jersey (1989).
30. Van Ness, H.C. "Adsorption of Gases on Solids", Industrial & Engineering Chemistry Fundamentals, 8, pp. 464-480 (1969).
31. Walas, S.M., "Phase Equilibria in Chemical Engineering", Butterworth, Stoneham, Massachusetts (1983).
32. Yang, R.T., "Gas Separation by Adsorption Processes", Butterworths, Boston, Massachusetts (1987).
33. Zhou, C., "AEMP Fortran Code for the Correlation and Prediction of Gas Adsorption Properties", Oklahoma State University, Stillwater, Oklahoma (1993).
34. Zhou, C., "Modeling and Prediction of Pure and Multicomponent Gas Adsorption", Ph.D. Dissertation, Oklahoma State University, Stillwater, Oklahoma (1994).

APPENDICES

... applied to calculate the amount of gas

...

... compressibility factor is very important

...

... especially at high pressures.

... and the pressure of the gas

... was calculated by the

...

... of the gas.

APPENDIX A

GAS COMPRESSIBILITY FACTOR

In the present work, an equation of state is applied to calculate the amount of gas injected and unadsorbed. The accuracy of the compressibility factor is very important for the calculation of the final experimental results, especially at high pressures.

Helium is used to test the void volume in the cell section; the pressure of helium is from 100 to 1000 psia. The compressibility factor of helium was calculated by the equation from *Thermodynamic and Thermophysical Properties of Helium* [14]. It is a virial expansion written as a function of pressure (atm) and temperature (Kelvin) and is truncated after the first term. The equation is given as

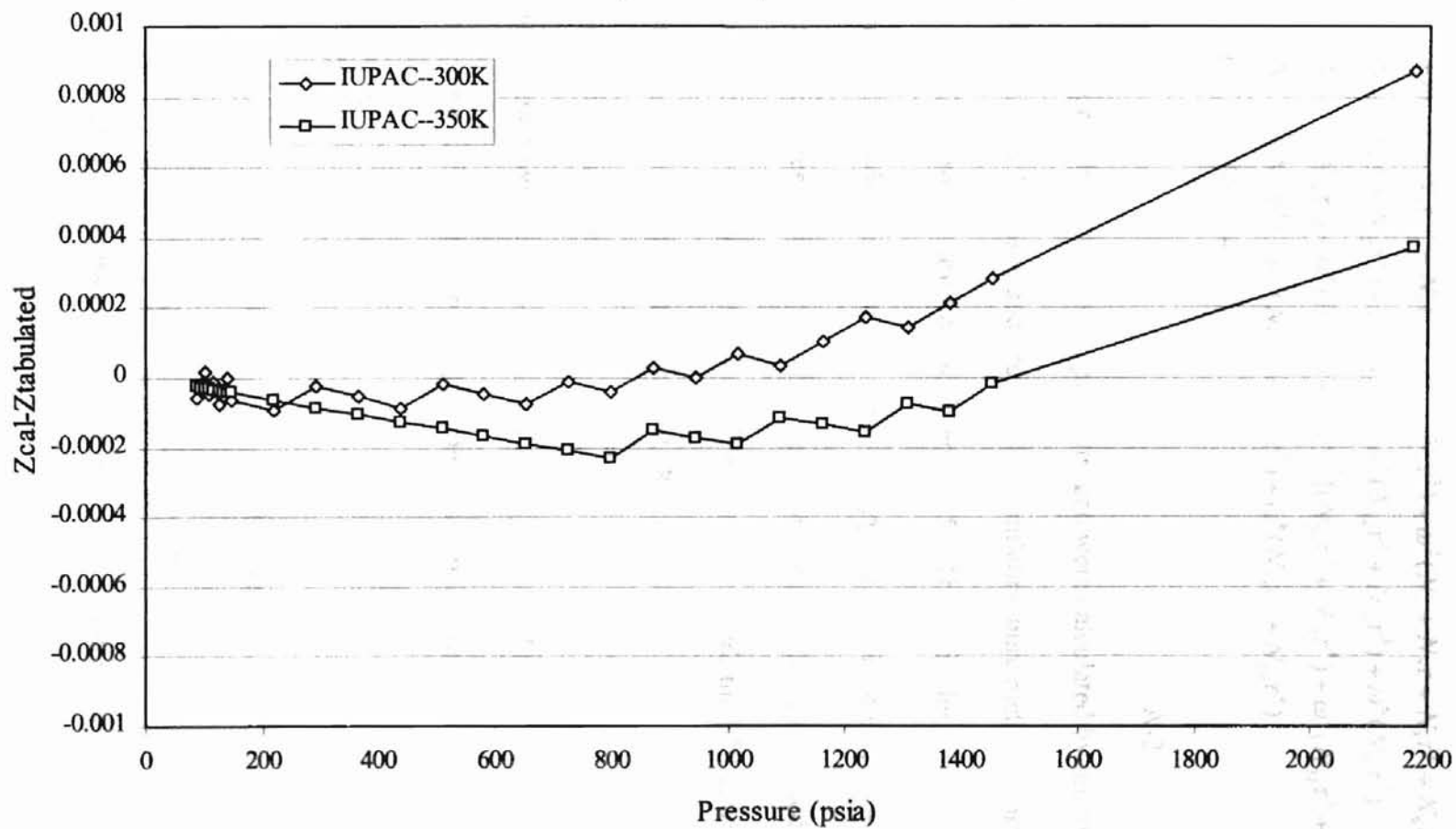
$$Z_{He} = 1 + B(T)P$$

$$B(T) = 0.001471 - (4.779E - 6)T + (4.920E - 9)T^2 \quad \text{A-1}$$

The compressibility factor calculated from the above equation has been compared with experimental data from the Reference 14 at temperatures of 310K and 320K, which are close to experimental temperatures of 309.1K (96.6 °F) and 319.3K (115 °F). The comparison between the calculated and the tabulated values are shown in Figure 53 and Table 30. The tabulated value was calculated by the author using the same equation.

Pure methane compressibility factors were calculated by the equation suggested by Jacobsen and Stewart, documented in the International Thermodynamic Tables for Methane [16]. The equation contains 32 constants with the ability to predict the compressibility factor at temperature from the triple point to over 400K and pressure to 400 bar. The equation is given in Equation A-2. The 32 constants are from the book [16], $\omega = \rho / \rho_c$, $\tau = T_c / T$, $\rho_c = 0.101095$ mole/cc, $T_c = 190.55$ K. The calculated compressibility factors of methane have been compared with the tabulated compressibility documented in the IUPAC book at temperatures of 310 K and

Figure 53. Deviation Between Calculated and Tabulated Compressibility Factor for Helium



very close to the experimental temperatures 309.1K (96.6°F) and
 300.15K (27.0°C) (the Figure 54 and Table 30)

320 K, which are very close to the experiment temperatures 309.1K (96.6 °F) and 319.3K (115 °F). The comparison is shown in the Figure 54 and Table 30.

$$\begin{aligned}
 Z = & 1 + \omega(N_1 + N_2\tau^{0.5} + N_3\tau + N_4\tau^2 + N_5\tau^3) + \omega^2(N_6 + N_7\tau + N_8\tau^2 + N_9\tau^3) \\
 & + \omega^3(N_{10} + N_{11}\tau + N_{12}\tau^2) + \omega^4(N_{13}\tau) + \omega^5(N_{14}\tau^2 + N_{15}\tau^3) + \omega^6(N_{16}\tau^2) \\
 & + \omega^7(N_{17}\tau^2 + N_{18}\tau^3) + \omega^8(N_{19}\tau^3) + \omega^2 e^{\omega\omega^2} [(N_{20}\tau^3 + N_{21}\tau^4) + \omega^2(N_{22}\tau^3 + N_{23}\tau^5) \\
 & + \omega^4(N_{24}\tau^3 + N_{25}\tau^4) + \omega^6(N_{26}\tau^3 + N_{27}\tau^5) + \omega^8(N_{28}\tau^3 + N_{29}\tau^4) \\
 & + \omega^{10}(N_{30}\tau^3 + N_{31}\tau^4 + N_{32}\tau^5)]
 \end{aligned}$$

A-2

The compressibility factors for pure nitrogen were calculated by the same equation suggested by Jacobsen and Stewart for calculating pure methane compressibility factor [15]. The 32 constants are from Reference [15]. The variables are the same as for methane expression, where $\omega = \rho / \rho_c$, $\tau = T_c / T$, $\rho_c = 0.01121$ mole/cc, $T_c = 126.20$ K. The calculated compressibility factors have been compared with the tabulated compressibility factor documented on the IUPAC book at 310K and 320K, which are close to the experimental temperatures of 309.1K and 319.3K. The comparison is shown in the Figure 55 and Table 30.

The carbon dioxide compressibility factor is calculated from the equation of state documented in the IUPAC reference [13]. The equation is listed below:

$$Z_{CO_2} = 1 + \sigma \left[\sum_{i=0}^9 \sum_{j=0}^{j_i} b_{ij} (\tau - 1)^j (\sigma - 1)^i \right] \quad \text{A-3}$$

The constants b_{ij} are from the book [13]. The variables are $\tau = T_c / T$, $\sigma = \rho / \rho_c$, the critical constants $T_c = 304.21K$, $\rho_c = 0.01063$ mole / cc .

The calculated compressibility factors have been compared with the tabulated compressibility factor documented in the IUPAC reference at 310K and 320 K, which are

Figure 54. Deviation Between Calculated and Tabulated Compressibility Factor for Methane

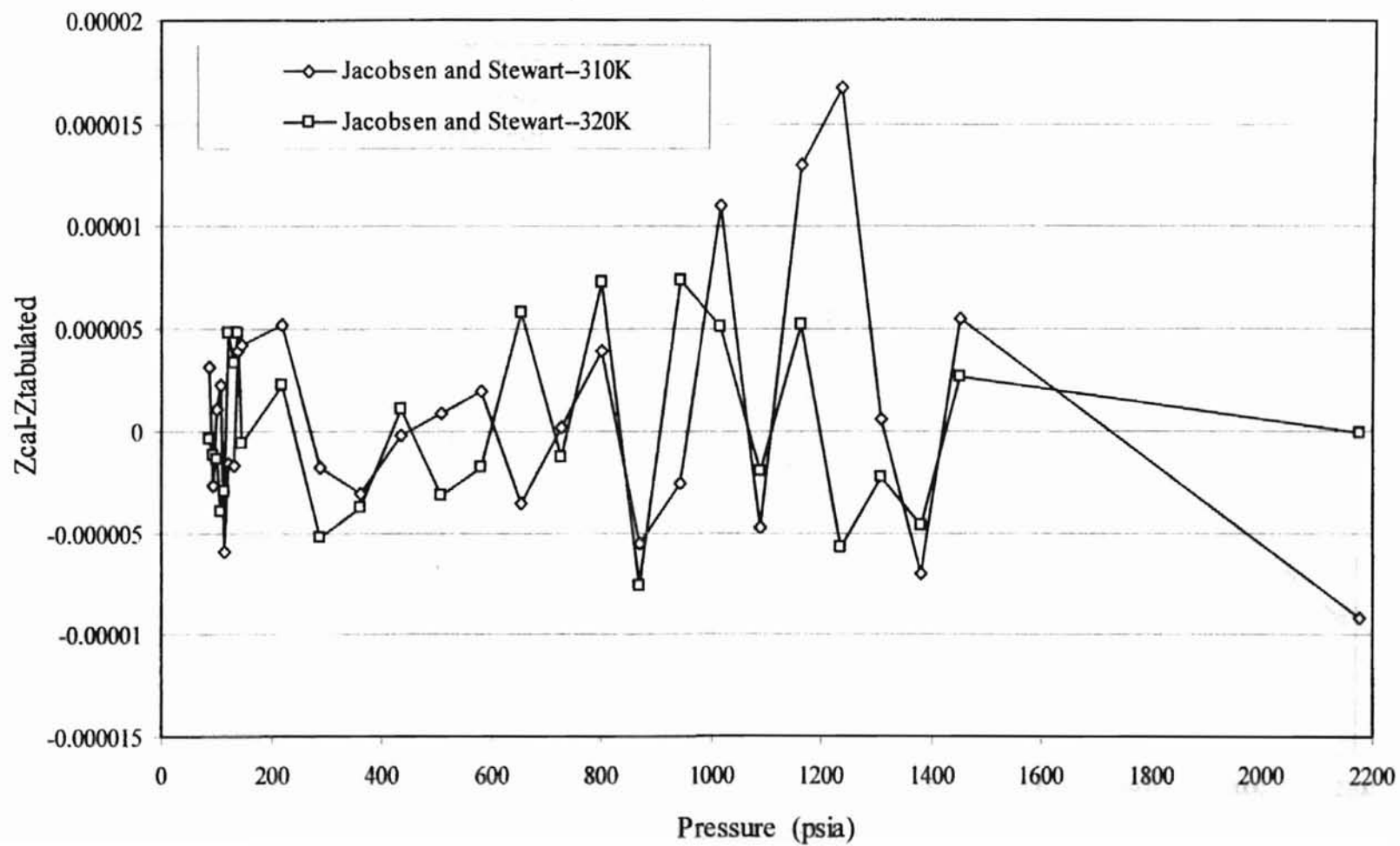


Figure 55. Deviation Between Calculated and Tabulated Compressibility Factor for Nitrogen

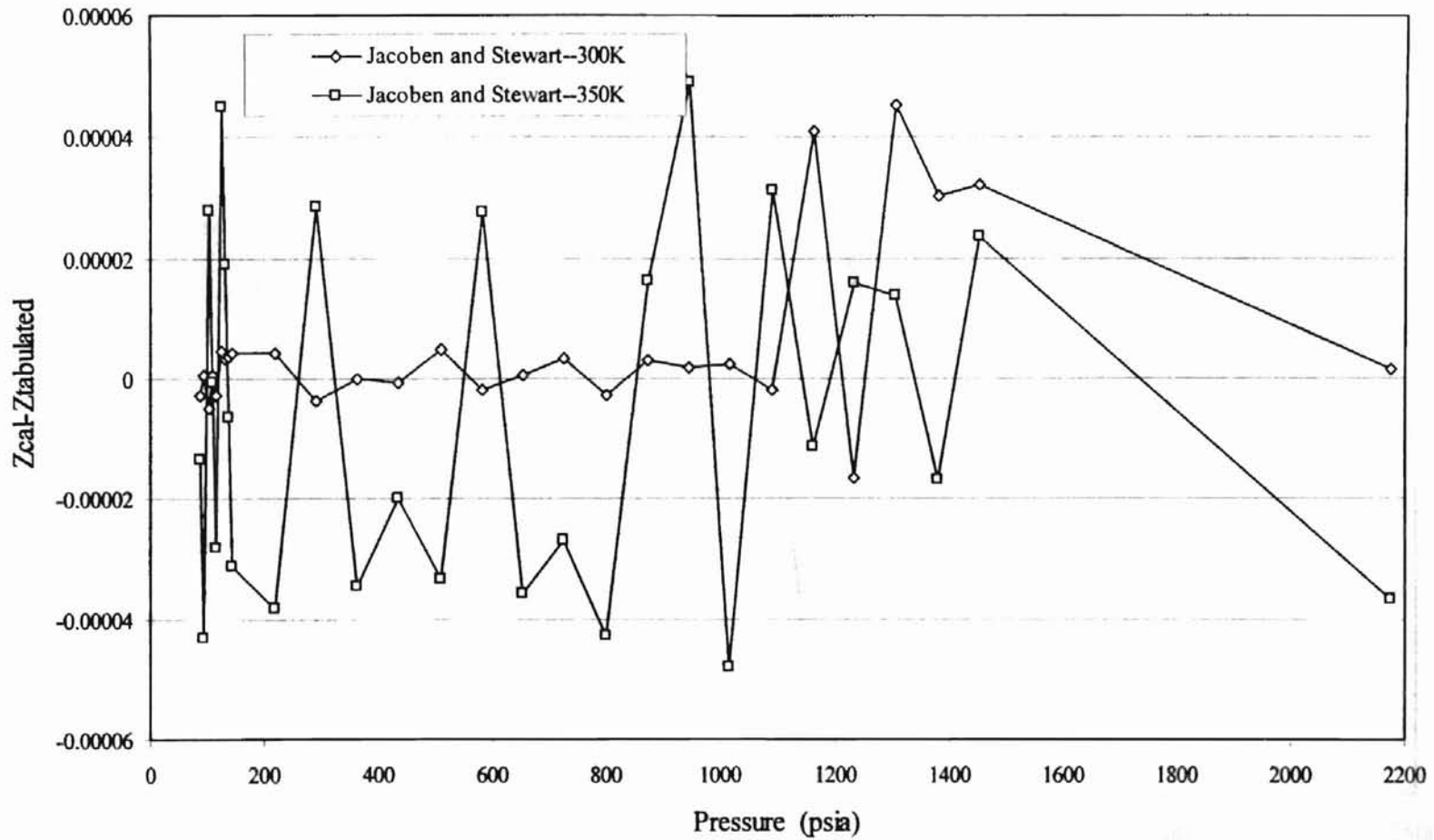
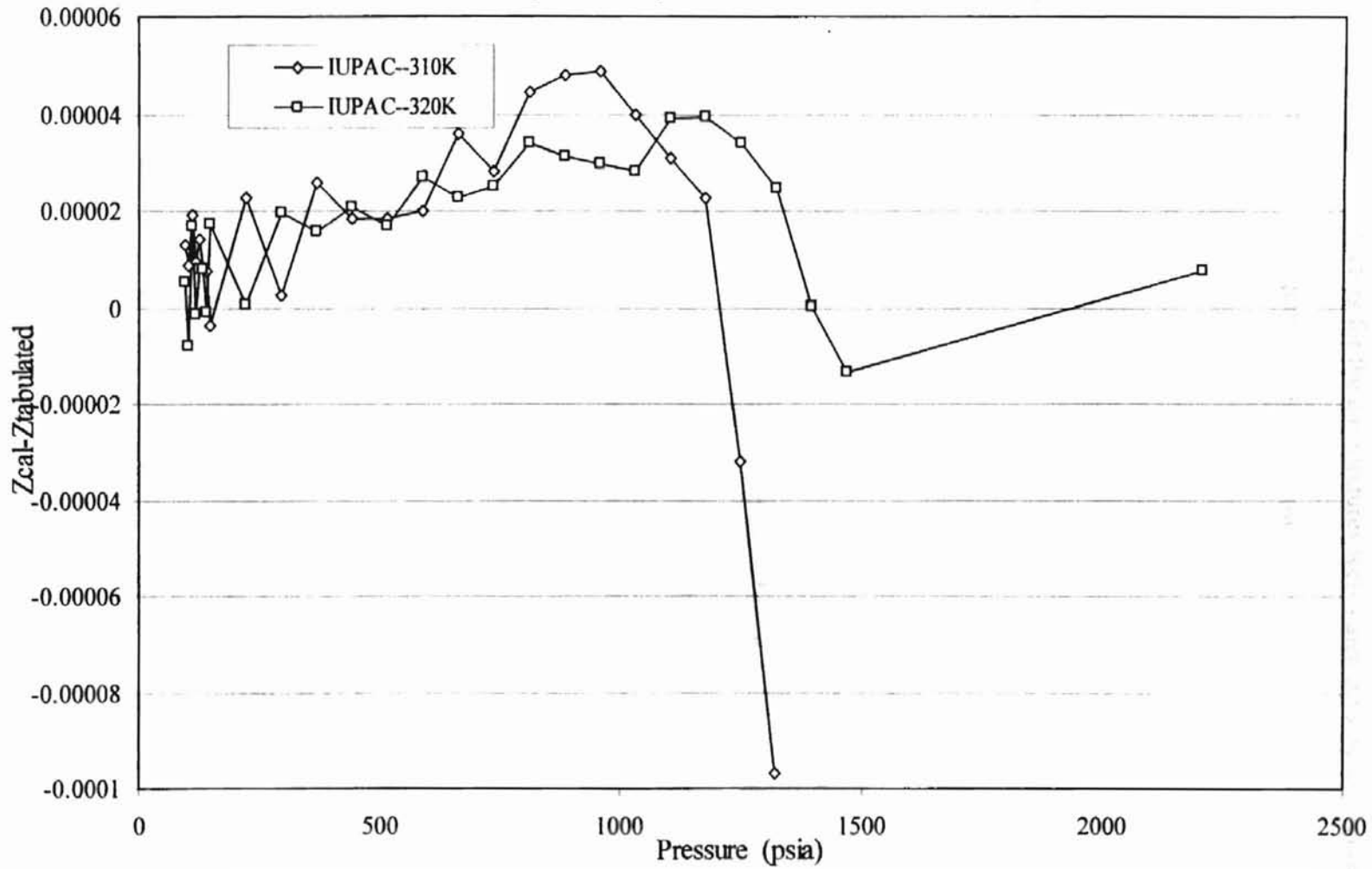


Figure 56. Deviation Between Calculated and Tabulated Compressibility Factor for Carbon Dioxide



close to the experimental temperatures of 309.1K (96.6° F) and 319.3K (115° F). The comparison is showed in the Figure 56 and Table 30.

The compressibility factors for the gas mixtures were calculated by the Redlich-Kwong equation of state. The equation is listed below:

$$\begin{aligned}
 P &= \frac{RT}{v - b_{mix}} - \frac{a_{mix}}{T^{0.5}v(v + b_{mix})} \\
 Z &= \frac{v}{v - b_{mix}} - \frac{a}{RT^{1.5}(v - b_{mix})} \\
 a_{mix} &= \sum_i \sum_j y_i y_j [a_i a_j]^{0.5} (1 - C_{ij}) \\
 b_{mix} &= \sum_i y_i b_i \\
 a &= \Omega_a R^2 T_c^{2.5} / P_c \\
 b &= \Omega_b R T_c / P_c
 \end{aligned}
 \tag{A-4}$$

The constants Ω_a and Ω_b for each pure gas were regressed from the experimental data documented in the IUPAC reference and are listed in the Table 29. The binary interaction parameters C_{ij} and D_{ij} are determined from experimental literature data on the binary systems, as discussed below.

TABLE 28. Regressed R-K EOS Constants for Different Gases

T(K)	Methane		Nitrogen		Carbon Dioxide	
	Ω_a	Ω_b	Ω_a	Ω_b	Ω_a	Ω_b
310	0.397254	0.07711	0.182463	0.087089	0.880066	0.08972
320	0.406831	0.080765	0.181059	0.087592	0.865688	0.088098

For the methane/nitrogen mixtures, the experimental data are from Keyes and Burks [17].

The optimum binary interaction parameter is determined from the experimental data.

The calculated data are compared with the experimental data collected by Keyes-Burks at

323.16K with compositions of 0.4331/0.5669, 0.7953/0.2047 and 0.8053/0.1947 from 500 psia to 2100 psia. The maximum absolute deviation in the compressibility factor is 0.0025. The result is shown in Figure 57 and Table 30.

TABLE 29. Regressed Binary Mixture Interaction Parameters

	C_{ij}	D_{ij}
Methane/Nitrogen	0.11440	0
Methane/Carbon Dioxide	0.13666	-0.06907
Nitrogen/Carbon Dioxide	0.070987	-0.12366

For methane/carbon dioxide mixture, the experimental data are from Holste and Hall [12], and Reamer, Olds, Sage and Lacey [23]. The binary interaction parameter was determined from the data collected by Holste and Hall at 320 K. The calculated data are compared with the experimental data of Holste-Hall at 300K and 320K with the composition of 0.5239/0.4761 from 72.5 psia to 1886 psia. The maximum absolute deviation is 0.0004. The calculated data have also been compared with the experimental data collected by Reamer et al. at 310.9K with the composition of 0.2035/0.7965, 0.4055/0.5945, 0.6050/0.3950, 0.8469/0.1531 from 200 psia to 2000 psia. The maximum absolute deviation is 0.005. The results are shown in Figures 58 and 59 and Table 30.

For nitrogen/carbon dioxide mixture, the experimental data are from Holste and Hall [12], and Haney and Bliss [11]. The binary interaction parameters were determined from the data collected by Holste and Hall at 320 K. The regressed parameters were used to calculate the methane/carbon dioxide mixture compressibility factor and compared with the experimental data from Holste and Hall and from Haney and Bliss. The calculated data are compared with the experimental data of Holste-Hall at 300K and

320K with the composition of 0.5530/0.4470 from 72.5 to 1886 psia, and the maximum absolute deviation is 0.001. The calculated data has been compared with the experimental data collected by Haney-Bliss at 323.15K with composition of 0.4952/0.5048, 0.7487/0.2513 from 441 psia to 1837 psia, the maximum absolute deviation is 0.001. The results are shown in Figure 60 and Table 30.

Table 30. Accuracy of Pure and Binary Mixture Compressibility Factor Predictions

	AAPD		RSME	
	300 K	350 K	300 K	350 K
Pure Helium	0.009652	0.0111	0.000189	0.000137
Pure Nitrogen	0.000808	0.00273	0.0000148	0.0000081
	310 K	320 K	310 K	320 K
Pure Methane	0.000440	0.00035	0.0000058	0.0000041
Pure Carbon Dioxide	0.00369	0.00183	0.0000529	0.0000218
Methane/Carbon Dioxide	0.130		0.00192	
	300 K	320 K	300 K	320 K
Methane/Carbon Dioxide	0.145	0.173	0.00224	0.00268
	323 K		323 K	
Methane/Nitrogen	0.113		0.00156	
	300 K	323 K	300 K	323 K
Nitrogen/Carbon Dioxide	0.030	0.026	0.000357	0.000454

Figure 57. Methane/Nitrogen Binary Mixture Compressibility Factor Calibration

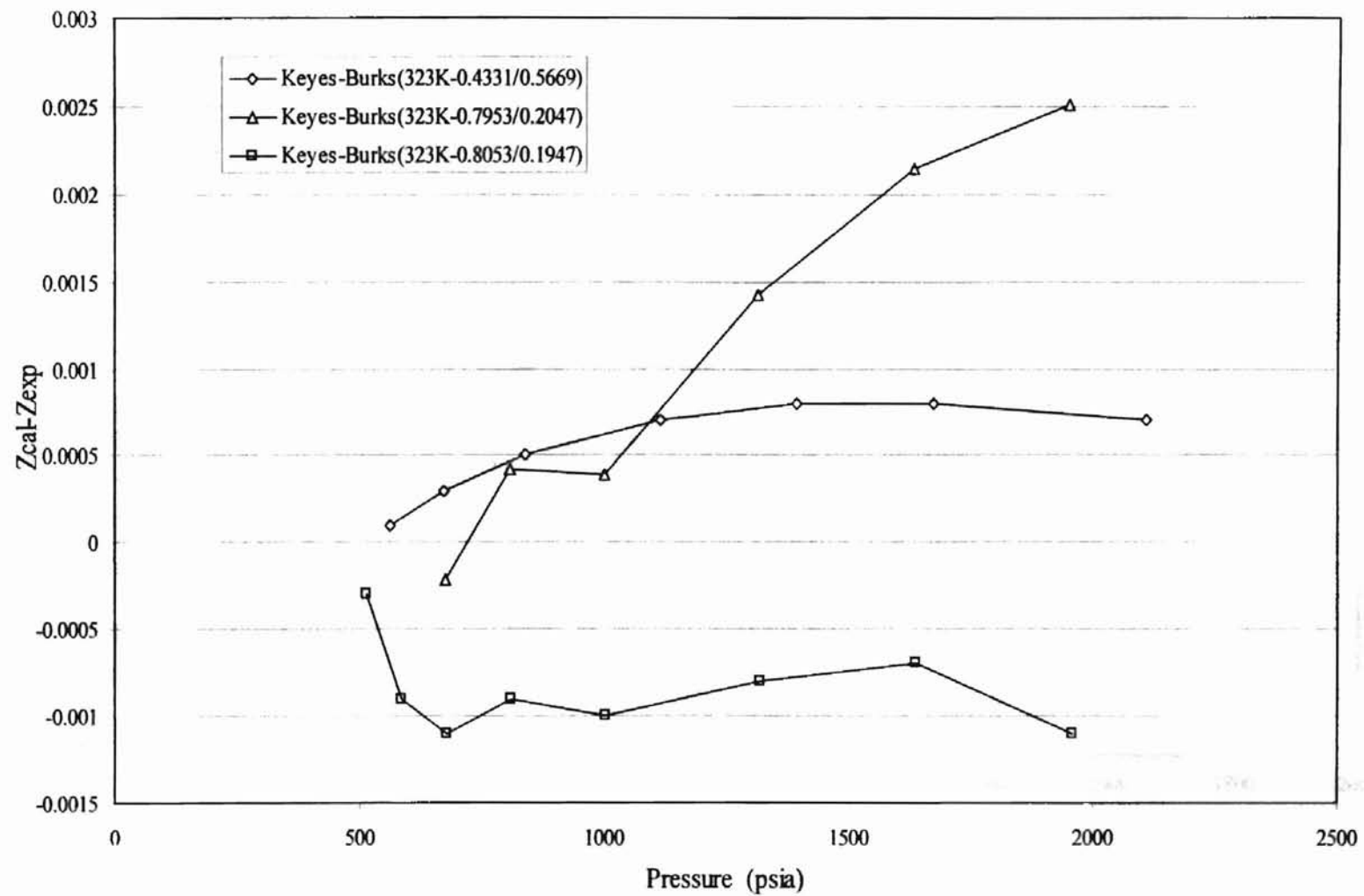


Figure 58. Methane/Carbon Dioxide Binary Mixture
Compressibility Factor Calibration: Reamer

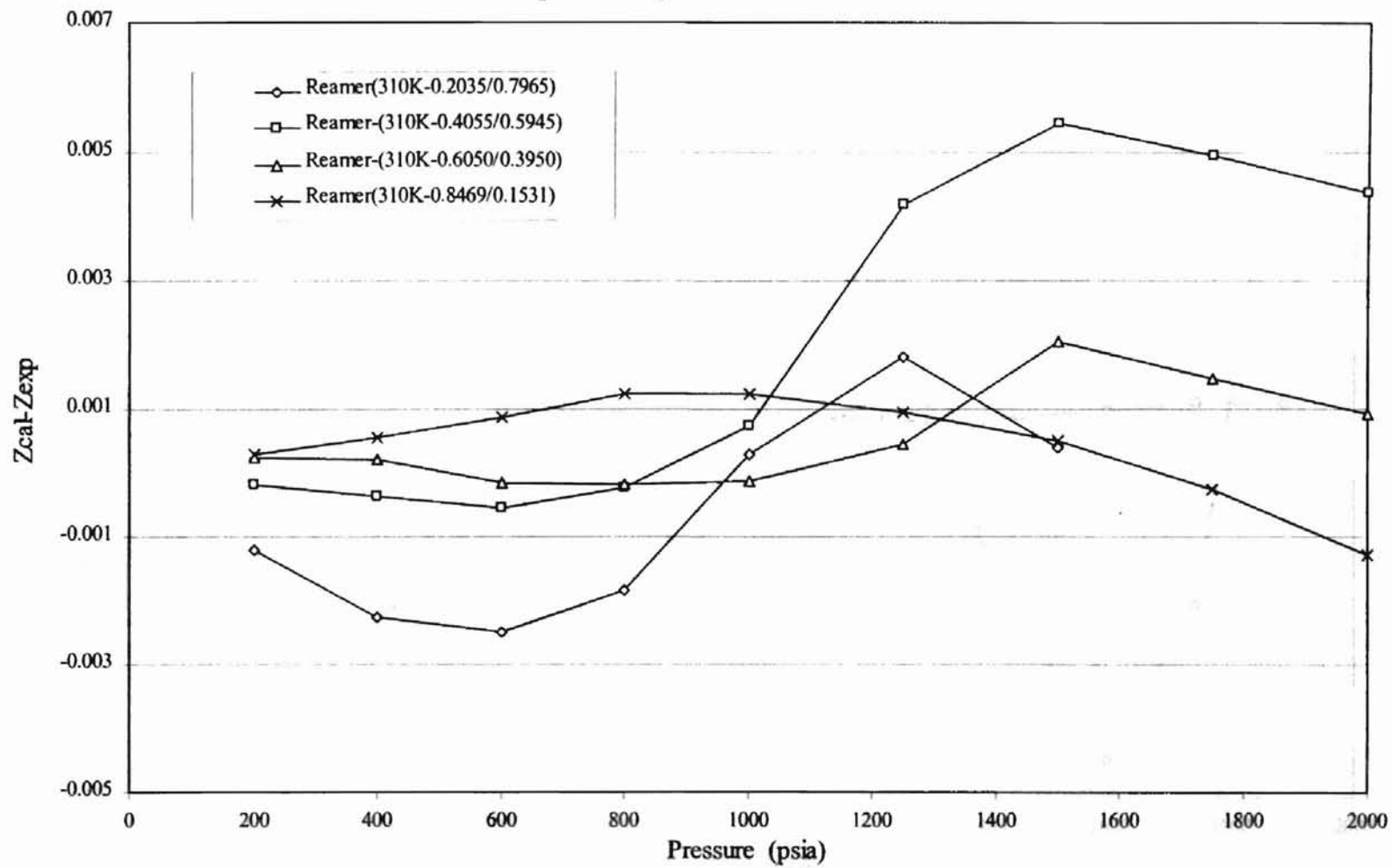


Figure 59. Methane/Carbon Dioxide Binary Mixture
Compressibility Factor Calibration: Holste-Hall

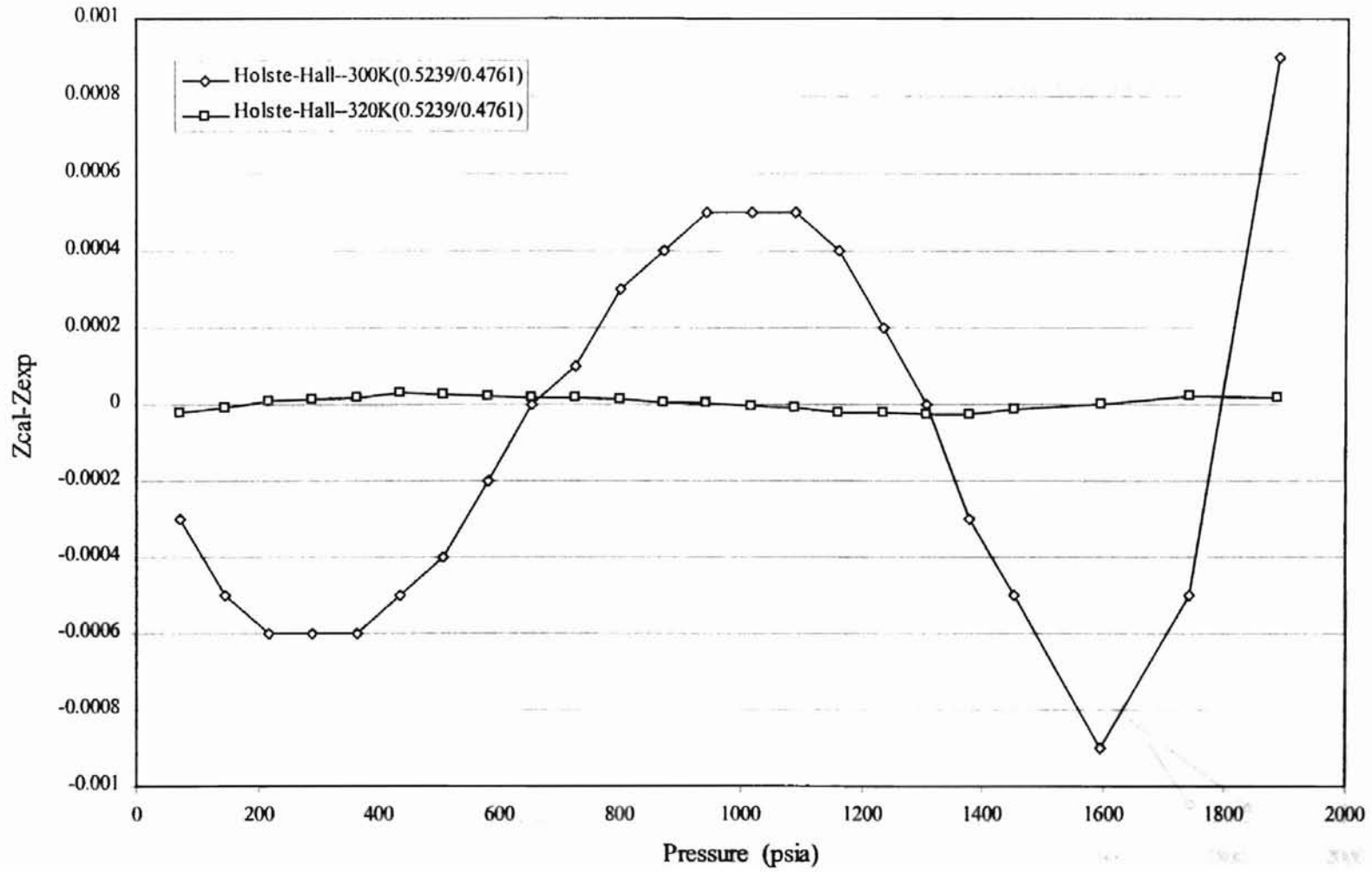
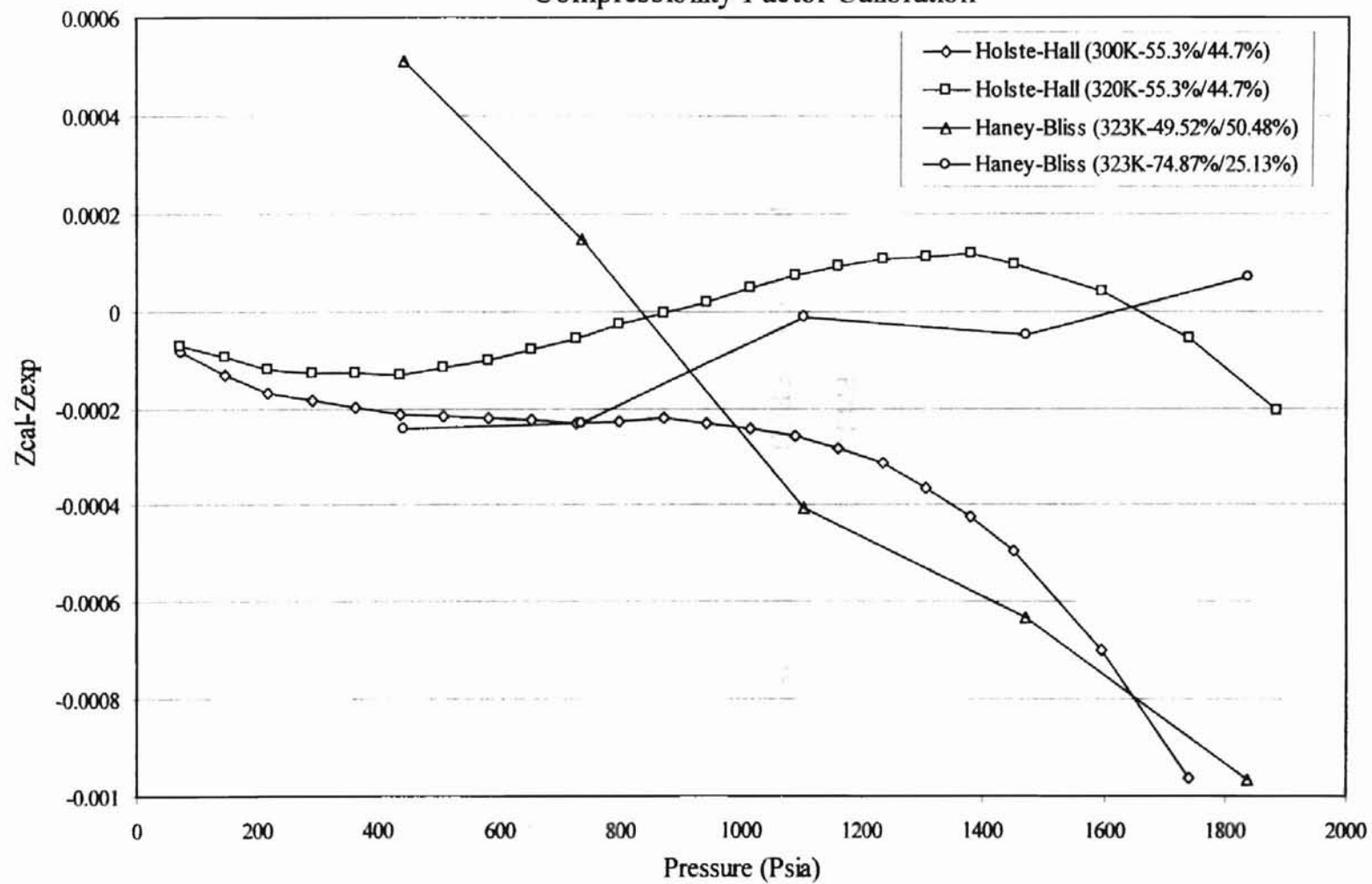


Figure 60. Nitrogen/Carbon Dioxide Binary Mixture
Compressibility Factor Calibration



In adsorbed phase fugacity coefficient is derived from the 2-D ZGP equation
state from Eq. Fugacity coefficient can be expressed as (24)

$$\ln \phi = \frac{1}{RT} \left(\frac{\partial \ln \gamma}{\partial \ln p} \right)_{T, \ln \gamma}$$

$$\ln \phi = \frac{1}{RT} \left(\frac{\partial \ln \gamma}{\partial \ln p} \right)_{T, \ln \gamma}$$

APPENDIX B DERIVATION OF FUGACITY EQUATIONS

The adsorbed phase fugacity coefficient is derived from the 2-D ZGR equation of state. From Equation 2-10, the fugacity coefficient can be expressed as [34]:

$$\ln \phi_i = \int_0^\omega \left\{ \frac{1}{RT\omega} \left[\frac{\partial(A\pi)}{\partial \omega_i} \right]_{T, M_s, n_j} - \frac{1}{\omega} \right\} d\omega - \ln Z_a \quad \text{B-1}$$

the 2-D equation of state is expressed as:

$$\left[A\pi + \frac{\alpha\omega^2}{1 + U\beta\omega + W(\beta\omega)^2} \right] [1 - (\beta\omega)^m] = \omega RT \quad \text{B-2}$$

the mixing rule is:

$$\alpha = \sum_i \sum_j x_i x_j \alpha_{ij} \quad \text{B-3}$$

$$\beta = \sum_i \sum_j x_i x_j \beta_{ij}$$

The Equation B-2 can be rearranged to:

$$A\pi = \frac{\omega RT}{1 - (\beta\omega)^m} - \frac{\alpha\omega^2}{1 + U\beta\omega + W(\beta\omega)^2} = S_1 + S_2 \quad \text{B-4}$$

Thus B-1 can be expressed as:

$$\ln \phi_i = F_1 + F_2 - \ln Z_a$$

where:

$$F_1 = \int_0^\omega \left\{ \frac{1}{RT\omega} \left[\frac{\partial S_1}{\partial \omega_i} \right] - \frac{1}{\omega} \right\} d\omega \quad \text{B-5}$$

$$F_2 = \int_0^\omega \left\{ \frac{1}{RT\omega} \left[\frac{\partial S_2}{\partial \omega_i} \right] \right\} d\omega \quad \text{B-6}$$

where,

$$\frac{\partial S_1}{\partial \omega_i} = \frac{RT}{1 - (\beta\omega)^m} + \frac{mRT(2\sum_j \beta_{ij}\omega_j - \beta\omega)(\beta\omega)^{m-1}}{[1 - (\beta\omega)^m]^2} \quad \text{B-7}$$

then substitute into Equation B-5,

$$F_1 = -\frac{1}{m} \ln[1 - (\beta\omega)^m] + \frac{[2\sum_j \beta_{ij}\omega_j - \beta\omega](\beta\omega)^m}{\beta\omega[1 - (\beta\omega)^m]^2} \quad \text{B-8}$$

for S_2 , the derivative is:

$$\frac{\partial S_2}{\partial \omega_i} = -\frac{2\sum_j \alpha_{ij}\omega_j}{1 + U\beta\omega + W(\beta\omega)^2} + \frac{\alpha\omega(2\sum_j \beta_{ij}\omega_j - \beta\omega)[U + 2W\beta\omega]}{[1 + U\beta\omega + W(\beta\omega)^2]^2} \quad \text{B-9}$$

substitute into Equation B-6,

$$F_2 = T_1 + T_2 \quad \text{B-10}$$

$$T_1 = -\frac{2\alpha\sum_j \beta_{ij}\omega_j - \alpha\beta\omega}{RT\beta(1 + U\beta\omega + W(\beta\omega)^2)} \quad \text{B-11}$$

$$T_2 = -\frac{\alpha\beta\omega + 2\beta\sum_j \alpha_{ij}\omega_j - 2\alpha\sum_j \beta_{ij}\omega_j}{RT\beta^2\omega\sqrt{U^2 - 4W}} \ln \left| \frac{2 + (U + \sqrt{U^2 - 4W})\beta\omega}{2 + (U - \sqrt{U^2 - 4W})\beta\omega} \right| \quad \text{B-12}$$

so the fugacity coefficient is expressed as [30]:

$$\ln \phi_i = -\frac{1}{m} \ln[1 - (\beta\omega)^m] + \frac{[2\sum_j \beta_{ij}\omega_j - \beta\omega](\beta\omega)^m}{\beta\omega[1 - (\beta\omega)^m]^2} - \ln Z_a + T_1 + T_2 \quad \text{B-13}$$

The dimensionless fugacity coefficient is derived from the 2-D PGR equation of state (Eq. 10.7) and Equation 10.15. The fugacity coefficient can be expressed as:

$$\ln \phi = \frac{1}{RT} \left[\int_0^P \frac{v - v^0}{P} dP - \int_0^P \frac{v^0}{P} dP \right]$$

or

or

APPENDIX C

DERIVATION OF FUGACITY FOR PGR EQUATION OF STATE

The adsorbed phase fugacity coefficient is derived from the 2-D PGR equation of state [27]. From Equation 2-15, the fugacity coefficient can be expressed as:

$$\ln \phi_i = \int_0^{\omega} \left\{ \frac{1}{RT\omega} \left[\frac{\partial(A\pi)}{\partial \omega_i} \right]_{T, M_s, n_j} - \frac{1}{\omega} \right\} d\omega - \ln Z_a \quad \text{C-1}$$

The 3-D PGR equation of state is expressed as:

$$\frac{Pv}{RT} = 1 + c \left(\frac{\beta_1 \tau}{v_r - \beta_2 \tau} - \frac{Z_M Y v_r}{v_r^2 + U v_r + W} - \frac{Q_1 Z_M Y}{v_r + Q_2} \right) \quad \text{C-2}$$

where,

$$v_r = \frac{v}{v^*}$$

$$Y = \exp(F_i) - 1$$

$$F_i = \omega_1 \left(\frac{1}{2\tilde{T}} \right)^{1/2} + \omega_2 \left(\frac{1}{2\tilde{T}} \right) + \omega_3 \left(\frac{1}{2\tilde{T}} \right)^{3/2} + \omega_4 \left(\frac{1}{2\tilde{T}} \right)^2$$

$$\tilde{T} = \frac{T}{T^*}$$

the 2-D equation of state is expressed as:

$$A\pi = \omega RT + cRT\omega \left(\frac{\beta_1 \tau l \omega}{1 - \beta_2 \tau l \omega} - \frac{Z_M Y l \omega}{1 + U l \omega + W (l \omega)^2} - \frac{Q_1 Z_M Y l \omega}{1 + Q_2 l \omega} \right) \quad \text{C-3}$$

the mixing rule is:

$$c = \sum_i x_i c_i$$

$$l = \sum_i \sum_j x_i x_j l_{ij} \quad \text{C-4}$$

$$Y = \sum_i \sum_j x_i x_j (\exp(F_i) - 1)$$

where,

$$F_i = \sum_{k=1} \omega_k \left(\frac{T^*}{2T} \right)^{\frac{1}{2}}$$

$$T^* = \sum_i \sum_j \frac{\epsilon_{ij} q_i}{c_{i,k}}$$

The Equation C-3 can be rearranged to:

$$S_1 = \omega RT + \frac{cRT\beta_1 \tau \omega^2}{1 - \beta_2 \tau \omega}$$

$$S_2 = \frac{cRTZ_M Y \omega^2}{1 + U\omega + W(\omega)^2}$$

C-5

$$S_3 = \frac{cRTQ_1 Z_M Y \omega^2}{1 + Q_2 \omega}$$

The C-1 can be expressed as:

$$\ln \phi_i = F_1 - F_2 - F_3 - \ln Z_a$$

where:

$$F_1 = \int_0^{\omega} \left\{ \frac{1}{RT\omega} \left[\frac{\partial S_1}{\partial \omega_i} \right] - \frac{1}{\omega} \right\} d\omega$$

C-6

$$F_2 = \int_0^{\omega} \left\{ \frac{1}{RT\omega} \left[\frac{\partial S_2}{\partial \omega_i} \right] \right\} d\omega$$

C-7

$$F_3 = \int_0^{\omega} \left\{ \frac{1}{RT\omega} \left[\frac{\partial S_3}{\partial \omega_i} \right] \right\} d\omega$$

C-8

where,

$$\frac{\partial S_1}{\partial \omega_i} = RT + cRT\beta_1 \tau \left(\frac{2\omega}{1 - \beta_2 \tau \omega} + \frac{\beta_2 \tau \omega}{(1 - \beta_2 \tau \omega)^2} \right)$$

C-9

then substitute into Equation C-6,

$$F_1 = \frac{c\beta_1}{\beta_2} \left[\frac{\beta_2 \tau \omega}{1 - \beta_2 \tau \omega} - \ln(1 - \beta_2 \tau \omega) \right]$$

C-10

for S_2 , the derivative is:

$$\frac{\partial S_2}{\partial \omega_i} = cRTIZ_M Y \left[\frac{2\omega}{1 + Ul\omega + W(l\omega)^2} - \frac{(Ul + 2Wl^2\omega)\omega^2}{(1 + Ul\omega + W(l\omega)^2)^2} \right] \quad \text{C-11}$$

substitute into Equation C-7,

$$F_2 = cZ_M Y \left[\frac{\omega}{1 + Ul\omega + U(l\omega)^2} + \frac{2}{l\sqrt{4W - U^2}} \left(\tanh^{-1} \left(\frac{U + 2Wl\omega}{\sqrt{4W - U^2}} \right) - \tanh^{-1} \left(\frac{U}{\sqrt{4W - U^2}} \right) \right) \right] \quad \text{C-12}$$

Similarly,

$$\frac{\partial S_3}{\partial \omega} = cRTQ_1 Z_M Y \omega \left[\frac{2}{1 + Q_2 l \omega} - \frac{Q_2 l \omega}{(1 + Q_2 l \omega)^2} \right] \quad \text{C-13}$$

$$F_3 = \frac{cQ_1 Z_M Y}{Q_2} \left[\frac{Q_2 l \omega}{1 + Q_2 l \omega} + \ln(1 + Q_2 l \omega) \right] \quad \text{C-14}$$

so the fugacity coefficient is expressed as.

$$\begin{aligned} \ln \phi = & \frac{c\beta_1}{\beta_2} \left[\frac{\beta_2 \tau l \omega}{1 - \beta_2 \tau l \omega} - \ln(1 - \beta_2 \tau l \omega) \right] - \\ & cZ_M Y v^* \left[\frac{\omega}{1 + Ul\omega + U(l\omega)^2} + \frac{2}{l\sqrt{4W - U^2}} \left(\tanh^{-1} \left(\frac{U + 2Wl\omega}{\sqrt{4W - U^2}} \right) - \tanh^{-1} \left(\frac{U}{\sqrt{4W - U^2}} \right) \right) \right] - \\ & \frac{cQ_1 Z_M Y}{Q_2} \left[\frac{Q_2 l \omega}{1 + Q_2 l \omega} + \ln(1 + Q_2 l \omega) \right] - \ln Z_a \end{aligned}$$

C-15

organic constituents [8]. The inorganic

and

amounts to the gas adsorption

amount. A quantitative

for coal analysis used

is

the amount of ash that is

APPENDIX D

ADSORPTION RESULTS ON ORGANIC COAL BASIS

All coals contain inorganic and organic constituents [8]. The inorganic constituents are called mineral matter, which does not contribute to the gas adsorption. The lower the mineral constituents, the higher the adsorption amount. A quantitative measure of the amount of mineral matter can be obtained from the coal analysis using Parr expression,

$$y_{pure} = 1 - [1.08A_{ash} + 0.55S_{sulfur}] \quad \text{D-1}$$

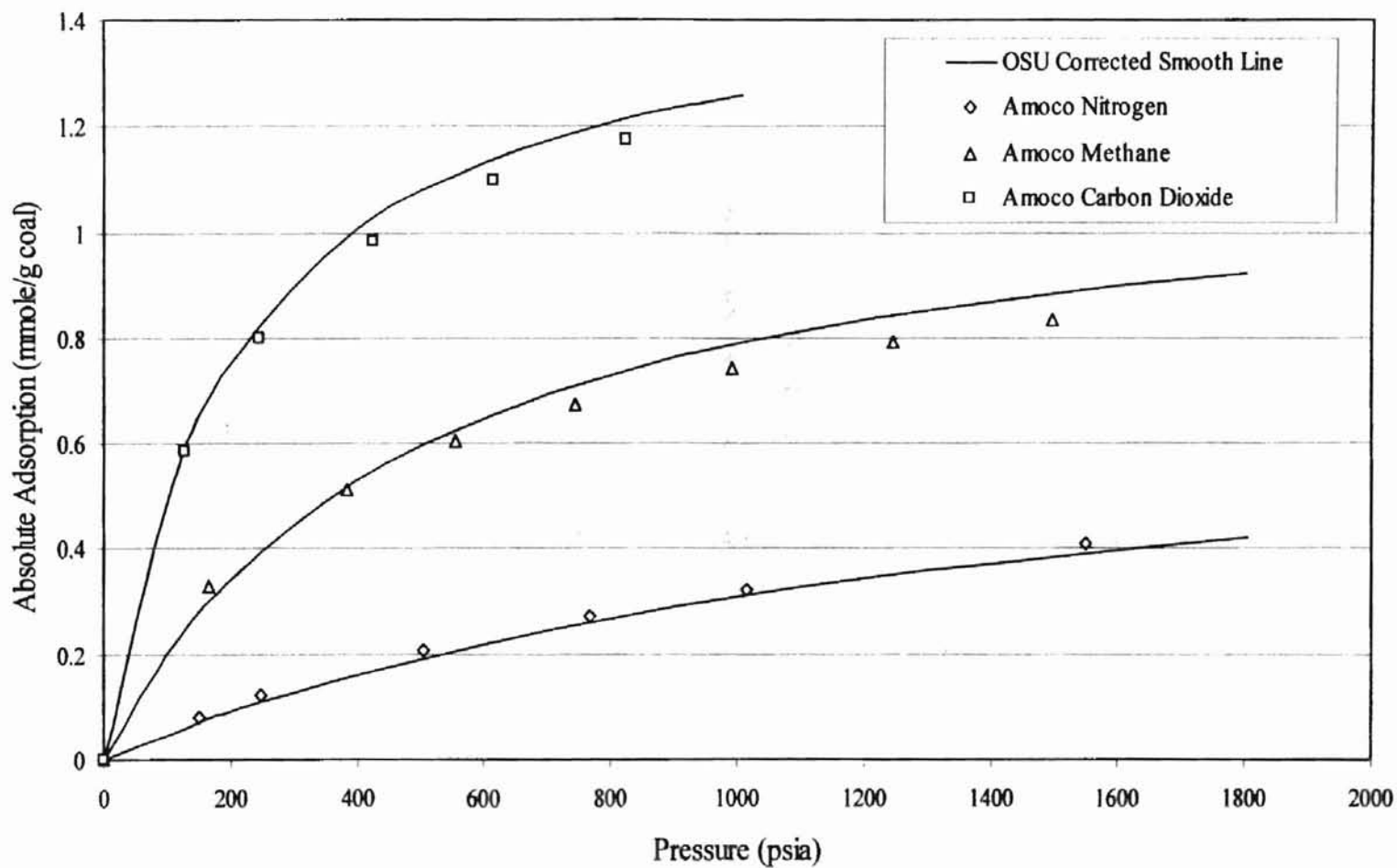
where y_{pure} , A_{ash} , S_{sulfur} are the mass fractions of pure(organic) coal, ash and sulfur respectively.

Adsorption results from the current work were compared to the Amoco data using an organic coal basis. The mass fraction of organic coal used in the current work was 75.7 percent, compared to 82.0 to Amoco results, which are reported from Hall's thesis [7]. The original data comparison shows that methane and carbon dioxide adsorption is about 5% lower than Amoco's, nitrogen is about 10% lower than Amoco's. The adjusted data comparison shows that nitrogen, methane and carbon dioxide adsorption is 5% higher than Amoco's data. The comparison is shown in Figure 61.

TABLE 31. Organic Coal Content of Coal Sample

	Current Work, Mass Percent	Amoco, Mass Percent
Ash Content A_{ash}	0.203	0.163
Sulfur Content S_{sulfur}	0.0419	0.0065
Pure(Organic) Coal y_{pure}	0.757	0.820

Figure 61. Comparison of Pure Gas Adsorption Data from OSU and Amoco
(Organic Coal Basis)



APPENDIX E
EXPERIMENTAL ADSORPTION DATA

TABLE 32. Pure Methane Adsorption Data on Wet Fruitland Coal (Run 1)

Void Volume	Percent Moisture	Dry Coal	Water Mass	Pump Temperature ($^{\circ}F$)	Cell Temperature ($^{\circ}F$)
78.05	9.7%	54.36g	5.84g	96.6	115

Pump Pressure (psia)	Pump Z factor	Injection Volume (cc)	Initial Cell Pressure (psia)	Final Cell Pressure (psia)	Cell Z factor	Total gas injected (gmole)	Total gas in water (mgmole)	Absolute Adsorption (mgmole/g coal)
996.3	0.9049	11.9	3	112.1	0.9900	0.0352	0.0461	0.2377
996.3	0.9049	8.62	112.1	208.1	0.9815	0.0608	0.0840	0.3427
996.3	0.9049	15.8	208.1	395.1	0.9650	0.1075	0.1542	0.4780
996.3	0.9049	17.55	395.1	607.2	0.9470	0.1595	0.2285	0.5855
996.3	0.9049	16.32	607.2	805.0	0.9312	0.2078	0.2933	0.6590
996.3	0.9049	16.89	805.0	1008.2	0.9164	0.2578	0.3559	0.7188
996.3	0.9049	16.9	1008.2	1214.8	0.9030	0.3079	0.4158	0.7431
996.3	0.9049	16.1	1214.8	1404.9	0.8925	0.3556	0.4680	0.7859
996.3	0.9049	16.82	1404.9	1602.8	0.8832	0.4054	0.5197	0.8274
996.3	0.9049	16.91	1602.8	1801.8	0.8744	0.4554	0.5692	0.8703

TABLE 33. Pure Methane Adsorption Data on Wet Fruitland Coal (Run 2)

Void Volume	Percent Moisture	Dry Coal	Water Mass	Pump Temperature (°F)	Cell Temperature (°F)
78.51	8.3%	54.63g	4.96g	96.6	115

Pump Pressure (psia)	Pump Z factor	Injection Volume (cc)	Initial Cell Pressure (psia)	Final Cell Pressure (psia)	Cell Z factor	Total gas injected (gmole)	Total gas in water (mgmole)	Absolute Adsorption (mgmole/g coal)
996.3	0.9049	10.5	2.8	102.6	0.9909	0.0311	0.0360	0.1942
996.3	0.9049	9.66	102.6	208.1	0.9815	0.0597	0.0717	0.3169
996.3	0.9049	16.4	208.1	398.9	0.9647	0.1083	0.1327	0.4650
996.3	0.9049	17.51	398.9	608.0	0.9469	0.1601	0.1952	0.5771
996.3	0.9049	16.64	608.0	808.0	0.9310	0.2094	0.2511	0.6547
996.3	0.9049	16.48	808.0	1004.8	0.9167	0.2582	0.3028	0.7160
996.3	0.9049	16.87	1004.8	1207.0	0.9030	0.3081	0.3530	0.7538
996.3	0.9049	16.91	1207.0	1407.3	0.8923	0.3582	0.3999	0.7931
996.3	0.9049	16.88	1407.3	1605.7	0.8831	0.4082	0.4442	0.8325
996.3	0.9049	16.67	1605.7	1802.3	0.8758	0.4575	0.4859	0.8676

TABLE 34. Pure Methane Adsorption Data on Wet Fruitland Coal (Run 3)

Void Volume	Percent Moisture	Dry Coal	Water Mass	Pump Temperature ($^{\circ}F$)	Cell Temperature ($^{\circ}F$)
78.96	7.6%	54.63g	4.51g	96.6	115

Pump Pressure (psia)	Pump Z factor	Injection Volume (cc)	Initial Cell Pressure (psia)	Final Cell Pressure (psia)	Cell Z factor	Total gas injected (gmole)	Total gas in water (mgmole)	Absolute Adsorption (mgmole/g coal)
996.3	0.9049	11.00	2.5	106.9	0.9905	0.0326	0.0341	0.2018
996.3	0.9049	9.41	106.9	209.1	0.9814	0.0604	0.0655	0.3213
996.3	0.9049	16.67	209.1	403.7	0.9643	0.1098	0.1221	0.4645
996.3	0.9049	16.63	403.7	602.0	0.9474	0.1590	0.1760	0.5674
996.3	0.9049	16.90	602.0	804.1	0.9313	0.2091	0.2274	0.6462
996.3	0.9049	17.02	804.1	1006.4	0.9166	0.2595	0.2758	0.7085
996.3	0.9049	16.92	1006.4	1207.9	0.9035	0.3096	0.3212	0.7504
996.3	0.9049	16.93	1207.9	1405.9	0.8924	0.3597	0.3634	0.7971
996.3	0.9049	16.69	1405.9	1601.8	0.8832	0.4091	0.4031	0.8317
996.3	0.9049	16.99	1601.8	1800.4	0.8758	0.4594	0.4415	0.8710

TABLE 35. Pure Carbon Dioxide Adsorption Data on Wet Fruitland Coal (Run 1)

Void Volume	Percent Moisture	Dry Coal	Water Mass	Pump Temperature (° F)	Cell Temperature (° F)
78.10	9.0%	54.63g	5.38g	96.6	115

Pump Pressure (psia)	Pump Z factor	Injection Volume (cc)	Initial Cell Pressure (psia)	Final Cell Pressure (psia)	Cell Z factor	Total gas injected (gmole)	Total gas in water (mgmole)	Absolute Adsorption (mgmole/g coal)
996.3	0.5709	10.6	2.7	105.1	0.9705	0.0496	0.745	0.5162
996.3	0.5709	7.72	105.1	210.0	0.9401	0.0836	1.483	0.7096
996.3	0.5709	12.72	210.0	402.1	0.8811	0.1432	2.685	0.9430
996.3	0.5709	14.46	402.1	612.4	0.8104	0.2104	4.291	1.0723
996.3	0.5709	14.49	612.4	798.0	0.7403	0.2782	4.535	1.1583
996.3	0.5709	20.69	798.0	1006.7	0.6479	0.3751	5.212	1.2163
996.3	0.5709	29.5	1006.7	1205.5	0.5355	0.5133	5.699	1.2373
996.3	0.5709	52.29	1205.5	1387.4	0.3982	0.7581	5.994	1.3177
996.3	0.5709	41.23	1387.4	1490.2	0.3364	0.9512	6.146	1.5744
996.3	0.5709	56.1	1490.2	1791.8	0.3105	1.2139	6.389	1.6498

TABLE 36. Pure Carbon Dioxide Adsorption Data on Wet Fruitland Coal (Run 2)

Void Volume	Percent Moisture	Dry Coal	Water Mass	Pump Temperature (°F)	Cell Temperature (°F)
79.79	6.3%	54.63g	3.68g	96.6	115

Pump Pressure (psia)	Pump Z factor	Injection Volume (cc)	Initial Cell Pressure (psia)	Final Cell Pressure (psia)	Cell Z factor	Total gas injected (gmole)	Total gas in water (mgmole)	Absolute Adsorption (mgmole/g coal)
996.3	0.5709	10.57	2.7	105.2	0.9706	0.0495	0.509	0.5105
996.3	0.5709	6.58	105.2	200.5	0.9429	0.0803	1.014	0.6810
996.3	0.5709	13.36	200.5	399.2	0.8821	0.1429	1.836	0.9318
996.3	0.5709	14.2	399.2	602.9	0.8138	0.2094	2.935	1.0739
996.3	0.5709	16.05	602.9	803.5	0.7381	0.2845	3.102	1.1773
996.3	0.5709	20.84	803.5	1007.0	0.6477	0.3821	3.565	1.2539
996.3	0.5709	29.99	1007.0	1201.6	0.5381	0.5225	3.897	1.3524
996.3	0.5709	53.3	1201.6	1383.5	0.4013	0.7721	4.100	1.5372
996.3	0.5709	60.66	1383.5	1547.8	0.3199	1.0562	4.244	1.7943
996.3	0.5709	37.82	1547.8	1772.3	0.3098	1.2333	4.369	1.8952

TABLE 37. Pure Carbon Dioxide Adsorption Data on Wet Fruitland Coal (Run 3)

Void Volume	Percent Moisture	Dry Coal	Water Mass	Pump Temperature ($^{\circ}F$)	Cell Temperature ($^{\circ}F$)
80.55	5.1%	54.63g	2.92g	96.6	115

Pump Pressure (psia)	Pump Z factor	Injection Volume (cc)	Initial Cell Pressure (psia)	Final Cell Pressure (psia)	Cell Z factor	Total gas injected (gmole)	Total gas in water (mgmole)	Absolute Adsorption (mgmole/g coal)
996.3	0.5709	10.00	2.8	102.1	0.9714	0.0468	0.404	0.4702
996.3	0.5709	8.00	102.1	210.7	0.9399	0.0843	0.805	0.7065
996.3	0.5709	13.25	210.7	407.5	0.8795	0.1463	1.457	0.9452
996.3	0.5709	13.41	407.5	601.2	0.8144	0.2091	2.328	1.0617
996.3	0.5709	16.38	601.2	802.3	0.7386	0.2858	2.461	1.1819
996.3	0.5709	20.38	802.3	1000.1	0.6511	0.3813	2.828	1.2669
996.3	0.5709	30.83	1000.1	1203.1	0.5371	0.5256	3.092	1.3059
996.3	0.5709	59.38	1203.1	1396.3	0.3914	0.8037	3.252	1.5809
996.3	0.5709	59.29	1396.3	1559.6	0.3178	1.0813	3.367	1.8792
996.3	0.5709	35.75	1559.6	1781.8	0.3101	1.2487	3.467	1.9014

TABLE 38. Pure Nitrogen Adsorption Data on Wet Fruitland Coal (Run 1)

Void Volume	Percent Moisture	Dry Coal	Water Mass	Pump Temperature ($^{\circ}F$)	Cell Temperature ($^{\circ}F$)
77.71	10.2%	54.36g	6.18g	96.6	115

Pump Pressure (psia)	Pump Z factor	Injection Volume (cc)	Initial Cell Pressure (psia)	Final Cell Pressure (psia)	Cell Z factor	Total gas injected (gmole)	Total gas in water (mgmole)	Absolute Adsorption (mgmole/g coal)
996.3	1.0023	8.91	3	107.8	0.9998	0.0238	0.0248	0.0489
996.3	1.0023	8.66	107.8	210.6	0.9998	0.0470	0.0480	0.0939
996.3	1.0023	15.62	210.6	403.7	1.0004	0.0887	0.0905	0.1487
996.3	1.0023	15.9	403.7	602.5	1.0016	0.1312	0.1329	0.2000
996.3	1.0023	16.09	602.5	805.9	1.0038	0.1742	0.1748	0.2498
996.3	1.0023	15.5	805.9	1007.9	1.0064	0.2157	0.2152	0.2812
996.3	1.0023	15.23	1007.9	1207.9	1.0098	0.2564	0.2539	0.3155
996.3	1.0023	14.75	1207.9	1405.9	1.0139	0.2958	0.2911	0.3419
996.3	1.0023	14.73	1405.9	1607.6	1.0188	0.3352	0.3279	0.3640
996.3	1.0023	14.31	1607.6	1805.0	1.0242	0.3735	0.3628	0.3934

TABLE 39. Pure Nitrogen Adsorption Data on Wet Fruitland Coal (Run 2)

Void Volume	Percent Moisture	Dry Coal	Water Mass	Pump Temperature ($^{\circ}F$)	Cell Temperature ($^{\circ}F$)
77.88	9.9%	54.36g	6.01g	96.6	115

Pump Pressure (psia)	Pump Z factor	Injection Volume (cc)	Initial Cell Pressure (psia)	Final Cell Pressure (psia)	Cell Z factor	Total gas injected (gmole)	Total gas in water (mgmole)	Absolute Adsorption (mgmole/g coal)
996.3	1.0023	8.84	2.7	105.6	0.9998	0.0236	0.0235	0.0522
996.3	1.0023	8.41	105.6	206.7	0.9998	0.0461	0.0457	0.0902
996.3	1.0023	15.98	206.7	402.5	1.0003	0.0888	0.0876	0.1511
996.3	1.0023	17.12	402.5	616.5	1.0017	0.1346	0.1318	0.2050
996.3	1.0023	14.81	616.5	804.9	1.0036	0.1742	0.1695	0.2447
996.3	1.0023	15.81	804.9	1008.5	1.0064	0.2165	0.2090	0.2848
996.3	1.0023	14.91	1008.5	1204.4	1.0098	0.2563	0.2458	0.3167
996.3	1.0023	15.12	1204.4	1406.7	1.0139	0.2967	0.2827	0.3527
996.3	1.0023	14.88	1406.7	1607.8	1.0188	0.3365	0.3183	0.3817
996.3	1.0023	14.01	1607.8	1801.8	1.0241	0.3740	0.3516	0.4041

TABLE 40. Pure Nitrogen Adsorption Data on Wet Fruitland Coal (Run 3)

Void Volume	Percent Moisture	Dry Coal	Water Mass	Pump Temperature ($^{\circ}F$)	Cell Temperature ($^{\circ}F$)
79.22	6.2%	56.69g	3.8g	96.6	115

Pump Pressure (psia)	Pump Z factor	Injection Volume (cc)	Initial Cell Pressure (psia)	Final Cell Pressure (psia)	Cell Z factor	Total gas injected (gmole)	Total gas in water (mgmole)	Absolute Adsorption (mgmole/g coal)
996.3	1.0023	8.66	2.9	102.6	0.9998	0.0232	0.0145	0.0470
996.3	1.0023	8.43	102.6	201.9	0.9998	0.0457	0.0283	0.0850
996.3	1.0023	16.49	201.9	399.5	1.0003	0.0898	0.0551	0.1495
996.3	1.0023	16.68	399.5	603.3	1.0016	0.1344	0.0818	0.2043
996.3	1.0023	16.06	603.3	802.8	1.0036	0.1773	0.1072	0.2511
996.3	1.0023	15.79	802.8	1002.4	1.0063	0.2195	0.1318	0.2912
996.3	1.0023	15.51	1002.4	1203.0	1.0097	0.2610	0.1557	0.3215
996.3	1.0023	15.22	1203.0	1402.5	1.0138	0.3017	0.1788	0.3516
996.3	1.0023	14.91	1402.5	1601.1	1.0186	0.3415	0.2010	0.3800
996.3	1.0023	14.53	1601.1	1799.9	1.0241	0.3804	0.2227	0.4002

TABLE 41. Pure Methane Adsorption Data on Wet Illinois-6 Coal (Run 1)

Void Volume	Percent Moisture	Dry Coal	Water Mass	Pump Temperature (°F)	Cell Temperature (°F)
74.7	13.6%	54.4g	8.5g	96.6	115

Pump Pressure (psia)	Pump Z factor	Injection Volume (cc)	Initial Cell Pressure (psia)	Final Cell Pressure (psia)	Cell Z factor	Total gas injected (gmole)	Total gas in water (mgmole)	Absolute Adsorption (mgmole/g coal)
996.3	0.9049	8.02	3.1	100.1	0.9910	0.0236	0.0461	0.0852
996.3	0.9049	8.18	100.1	204.8	0.9818	0.0476	0.0840	0.1455
996.3	0.9049	14.68	204.8	396.5	0.9649	0.0908	0.1542	0.2226
996.3	0.9049	16.06	396.5	605.6	0.9470	0.1380	0.2285	0.2836
996.3	0.9049	15.39	605.6	803.2	0.9310	0.1833	0.2933	0.3287
996.3	0.9049	15.76	803.2	1003.5	0.9161	0.2296	0.3559	0.3611
996.3	0.9049	16.25	1003.5	1208	0.9026	0.2774	0.4158	0.3836
996.3	0.9049	13.49	1208	1373.8	0.8930	0.3170	0.4680	0.4104
996.3	0.9049	18.69	1373.8	1603.6	0.8819	0.3720	0.5197	0.4378
996.3	0.9049	16.93	1603.6	1810.9	0.8742	0.4218	0.5692	0.4662

TABLE 42. Pure Methane Adsorption Data on Wet Illinois-6 Coal (Run 2)

Void Volume	Percent Moisture	Dry Coal	Water Mass	Pump Temperature ($^{\circ}F$)	Cell Temperature ($^{\circ}F$)
74.7	12.6%	54.4g	7.84g	96.6	115

Pump Pressure (psia)	Pump Z factor	Injection Volume (cc)	Initial Cell Pressure (psia)	Final Cell Pressure (psia)	Cell Z factor	Total gas injected (gmole)	Total gas in water (mgmole)	Absolute Adsorption (mgmole/g coal)
996.3	0.9049	8.24	2	98.6	0.9997	0.0242	0.0461	0.1010
996.3	0.9049	7.89	98.6	203	0.9912	0.0474	0.0840	0.1445
996.3	0.9049	15.13	203	399.6	0.9819	0.0919	0.1542	0.2237
996.3	0.9049	16.03	399.6	605.3	0.9646	0.1390	0.2285	0.2923
996.3	0.9049	15.61	605.3	807.9	0.9470	0.1849	0.2933	0.3237
996.3	0.9049	15.68	807.9	1005.7	0.9307	0.2310	0.3559	0.3574
996.3	0.9049	16.41	1005.7	1209.2	0.9160	0.2792	0.4158	0.3893
996.3	0.9049	15.82	1209.2	1404.3	0.9025	0.3257	0.4680	0.4114
996.3	0.9049	16.31	1404.3	1604.4	0.8914	0.3737	0.5197	0.4314
996.3	0.9049	16.09	1604.4	1801.7	0.8819	0.4210	0.5692	0.4508

TABLE 43. Pure Nitrogen Adsorption Data on Wet Illinois-6 Coal (Run 1)

Void Volume	Percent Moisture	Dry Coal	Water Mass	Pump Temperature (°F)	Cell Temperature (°F)
74.3	15.6%	54.4g	10.0g	96.6	115

Pump Pressure (psia)	Pump Z factor	Injection Volume (cc)	Initial Cell Pressure (psia)	Final Cell Pressure (psia)	Cell Z factor	Total gas injected (gmole)	Total gas in water (mgmole)	Absolute Adsorption (mgmole/g coal)
996.3	1.0023	8.6	2.7	114.8	0.9998	0.0228	0.0145	0.0209
996.3	1.0023	6.8	114.8	204.2	0.9998	0.0408	0.0283	0.0351
996.3	1.0023	15.07	204.2	402.3	1.0004	0.0807	0.0551	0.0681
996.3	1.0023	15.2	402.3	605	1.0016	0.1210	0.0818	0.0943
996.3	1.0023	15.35	605	812.2	1.0038	0.1617	0.1072	0.1168
996.3	1.0023	14.16	812.2	1005.4	1.0065	0.1992	0.1318	0.1362
996.3	1.0023	14.49	1005.4	1206.4	1.0100	0.2376	0.1557	0.1518
996.3	1.0023	14.36	1206.4	1407.9	1.0144	0.2757	0.1788	0.1687
996.3	1.0023	13.69	1407.9	1603.2	1.0193	0.3119	0.2010	0.1837
996.3	1.0023	13.88	1603.2	1804.1	1.0250	0.3487	0.2227	0.2010

TABLE 44. Pure Nitrogen Adsorption Data on Wet Illinois-6 Coal (Run 1)

Void Volume	Percent Moisture	Dry Coal	Water Mass	Pump Temperature (°F)	Cell Temperature (°F)
74.5	14.6%	54.4g	9.3g	96.6	115

Pump Pressure (psia)	Pump Z factor	Injection Volume (cc)	Initial Cell Pressure (psia)	Final Cell Pressure (psia)	Cell Z factor	Total gas injected (gmole)	Total gas in water (mgmole)	Absolute Adsorption (mgmole/g coal)
996.3	1.0023	8.6	2.7	99.9	0.9998	0.0228	0.0145	0.0219
996.3	1.0023	6.8	99.9	202.9	0.9998	0.0408	0.0283	0.0395
996.3	1.0023	15.07	202.9	403.6	1.0004	0.0807	0.0551	0.0720
996.3	1.0023	15.2	403.6	625.5	1.0016	0.1210	0.0818	0.1012
996.3	1.0023	15.35	625.5	803.6	1.0038	0.1617	0.1072	0.1206
996.3	1.0023	14.16	803.6	996.3	1.0065	0.1992	0.1318	0.1410
996.3	1.0023	14.49	996.3	1199.7	1.0100	0.2376	0.1557	0.1552
996.3	1.0023	14.36	1199.7	1405.7	1.0144	0.2757	0.1788	0.1769
996.3	1.0023	13.69	1405.7	1600.1	1.0193	0.3119	0.2010	0.1918
996.3	1.0023	13.88	1600.1	1799	1.0250	0.3487	0.2227	0.2062

TABLE 45. Methane/Carbon Dioxide (80%/20%) Adsorption Data on Wet Fruitland Coal

Methane Feed Composition	Void Volume (cc)	Percent Moisture	Dry Coal	Water Mass (g)	Pump Temperature (°F)	Cell Temperature (°F)
0.798	73.1	9.7%	58.7	6.32	96.6	115

Pump Pressure (psia)	Pump Z factor	Injection Volume (cc)	Initial Cell Pressure (psia)	Final Cell Pressure (psia)	Initial Cell Z Factor	Final Cell Z factor	Total gas injected (gmole)	Methane Mole Fraction	Methane Adsorption mgmole/g coal	Carbon Dioxide Adsorption mgmole/g coal
996.3	0.8747	11.15	3	105.0	0.9996	0.9890	0.0342	0.8921	0.16489	0.07921
996.3	0.8747	9.01	105.0	207.8	0.9890	0.9784	0.0618	0.8810	0.24642	0.12827
996.3	0.8747	15.68	207.8	401.0	0.9784	0.9592	0.1099	0.8774	0.33547	0.21029
996.3	0.8747	16.68	401.0	605.4	0.9592	0.9381	0.1610	0.8702	0.39704	0.27511
996.3	0.8747	16.3	605.4	810.2	0.9381	0.9176	0.2110	0.8612	0.4411	0.31354
996.3	0.8747	16.05	810.2	1008.5	0.9176	0.8989	0.2602	0.8536	0.47564	0.34617
996.3	0.8747	15.92	1008.5	1204.8	0.8989	0.8810	0.3090	0.8461	0.5163	0.36012
996.3	0.8747	16.3	1204.8	1404.3	0.8810	0.8640	0.3589	0.8377	0.55716	0.35906
996.3	0.8747	16.85	1404.3	1603.2	0.8640	0.8497	0.4106	0.8302	0.6042	0.3612
996.3	0.8747	17.55	1603.2	1805.8	0.8497	0.8347	0.4644	0.8261	0.63473	0.37099

TABLE 46. Methane/Carbon Dioxide (60%/40%) Data on Wet Fruitland Coal

Methane Feed Composition	Void Volume (cc)	Percent Moisture	Dry Coal	Water Mass (g)	Pump Temperature (°F)	Cell Temperature (°F)
0.628	73.2	9.6%	58.7	6.22	96.6	115

Pump Pressure (psia)	Pump Z factor	Injection Volume (cc)	Initial Cell Pressure (psia)	Final Cell Pressure (psia)	Initial Cell Z Factor	Final Cell Z factor	Total gas injected (gmole)	Methane Mole Fraction	Methane Adsorption mgmole/g coal	Carbon Dioxide Adsorption mgmole/gcoal
996.3	0.8401	11.48	3	107.6	0.9995	0.9874	0.0366	0.7787	0.1283	0.1526
996.3	0.8401	9.38	107.6	209.4	0.9874	0.9748	0.0666	0.7625	0.1860	0.2502
996.3	0.8401	15.81	209.4	403.5	0.9748	0.9517	0.1170	0.7521	0.2340	0.3927
996.3	0.8401	15.9	403.5	602.2	0.9517	0.9269	0.1677	0.7323	0.2636	0.4896
996.3	0.8401	16.47	602.2	807.9	0.9269	0.9017	0.2203	0.7165	0.2901	0.5620
996.3	0.8401	16.24	807.9	1005.5	0.9017	0.8772	0.2721	0.7048	0.3121	0.6117
996.3	0.8401	16.65	1005.5	1206.8	0.8772	0.8520	0.3253	0.6921	0.3435	0.6231
996.3	0.8401	17.28	1206.8	1404.9	0.8520	0.8291	0.3804	0.6831	0.3685	0.6427
996.3	0.8401	17.6	1404.9	1605.3	0.8291	0.8090	0.4366	0.6731	0.4040	0.6535
996.3	0.8401	17.79	1605.3	1801.0	0.8090	0.7896	0.4933	0.6662	0.4210	0.6617

TABLE 47. Methane/Carbon Dioxide (40%/60%) Adsorption Data on Wet Fruitland Coal

Methane Feed Composition	Void Volume (cc)	Percent Moisture	Dry Coal	Water Mass (g)	Pump Temperature ($^{\circ}F$)	Cell Temperature ($^{\circ}F$)
0.442	73.5	9.2%	58.7	5.92	96.6	115

Pump Pressure (psia)	Pump Z factor	Injection Volume (cc)	Initial Cell Pressure (psia)	Final Cell Pressure (psia)	Initial Cell Z Factor	Final Cell Z factor	Total gas injected (gmole)	Methane Mole Fraction	Methane Adsorption mgmole/g coal	Carbon Dioxide Adsorption mgmole/g coal
996.3	0.7923	11.38	3.1	111.4	0.9994	0.9836	0.0384	0.5916	0.0774	0.2204
996.3	0.7923	8.2	111.4	208.2	0.9836	0.9692	0.0662	0.5850	0.0957	0.3466
996.3	0.7923	16.88	208.2	410.2	0.9692	0.9382	0.1233	0.5826	0.1065	0.5935
996.3	0.7923	15.15	410.2	602.7	0.9382	0.9074	0.1745	0.5512	0.1313	0.7152
996.3	0.7923	15.96	602.7	802.1	0.9074	0.8735	0.2285	0.5288	0.1508	0.8039
996.3	0.7923	16.84	802.1	1002.8	0.8735	0.8400	0.2854	0.5148	0.1623	0.8851
996.3	0.7923	17.93	1002.8	1203.8	0.8400	0.8046	0.3461	0.5009	0.1833	0.9351
996.3	0.7923	18.77	1203.8	1402.2	0.8046	0.7700	0.4095	0.4865	0.2224	0.9439
996.3	0.7923	20.08	1402.2	1601.5	0.7700	0.7378	0.4774	0.4768	0.2555	0.9572
996.3	0.7923	21.15	1601.5	1801.6	0.7378	0.7089	0.5490	0.4700	0.2822	0.9721

TABLE 48. Methane/Carbon Dioxide (20%/80%) Adsorption Data on Wet Fruitland Coal

Methane Feed Composition	Void Volume (cc)	Percent Moisture	Dry Coal	Water Mass (g)	Pump Temperature (°F)	Cell Temperature (°F)
0.21	75.0	7.6%	58.7	4.85	96.6	115

Pump Pressure (psia)	Pump Z factor	Injection Volume (cc)	Initial Cell Pressure (psia)	Final Cell Pressure (psia)	Initial Cell Z Factor	Final Cell Z factor	Total gas injected (gmole)	Methane Mole Fraction	Methane Adsorption mgmole/g coal	Carbon Dioxide Adsorption mgmole/g coal
996.3	0.7073	12.36	3	112	0.9993	0.9779	0.0468	0.3318	0.044	0.3744
996.3	0.7073	8.15	112	207.7	0.9779	0.9578	0.0776	0.3089	0.0586	0.5422
996.3	0.7073	15.43	207.7	398.2	0.9578	0.9177	0.1361	0.2950	0.0651	0.8094
996.3	0.7073	15.82	398.2	608.6	0.9177	0.8689	0.1960	0.2764	0.0619	0.9531
996.3	0.7073	15.56	608.6	804.8	0.8689	0.8224	0.2550	0.2607	0.0688	1.038
996.3	0.7073	17.88	804.8	1006.1	0.8224	0.7673	0.3227	0.2486	0.0764	1.100
996.3	0.7073	20.09	1006.1	1203.8	0.7673	0.7084	0.3988	0.2386	0.0854	1.125
996.3	0.7073	23.49	1203.8	1400	0.7084	0.6503	0.4878	0.2308	0.1020	1.156
996.3	0.7073	28.22	1400	1600.3	0.6503	0.5921	0.5947	0.2253	0.1143	1.191
996.3	0.7073	29.4	1600.3	1790	0.5921	0.5476	0.7061	0.2202	0.1477	1.240

TABLE 49. Methane/Nitrogen (80%/20%) Adsorption Data on Wet Fruitland Coal

Methane Feed Composition	Void Volume (cc)	Percent Moisture	Dry Coal	Water Mass (g)	Pump Temperature ($^{\circ}F$)	Cell Temperature ($^{\circ}F$)
0.791	73.6	8.5%	62.0	5.75	96.6	115

Pump Pressure (psia)	Pump Z factor	Injection Volume (cc)	Initial Cell Pressure (psia)	Final Cell Pressure (psia)	Initial Cell Z Factor	Final Cell Z factor	Total gas injected (gmole)	Methane Mole Fraction	Methane Adsorption mgmole/g coal	Nitrogen Adsorption mgmole/gcoal
996.3	0.9339	10.25	3	105.1	0.9997	0.9934	0.0294	0.7424	0.1411	0.0164
996.3	0.9339	9.24	105.1	208.8	0.9934	0.9871	0.0559	0.7483	0.2363	0.0249
996.3	0.9339	16.33	208.8	405.3	0.9871	0.9758	0.1027	0.7525	0.3664	0.0287
996.3	0.9339	16.12	405.3	606.2	0.9758	0.9649	0.1490	0.7577	0.4633	0.0311
996.3	0.9339	15.94	606.2	808.2	0.9649	0.9548	0.1947	0.7640	0.5331	0.0379
996.3	0.9339	15.43	808.2	1005.2	0.9548	0.9459	0.2390	0.7697	0.5836	0.0480
996.3	0.9339	15.66	1005.2	1205.8	0.9459	0.9384	0.2839	0.7720	0.6358	0.0499
996.3	0.9339	15.31	1205.8	1402	0.9384	0.9318	0.3278	0.7742	0.6792	0.0534
996.3	0.9339	15.68	1402	1605.2	0.9318	0.9261	0.3728	0.7762	0.7135	0.0564
996.3	0.9339	15.27	1605.2	1803.2	0.9261	0.9222	0.4166	0.7802	0.7336	0.0768

TABLE 50. Methane/Nitrogen (60%/40%) Adsorption Data on Wet Fruitland Coal

Methane Feed Composition	Void Volume (cc)	Percent Moisture	Dry Coal	Water Mass (g)	Pump Temperature (°F)	Cell Temperature (°F)
0.600	72.3	8.7	60.48	5.77	96.6	115

Pump Pressure (psia)	Pump Z factor	Injection Volume (cc)	Initial Cell Pressure (psia)	Final Cell Pressure (psia)	Initial Cell Z Factor	Final Cell Z factor	Total gas injected (gmole)	Methane Mole Fraction	Methane Adsorption mgmole/g coal	Nitrogen Adsorption mgmole/gcoal
996.3	0.9540	9.90	3	108.8	0.9999	0.9951	0.0280	0.5442	0.1010	0.0333
996.3	0.9540	8.27	108.8	208.1	0.9951	0.9913	0.0515	0.5535	0.1654	0.0525
996.3	0.9540	15.62	208.1	402.2	0.9913	0.9837	0.0954	0.5639	0.2547	0.0820
996.3	0.9540	15.99	402.2	601.5	0.9837	0.9766	0.1404	0.5678	0.3298	0.0973
996.3	0.9540	15.62	601.5	808.1	0.9766	0.9707	0.1839	0.5699	0.3943	0.1036
996.3	0.9540	15.10	808.1	1004.5	0.9707	0.9656	0.2261	0.5728	0.4423	0.1136
996.3	0.9540	15.42	1004.5	1209.3	0.9656	0.9612	0.2698	0.5780	0.4752	0.1299
996.3	0.9540	14.39	1209.3	1408.0	0.9612	0.9583	0.3100	0.5810	0.5092	0.1377
996.3	0.9540	14.50	1408.0	1605.1	0.9583	0.9565	0.3510	0.5835	0.5311	0.1487
996.3	0.9540	14.81	1605.1	1801.8	0.9565	0.9556	0.3924	0.5848	0.5705	0.1594

TABLE 51. Methane/Nitrogen (40%/60%) Adsorption Data on Wet Fruitland Coal

Methane Feed Composition	Void Volume (cc)	Percent Moisture	Dry Coal	Water Mass (g)	Pump Temperature ($^{\circ}F$)	Cell Temperature ($^{\circ}F$)
0.400	72.5	9.4	60.48	5.57	96.6	115

Pump Pressure (psia)	Pump Z factor	Injection Volume (cc)	Initial Cell Pressure (psia)	Final Cell Pressure (psia)	Initial Cell Z Factor	Final Cell Z factor	Total gas injected (gmole)	Methane Mole Fraction	Methane Adsorption mgmole/g coal	Nitrogen Adsorption mgmole/gcoal
996.3	0.9737	9.60	3	109.7	0.9999	0.9973	0.0260	0.3326	0.0672	0.0368
996.3	0.9737	8.15	109.7	202.6	0.9973	0.9951	0.0484	0.3435	0.1166	0.0697
996.3	0.9737	16.15	202.6	409.4	0.9951	0.9908	0.0927	0.3539	0.1820	0.0987
996.3	0.9737	15.82	409.4	612.2	0.9908	0.9874	0.1359	0.3606	0.2366	0.1227
996.3	0.9737	15.54	612.2	808.7	0.9874	0.9847	0.1785	0.3662	0.2757	0.1487
996.3	0.9737	15.05	808.7	1011.1	0.9847	0.9829	0.2198	0.3719	0.3082	0.1764
996.3	0.9737	14.71	1011.1	1213.9	0.9829	0.9819	0.2599	0.3769	0.3254	0.1984
996.3	0.9737	14.52	1213.9	1404.6	0.9819	0.9821	0.2992	0.3792	0.3551	0.2141
996.3	0.9737	14.62	1404.6	1605.7	0.9821	0.9829	0.3393	0.3825	0.3670	0.2373
996.3	0.9737	14.65	1605.7	1805.0	0.9829	0.9849	0.3793	0.3841	0.4000	0.2526

TABLE 52. Methane/Nitrogen (20%/80%) Adsorption Data on Wet Fruitland Coal

Methane Feed Composition	Void Volume (cc)	Percent Moisture	Dry Coal	Water Mass (g)	Pump Temperature ($^{\circ}F$)	Cell Temperature ($^{\circ}F$)
0.207	73.8	8.1%	62.0	5.5	96.6	115

Pump Pressure (psia)	Pump Z factor	Injection Volume (cc)	Initial Cell Pressure (psia)	Final Cell Pressure (psia)	Initial Cell Z Factor	Final Cell Z factor	Total gas injected (gmole)	Methane Mole Fraction	Methane Adsorption mgmole/g coal	Nitrogen Adsorption mgmole/gcoal
996.3	0.9906	9.95	2.7	115.2	0.9999	0.9986	0.0269	0.1481	0.0388	0.0478
996.3	0.9906	7.81	115.2	207.8	0.9986	0.9977	0.0480	0.1526	0.0645	0.0769
996.3	0.9906	16.01	207.8	404.1	0.9977	0.9962	0.0913	0.1581	0.1106	0.1223
996.3	0.9906	15.83	404.1	603.7	0.9962	0.9954	0.1341	0.1634	0.1473	0.1592
996.3	0.9906	15.15	603.7	800.2	0.9954	0.9954	0.1751	0.1683	0.1741	0.1870
996.3	0.9906	15.38	800.2	1002.4	0.9954	0.9961	0.2167	0.1731	0.1948	0.2160
996.3	0.9906	15.13	1002.4	1205	0.9961	0.9978	0.2576	0.1753	0.2177	0.2354
996.3	0.9906	14.54	1205	1402.4	0.9978	1.0002	0.2969	0.1792	0.2289	0.2621
996.3	0.9906	14.19	1402.4	1600.2	1.0002	1.0032	0.3353	0.1828	0.2345	0.2839
996.3	0.9906	13.66	1600.2	1803.5	1.0032	1.0071	0.3723	0.1854	0.2448	0.3264

TABLE 53. Nitrogen/Carbon Dioxide (80%/20%) Adsorption Data on Wet Fruitland Coal

Nitrogen Feed Composition	Void Volume (cc)	Percent Moisture	Dry Coal	Water Mass (g)	Pump Temperature ($^{\circ}F$)	Cell Temperature ($^{\circ}F$)
0.820	75.7	10.5%	57.2	6.68	96.6	115

Pump Pressure (psia)	Pump Z factor	Injection Volume (cc)	Initial Cell Pressure (psia)	Final Cell Pressure (psia)	Initial Cell Z Factor	Final Cell Z factor	Total gas injected (gmole)	Nitrogen Mole Fraction	Nitrogen Adsorption mgmole/g coal	Carbon Dioxide Adsorption mgmole/gcoal
996.3	0.9629	10.52	2	117.4	0.9997	0.9989	0.0292	0.0412	0.0380	0.0754
996.3	0.9629	8.16	117.4	211.2	0.9989	0.9978	0.0519	0.0508	0.0612	0.1253
996.3	0.9629	16.13	211.2	402.8	0.9978	0.9956	0.0968	0.0671	0.0996	0.2080
996.3	0.9629	16.41	402.8	605.9	0.9956	0.9930	0.1425	0.0823	0.1296	0.2696
996.3	0.9629	15.74	605.9	802.5	0.9930	0.9913	0.1863	0.0905	0.1548	0.3256
996.3	0.9629	16.03	802.5	1004.2	0.9913	0.9910	0.2309	0.0950	0.1769	0.3849
996.3	0.9629	15.39	1004.2	1193.3	0.9910	0.9905	0.2737	0.0985	0.2160	0.4405
996.3	0.9629	16.17	1193.3	1395	0.9905	0.9897	0.3187	0.1027	0.2544	0.4905
996.3	0.9629	15.56	1395	1602	0.9897	0.9893	0.3620	0.1090	0.2687	0.5152
996.3	0.9629	15.29	1602	1803	0.9893	0.9908	0.4045	0.1338	0.2836	0.5553

TABLE 54. Nitrogen/Carbon Dioxide (60%/40%) Adsorption Data on Wet Fruitland Coal

Nitrogen Feed Composition	Void Volume (cc)	Percent Moisture	Dry Coal	Water Mass (g)	Pump Temperature ($^{\circ}F$)	Cell Temperature ($^{\circ}F$)
0.630	77.0	10.0%	57.7	6.42	96.6	115

Pump Pressure (psia)	Pump Z factor	Injection Volume (cc)	Initial Cell Pressure (psia)	Final Cell Pressure (psia)	Initial Cell Z Factor	Final Cell Z factor	Total gas injected (gmole)	Nitrogen Mole Fraction	Nitrogen Adsorption mgmole/g coal	Carbon Dioxide Adsorption mgmole/gcoal
996.3	0.9077	11.43	2.8	116.2	0.9997	0.9957	0.0337	0.8193	0.0271	0.1537
996.3	0.9077	8.19	116.2	205	0.9957	0.9923	0.0579	0.8128	0.0380	0.2542
996.3	0.9077	16.8	205	398.7	0.9923	0.9850	0.1075	0.8011	0.0581	0.4034
996.3	0.9077	17.26	398.7	604.9	0.9850	0.9755	0.1584	0.7753	0.0725	0.5222
996.3	0.9077	16.37	604.9	806	0.9755	0.9657	0.2067	0.7549	0.0837	0.6024
996.3	0.9077	16.28	806	1006.1	0.9657	0.9575	0.2548	0.7427	0.0882	0.6803
996.3	0.9077	16.41	1006.1	1208	0.9575	0.9484	0.3032	0.7304	0.0990	0.7359
996.3	0.9077	16.06	1208	1405.8	0.9484	0.9402	0.3506	0.7190	0.1176	0.7725
996.3	0.9077	16.19	1405.8	1606.3	0.9402	0.9339	0.3984	0.7106	0.1322	0.8098
996.3	0.9077	16.26	1606.3	1805.3	0.9339	0.9278	0.4464	0.7046	0.1433	0.8519

TABLE 55. Nitrogen/Carbon Dioxide (40%/60%) Adsorption Data on Wet Fruitland Coal

Nitrogen Feed Composition	Void Volume (cc)	Percent Moisture	Dry Coal	Water Mass (g)	Pump Temperature ($^{\circ}F$)	Cell Temperature ($^{\circ}F$)
0.422	75.0	7.7%	62.0	5.2	96.6	115

Pump Pressure (psia)	Pump Z factor	Injection Volume (cc)	Initial Cell Pressure (psia)	Final Cell Pressure (psia)	Initial Cell Z Factor	Final Cell Z factor	Total gas injected (gmole)	Nitrogen Mole Fraction	Nitrogen Adsorption mgmole/g coal	Carbon Dioxide Adsorption mgmole/gcoal
996.3	0.8373	10.96	3.1	102.5	0.9997	0.9927	0.0350	0.6664	0.0287	0.2186
996.3	0.8373	9.35	102.5	202.9	0.9927	0.9843	0.0649	0.6343	0.0375	0.3666
996.3	0.8373	16.21	202.9	394.8	0.9843	0.9658	0.1168	0.5904	0.0429	0.5582
996.3	0.8373	16.79	394.8	604.5	0.9658	0.9432	0.1705	0.5553	0.0487	0.6891
996.3	0.8373	16.05	604.5	805.8	0.9432	0.9201	0.2219	0.5293	0.0606	0.7697
996.3	0.8373	15.94	805.8	1002	0.9201	0.8981	0.2729	0.5132	0.0657	0.8383
996.3	0.8373	16.72	1002	1202.6	0.8981	0.8760	0.3264	0.5004	0.0713	0.8956
996.3	0.8373	17.1	1202.6	1400	0.8760	0.8550	0.3811	0.4898	0.0833	0.9456
996.3	0.8373	18.04	1400	1602	0.8550	0.8339	0.4389	0.4791	0.1069	0.9756
996.3	0.8373	18.19	1602	1802	0.8339	0.8178	0.4971	0.4744	0.1122	1.0397

TABLE 56. Nitrogen/Carbon Dioxide (20%/80%) Adsorption Data on Wet Fruitland Coal

Nitrogen Feed Composition	Void Volume (cc)	Percent Moisture	Dry Coal	Water Mass (g)	Pump Temperature ($^{\circ}F$)	Cell Temperature ($^{\circ}F$)
0.18	75.7	10.5%	57.2	6.68	96.6	115

Pump Pressure (psia)	Pump Z factor	Injection Volume (cc)	Initial Cell Pressure (psia)	Final Cell Pressure (psia)	Initial Cell Z Factor	Final Cell Z factor	Total gas injected (gmole)	Nitrogen Mole Fraction	Nitrogen Adsorption mgmole/g coal	Carbon Dioxide Adsorption mgmole/gcoal
996.3	0.7418	12.03	3.1	110.6	0.9993	0.9839	0.0434	0.3983	0.0170	0.3363
996.3	0.7418	8.27	110.6	206.5	0.9839	0.9683	0.0733	0.3703	0.0152	0.5021
996.3	0.7418	15.62	206.5	406.7	0.9683	0.9326	0.1297	0.3240	0.0190	0.7113
996.3	0.7418	15.16	406.7	605.7	0.9326	0.8930	0.1844	0.2967	0.0249	0.8369
996.3	0.7418	15.89	605.7	807.5	0.8930	0.8494	0.2418	0.2795	0.0257	0.9222
996.3	0.7418	16.75	807.5	1003.7	0.8494	0.8090	0.3023	0.2682	0.0300	1.0065
996.3	0.7418	18.62	1003.7	1202.5	0.8090	0.7638	0.3696	0.2566	0.0449	1.0596
996.3	0.7418	15.67	1202.5	1354.7	0.7638	0.7295	0.4262	0.2505	0.0541	1.1069
996.3	0.7418	16.32	1354.7	1500.1	0.7295	0.6973	0.4851	0.2454	0.0664	1.1574
996.3	0.7418	29.3	1500.1	1752	0.6973	0.6495	0.5909	0.2392	0.0750	1.2084

VITA

Xudong Liang

Candidate for the Degree of

Master of Science

Thesis: ADSORPTION OF PURE AND MULTICOMPONENT GASES
ON WET COAL

Major Field: Chemical Engineering

Biographical:

Personal Data: Born in Shanghai, P.R.China, Dec. 15, 1968, the son of Jinlai Liang and Lianzheng Yang.

Education: Graduated from KongJiang Middle School, Shanghai, China, in July 1987; received Bachelor of Science Degree in Petro-Chemical Engineering from East China University of Chemical Technology, Shanghai, China, in July 1991.

Professional Experience: Process Engineer, Sinopec Shanghai Oil Refinery, Shanghai, China, July 1991 to Dec., 1994; Process & Project Engineer, Shell Companies in Greater China, Shanghai, China, Jan., 1994 to Dec., 1996; Lubricant Engineer, Caltex Petroleum Corporation, Shanghai China, Jan., 1997 to Aug., 1997; Teaching Assistant, School of Chemical Engineering, Oklahoma State University, Aug., 1997 to Dec. 1998; Research Assistant, School of Chemical Engineering, Oklahoma State University, Aug., 1997 to Dec., 1999.